frontiers | Research Topics

Emerging talents in renal endocrinology 2023

Edited by
Federica Mescia

Published in
Frontiers in Endocrinology

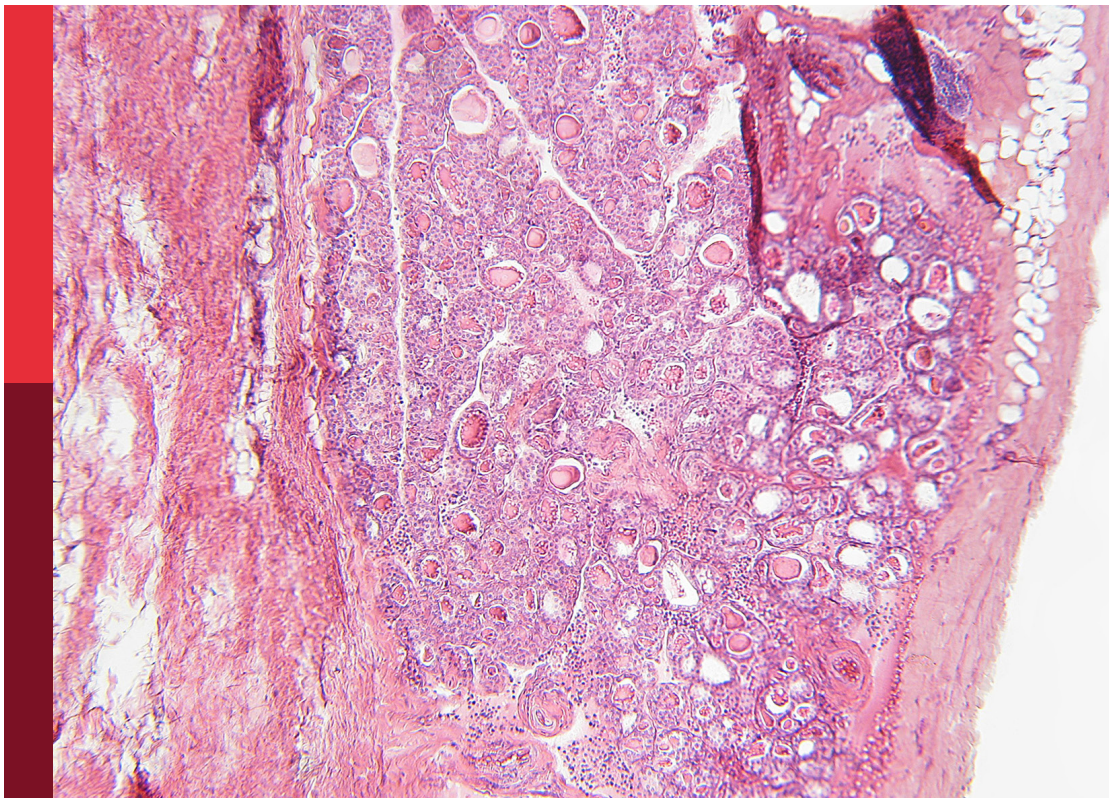

ISSN 1664-8714
ISBN 978-2-8325-6003-7
DOI 10.3389/978-2-8325-6003-7

About Frontiers

Frontiers is more than just an open access publisher of scholarly articles: it is a pioneering approach to the world of academia, radically improving the way scholarly research is managed. The grand vision of Frontiers is a world where all people have an equal opportunity to seek, share and generate knowledge. Frontiers provides immediate and permanent online open access to all its publications, but this alone is not enough to realize our grand goals.

Frontiers journal series

The Frontiers journal series is a multi-tier and interdisciplinary set of open-access, online journals, promising a paradigm shift from the current review, selection and dissemination processes in academic publishing. All Frontiers journals are driven by researchers for researchers; therefore, they constitute a service to the scholarly community. At the same time, the *Frontiers journal series* operates on a revolutionary invention, the tiered publishing system, initially addressing specific communities of scholars, and gradually climbing up to broader public understanding, thus serving the interests of the lay society, too.

Dedication to quality

Each Frontiers article is a landmark of the highest quality, thanks to genuinely collaborative interactions between authors and review editors, who include some of the world's best academicians. Research must be certified by peers before entering a stream of knowledge that may eventually reach the public - and shape society; therefore, Frontiers only applies the most rigorous and unbiased reviews. Frontiers revolutionizes research publishing by freely delivering the most outstanding research, evaluated with no bias from both the academic and social point of view. By applying the most advanced information technologies, Frontiers is catapulting scholarly publishing into a new generation.

What are Frontiers Research Topics?

Frontiers Research Topics are very popular trademarks of the *Frontiers journals series*: they are collections of at least ten articles, all centered on a particular subject. With their unique mix of varied contributions from Original Research to Review Articles, Frontiers Research Topics unify the most influential researchers, the latest key findings and historical advances in a hot research area.

Find out more on how to host your own Frontiers Research Topic or contribute to one as an author by contacting the Frontiers editorial office: frontiersin.org/about/contact

Emerging talents in renal endocrinology: 2023

Topic editor
Federica Mescia — University of Brescia, Italy

Citation
Mescia, F., ed. (2025). *Emerging talents in renal endocrinology: 2023*. Lausanne: Frontiers Media SA. doi: 10.3389/978-2-8325-6003-7

Table of contents

05 Fibroblast growth factor 23 is independently associated with renal magnesium handling in patients with chronic kidney disease
Teodora V. Grigore, Malou Zuidscherwoude, Anna Witasp, Peter Barany, Annika Wernerson, Annette Bruchfeld, Hong Xu, Hannes Olauson and Joost Hoenderop

15 Crosstalk between bone and muscle in chronic kidney disease
Limy Wong and Lawrence P. McMahon

25 Diagnostic efficacy of the triglyceride–glucose index in the prediction of contrast-induced nephropathy following percutaneous coronary intervention
Wei–Ting Chang, Chien-Cheng Liu, Yen-Ta Huang, Jheng-Yan Wu, Wen-Wen Tsai, Kuo–Chuan Hung, I–Wen Chen and Ping-Hsun Feng

36 Overview of the safety, efficiency, and potential mechanisms of finerenone for diabetic kidney diseases
Wenmin Chen, Lingqian Zheng, Jiali Wang, Yongda Lin and Tianbiao Zhou

51 Association between systemic inflammation response index and chronic kidney disease: a population-based study
Xiaowan Li, Lan Cui and Hongyang Xu

67 External validation of a minimal-resource model to predict reduced estimated glomerular filtration rate in people with type 2 diabetes without diagnosis of chronic kidney disease in Mexico: a comparison between country-level and regional performance
Camilla Sammut-Powell, Rose Sisk, Ruben Silva-Tinoco, Gustavo de la Pena, Paloma Almeda-Valdes, Sonia Citlali Juarez Comboni, Susana Goncalves and Rory Cameron

76 Hair cortisol and changes in cortisol dynamics in chronic kidney disease
Laura Boswell, Arturo Vega-Beyhart, Miquel Blasco, Luis F. Quintana, Gabriela Rodríguez, Daniela Díaz-Catalán, Carme Vilardell, María Claro, Mireia Mora, Antonio J. Amor, Gregori Casals and Felicia A. Hanzu

89 Urinary hyaluronidase activity is closely related to vasopressinergic system following an oral water load in men: a potential role in blood pressure regulation and early stages of hypertension development
Anna Calvi, Alice Bongrani, Ignazio Verzicco, Giuliano Figus, Vanni Vicini, Pietro Coghi, Alberto Montanari and Aderville Cabassi

101 Causal effects of serum calcium, phosphate, and 25-hydroxyvitamin D on kidney function: a genetic correlation, pleiotropic analysis, and Mendelian randomization study
Yanjun Liang, Shuang Liang, Dayang Xie, Xinru Guo, Chen Yang, Tuo Xiao, Kaiting Zhuang, Yongxing Xu, Yong Wang, Bin Wang, Zhou Zhang, Xiangmei Chen, Yizhi Chen and Guangyan Cai

113 Dysregulation of the 3β-hydroxysteroid dehydrogenase type 2 enzyme and steroid hormone biosynthesis in chronic kidney disease
Yiyi Zuo, Dongqing Zha, Yue Zhang, Wan Yang, Jie Jiang, Kangning Wang, Runze Zhang, Ziyi Chen and Qing He

frontiers | Frontiers in Endocrinology

TYPE Original Research
PUBLISHED 09 January 2023
DOI 10.3389/fendo.2022.1046392

OPEN ACCESS

EDITED BY
Seerapani Gopaluni,
University of Cambridge,
United Kingdom

REVIEWED BY
Lorenza Magagnoli,
University of Milan, Italy
Erica Clinkenbeard,
Purdue University Indianapolis,
United States

*CORRESPONDENCE
Joost Hoenderop
joost.hoenderop@radboudumc.nl

†These authors have contributed equally to this work and share last authorship

SPECIALTY SECTION
This article was submitted to Renal Endocrinology, a section of the journal Frontiers in Endocrinology

RECEIVED 16 September 2022
ACCEPTED 28 November 2022
PUBLISHED 09 January 2023

CITATION
Grigore TV, Zuidscherwoude M, Witasp A, Barany P, Wernerson A, Bruchfeld A, Xu H, Olauson H and Hoenderop J (2023) Fibroblast growth factor 23 is independently associated with renal magnesium handling in patients with chronic kidney disease. *Front. Endocrinol.* 13:1046392. doi: 10.3389/fendo.2022.1046392

Fibroblast growth factor 23 is independently associated with renal magnesium handling in patients with chronic kidney disease

Teodora V. Grigore[1], Malou Zuidscherwoude[1], Anna Witasp[2], Peter Barany[2], Annika Wernerson[2], Annette Bruchfeld[2,3], Hong Xu[4], Hannes Olauson[2†] and Joost Hoenderop[1*†]

[1]Radboud Institute for Molecular Life Sciences, Department of Physiology, Radboudumc, Nijmegen, Netherlands, [2]Karolinska Institutet, Division of Renal Medicine, Department of Clinical Science, Intervention and Technology, Stockholm, Sweden, [3]Linköpings universitet Hälsouniversitetet, Department of Health, Medicine and Caring Sciences, Linköping, Sweden, [4]Karolinska Institutet, Division of Clinical Geriatrics, Department of Neurobiology, Department of Care Sciences and Society, Stockholm, Sweden

Background: Disturbances in magnesium homeostasis are common in patients with chronic kidney disease (CKD) and are associated with increased mortality. The kidney is a key organ in maintaining normal serum magnesium concentrations. To this end, fractional excretion of magnesium (FEMg) increases as renal function declines. Despite recent progress, the hormonal regulation of renal magnesium handling is incompletely understood. Fibroblast Growth Factor 23 (FGF23) is a phosphaturic hormone that has been linked to renal magnesium handling. However, it has not yet been reported whether FGF23 is associated with renal magnesium handling in CKD patients.

Methods: The associations between plasma FGF23 levels, plasma and urine magnesium concentrations and FEMg was investigated in a cross-sectional cohort of 198 non-dialysis CKD patients undergoing renal biopsy.

Results: FGF23 was significantly correlated with FEMg (Pearson's correlation coefficient = 0.37, $p<0.001$) and urinary magnesium (-0.14, $p=0.04$), but not with plasma magnesium. The association between FGF23 and FEMg remained significant after adjusting for potential confounders, including estimated glomerular filtration rate (eGFR), parathyroid hormone and 25-hydroxyvitamin D.

Conclusions: We report that plasma FGF23 is independently associated with measures of renal magnesium handling in a cohort of non-dialysis CKD patients. A potential causal relationship should be investigated in future studies.

KEYWORDS

FGF23, FEMg, CKD, Klotho, phosphate

1 Introduction

Magnesium ions (Mg^{2+}) are essential in several biological processes such as cell signaling, energy metabolism, growth and proliferation. Normomagnesemia is maintained between 0.7 and 1.1 mmol/L through an elaborate coordination between the kidney, bone and intestine. Renal excretion of Mg^{2+} is a controlled process (1) fine-tuned in the distal convoluted tubule (DCT). In the DCT, regulated Mg^{2+} reabsorption occurs through the transient receptor potential melastatin (TRPM) 6 (2). 10-25% filtered Mg^{2+} is reabsorbed in the proximal tubule and 50-70% is reabsorbed in the thick ascending limb of Henle's loop. Fine-tuning of Mg^{2+} reabsorption occurs in the DCT (10%) *via* an active transcellular process (1). The Mg^{2+} handling in the kidney is influenced by several factors. Generally, peptide hormones, such as parathyroid hormone (PTH) or vasopressin, increase the Mg^{2+} transport (3). Interestingly, vitamin D does not influence, in physiological conditions, the Mg^{2+} homeostasis, yet rodents treated with vitamin D showed an increase in serum levels of Mg^{2+} and a decrease in renal Mg^{2+} excretion (4). Electrolytes play an important role in the transport of Mg^{2+}. Calcium (Ca^{2+}) and Mg^{2+} ions have been shown to activate Calcium Sensing Receptor (CaSR) and regulate paracellular Mg^{2+} transport (5), while potassium (K^{+}) indirectly influences the Mg^{2+} transport in the DCT through the voltage-gated channel Kv1.1, which provides an electrical driving force for transcellular Mg^{2+} transport (6, 7). Nevertheless, the exact regulation of renal Mg^{2+} handling remains largely unkown. Mutations in the *TRPM6* gene results in primary hypomagnesemia with secondary hypocalcemia (PHSH, OMIM# 602014), an autosomal recessive condition characterized by abnormally low serum Mg^{2+}. However, the precise hormonal regulation of TRPM6 in health and in disease has not yet been characterized (8).

Chronic kidney disease (CKD) affects approximately 10% of the population globally and is associated with increased cardiovascular morbidity and mortality (9). Vascular calcification is a key mechanism behind the increased cardiovascular risk associated with CKD (10, 11). In CKD patients the fractional excretion of Mg^{2+} (FEMg) gradually increases to compensate for the reduced number of functioning nephrons (12). In patients with end stage renal disease (ESRD) the adaptive mechanisms are no longer sufficient to fully compensate for the loss of glomerular filtration capacity, which can lead to hypermagnesemia (13). Also, hypomagnesemia is commonly observed in CKD patients due to reduced intestinal uptake or increased renal losses caused by use of medication such as diuretics and proton-pump inhibitors (14, 15), comorbidities including diabetes and hypertension, or low dietary Mg^{2+} intake (1).

Both hyper- and hypomagnesemia have been linked to cardiovascular disease and higher overall mortality in patients with CKD (16, 17). Mechanistically, Mg^{2+} has been demonstrated to inhibit phosphate-induced vascular calcification, and Mg^{2+} supplementation or Mg^{2+}-based therapies have shown promise in reducing cardiovascular disease in CKD patients (18–22). A better understanding of the hormonal regulation of renal Mg^{2+} handling, especially in the setting of reduced renal function, is therefore of outmost clinical importance.

Fibroblast Growth Factor 23 (FGF23) is a bone-derived hormone that reduces the apical abundance of the sodium-phosphate co-transporters NPT2A and NPT2C in the proximal tubule, thereby lowering phosphate (Pi) reabsorption and increasing urinary Pi excretion. FGF23 concentrations increase dramatically in CKD patients, likely as an adaptive mechanism to counteract Pi retention (23–25). FGF23 plays an active role in the inhibition of renal 1,25-dihydroxyvitamin D ($1,25(OH)_2D$) synthesis by increasing the expression of the calcitriol-inactivating enzyme 24-hydroxylase, whereas PTH stimulates the 25-hydroxyvitamin D-1α-hydroxylase, which generates $1,25(OH)_2D$ (26). FGF23 and $1,25(OH)_2D$ regulate each other through a feedback loop, as $1,25(OH)_2D$ stimulates FGF23 synthesis in osteoblasts through the presence of a vitamin D response element in the FGF23 promoter (27). Animal studies show that FGF23 inhibits PTH secretion by activating the MAPK pathway, which decreases PTH expression and secretion (28, 29). This mechanism may not be important in humans, as CKD patients display a simultaneous increase in PTH and FGF23 levels (30–32).

Many epidemiological studies have linked increased FGF23 concentrations to worse clinical outcomes, including cardiovascular morbidity and mortality (33, 34), although the evidence of a causal relationship from prospective trials is still lacking.

In addition to regulating Pi balance, FGF23 and its co-receptor Klotho have been linked to renal handling of other electrolytes, including Ca^{2+}, sodium (Na^{+}) and K^{+} (35–37). There are also some indications that FGF23 may be involved in controlling renal Mg^{2+} reabsorption. First, mice with diet-induced hypomagnesemia have increased serum FGF23 levels and reduced renal Klotho expression (38, 39), suggesting that dietary Mg^{2+} can influence the regulation of the FGF23-Klotho axis. Similarly, low plasma Mg^{2+} concentrations are associated with high plasma FGF23 concentrations and high mortality rates in azotemic cats with CKD (40). Second, a negative association between serum FGF23 and Mg^{2+} was observed in patients undergoing hemodialysis, supporting a possible interrelationship (41). Third, Mg^{2+} supplementation was recently reported to reduce vascular calcification in hyperphosphatemic Klotho-deficient mice with high FGF23 concentrations (8).

Herein we set out to test whether FGF23 could be involved in renal Mg^{2+} handling in patients with non-dialysis CKD, and particularly we hypothesize that FGF23 and FEMg are positively associated.

10.3389/fendo.2022.1046392

2 Materials and methods

2.1 Study design and patient inclusion

For the present study we used a cohort of non-dialysis patients with CKD stage 1-5 undergoing kidney biopsy at the Karolinska University Hospital between 2011 and 2017 (KaroKidney – karokidney.org) (23). All patients in which plasma and spot urine Mg^{2+} were available were included in the analysis. The study received ethical approval (Ethical Review Board, Stockholm, Sweden, DNR 2010/579-31), and informed consent was obtained from all participants.

2.2 Exposure, outcome and covariates

Prior to the kidney biopsy, blood and urine samples were collected and directly analyzed or frozen and stored at -80°C for later biochemical measurements. Intact FGF23 was measured in plasma using a second-generation enzyme-linked immunosorbent assay (ELISA) (Immutopics, San Clemente, CA, USA). Plasma (normal values equal to 0.7-1.1 mmol/L) and urine Mg^{2+} concentrations were measured using a colorimetric assay (Roche/Hitachi, Tokyo, Japan) according to the manufacturer's protocol. Absorbance was measured at a 600 nm wavelength on a microplate spectrophotometer (Bio-Rad Laboratories, CA, USA). All Mg^{2+} measurements were carried out in triplicate. The FEMg (normal range defined as FEMg under 4%) was calculated using the formula $[(U_{Mg}{}^{2+} \times P_{Crea})/(U_{Crea} \times P_{Mg}{}^{2+} \times 0.7)] \times 100$ (where U = urinary, P = plasma, Mg^{2+} = ionized magnesium, Crea = creatinine) (42). Soluble Klotho and aldosterone were analyzed in serum using ELISA methods (IBL International, Germany and DRG Diagnostics, Germany, respectively). Estimated eGFR was calculated using plasma Cystatin C values.

2.3 Statistical analysis

Data were expressed as mean ± standard deviation (SD) or median with interquartile range (IQR) for continuous variables and percentage of total for categorical variables. Plasma FGF23, Klotho, 25-hydroxyvitamin D, PTH, aldosterone, fractional excretion of Ca^{2+} (FECa), FEMg, fraction excretion of K^+ (FEK), plasma Pi, Ca^{2+}, creatinine, and urinary Ca^{2+}, Mg^{2+}, Pi and creatinine were $\log_{10}$ transformed when used in models, to improve their distribution towards normal. Missing data were imputed by using Predictive Mean Matching with 15 iterations and can be found in Supplementary Table 1.

The cohort was stratified into quartiles, based on the plasma levels of FGF23, and the quartiles were tested for group comparisons using one-way ANOVA and Tukey's *post-hoc* test to correct for multiple comparisons.

Pearson's correlation was used to explore the relationships between FGF23, FEMg, eGFR, age, sex, aldosterone, PTH, Klotho, 25-hydroxyvitamin D, FEK, fractional excretion of Pi (FEPi), FECa, plasma Na^+, K^+, Ca^{2+}, Pi, Mg^{2+}, urinary Ca^{2+}, and Pi concentrations. All data were compiled in a correlation matrix with all covariates included.

Univariate linear regression models were performed to investigate the effect of FGF23 on FEMg values. Data were expressed as regression coefficient (β), 95% confidence intervals (CI), adjusted R^2 and *p*-value. Multivariate general linear regression models were run to investigate the effect of FGF23 on FEMg. The first model (model 1) consisted of age (years), sex and eGFR (mL/min/1.73 m^2). The second model (model 2) included the same parameters as model 1 plus Klotho (pg/mL), 25-hydroxyvitamin D (nmol/L), and PTH (ng/L). The third model (model 3) included model 1 and medication (yes/no): loop diuretics, thiazide, PPI, and beta blockers. The fourth model (model 4) included model 2 and model 3, and the fifth model (model 5) included model 4 and comorbidities (yes/no): hypertension and diabetes. The sixth model (model 6) included model 2 and FECa, while the seventh model (model 7) included model 1 and FECa, FEK and FEPi.

The cohort was divided into quartiles of FGF23 concentrations and quartiles of eGFR, to investigate if the $\log_{10}$FEMg associations are consistent even if the cohort is divided and we see the same trend. Linear regression analysis was used to show the associations.

Differences with a *p*-value of <0.05 were considered statistically significant. Statistical analyses were performed using statistical software SPSS for Windows, version 25, release 25.0.0.1, 64-bit edition and GraphPad Prism 8 for macOS, version 8.4.3 (471).

3 Results

3.1 Baseline characteristics of study population

The study cohort included a total of 198 CKD patients. Clinical characteristics and relevant laboratory results for the full cohort and FGF23 strata are reported in Table 1. Of the 198 patients, 62.7% were male, the mean age was 50.5 (± 17.0) years, the median for FGF23 was 81 (58 – 154) pg/mL and the mean eGFR was 48.7 (± 22.3) mL/min/1.73m^2. Of the patients, 13.1% were hypomagnesemic and 57.1% presented FEMg values higher than the normal range. Of note, FEMg, FEPi and FEK increased over quartiles of FGF23. All plasma and urine electrolyte values are shown in Supplementary Figure 1.

10.3389/fendo.2022.1046392

TABLE 1 Baseline characteristics of patients in the CKD cohort (N=198) and of each FGF23 strata.

N	Full cohort 198	Quartile 1 48	Quartile 2 52	Quartile 3 48	Quartile 4 50	p value for trend
Demographics						
Age (years), mean ± SD	50.5 (± 17.0)	48.0 (± 17.4)	48.6 (± 16.1)	49.8 (± 18.2)	55.6 (± 15.7)	0.10
Sex (male), %	62.7	54.8	64.6	58.5	71.7	
Laboratory analyses						
FGF23 (pg/mL), median (IQR)	81.0 (58.0-154.0)	44.0 (33.2-53.0)	65.2 (61.1-71.0)	107.0 (94.3-125.0)	243.0 (186.5-373.5)	<0.0001
GFR Cystatin C (mL/min/1.73 m^2), mean ± SD	48.7 (± 22.3)	61.9 (± 19.1)	57.3 (± 18.3)	48.3 (± 20.8)	27.4 (± 13.2)	<0.0001
Klotho (pg/mL), median (IQR)	640.5 (536.2-780.5)	748.5 (575.7-932.5)	653.5 (560.2-737.0)	637.5 (553.0-732.5)	571.0 (487.5-745.2)	0.005
PTH (ng/L), median (IQR)	9.1 (4.6-33.0)	6.4 (3.8-29.0)	9.6 (5.2-37.0)	6.7 (4.7-13.0)	11.5 (5.6-33.2)	0.05
25-hydroxyvitamin D (nmol/L), median (IQR)	37.5 (24.0-53.2)	39.5 (33.2-54.5)	39.0 (28.2-57.2)	31.0 (18.2-49.7)	35.5 (25.5-49.0)	0.78
Plasma creatinine (µmol/L), median (IQR)	121.5 (82.7-182.2)	82.0 (69.2-117.2)	100.0 (78.2-132.2)	123.0 (98.0-186.0)	209.0 (157.0-300.7)	<0.0001
Urinary creatinine (mmol/L), median (IQR)	6.4 (4.9-9.4)	6.8 (5.3-11.1)	6.7 (5.4-9.4)	6.3 (5.0-8.3)	5.6 (4.6-8.3)	0.55
Plasma Mg^{2+} (mmol/L), mean ± SD	0.8 (± 0.1)	0.8 (± 0.1)	0.8 (± 0.1)	0.8 (± 0.1)	0.8 (± 0.1)	0.81
Urinary Mg^{2+} (mmol/L), median (IQR)	2.0 (1.1-3.0)	2.3 (1.4-3.0)	2.2 (1.3-3.5)	1.9 (1.1-2.8)	1.7 (1.1-2.3)	0.13
FEMg (%), median (IQR)	4.8 (2.5-8.1)	3.2 (1.9-4.7)	4.1 (2.3-8.6)	5.0 (3.3-7.5)	7.5 (4.7-13.1)	<0.0001
Plasma Ca^{2+} (mmol/L), median (IQR)	2.2 (2.1-2.3)	2.2 (2.1-2.3)	2.2 (2.2-2.3)	2.2 (2.1-2.3)	2.2 (2.1-2.3)	0.56
Urinary Ca^{2+} (mmol/L), median (IQR)	0.5 (0.1-1.2)	0.9 (0.3-1.7)	0.5 (0.2-1.4)	0.4 (0.1-1.2)	0.2 (0.1-0.6)	0.002
FECa (%), median (IQR)	0.4 (0.1-0.7)	0.4 (0.1-0.7)	0.3 (0.1-0.9)	0.3 (0.1-0.7)	0.4 (0.1-1.1)	0.24
Plasma PO_4^{3-} (mmol/L), median (IQR)	1.1 (0.9-1.3)	1.0 (0.8-1.1)	1.0 (0.8-1.2)	1.2 (1.0-1.3)	1.3 (1.1-1.5)	<0.0001
Urinary PO_4^{3-} (mmol/L), median (IQR)	14.0 (8.6-20.0)	14.0 (7.8-22.9)	15.4 (10.5-20.6)	13.0 (7.4-19.4)	13.4 (9.4-16.3)	0.65
FEPi (%), mean ± SD	23.3 (± 14.3)	16.3 (± 10.8)	19.8 (± 12.4)	21.2 (± 11.1)	35.2 (± 14.8)	<0.0001
Plasma K^+ (mmol/L), mean ± SD	4.0 (± 0.46)	3.8 (± 0.3)	3.9 (± 0.2)	4.1 (± 0.5)	4.2 (± 0.5)	<0.0001
FEK (%), median (IQR)	15.7 (10.1-22.5)	12.8 (7.4-18.5)	14.3 (10.1-19.4)	15.2 (10.2-21.6)	26.0 (16.3-34.9)	<0.0001
Medication, (%)						
Betablockers	34.8	24.4	23.1	43.2	46.9	
Loop diuretics	35.3	19.5	23.1	38.6	57.1	
Thiazides	4.9	4.9	5.8	4.7	4.1	
Ca^{2+}-based PO_4^{3-} binders	10.3	12.2	9.6	6.8	12.2	
Non-Ca^{2+}-based PO_4^{3-} binders	4.9	2.4	1.9	0	14.3	
PPI	17.4	22.0	13.5	13.6	20.4	
Comorbidities, (%)						
Hypertension	45.5	33.3	40.4	47.9	60.0	
T1D	1.5	2.1	0	43.2	4.0	
T2D	12.1	10.4	9.6	0	18.0	

Data reported as mean and SD for variables with normal distribution, and as median and IQR for skewed variables.

3.2 Associations between FGF23, covariates and renal magnesium handling

Initially, the relationships between FGF23 and plasma Mg^{2+}, urinary Mg^{2+} concentrations, and FEMg were explored using Pearson's correlation (as shown in Figure 1 and Supplementary Table 2). This analysis showed a significant correlation between FGF23, FEMg and urinary Mg^{2+}, but no significant correlation with plasma Mg^{2+} concentration. Furthermore, plasma FGF23 was negatively correlated with plasma Klotho (r=-0.281, p<0.001), and positively correlated with FEPi (r=0.527, p<0.001) (shown in Figure 1 and Supplementary Table 2).

Next, Pearson's correlation was used to assess the relationship between FEMg and several clinical characteristics. The bivariate analysis demonstrated a negative correlation between FEMg and eGFR (r=-0.397, p<0.001) and an inversed correlation with plasma Klotho (r=-0.261, p<0.001), as seen in Figure 1 and Supplementary Table 2. Further, FEMg was positively and moderately correlated with FEPi (r=0.394, p<0.001) and plasma Pi (r=0.229, p=0.001) (shown in Figure 1 and Supplementary Table 2).

3.3 Univariate and multivariate analyses between FGF23 and renal magnesium handling

Univariate linear regression analysis revealed a significant correlation between plasma FGF23 and FEMg (in Table 2). Conversely, there was no significant correlation between FGF23 and plasma Mg^{2+} concentration and only a very weak

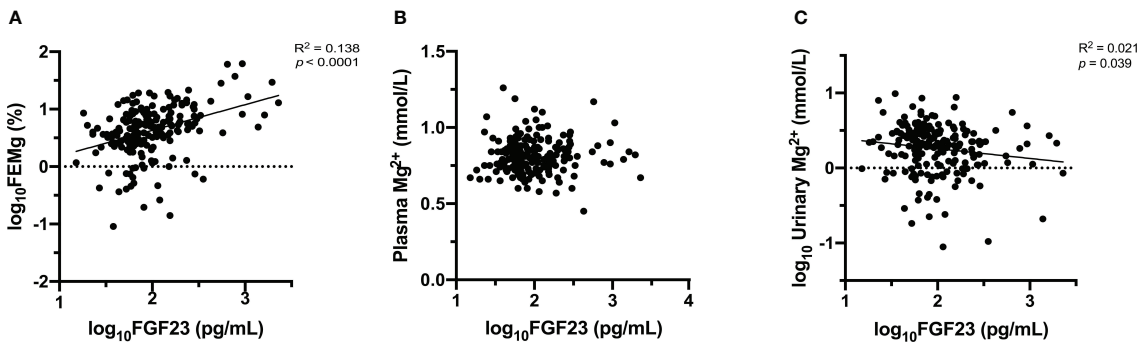

FIGURE 1
Association between FGF23 and Mg^{2+} [FEMg **(A)**, plasma Mg^{2+} **(B)**, urinary Mg^{2+} **(C)**]. Data are the outcomes of simple linear regression analysis.

TABLE 2 Linear regression models exploring the association between FGF23 and FEMg.

	Unstandardized β coefficient	95% CI	Adjusted R^2	*p*-value
Crude	0.449	0.292 to 0.606	0.135	<0.001
Model 1	0.236	0.034 to 0.438	0.184	0.022
Model 2	0.204	-0.026 to 0.434	0.182	0.081
Model 3	0.269	0.032 to 0.506	0.181	0.026
Model 4	0.283	0.021 to 0.545	0.176	0.034
Model 5	0.295	0.029 to 0.562	0.167	0.030
Model 6	0.210	0.004 to 0.416	0.197	0.046
Model 7	0.189	-0.023 to 0.401	0.203	0.080

model 1 adjusted for age, sex and GFR Cystatin C.
model 2 adjusted for age, sex, GFR Cystatin C, log_{10} Klotho, log_{10} 25-hydroxyvitamin D, log_{10} PTH, log_{10} plasma PO_4^{3-}, log_{10} urinary PO_4^{3-}.
model 3 adjusted for age, sex, GFR Cystatin C, loop diuretics, thiazide, PPI, beta blockers, Ca^{2+}-based PO_4^{3-} binders, non-Ca^{2+}-based PO_4^{3-} binders.
model 4 adjusted for age, sex, GFR Cystatin C, log_{10} Klotho, log_{10} 25-hydroxyvitamin D, log_{10} PTH, log_{10} plasma PO_4^{3-}, log_{10} urinary PO_4^{3-}, loop diuretics, thiazide, PPI, beta blockers, Ca^{2+}-based PO_4^{3-} binders, non-Ca^{2+}-based PO_4^{3-} binders.
model 5 adjusted for age, sex, GFR Cystatin C, log_{10} Klotho, log_{10} 25-hydroxyvitamin D, log_{10} PTH, log_{10} plasma PO_4^{3-}, log_{10} urinary PO_4^{3-}, loop diuretics, thiazide, PPI, beta blockers, Ca^{2+}-based PO_4^{3-} binders, non-Ca^{2+}-based PO_4^{3-} binders, hypertension, diabetes.
model 6 adjusted for age, sex and GFR Cystatin C, log_{10} Klotho, log_{10} 25-hydroxyvitamin D, log_{10} PTH, log_{10}FECa.
model 7 adjusted for age, sex, GFR Cystatin C, log_{10}FECa, log_{10}FEK, FEPi.

10.3389/fendo.2022.1046392

correlation between FGF23 and urinary Mg^{2+} concentration (as seen in Figure 2).

Next, we explored the relationship between FEMg and FGF23 after adjustment for potential confounders. In crude linear regression, FGF23 accounts for 37.4% of the variation in FEMg, with an adjusted R^2 of 0.135 ($p<0.001$). After adjustment for age, sex and eGFR (model 1) there was an overall adjusted R^2 of 0.184 (p=0.022). In a multiple adjusted linear regression model including age, sex, eGFR, Klotho, 25-hydroxyvitamin D, PTH, there was an overall adjusted R^2 of 0.189, (p=0.059). In model 3 (adjusted for use of medication) there was an adjusted R^2 of 0.179 (p=0.016), while model 4 showed an overall adjusted R^2 of 0.174 (p=0.032). In the adjustment for medication and comorbidities (model 5) there was an adjusted R^2 of 0.164 (p=0.029), while in the adjustment for fractional excretions (model 7) there was an adjusted R^2 of 0.203 (p=0.080). The adjustment for the Klotho-FGF23 axis (model 6) showed an overall adjusted R^2 of 0.197 (p=0.046). Supplementary Tables 3, 4 show that the models in Table 2 were not over-adjusted, using the variance inflation factor and two linear regression models.

3.4 Subgroup analysis by different eGFR and FGF23 stages

To investigate if the associations to FEMg are consistent over the full spectra of FGF23 concentrations and eGFR observed in our cohort we performed sub-group analysis in the different strata of FGF23 and eGFR (shown in Figure 3). The results show that, in the FGF23 strata, the association between FEMg and FGF23 is significant only in the fourth quartile, while the association between FEMg and eGFR is significant in the first, third and fourth quartile. The division in eGFR quartiles demonstrated that FEMg correlates only in the first quartile with FGF23 (in Table 3). The pattern of FEMg is similar throughout FGF23 and eGFR strata – it decreases with the increase of eGFR and it simultaneously increases with FGF23 (Figure 3). Supplementary Figures 2, 3 explore Klotho in CKD using similar analysis.

4 Discussion

In this study of 198 non-dialysis CKD patients, we demonstrate that FGF23 is positively associated with FEMg independently of renal function and other potential confounders. This finding is consistent with the hypothesis that FGF23 may influence renal magnesium handling in patients with decreased renal function, and/or vice versa (23, 33, 34, 43).

The role of FGF23 in CKD and the associated cardiovascular disease has been the subject of many studies over the last decade (18, 39, 44, 45). As a master regulator of phosphate (46), it is well established that the increase in FGF23 contributes to maintaining phosphate homeostasis in early stages of CKD, and as such protects against vascular calcification. This is evidenced by studies (47) in which FGF23 neutralizing antibodies were given to rats with CKD, where the reduction of FGF23 resulted in hyperphosphatemia and significantly

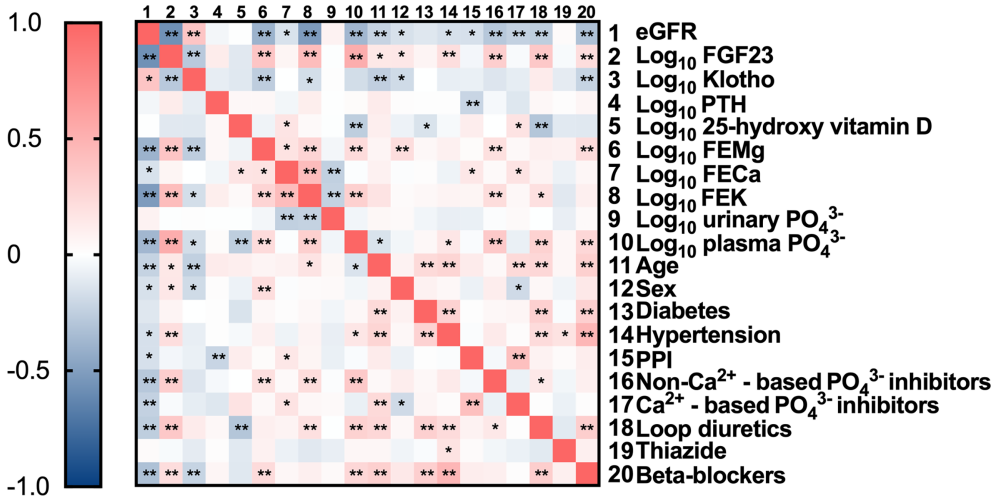

FIGURE 2
Correlation matrix with relevant parameters included. Data are the outcomes of bivariate analysis; *Correlation is significant at the 0.05 level; **Correlation is significant at the 0.01 level.

10.3389/fendo.2022.1046392

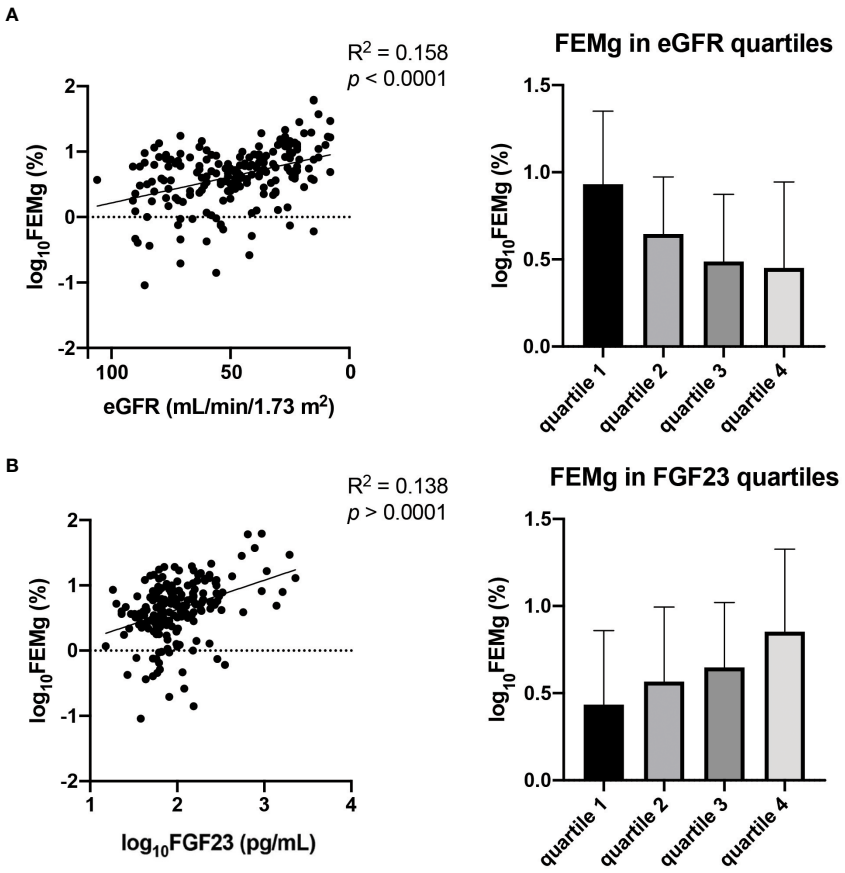

FIGURE 3
Association between eGFR and FEMg **(A)** in comparison with the association of FGF23 and FEMg **(B)**. Data are the outcomes of simple linear regression analysis.

worsen vascular calcification. However, it is still debated whether the dramatically increased FGF23 concentrations commonly observed in late-stage CKD patients have direct and detrimental effects on the cardiovascular system.

Similarly, the role of Mg^{2+} homeostasis in CKD patients has received increasing attention over the last few years, especially in the context of vascular calcification and other cardiovascular morbidities (17, 20, 48). There have been some indications that

TABLE 3 Subgroup analysis of FEMg associated with FGF23 or eGFR in FGF23 or eGFR quartiles.

		FGF23		eGFR	
	Quartile range	R^2	*p*-value	R^2	*p*-value
FGF23 (pg/mL)					
quartile 1	15.1-57	0.013	0.932	-0.379	0.008
quartile 2	58-81	-0.162	0.252	-0.069	0.627
quartile 3	83-152	-0.035	0.810	-0.310	0.029
quartile 4	154-2307	0.340	0.018	-0.324	0.025
eGFR (mL/min/1.73 m^2)					
quartile 1	8-30	0.300	0.035	-0.260	0.068
quartile 2	31-47	0.154	0.272	-0.233	0.093
quartile 3	48-66	0.155	0.310	-0.140	0.360
quartile 4	67-106	0.122	0.400	-0.162	0.262

Mg^{2+} is involved in controlling FGF23 levels (38, 39), and that FGF23-Klotho signaling might influence renal magnesium handling. A potential mechanism for such relationship might be that FGF23-Klotho signaling in the DCT controls TRPM6 expression and/or activity. This is supported by the co-expression of Klotho and TRPM6 in distal tubular cells (49, 50), and by the fact that the renal expression of Klotho and TRPM6 are strongly correlated in healthy individuals as well as in patients with diabetic nephropathy (51).

Although a few studies have reported on associations between FGF23 and Mg^{2+} in animals or in patients with ESRD, no studies have explored their potential relationship in human non-dialysis CKD (40, 41). In the present study we report a direct and independent association between FGF23 and FEMg, whereas there are no or only weak associations to plasma or urinary Mg^{2+}. This is supportive of the hypothesis that FGF23 may participate in controlling renal Mg^{2+} reabsorption, to maintain Mg^{2+} homeostasis as renal function declines (23, 33, 34, 43). The plasma Mg^{2+} levels were stable across all quartiles, which indicates a sustained intestinal absorption of Mg^{2+} due to dietary Mg^{2+} intake (4, 52). However, the cross-sectional nature of this study restricts us from drawing conclusions about any possible causality behind the observed relationship between FEMg and FGF23.

Importantly, as the hormonal regulation of Mg^{2+} handling is incompletely understood, there could be confounders that we did not consider in our models and that might explain the observed relationship, which could provide a potential mechanism and explanation to the observed associations.

In conclusion, our study demonstrates that FGF23 is positively associated with FEMg in patients with CKD, independently of renal function and other potential confounders. These finding warrants further investigations of the FGF23-Klotho-Pi-Mg^{2+} axis in patients with CKD and vascular calcification.

Data availability statement

The data that support the findings of this study are not publicly available due to their containing information that could compromise the privacy of research participants, but are available from KaroKidney upon reasonable request.

Ethics statement

The study received ethical approval from the Ethical Review Board, Stockholm, Sweden (DNR 2010/579-31), and informed consent was obtained from all participants.

Author contributions

TG, HO, and JH were involved in the conception and design of the study. TG performed experiments and statistical analysis. AWi, PB, AWe, AB and HO created the biobank. TG, MZ, HO and JH drafted the manuscript. TG, MZ, HX, AWi, PB, AWe, AB, HO and JH critically revised the manuscript. TG, MZ, AWi, PB, AWe, AB, HX, HO and JH approved the final version of the manuscript. All authors contributed to the article and approved the submitted version.

Funding

This work was supported by grants from Region Stockholm (ALF), CIMED, the Swedish Kidney Foundation and Radboud Institute for Molecular Life Sciences.

Acknowledgments

The authors would like to thank Wouter van Megen for his valuable advice when processing the samples.

Conflict of interest

The authors declare that the research was conducted in the absence of any commercial or financial relationships that could be construed as a potential conflict of interest.

Publisher's note

Supplementary material

The Supplementary Material for this article can be found online at: https://www.frontiersin.org/articles/10.3389/fendo.2022.1046392/full#supplementary-material

References

1. de Baaij JH, Hoenderop JG, Bindels RJ. Magnesium in man: Implications for health and disease. *Physiol Rev* (2015) 95(1):1–46. doi: 10.1152/physrev.00012.2014

2. Cao G, Hoenderop JG, Bindels RJ. Insight into the molecular regulation of the epithelial magnesium channel Trpm6. *Curr Opin Nephrol Hypertens* (2008) 17 (4):373–8. doi: 10.1097/MNH.0b013e328303e184

3. Dai LJ, Ritchie G, Kerstan D, Kang HS, Cole DE, Quamme GA. Magnesium transport in the renal distal convoluted tubule. *Physiol Rev* (2001) 81(1):51–84. doi: 10.1152/physrev.2001.81.1.51

4. Lameris AL, Nevalainen PI, Reijnen D, Simons E, Eygensteyn J, Monnens L, et al. Segmental transport of Ca(2)(+) and Mg(2)(+) along the gastrointestinal tract. *Am J Physiol Gastrointest Liver Physiol* (2015) 308(3):G206–16. doi: 10.1152/ajpgi.00093.2014

5. Gong Y, Renigunta V, Himmerkus N, Zhang J, Renigunta A, Bleich M, et al. Claudin-14 regulates renal ca(+)(+) transport in response to casr signalling *Via* a novel microrna pathway. *EMBO J* (2012) 31(8):1999–2012. doi: 10.1038/emboj.2012.49

6. Curry JN, Yu ASL. Magnesium handling in the kidney. *Adv Chronic Kidney Dis* (2018) 25(3):236–43. doi: 10.1053/j.ackd.2018.01.003

7. Glaudemans B, van der Wijst J, Scola RH, Lorenzoni PJ, Heister A, van der Kemp AW, et al. A missense mutation in the Kv1.1 voltage-gated potassium channel-encoding gene Kcna1 is linked to human autosomal dominant hypomagnesemia. *J Clin Invest* (2009) 119(4):936–42. doi: 10.1172/JCI36948

8. Ter Braake AD, Smit AE, Bos C, van Herwaarden AE, Alkema W, van Essen HW, et al. Magnesium prevents vascular calcification in klotho deficiency. *Kidney Int* (2020) 97(3):487–501. doi: 10.1016/j.kint.2019.09.034

9. Jha V, Garcia-Garcia G, Iseki K, Li Z, Naicker S, Plattner B, et al. Chronic kidney disease: Global dimension and perspectives. *Lancet* (2013) 382(9888):260–72. doi: 10.1016/S0140-6736(13)60687-X

10. Guerin AP, London GM, Marchais SJ, Metivier F. Arterial stiffening and vascular calcifications in end-stage renal disease. *Nephrol Dial Transplant* (2000) 15 (7):1014–21. doi: 10.1093/ndt/15.7.1014

11. Floege J, Ketteler M. Vascular calcification in patients with end-stage renal disease. *Nephrol Dial Transplant* (2004) 19(Suppl 5):V59–66. doi: 10.1093/ndt/gfh1058

12. Rodelo-Haad C, Pendon-Ruiz de Mier MV, Diaz-Tocados JM, Martin-Malo A, Santamaria R, Munoz-Castaneda JR, et al. The role of disturbed mg homeostasis in chronic kidney disease comorbidities. *Front Cell Dev Biol* (2020) 8:543099. doi: 10.3389/fcell.2020.543099

13. Coburn JW, Popovtzer MM, Massry SG, Kleeman CR. The physicochemical state and renal handling of divalent ions in chronic renal failure. *Arch Intern Med* (1969) 124(3):302–11. doi: 10.1001/archinte.1969.00300190042007

14. Mikolasevic I, Milic S, Stimac D, Zaputovic L, Lukenda Zanko V, Gulin T, et al. Is there a relationship between hypomagnesemia and proton-pump inhibitors in patients on chronic hemodialysis? *Eur J Intern Med* (2016) 30:99–103. doi: 10.1016/j.ejim.2016.01.026

15. Nakashima A, Ohkido I, Yokoyama K, Mafune A, Urashima M, Yokoo T. Proton pump inhibitor use and magnesium concentrations in hemodialysis patients: A cross-sectional study. *PloS One* (2015) 10(11):e0143656. doi: 10.1371/journal.pone.0143656

16. Celi LA, Scott DJ, Lee J, Nelson R, Alper SL, Mukamal KJ, et al. Association of hypermagnesemia and blood pressure in the critically ill. *J Hypertens* (2013) 31 (11):2136–41. doi: 10.1097/HJH.0b013e3283642f18

17. Azem R, Daou R, Bassil E, Anvari EM, Taliercio JJ, Arrigain S, et al. Serum magnesium, mortality and disease progression in chronic kidney disease. *BMC Nephrol* (2020) 21(1):49. doi: 10.1186/s12882-020-1713-3

18. Ter Braake AD, Shanahan CM, de Baaij JHF. Magnesium counteracts vascular calcification: Passive interference or active modulation? *Arterioscler Thromb Vasc Biol* (2017) 37(8):1431–45. doi: 10.1161/ATVBAHA.117.309182

19. Turgut F, Kanbay M, Metin MR, Uz E, Akcay A, Covic A. Magnesium supplementation helps to improve carotid intima media thickness in patients on hemodialysis. *Int Urol Nephrol* (2008) 40(4):1075–82. doi: 10.1007/s11255-008-9410-3

20. Massy ZA, Drueke TB. Magnesium and outcomes in patients with chronic kidney disease: Focus on vascular calcification, atherosclerosis and survival. *Clin Kidney J* (2012) 5(Suppl 1):i52–61. doi: 10.1093/ndtplus/sfr167

21. Leenders NHJ, Bos C, Hoekstra T, Schurgers LJ, Vervloet MG, Hoenderop JGJ. Dietary magnesium supplementation inhibits abdominal vascular calcification in an experimental animal model of chronic kidney disease. *Nephrol Dial Transplant* (2022) 37(6):1049-58. doi: 10.1093/ndt/gfac026

22. Xu C, Smith ER, Tiong MK, Ruderman I, Toussaint ND. Interventions to attenuate vascular calcification progression in chronic kidney disease: A systematic review of clinical trials. *J Am Soc Nephrol* (2022) 33(5):1011–32. doi: 10.1681/ASN.2021101327

23. Xu H, Hashem A, Witasp A, Mencke R, Goldsmith D, Barany P, et al. Fibroblast growth factor 23 is associated with fractional excretion of sodium in patients with chronic kidney disease. *Nephrol Dial Transplant* (2019) 34(12):2051–7. doi: 10.1093/ndt/gfy315

24. Vervloet MG. Fgf23 measurement in chronic kidney disease: What is it really reflecting? *Clin Chim Acta* (2020) 505:160–6. doi: 10.1016/j.cca.2020.03.013

25. Larsson T, Nisbeth U, Ljunggren O, Juppner H, Jonsson KB. Circulating concentration of fgf-23 increases as renal function declines in patients with chronic kidney disease, but does not change in response to variation in phosphate intake in healthy volunteers. *Kidney Int* (2003) 64(6):2272–9. doi: 10.1046/j.1523-1755.2003.00328.x

26. Prie D, Friedlander G. Reciprocal control of 1,25-dihydroxyvitamin d and Fgf23 formation involving the Fgf23/Klotho system. *Clin J Am Soc Nephrol* (2010) 5(9):1717–22. doi: 10.2215/CJN.02680310

27. Liu S, Tang W, Zhou J, Stubbs JR, Luo Q, Pi M, et al. Fibroblast growth factor 23 is a counter-regulatory phosphaturic hormone for vitamin d. *J Am Soc Nephrol* (2006) 17(5):1305–15. doi: 10.1681/ASN.2005111185

28. Ben-Dov IZ, Galitzer H, Lavi-Moshayoff V, Goetz R, Kuro-o M, Mohammadi M, et al. The parathyroid is a target organ for Fgf23 in rats. *J Clin Invest* (2007) 117(12):4003–8. doi: 10.1172/JCI32409

29. Olauson H, Lindberg K, Amin R, Sato T, Jia T, Goetz R, et al. Parathyroid-specific deletion of klotho unravels a novel calcineurin-dependent Fgf23 signaling pathway that regulates pth secretion. *PloS Genet* (2013) 9(12):e1003975. doi: 10.1371/journal.pgen.1003975

30. Isakova T, Wahl P, Vargas GS, Gutierrez OM, Scialla J, Xie H, et al. Fibroblast growth factor 23 is elevated before parathyroid hormone and phosphate in chronic kidney disease. *Kidney Int* (2011) 79(12):1370–8. doi: 10.1038/ki.2011.47

31. Galitzer H, Ben-Dov IZ, Silver J, Naveh-Many T. Parathyroid cell resistance to fibroblast growth factor 23 in secondary hyperparathyroidism of chronic kidney disease. *Kidney Int* (2010) 77(3):211–8. doi: 10.1038/ki.2009.464

32. Komaba H, Fukagawa M. Fgf23-parathyroid interaction: Implications in chronic kidney disease. *Kidney Int* (2010) 77(4):292–8. doi: 10.1038/ki.2009.466

33. Fragoso A, Silva AP, Gundlach K, Buchel J, Neves PL. Magnesium and fgf-23 are independent predictors of pulse pressure in pre-dialysis diabetic chronic kidney disease patients. *Clin Kidney J* (2014) 7(2):161–6. doi: 10.1093/ckj/sfu003

34. Musgrove J, Wolf M. Regulation and effects of Fgf23 in chronic kidney disease. *Annu Rev Physiol* (2020) 82:365–90. doi: 10.1146/annurev-physiol-021119-034650

35. Cha SK, Hu MC, Kurosu H, Kuro-o M, Moe O, Huang CL. Regulation of renal outer medullary potassium channel and renal k(+) excretion by klotho. *Mol Pharmacol* (2009) 76(1):38–46. doi: 10.1124/mol.109.055780

36. Imura A, Tsuji Y, Murata M, Maeda R, Kubota K, Iwano A, et al. Alpha-klotho as a regulator of calcium homeostasis. *Science* (2007) 316(5831):1615–8. doi: 10.1126/science.1135901

37. Hu MC, Kuro-o M, Moe OW. Renal and extrarenal actions of klotho. *Semin Nephrol* (2013) 33(2):118–29. doi: 10.1016/j.semnephrol.2012.12.013

38. Matsuzaki H, Katsumata S, Maeda Y, Kajita Y. Changes in circulating levels of fibroblast growth factor 23 induced by short-term dietary magnesium deficiency in rats. *Magnes Res* (2016) 29(2):48–54. doi: 10.1684/mrh.2016.0401

39. Matsuzaki H, Kajita Y, Miwa M. Magnesium deficiency increases serum fibroblast growth factor-23 levels in rats. *Magnes Res* (2013) 26(1):18–23. doi: 10.1684/mrh.2013.0331

40. van den Broek DHN, Chang YM, Elliott J, Jepson RE. Prognostic importance of plasma total magnesium in a cohort of cats with azotemic chronic kidney disease. *J Vet Intern Med* (2018) 32(4):1359–71. doi: 10.1111/jvim.15141

41. Iguchi A, Watanabe Y, Iino N, Kazama JJ, Iesato H, Narita I. Serum magnesium concentration is inversely associated with fibroblast growth factor 23 in haemodialysis patients. *Nephrol (Carlton)* (2014) 19(11):667–71. doi: 10.1111/nep.12287

42. Ayuk J, Gittoes NJ. Contemporary view of the clinical relevance of magnesium homeostasis. *Ann Clin Biochem* (2014) 51(Pt 2):179–88. doi: 10.1177/0004563213517628

43. Felsenfeld AJ, Levine BS, Rodriguez M. Pathophysiology of calcium, phosphorus, and magnesium dysregulation in chronic kidney disease. *Semin Dial* (2015) 28(6):564–77. doi: 10.1111/sdi.12411

44. Olauson H, Qureshi AR, Miyamoto T, Barany P, Heimburger O, Lindholm B, et al. Relation between serum fibroblast growth factor-23 level and mortality in incident dialysis patients: Are gender and cardiovascular disease confounding the

relationship? *Nephrol Dial Transplant* (2010) 25(9):3033–8. doi: 10.1093/ndt/gfq191

45. Sakaguchi Y, Fujii N, Shoji T, Hayashi T, Rakugi H, Isaka Y. Hypomagnesemia is a significant predictor of cardiovascular and non-cardiovascular mortality in patients undergoing hemodialysis. *Kidney Int* (2014) 85(1):174–81. doi: 10.1038/ki.2013.327

46. Bacchetta J, Bardet C, Prie D. Physiology of Fgf23 and overview of genetic diseases associated with renal phosphate wasting. *Metabolism* (2020) 103S:153865. doi: 10.1016/j.metabol.2019.01.006

47. Shalhoub V, Shatzen EM, Ward SC, Davis J, Stevens J, Bi V, et al. Fgf23 neutralization improves chronic kidney disease-associated hyperparathyroidism yet increases mortality. *J Clin Invest* (2012) 122(7):2543–53. doi: 10.1172/JCI61405

48. Massy ZA, Drueke TB. Magnesium and cardiovascular complications of chronic kidney disease. *Nat Rev Nephrol* (2015) 11(7):432–42. doi: 10.1038/nrneph.2015.74

49. Chen L, Chou CL, Knepper MA. A comprehensive map of mrnas and their isoforms across all 14 renal tubule segments of mouse. *J Am Soc Nephrol* (2021) 32 (4):897-912. doi: 10.1681/ASN.2020101406

50. He B, Chen P, Zambrano S, Dabaghie D, Hu Y, Moller-Hackbarth K, et al. Single-cell rna sequencing reveals the mesangial identity and species diversity of glomerular cell transcriptomes. *Nat Commun* (2021) 12(1):2141. doi: 10.1038/s41467-021-22331-9

51. Levin A, Reznichenko A, Witasp A, Liu P, Greasley PJ, Sorrentino A, et al. Novel insights into the disease transcriptome of human diabetic glomeruli and tubulointerstitium. *Nephrol Dial Transplant* (2020) 35(12):2059–72. doi: 10.1093/ndt/gfaa121

52. Fine KD, Santa Ana CA, Porter JL, Fordtran JS. Intestinal absorption of magnesium from food and supplements. *J Clin Invest* (1991) 88(2):396–402. doi: 10.1172/JCI115317

frontiers | Frontiers in Endocrinology

TYPE Mini Review
PUBLISHED 23 March 2023
DOI 10.3389/fendo.2023.1146868

OPEN ACCESS

EDITED BY
Andrea Galassi,
Santi Paolo e Carlo Hospital, Italy

REVIEWED BY
Renqing Zhao,
Yangzhou University, China

*CORRESPONDENCE
Limy Wong
limywong@gmail.com

SPECIALTY SECTION
This article was submitted to Renal Endocrinology, a section of the journal Frontiers in Endocrinology

RECEIVED 18 January 2023
ACCEPTED 14 March 2023
PUBLISHED 23 March 2023

CITATION
Wong L and McMahon LP (2023) Crosstalk between bone and muscle in chronic kidney disease.
Front. Endocrinol. 14:1146868.
doi: 10.3389/fendo.2023.1146868

Crosstalk between bone and muscle in chronic kidney disease

Limy Wong [1,2]* and Lawrence P. McMahon [1,2]

[1]Department of Renal Medicine, Monash University Eastern Health Clinical School, Box Hill, VIC, Australia, [2]Department of Renal Medicine, Eastern Health, Box Hill, VIC, Australia

With increasing life expectancy, the related disorders of bone loss, metabolic dysregulation and sarcopenia have become major health threats to the elderly. Each of these conditions is prevalent in patients with chronic kidney disease (CKD), particularly in more advanced stages. Our current understanding of the bone-muscle interaction is beyond mechanical coupling, where bone and muscle have been identified as interrelated secretory organs, and regulation of both bone and muscle metabolism occurs through osteokines and myokines *via* autocrine, paracrine and endocrine systems. This review appraises the current knowledge regarding biochemical crosstalk between bone and muscle, and considers recent progress related to the role of osteokines and myokines in CKD, including modulatory effects of physical exercise and potential therapeutic targets to improve musculoskeletal health in CKD patients.

KEYWORDS

osteokines, myokines, chronic kidney disease, crosstalk, bone, muscle

Introduction

Chronic kidney disease (CKD) has a complex relationship with ageing, where the CKD phenotype provides an accelerated model of ageing through various mechanisms while ageing also hastens the progression of kidney disease. Patients affected by CKD experience profound musculoskeletal functional decline at a younger age, which is compounded by concurrent losses in bone and skeletal muscle mass, leading to reduced mobility and excessively high rates of falls and fractures, the effects of which are often life-limiting.

Disturbances in mineral and bone metabolism in CKD are conventionally jointly referred to as CKD-Mineral Bone Disorder (CKD-MBD), and comprises abnormalities in the homeostasis of calcium, phosphorus, vitamin D and parathyroid hormone (PTH); abnormalities of bone turnover, mineralisation or volume; and vascular or soft tissue calcification (1). Despite earlier research and vigorous exploration of therapeutic strategies in managing skeletal health focusing on bone and mineral abnormalities, a disturbing limitation in patient care persists, particularly in those with advanced CKD and/or who are dialysis-dependent. Meaningful clinical and biological targets are lacking in this population, resulting in management uncertainty for the prevention of bone loss and fractures.

Furthermore, it is increasingly recognised that sarcopenia plays a detrimental role in musculoskeletal health in CKD. Sarcopenia is a condition characterised by a reduction in muscle mass, strength and/or performance that accrues over many years and is associated with ageing (2). However, it is now recognised that sarcopenia begins earlier in life with many contributing factors beyond ageing alone. CKD patients suffer severe skeletal muscle wasting, and again this is particularly evident in its advanced stages. There is no pharmacological treatment available at present to reverse or halt the progression of muscle atrophy, although aerobic and resistance-training exercise and nutritional interventions have been shown to be of some benefit (3–5).

Our understanding of the interaction between bone and skeletal muscle now exceeds the concept of purely mechanical coupling, with evidence that these tissues communicate at a biomolecular level (6). Bone and muscle have been shown to be interrelated secretory organs, which produce osteokines (bone-derived factors) and myokines (muscle-derived factors) respectively. Each of these is important in regulating bone and muscle metabolism through autocrine, paracrine and endocrine signalling. The growing knowledge about the crosstalk between bone and muscle, and the likely influence of exercise on both tissues has important implications for clinical practice and introduces potential therapeutic targets to improve bone and muscle parameters, and consequently, the patient's overall health and wellbeing. However, the biochemical relationship between bone and muscle in tandem is less well understood in the uraemic milieu.

This review presents an in-depth discussion about the known endocrine and other crosstalk between bone and muscle, the modulatory effects of physical exercise on these tissues, potential therapeutic targets and, lastly, important research questions in this field.

Bone fragility in patients with chronic kidney disease

In the general population, osteoporosis is defined as a reduction in bone density; while bone disorders in CKD are more complex. The diagnosis and management of bone disorders in CKD is challenging for several reasons: (i) heterogeneous changes in bone tissue other than osteoporosis that could compromise bone strength such as osteomalacia, osteitis fibrosa cystica, adynamic bone disease (with inadequate bone turnover) and mixed bone lesions; (ii) the inability of dual-energy X-ray absorptiometry to provide meaningful details regarding underlying bone mineral density; (iii) inaccuracy of serum-derived bone turnover markers due to reduced renal clearance and (iv) infrequent use of bone biopsy, the gold standard determinant of bone pathology, due to its restricted availability, invasive nature, and limited interpretative expertise (7). Dialysis-dependent patients have a 4- to 14-fold higher risk of developing fractures than the healthy general population, a risk which extends to those with an estimated glomerular filtration rate (eGFR) between 15 to 60 mL/min/1.73m^2 (8–12).

Despite early research efforts to identify better management strategies, the incidence of fractures has continued to rise in recent years, with no therapeutic agent yet approved for patients with kidney-related bone disease. Agents that have been targeted include vitamin D analogues and calcimimetics to suppress PTH and improve bone remodelling, thus potentially reducing fracture risk, and antiresorptive and osteoanabolic agents. The latter are approved for osteoporosis in the general population and have been administered off-label in CKD Stage 3B-5 high-risk patients. However, their use has been limited due to the lack of large-scale clinical trials and concern regarding their contribution to further kidney dysfunction and adynamic bone disease, which has now evolved as the predominant form of renal osteodystrophy associated with poor outcomes (13, 14).

Muscle health in patients with chronic kidney disease

Skeletal muscle is the largest tissue in the human body, accounting for about 40-50% of body mass (15). It is imperative for gait and posture and also functions as an endocrine organ. Maximal muscle mass is achieved during young adulthood but after the age of 50, muscle loss occurs at a rate of ~1-2% per annum (16). Sarcopenia, a recently recognised disease entity, is common in older-aged adults but can also occur earlier in life from systemic illnesses, particularly conditions that trigger an inflammatory response such as CKD and malignancy. Sarcopenia is thus prevalent in the CKD population and is associated with an increased risk of hospitalisation and mortality in both dialysis and non-dialysis dependent patients. Low skeletal muscle mass (determined by radiological measures) is associated both with a higher waitlist mortality among kidney transplant candidates and an increase hospital readmission rate within the first 30 days after kidney transplant discharge (17, 18).

Several risk factors have been proposed to contribute to the development of sarcopenia in CKD including ageing, chronic inflammation, hormonal changes/resistance, metabolic acidosis, a more sedentary lifestyle and poor nutritional status leading to an imbalance between protein synthesis and degradation. We recently reported that the differentially expressed genes and proteins in skeletal muscle of CKD subjects belong to 8 major biological and signalling pathways, namely apoptosis, autophagy, inflammation, insulin/insulin-like growth factor 1 (IGF1) signalling, lipid metabolism, mitochondrial function, muscle cell growth and differentiation, and protein turnover (19).

Bone metabolism and remodelling

The overall composition of bone tissue is altered in CKD due to abnormal systemic mineral metabolism and bone remodelling. Cells within bone include osteocytes (90-95%), osteoblasts (5%), and osteoclasts (1%) (20). It is a dynamic tissue and its structural integrity is maintained by bone remodelling, consisting of coordinated actions of the three cell types in a process tightly regulated by both local and systemic factors (21). The presence of the myogenic interleukin-6 (IL-6) activates the secretion of

osteoblast and osteocyte-induced receptor activator of nuclear factor-κB (RANK), which drives osteoclastogenesis (22). This also results in an increased expression of RANKL, which binds to its receptor and triggers a cascade of signalling events that induce osteoclast differentiation, activation and survival. By contrast, osteoprotegerin (OPG), a soluble decoy receptor, binds RANKL to prevent the latter binding to RANK, thereby inhibiting osteoclastogenesis (23) and restraining bone loss. Dysregulation of the RANK-RANKL-OPG axis can lead to osteoporosis. Studies investigating RANKL levels in CKD patients have demonstrated conflicting findings (24–26), whereas OPG concentrations have consistently been reported to be higher in haemodialysis patients (24, 27, 28), which could reflect a compensatory protective mechanism to moderate bone remodelling.

Osteokines and muscle metabolism

The discovery that osteocytes produced fibroblast growth factor 23 (FGF23), which circulates in different forms targeting the kidney and other organs including muscle, led to the recognition of bone as an endocrine organ. The list of osteokines has since continued to expand. Herein, we describe several osteokines that have been demonstrated to have regulatory effects on muscles (see Table 1).

Fibroblast growth factor 23

FGF23 was first discovered in 2000 as a cause of autosomal dominant hypophosphataemic rickets (29). It is part of a superfamily of 22 peptides grouped into 7 subfamilies. FGF23 is mainly secreted by osteocytes and osteoblasts. It downregulates the luminal expression of sodium/phosphorus co-transporters in the proximal renal tubules to stimulate phosphaturia (30). FGF23 also suppresses the production of 1,25$(OH)_2$Vitamin D by inhibiting 1-alpha hydroxylase, leading to phosphate wasting (31) and consequently poor bone mineralisation. The canonical FGF23 signalling pathway requires the obligatory co-receptor alpha klotho (α-KL), a transmembrane protein with extracellular glucuronidase activity, for binding to the first of four tissue-specific fibroblast growth factor receptors (FGFR), FGFR1 (32). However, some FGF23 signalling occurs independent of α-KL and is referred to as non-canonical FGF23 signalling, through binding and activation of other receptors: FGFR3/FGFR4/calcineurin/nuclear factor of activated T-cells (33), mainly in the setting of markedly elevated circulating FGF23 levels. Effects include distinct changes in several organs. Treatment of neonatal rat ventricular myocytes for 48 hours with varying concentrations of FGF23 induced morphometric hypertrophy in a similar extent to treatment with fibroblast growth factor 2 (FGF2). Moreover, *in vivo* experiments using both intravenous and intramyocardial injection of FGF23 showed induction of left ventricular hypertrophy in non-CKD mice (34).

What effects FGF23 has *in vivo*, with or without α-KL, remains uncertain. Higher serum levels have been shown to be independently associated with pre-frailty and frailty in a large

TABLE 1 Biochemical crosstalk between bone and skeletal muscle.

Myokines	Effect on muscle	Effect on bone formation	Effect on bone resorption	Effect from exercise	Osteokines	Effect on bone formation	Effect on bone resorption	Effect on muscle	Effect from exercise
Myostatin	●	●	●	●	FGF23	○	○	○	○
Irisin	●	●	○	●	Osteocalcin	○	○	○	●
IL-6	●	○	●	●	RANK/RANKL	●	●	●	○
IL-15	●	○	●	●	OPG	●	●	●	●
FGF2	●	●	●	●	Sclerostin	●	●	●	○
IGF-1	●	●	●	●	IGF-1	●	●	●	●

FGF2, fibroblast growth factor 2; FGF23, fibroblast growth factor 23; IGF-1, insulin-like growth factor-1; IL-6, interleukin-6; IL-15, interleukin-15; OPG, osteoprotegerin; RANK, receptor activator of nuclear factor-κB; RANKL, receptor activator of nuclear factor-κB ligand.
Red filled circles indicate inhibition/downregulation, blue filled circles indicate stimulation/upregulation and empty circles indicate uncertain effects or conflicting findings based on current literature.

cohort of community-dwelling elderly inhabitants (35). Similarly, as part of the SPRINT trial, Jovanovich et al. reported that FGF23 was associated with increased frailty among older adults with CKD (36), suggesting that FGF23 might have more diverse negative biological effects. Both FGF23 and α-KL were previously shown to inhibit differentiation of cultured skeletal muscle cells through downregulation of insulin/IGF-1 signalling (37). FGF23 was also found to induce premature senescence of human skeletal muscle mesenchymal stem cells *via* the p53/p21 pathway in an α-KL-independent manner, supporting its inhibitory effects (38). However, plasma FGF23 concentrations have also been reported to be positively correlated with muscle mass indices in a small haemodialysis cohort (39). As a potential therapeutic target, exercise endurance was found to improve significantly in C57BL/6J mice following exogenous administration of recombinant FGF23 (40). However, Avin et al. found that FGF23 did not influence C2C12 myoblast proliferation and differentiation and *ex-vivo* FGF23 treatment did not alter soleus contractility (41). Thus, the regulatory effect of FGF23 on skeletal muscle remains unresolved and further research is required to address this question.

Osteocalcin

Osteocalcin (OCN) is the most abundant non-collagenous osteoblast-derived protein. There are two main forms of OCN in the circulation: γ–carboxylated and uncarboxylated (uOCN). Considered to be the active form, the latter has been shown to be involved in the regulation of insulin secretion and sensitivity (42), glucose metabolism (43), male fertility (44) and brain function (45). Although the data from *in vitro* and *in vivo* studies are controversial (46–49), OCN is thought to play an important role in bone remodelling by modulating osteoblast and osteoclast activity. High levels of circulating OCN and uOCN were observed in CKD patients (50–52), potentially due to increased bone metabolism, decreased renal clearance or both, with progression correlating with serum intact PTH and alkaline phosphatase (ALP) (50, 51), most probably reflecting the severity of the underlying bone disorder.

OCN was also discovered to promote muscle uptake and utilisation of glucose and fatty acids. $Ocn^{-}/^{-}$ mice were found to have impaired exercise capacity, which was rescued by exogenous OCN administration (53). OCN was also shown to be a major regulator of IL-6 expression in the muscle during exercise and the rise in circulating IL-6 levels was proposed to originate from muscle, eventually forming a feed-forward axis to amplify adaptation to exercise (53). Moreover, using mice lacking OCN ($Ocn^{-}/^{-}$), its receptor in all cells ($Gprc6a^{-}/^{-}$) and specifically in myofibres ($Gprc6a_{Mck}^{-}/^{-}$), Mera et al. showed that OCN signalling is essential in maintaining muscle mass by promoting protein synthesis in myotubes (54). uOCN was later found to enhance C2C12 myoblast cell proliferation and differentiation through activation of the PI3k/Akt, p38 MAPK and GPRC6A-ERK1/2 signalling pathways (55). Taken together, these findings strongly support that OCN, especially its active form, plays an important role in regulating muscle mass and might potentially be a therapeutic target in sarcopenia. However, recent studies have found to be contrary. Using a newly generated *Ocn*-deficient mouse model by deleting *Bglap* and *Bglap2*, Moriishi et al. showed that OCN played no role in bone formation or resorption, glucose metabolism, testosterone synthesis, or muscle mass (56). Similarly, Diegel et al. generated *Ocn*-deficient mouse using a CRISPR/Cas9-mediated gene editing tool and found that these mice displayed normal bone mass, serum glucose and fertility (57). The apparent discrepancies between studies remain inexplicable and additional efforts are required to confirm these findings.

Receptor activator of nuclear factor-κB/ Receptor activator of nuclear factor-κB ligand/Osteoprotegerin

RANK and RANKL are expressed in osteoclasts and osteoblasts respectively, as well as in skeletal muscle, and their interaction activates the nuclear factor-κB (NF-κB) signalling pathway, a key transcription factor inducing the expression of various proinflammatory genes, which can inhibit myogenic differentiation and activate the local ubiquitin proteasome system, ultimately leading to muscle atrophy (58). In addition, RANK has been shown to regulate calcium storage and muscle performance during denervation (59). Both genetic deletion of muscle RANK and short-term anti-RANKL treatment were shown to improve muscle integrity and strength of young dystrophic *mdx* mice (60). Hamoudi et al. demonstrated that anti-RANKL treatment inhibited NF-κB signalling and increased the proportion of M2 macrophages in dystrophic mice, thus reducing muscle inflammation and improving its mechanical properties (61). Similar findings were also observed in young dystrophic *mdx* mice when treated with recombinant full length OPG-Fc, a decoy receptor for RANKL (62). Furthermore, postmenopausal women who were treated with denosumab, a neutralising antibody against RANKL, for an average duration of 3 years were found to have improved appendicular lean mass and handgrip strength and these gains were absent in the bisphosphate treatment group (63). Altogether, it seems that the RANK-RANKL-OPG axis plays a pivotal role in bone and muscle metabolism. Given that coexistence of osteoporosis and sarcopenia is prevalent in the elderly population, the potential benefit of anti-RANKL treatment in possibly mitigating skeletal muscle atrophy while enhancing bone mechanical properties should be further investigated. However, any relationship between higher OPG concentrations (and OPG/RANKL ratio) and sarcopenia in CKD is yet to be determined.

Sclerostin

Sclerostin is primarily secreted by mature osteocytes (64) and is a negative regulator of bone formation *via* inhibition of the Wnt/β-catenin pathway through binding to Wnt coreceptors, low-density lipoprotein receptor-related proteins 5 and 6 (65). Wnt-3a was also found to promote C2C12 myoblast differentiation through upregulation of *MyoD* and *Myogenin* while sclerostin treatment

inhibited the effect of Wnt-3a on the C2C12 myoblast differentiation (65). A recent cross-sectional study of 240 healthy non-diabetic Korean individuals found that serum sclerostin levels were significantly higher in the low muscle mass group (66) and similar findings were observed in haemodialysis patients with diabetes (67). Interestingly, in a breast cancer mice model with bone metastasis, treatment with anti-sclerostin antibody prevented tumour growth in bone and bone destruction, as well as improvement in muscle function (68). Romosozumab, a human monoclonal antibody directed against sclerostin, has recently been approved for treatment of osteoporosis in postmenopausal women with high fracture risk. Its effect on skeletal muscle remains to be confirmed in larger human studies. Interestingly, skeletal muscle has also been found to secrete sclerostin, which works synergistically with bone-derived sclerostin to strengthen the negative regulatory mechanism of osteogenesis (69).

Insulin-like growth factor 1

IGF1 is an anabolic hormone with about 50% structural homology with proinsulin. It is primarily synthesised in the liver, but also in extrahepatic tissues including bone and acts on skeletal muscle in a paracrine manner, primarily through the Type 1 IGF receptor (IGF1R) to stimulate cellular uptake of glucose and amino acids, enhance protein synthesis and suppress protein degradation (70). It is an important determinant of muscle mass and function. pAkt, which is a major cellular signalling effector of insulin and IGF-1, was consistently found to be reduced in the skeletal muscle of CKD individuals (19). A reduction of Akt activity induces activation of FOXO transcription factors, ultimately resulting in overexpression of genes that are involved in catabolic processes as well as autophagy (71). Moreover, reduced IGF1 concentrations in CKD patients have been associated with body composition and lower bone mineral density (72, 73). However, IGF1 therapy has not been shown to have beneficial effects on bone density, muscle strength or muscle mass in older women (74).

Myokines and bone metabolism

Muscle-derived factors are called myokines, a term first proposed by Pedersen and colleagues in 2010 (75). These molecules include but are not limited to myostatin, irisin, IL-6, IL-8, IL-15, leukaemia inhibitory factor, brain-derived neurotrophic factor, IGF-1 and FGF2 (76).

Myostatin

Myostatin was the first myokine identified in 1997 (77) and is primarily produced in skeletal muscle. It is a highly conserved member of the transforming growth factor-β superfamily and is one of the most potent negative regulators of skeletal myogenesis. It inhibits muscle cell growth and differentiation by interacting with the activin type II receptors (ActRIIA and ActRIIB), leading to upregulation of the cytokines and other signalling mediators that disrupt protein metabolism (71). Myostatin knockout results in excessive skeletal muscle hypertrophy in mice (78, 79) and notably, myostatin deficiency also increases bone mineral density (80–82), which might be attributed to both loading-associated effects and biochemical interaction between bone and muscle. Myostatin was later discovered to have a negative impact on bone remodelling by enhancing osteoclastogenesis and reducing bone formation (83). Enhancement of osteogenic differentiation was observed in bone-marrow derived mesenchymal stem cells from *Mstn-/-* mice as compared to wild-type mice, which was load-dependent (81). Furthermore, myostatin was shown to accelerate RANKL-mediated osteoclast formation *via* activation of the NFAT signalling pathway (84).

Several studies have investigated the plasma concentrations of myostatin in CKD patients, the majority of them reporting higher levels in CKD and dialysis-dependent patients compared to healthy subjects (85). A few novel myostatin-targeted agents such as LY2495655 (humanised myostatin antibody that neutralises myostatin) and bimagrumab (humanised monoclonal antibody that binds to ActRII) have been tested in Phase II clinical trials with inconsistent results; some demonstrating positive outcomes with increased lean body mass and improved handgrip strength and gait speed (86, 87), while others did not (88).

Irisin

Irisin, a cleaved product of fibronectin Type III domain containing 5 (FNDC5), is secreted from skeletal muscle in response to an increased expression of peroxisome proliferator-activated receptor-γ co-activator-1-α (PGC1α) following exercise, to promote thermogenesis by browning white fat. It is also possibly involved in glucose metabolism (89). Irisin has been shown to promote myogenesis by enhancing myoblast proliferation and differentiation, increasing protein synthesis *via* activation of Akt and ERK, expanding the satellite cell pool and upregulating the expression of exercise-related genes, for example IL-6 (90, 91). Its anabolic effects on bone tissue are supported by *in vivo* studies, where low-dose weekly irisin injections for 4 weeks in young male mice resulted in increased cortical bone mass and strength, stimulating bone formation *via* upregulation of osteogenic transcription factors including activating transcription factor 4, Runt-related transcription factor 2 and Sp7 transcription factor. Interestingly, a lower number of osteoclasts were also observed in mice treated with irisin, which might contribute to the increase in bone strength (92). Recent findings raise the possibility that irisin could be a potential target for treating osteoporosis/CKD-MBD and sarcopenia. There is a known negative correlation between circulating irisin levels and osteoporotic fractures in postmenopausal women (93). Furthermore, plasma irisin levels are known to be lower in CKD patients (94), and recently, reduced irisin expression in the gastrocnemius muscle of 5/6 nephrectomised mice was found to be correlated with cortical bone mineral density (95).

Interleukins

Some circulating inflammatory cytokines (e.g. IL-6, IL-7 and IL-15) are important for muscle development and growth as well as

activation of muscle repair mechanisms. As mentioned previously, muscle-derived IL-6 promotes myogenesis and skeletal muscle growth *via* the regulation of proliferative capability of muscle stem cells (96). Apart from its glucose uptake and fatty acid oxidation, IL-6 stimulates bone resorption by inducing RANK and RANKL expression and the resorptive process has been demonstrated to be dependent on osteoblast signalling (22). *IL-6*$^{-/-}$ mice have increased bone formation and higher osteoclast numbers, but with a greater osteoclast apoptosis rate and reduction in resorption capacity (97). Its role in osteoblastogenesis remains controversial. Low grade chronic inflammation is prevalent in CKD patients and the interactions between cytokines, inflammation and muscle wasting are complex. On the one hand, systemic inflammation strongly correlates with muscle wasting, malnutrition, cardiovascular disease and mortality in patients with end-stage kidney disease (ESKD) (98–100). Higher expression of tumour necrosis factor-alpha (TNF-α) and IL-6 were observed in the muscle of CKD patients and mice compared to healthy controls and were associated with the development of muscle atrophy (19). Contrarily, both TNF-α and IL-6 have pleiotropic functions with a positive effect on muscle growth and regeneration. IL-6 was also shown to facilitate the local infiltration of macrophages and stimulate local IGF-1 production in muscle tissue of CKD mice (101). Furthermore, increased IL-6 efflux from muscle was found to correlate with increased muscle protein synthesis during haemodialysis (102). Similarly, IL-15, another anabolic factor in skeletal muscle, has also been demonstrated to have conflicting effects on osteoclast activity and bone mass (103, 104). Finally, higher circulating IL-15 levels correlate with a reduction in body fat and increased bone mineral content in mice (105).

Others

Each of muscle-derived IGF1 and FGF2 exert anabolic effects on bone metabolism by promoting osteoblast proliferation and hastening bone formation. IGF1 regulates bone anabolism as a response to enhanced osteoblast survival and proliferation, whereas FGF2 has been proposed to be secreted following disruption of the plasma membrane in response to injury or mechanical muscle contraction, rather than by exocytosis (106). Moreover, FGF2 was found to reduce glucocorticoid-mediated bone resorption *via* inhibition of sclerostin signalling, reinforcing its anabolic effects on bone metabolism (107). Circulating FGF2 levels have been reported to be lower in patients with more advanced CKD (108, 109), though its role in the development of sarcopenia in CKD is yet to be determined.

Effects of exercise on osteokines and myokines in chronic kidney disease

Observational studies have shown that patients with advanced CKD, particularly those on maintenance haemodialysis often have a sedentary lifestyle (110, 111) and about 45% of end-stage kidney disease (ESKD) patients report not performing any exercise at all (112). The health benefits of regular physical activity include a reduced risk of non-communicable diseases (e.g. heart disease, stroke and diabetes), better blood pressure control and improved mental health as well as overall quality of life. Physical activity improves physical function and reduces both pain and fall risk among adults with arthritis (113). In the CKD population, a highly active treatment group had a 25% risk reduction of all-cause mortality in comparison to inactive patients, even when factored for the presence of ESKD (114). Physical exercise also has a beneficial impact on bone mass, through promotion of bone formation and inhibition of bone resorption (115–117).

Several osteokines and myokines such as uOCN, OPG, irisin, IL-7, IL-15 and IL-6 are released in response to exercise training, exerting favourable physiological and metabolic effects in skeletal muscle and bone, in conjunction with a systemic anti-inflammatory effect (118, 119). In addition, both plasma and muscle myostatin levels were shown to decrease following aerobic and resistive training (120, 121). However, Gomes et al. investigated the effect of aerobic exercise on bone metabolism biomarkers (OCN, uOCN, sclerostin, PTH and total ALP) in non-dialysis CKD patients and found no differences in these biomarkers following a 24-week period of low-moderate intensity aerobic training except the total ALP (122). Similarly, both irisin and OCN levels were unaffected by resistance exercise in haemodialysis patients, though an increase in OPG was observed (123, 124). Yet, Zhou et al. reported higher plasma myostatin levels following 12 months of exercise training in a cohort of 151 non-dialysis-dependent CKD patients (125). These contrasting results underline the need for further studies in determining the effects of exercise (aerobic, resistance or alternative forms) on these bone-muscle biomarkers in CKD. Notwithstanding inconsistent findings from previous studies, a recent systematic review investigating the effects of physical activity in CKD patients reported beneficial effects of resistance exercise on bone health (126).

Conclusions and directions

Over the last thirty years, studies in CKD patients have mostly focused either on bone or on muscle separately without recognition of an interplay between the two organs. This oversight has perhaps driven the bias and associated interpretative limitations of mechanical coupling. A better understanding of the secretory crosstalk and associated biochemical coupling between these two organs represents a subject of great interest, with conceivable potential in identifying novel therapeutic targets and ultimately addressing the major unmet needs in managing renal osteodystrophy and sarcopenia in CKD population.

That said, the well-documented beneficial effects of exercise on bone and skeletal muscle in CKD cannot be understated. Although many dialysis-dependent patients might be too frail to engage in vigorous exercise, a less intense regimen may still be valuable. It is of note that the incorporation of exercise programs into standard clinical care has been slow, possibly because of feasibility concerns (127). However, in line with the World Health Organisation 2018-2030 Global Action Plan to promote physical activity for each according to their ability across the life course, health professionals play an essential role in improving access and quality of health care

in the CKD population. There are also potential opportunities for digital innovations to promote and support participation in physical activity to improve the health and well-being of our patients.

To finish, several key questions remain unanswered: (1) Is there a connection between osteoporosis, renal osteodystrophy and sarcopenia? (2) Does one condition precede or metabolically influence the other? (3) Is the phenotypic loss of muscle tissue simply related to comparable changes in bone over the course of CKD progression, each profoundly influenced by uraemia and a profoundly sedentary lifestyle? (4) Are other tissues, notably adipocytes, involved in the observed deleterious changes to bone and muscle in CKD?

Author contributions

LW contributed to conception and design of the article. LW wrote the first draft of the manuscript. All authors contributed to the article and approved the submitted version.

Funding

LW is supported by the Royal Australasian College of Physicians Jacquot Establishment Fellowship 2021 (2021REF00021) and 2022 (2022REF00084). The aim of the Jacquot Research Establishment Fellowship is to assist establishment of a career in nephrology research for a nephrologist who has completed a research higher degree in an area of relevance. The Fellowship is supported by the Estate of the late Don and Lorraine Jacquot and co-administered with the Australian and New Zealand Society of Nephrology Fellowship.

Conflict of interest

The authors declare that the research was conducted in the absence of any commercial or financial relationships that could be construed as a potential conflict of interest.

Publisher's note

References

1. Moe S, Drueke T, Cunningham J, Goodman W, Martin K, Olgaard K, et al. Definition, evaluation, and classification of renal osteodystrophy: A position statement from kidney disease: Improving global outcomes (KDIGO). *Kidney Int* (2006) 69 (11):1945–53. doi: 10.1038/sj.ki.5000414

2. Cruz-Jentoft AJ, Bahat G, Bauer J, Boirie Y, Bruyere O, Cederholm T, et al. Sarcopenia: revised European consensus on definition and diagnosis. *Age Ageing* (2019) 48(1):16–31. doi: 10.1093/ageing/afy169

3. Cheema BS, Singh MA. Exercise training in patients receiving maintenance hemodialysis: A systematic review of clinical trials. *Am J Nephrol* (2005) 25(4):352–64. doi: 10.1159/000087184

4. Heiwe S, Jacobson SH. Exercise training for adults with chronic kidney disease. *Cochrane Database Syst Rev* (2011) 10:CD003236. doi: 10.1002/14651858.CD003236.pub2

5. Morley JE, Argiles JM, Evans WJ, Bhasin S, Cella D, Deutz NE, et al. Nutritional recommendations for the management of sarcopenia. *J Am Med Dir Assoc* (2010) 11 (6):391–6. doi: 10.1016/j.jamda.2010.04.014

6. Brotto M, Johnson ML. Endocrine crosstalk between muscle and bone. *Curr Osteoporos Rep* (2014) 12(2):135–41. doi: 10.1007/s11914-014-0209-0

7. Iseri K, Dai L, Chen Z, Qureshi AR, Brismar TB, Stenvinkel P, et al. Bone mineral density and mortality in end-stage renal disease patients. *Clin Kidney J* (2020) 13 (3):307–21. doi: 10.1093/ckj/sfaa089

8. Alem AM, Sherrard DJ, Gillen DL, Weiss NS, Beresford SA, Heckbert SR, et al. Increased risk of hip fracture among patients with end-stage renal disease. *Kidney Int* (2000) 58(1):396–9. doi: 10.1046/j.1523-1755.2000.00178.x

9. Coco M, Rush H. Increased incidence of hip fractures in dialysis patients with low serum parathyroid hormone. *Am J Kidney Dis* (2000) 36(6):1115–21. doi: 10.1053/ajkd.2000.19812

10. Dooley AC, Weiss NS, Kestenbaum B. Increased risk of hip fracture among men with CKD. *Am J Kidney Dis* (2008) 51(1):38–44. doi: 10.1053/j.ajkd.2007.08.019

11. Jadoul M, Albert JM, Akiba T, Akizawa T, Arab L, Bragg-Gresham JL, et al. Incidence and risk factors for hip or other bone fractures among hemodialysis patients in the dialysis outcomes and practice patterns study. *Kidney Int* (2006) 70(7):1358–66. doi: 10.1038/sj.ki.5001754

12. Nickolas TL, McMahon DJ, Shane E. Relationship between moderate to severe kidney disease and hip fracture in the united states. *J Am Soc Nephrol* (2006) 17 (11):3223–32. doi: 10.1681/ASN.2005111194

13. Malluche HH, Mawad HW, Monier-Faugere MC. Renal osteodystrophy in the first decade of the new millennium: Analysis of 630 bone biopsies in black and white patients. *J Bone Miner Res* (2011) 26(6):1368–76. doi: 10.1002/jbmr.309

14. Sprague SM, Bellorin-Font E, Jorgetti V, Carvalho AB, Malluche HH, Ferreira A, et al. Diagnostic accuracy of bone turnover markers and bone histology in patients with CKD treated by dialysis. *Am J Kidney Dis* (2016) 67(4):559–66. doi: 10.1053/j.ajkd.2015.06.023

15. Griffiths RD. Muscle mass, survival, and the elderly ICU patient. *Nutrition* (1996) 12(6):456–8. doi: 10.1016/S0899-9007(96)00141-4

16. von Haehling S, Morley JE, Anker SD. From muscle wasting to sarcopenia and myopenia: update 2012. *J Cachexia Sarcopenia Muscle* (2012) 3(4):213–7. doi: 10.1007/s13539-012-0089-z

17. Wong L, Kent AB, Lee D, Roberts MA, McMahon LP. Low muscle mass and early hospital readmission post-kidney transplantation. *Int Urol Nephrol* (2022) 54 (8):1977–86. doi: 10.1007/s11255-021-03085-1

18. Locke JE, Carr JJ, Nair S, Terry JG, Reed RD, Smith GD, et al. Abdominal lean muscle is associated with lower mortality among kidney waitlist candidates. *Clin Transplant* (2017) 31(3). doi: 10.1111/ctr.12911

19. Wong L, Kenny R, Howard JL, McMahon LP. Molecular mechanisms underpinning muscle atrophy in CKD (TH-PO828). *J Am Soc Nephrol* (2022) 33:285.

20. Lu W, Xiao W, Xie W, Fu X, Pan L, Jin H, et al. The role of osteokines in sarcopenia: Therapeutic directions and application prospects. *Front Cell Dev Biol* (2021) 9:735374. doi: 10.3389/fcell.2021.735374

21. Kular J, Tickner J, Chim SM, Xu J. An overview of the regulation of bone remodelling at the cellular level. *Clin Biochem* (2012) 45(12):863–73. doi: 10.1016/j.clinbiochem.2012.03.021

22. Udagawa N, Takahashi N, Katagiri T, Tamura T, Wada S, Findlay DM, et al. Interleukin (IL)-6 induction of osteoclast differentiation depends on IL-6 receptors expressed on osteoblastic cells but not on osteoclast progenitors. *J Exp Med* (1995) 182 (5):1461–8. doi: 10.1084/jem.182.5.1461

23. Mizuno A, Amizuka N, Irie K, Murakami A, Fujise N, Kanno T, et al. Severe osteoporosis in mice lacking osteoclastogenesis inhibitory factor/osteoprotegerin. *Biochem Biophys Res Commun* (1998) 247(3):610–5. doi: 10.1006/bbrc.1998.8697

24. Doumouchtsis KK, Kostakis AI, Doumouchtsis SK, Tziamalis MP, Tsigris C, Kostaki MA, et al. sRANKL/osteoprotegerin complex and biochemical markers in a

cohort of male and female hemodialysis patients. *J Endocrinol Invest* (2007) 30(9):762–6. doi: 10.1007/BF03350814

25. Avbersek-Luznik I, Balon BP, Rus I, Marc J. Increased bone resorption in HD patients: is it caused by elevated RANKL synthesis? *Nephrol Dial Transplant* (2005) 20 (3):566–70. doi: 10.1093/ndt/gfh672

26. Albalate M, de la Piedra C, Fernandez C, Lefort M, Santana H, Hernando P, et al. Association between phosphate removal and markers of bone turnover in haemodialysis patients. *Nephrol Dial Transplant* (2006) 21(6):1626–32. doi: 10.1093/ndt/gfl034

27. Avbersek-Luznik I, Malesic I, Rus I, Marc J. Increased levels of osteoprotegerin in hemodialysis patients. *Clin Chem Lab Med* (2002) 40(10):1019–23. doi: 10.1515/CCLM.2002.177

28. Kazama JJ, Shigematsu T, Yano K, Tsuda E, Miura M, Iwasaki Y, et al. Increased circulating levels of osteoclastogenesis inhibitory factor (osteoprotegerin) in patients with chronic renal failure. *Am J Kidney Dis* (2002) 39(3):525–32. doi: 10.1053/ajkd.2002.31402

29. ADHR Consortium. Autosomal dominant hypophosphataemic rickets is associated with mutations in FGF23. *Nat Genet* (2000) 26(3):345–8. doi: 10.1038/81664

30. Shimada T, Urakawa I, Yamazaki Y, Hasegawa H, Hino R, Yoneya T, et al. FGF-23 transgenic mice demonstrate hypophosphatemic rickets with reduced expression of sodium phosphate cotransporter type IIa. *Biochem Biophys Res Commun* (2004) 314 (2):409–14. doi: 10.1016/j.bbrc.2003.12.102

31. Shimada T, Hasegawa H, Yamazaki Y, Muto T, Hino R, Takeuchi Y, et al. FGF-23 is a potent regulator of vitamin d metabolism and phosphate homeostasis. *J Bone Miner Res* (2004) 19(3):429–35. doi: 10.1359/JBMR.0301264

32. Urakawa I, Yamazaki Y, Shimada T, Iijima K, Hasegawa H, Okawa K, et al. Klotho converts canonical FGF receptor into a specific receptor for FGF23. *Nature* (2006) 444(7120):770–4. doi: 10.1038/nature05315

33. Ho BB, Bergwitz C. FGF23 signalling and physiology. *J Mol Endocrinol* (2021) 66(2):R23–32. doi: 10.1530/JME-20-0178

34. Faul C, Amaral AP, Oskouei B, Hu MC, Sloan A, Isakova T, et al. FGF23 induces left ventricular hypertrophy. *J Clin Invest* (2011) 121(11):4393–408. doi: 10.1172/JCI46122

35. Beben T, Ix JH, Shlipak MG, Sarnak MJ, Fried LF, Hoofnagle AN, et al. Fibroblast growth factor-23 and frailty in elderly community-dwelling individuals: The cardiovascular health study. *J Am Geriatr Soc* (2016) 64(2):270–6. doi: 10.1111/jgs.13951

36. Jovanovich A, Ginsberg C, You Z, Katz R, Ambrosius WT, Berlowitz D, et al. FGF23, frailty, and falls in SPRINT. *J Am Geriatr Soc* (2021) 69(2):467–73. doi: 10.1111/jgs.16895

37. Kido S, Hashimoto Y, Segawa H, Tatsumi S, Miyamoto K. Muscle atrophy in patients with CKD results from FGF23/klotho-mediated suppression of insulin/IGF-1 signalling. *Kidney Res Clin Pract* (2012) 31:A44.

38. Sato C, Iso Y, Mizukami T, Otabe K, Sasai M, Kurata M, et al. Fibroblast growth factor-23 induces cellular senescence in human mesenchymal stem cells from skeletal muscle. *Biochem Biophys Res Commun* (2016) 470(3):657–62. doi: 10.1016/j.bbrc.2016.01.086

39. Fukasawa H, Ishigaki S, Kinoshita-Katahashi N, Niwa H, Yasuda H, Kumagai H, et al. Plasma levels of fibroblast growth factor-23 are associated with muscle mass in haemodialysis patients. *Nephrol (Carlton)* (2014) 19(12):784–90. doi: 10.1111/nep.12333

40. Li DJ, Fu H, Zhao T, Ni M, Shen FM. Exercise-stimulated FGF23 promotes exercise performance *via* controlling the excess reactive oxygen species production and enhancing mitochondrial function in skeletal muscle. *Metabolism* (2016) 65(5):747–56. doi: 10.1016/j.metabol.2016.02.009

41. Avin KG, Vallejo JA, Chen NX, Wang K, Touchberry CD, Brotto M, et al. Fibroblast growth factor 23 does not directly influence skeletal muscle cell proliferation and differentiation or ex vivo muscle contractility. *Am J Physiol Endocrinol Metab* (2018) 315(4):E594–604. doi: 10.1152/ajpendo.00343.2017

42. Lee NK, Sowa H, Hinoi E, Ferron M, Ahn JD, Confavreux C, et al. Endocrine regulation of energy metabolism by the skeleton. *Cell* (2007) 130(3):456–69. doi: 10.1016/j.cell.2007.05.047

43. Ferron M, McKee MD, Levine RL, Ducy P, Karsenty G. Intermittent injections of osteocalcin improve glucose metabolism and prevent type 2 diabetes in mice. *Bone* (2012) 50(2):568–75. doi: 10.1016/j.bone.2011.04.017

44. Oury F, Sumara G, Sumara O, Ferron M, Chang H, Smith CE, et al. Endocrine regulation of male fertility by the skeleton. *Cell* (2011) 144(5):796–809. doi: 10.1016/j.cell.2011.02.004

45. Puig J, Blasco G, Daunis-i-Estadella J, Moreno M, Molina X, Alberich-Bayarri A, et al. Lower serum osteocalcin concentrations are associated with brain microstructural changes and worse cognitive performance. *Clin Endocrinol (Oxf)* (2016) 84(5):756–63. doi: 10.1111/cen.12954

46. Ducy P, Desbois C, Boyce B, Pinero G, Story B, Dunstan C, et al. Increased bone formation in osteocalcin-deficient mice. *Nature* (1996) 382(6590):448–52. doi: 10.1038/382448a0

47. Chenu C, Colucci S, Grano M, Zigrino P, Barattolo R, Zambonin G, et al. Osteocalcin induces chemotaxis, secretion of matrix proteins, and calcium-mediated intracellular signaling in human osteoclast-like cells. *J Cell Biol* (1994) 127(4):1149–58. doi: 10.1083/jcb.127.4.1149

48. Boskey AL, Gadaleta S, Gundberg C, Doty SB, Ducy P, Karsenty G. Fourier Transform infrared microspectroscopic analysis of bones of osteocalcin-deficient mice provides insight into the function of osteocalcin. *Bone* (1998) 23(3):187–96. doi: 10.1016/S8756-3282(98)00092-1

49. Bodine PV, Komm BS. Evidence that conditionally immortalized human osteoblasts express an osteocalcin receptor. *Bone* (1999) 25(5):535–43. doi: 10.1016/S8756-3282(99)00213-6

50. Delmas PD, Wilson DM, Mann KG, Riggs BL. Effect of renal function on plasma levels of bone gla-protein. *J Clin Endocrinol Metab* (1983) 57(5):1028–30. doi: 10.1210/jcem-57-5-1028

51. Alpdemir M, Fidanci V, Alpdemir MF, Azak A, Saydam G, Duranay M, et al. Serum undercarboxylated osteocalcin levels are related to bone disease in hemodialysis and peritoneal dialysis patients. *Eur Res J* (2021) 7(3):225–34. doi: 10.18621/eurj.734216

52. Millar SA, John SG, McIntyre CW, Ralevic V, Anderson SI, O'Sullivan SE. An investigation into the role of osteocalcin in human arterial smooth muscle cell calcification. *Front Endocrinol (Lausanne)* (2020) 11:369. doi: 10.3389/fendo.2020.00369

53. Mera P, Laue K, Ferron M, Confavreux C, Wei J, Galan-Diez M, et al. Osteocalcin signaling in myofibers is necessary and sufficient for optimum adaptation to exercise. *Cell Metab* (2016) 23(6):1078–92. doi: 10.1016/j.cmet.2016.05.004

54. Mera P, Laue K, Wei J, Berger JM, Karsenty G. Osteocalcin is necessary and sufficient to maintain muscle mass in older mice. *Mol Metab* (2016) 5(10):1042–7. doi: 10.1016/j.molmet.2016.07.002

55. Liu S, Gao F, Wen L, Ouyang M, Wang Y, Wang Q, et al. Osteocalcin induces proliferation *via* positive activation of the PI3K/Akt, P38 MAPK pathways and promotes differentiation through activation of the GPRC6A-ERK1/2 pathway in C2C12 myoblast cells. *Cell Physiol Biochem* (2017) 43(3):1100–12. doi: 10.1159/000481752

56. Moriishi T, Ozasa R, Ishimoto T, Nakano T, Hasegawa T, Miyazaki T, et al. Osteocalcin is necessary for the alignment of apatite crystallites, but not glucose metabolism, testosterone synthesis, or muscle mass. *PloS Genet* (2020) 16(5):e1008586. doi: 10.1371/journal.pgen.1008586

57. Diegel CR, Hann S, Ayturk UM, Hu JCW, Lim KE, Droscha CJ, et al. An osteocalcin-deficient mouse strain without endocrine abnormalities. *PloS Genet* (2020) 16(5):e1008361. doi: 10.1371/journal.pgen.1008361

58. Langen RC, Schols AM, Kelders MC, Wouters EF, Janssen-Heininger YM. Inflammatory cytokines inhibit myogenic differentiation through activation of nuclear factor-kappaB. *FASEB J* (2001) 15(7):1169–80. doi: 10.1096/fj.00-0463

59. Dufresne SS, Dumont NA, Boulanger-Piette A, Fajardo VA, Gamu D, Kake-Guena SA, et al. Muscle RANK is a key regulator of Ca2+ storage, SERCA activity, and function of fast-twitch skeletal muscles. *Am J Physiol Cell Physiol* (2016) 310(8):C663–72. doi: 10.1152/ajpcell.00285.2015

60. Dufresne SS, Boulanger-Piette A, Bosse S, Argaw A, Hamoudi D, Marcadet L, et al. Genetic deletion of muscle RANK or selective inhibition of RANKL is not as effective as full-length OPG-fc in mitigating muscular dystrophy. *Acta Neuropathol Commun* (2018) 6(1):31. doi: 10.1186/s40478-018-0533-1

61. Hamoudi D, Marcadet L, Piette Boulanger A, Yagita H, Bouredji Z, Argaw A, et al. An anti-RANKL treatment reduces muscle inflammation and dysfunction and strengthens bone in dystrophic mice. *Hum Mol Genet* (2019) 28(18):3101–12. doi: 10.1093/hmg/ddz124

62. Dufresne SS, Dumont NA, Bouchard P, Lavergne E, Penninger JM, Frenette J. Osteoprotegerin protects against muscular dystrophy. *Am J Pathol* (2015) 185(4):920–6. doi: 10.1016/j.ajpath.2015.01.006

63. Bonnet N, Bourgoin L, Biver E, Douni E, Ferrari S. RANKL inhibition improves muscle strength and insulin sensitivity and restores bone mass. *J Clin Invest* (2019) 129 (8):3214–23. doi: 10.1172/JCI125915

64. Winkler DG, Sutherland MK, Geoghegan JC, Yu C, Hayes T, Skonier JE, et al. Osteocyte control of bone formation *via* sclerostin, a novel BMP antagonist. *EMBO J* (2003) 22(23):6267–76. doi: 10.1093/emboj/cdg599

65. Li X, Zhang Y, Kang H, Liu W, Liu P, Zhang J, et al. Sclerostin binds to LRP5/6 and antagonizes canonical wnt signaling. *J Biol Chem* (2005) 280(20):19883–7. doi: 10.1074/jbc.M413274200

66. Kim JA, Roh E, Hong SH, Lee YB, Kim NH, Yoo HJ, et al. Association of serum sclerostin levels with low skeletal muscle mass: The Korean sarcopenic obesity study (KSOS). *Bone* (2019) 128:115053. doi: 10.1016/j.bone.2019.115053

67. Medeiros MC, Rocha N, Bandeira E, Dantas I, Chaves C, Oliveira M, et al. Serum sclerostin, body composition, and sarcopenia in hemodialysis patients with diabetes. *Int J Nephrol* (2020) 2020:4596920. doi: 10.1155/2020/4596920

68. Hesse E, Schroder S, Brandt D, Pamperin J, Saito H, Taipaleenmaki H. Sclerostin inhibition alleviates breast cancer-induced bone metastases and muscle weakness. *JCI Insight* (2019) 5(9). doi: 10.1172/jci.insight.125543

69. Magaro MS, Bertacchini J, Florio F, Zavatti M, Poti F, Cavani F, et al. Identification of sclerostin as a putative new myokine involved in the muscle-to-Bone crosstalk. *Biomedicines* (2021) 9(1). doi: 10.3390/biomedicines9010071

70. Le Roith D. Seminars in medicine of the Beth Israel deaconess medical center. insulin-like growth factors. *N Engl J Med* (1997) 336(9):633–40. doi: 10.1056/NEJM199702273360907

71. Wang XH, Mitch WE, Price SR. Pathophysiological mechanisms leading to muscle loss in chronic kidney disease. *Nat Rev Nephrol* (2022) 18(3):138–52. doi: 10.1038/s41581-021-00498-0

72. Park SH, Jia T, Qureshi AR, Barany P, Heimburger O, Larsson TE, et al. Determinants and survival implications of low bone mineral density in end-stage renal disease patients. *J Nephrol* (2013) 26(3):485–94. doi: 10.5301/jn.5000185

73. Jia T, Gama Axelsson T, Heimburger O, Barany P, Lindholm B, Stenvinkel P, et al. IGF-1 and survival in ESRD. *Clin J Am Soc Nephrol* (2014) 9(1):120–7. doi: 10.2215/CJN.02470213

74. Friedlander AL, Butterfield GE, Moynihan S, Grillo J, Pollack M, Holloway L, et al. One year of insulin-like growth factor I treatment does not affect bone density, body composition, or psychological measures in postmenopausal women. *J Clin Endocrinol Metab* (2001) 86(4):1496–503. doi: 10.1210/jcem.86.4.7377

75. Pedersen BK. Muscles and their myokines. *J Exp Biol* (2011) 214(Pt 2):337–46. doi: 10.1242/jeb.048074

76. Brotto M, Bonewald L. Bone and muscle: Interactions beyond mechanical. *Bone* (2015) 80:109–14. doi: 10.1016/j.bone.2015.02.010

77. Lee JH, Jun HS. Role of myokines in regulating skeletal muscle mass and function. *Front Physiol* (2019) 10:42. doi: 10.3389/fphys.2019.00042

78. McPherron AC, Lawler AM, Lee SJ. Regulation of skeletal muscle mass in mice by a new TGF-beta superfamily member. *Nature* (1997) 387(6628):83–90. doi: 10.1038/387083a0

79. Lin J, Arnold HB, Della-Fera MA, Azain MJ, Hartzell DL, Baile CA. Myostatin knockout in mice increases myogenesis and decreases adipogenesis. *Biochem Biophys Res Commun* (2002) 291(3):701–6. doi: 10.1006/bbrc.2002.6500

80. Kellum E, Starr H, Arounleut P, Immel D, Fulzele S, Wenger K, et al. Myostatin (GDF-8) deficiency increases fracture callus size, sox-5 expression, and callus bone volume. *Bone* (2009) 44(1):17–23. doi: 10.1016/j.bone.2008.08.126

81. Hamrick MW, Shi X, Zhang W, Pennington C, Thakore H, Haque M, et al. Loss of myostatin (GDF8) function increases osteogenic differentiation of bone marrow-derived mesenchymal stem cells but the osteogenic effect is ablated with unloading. *Bone* (2007) 40(6):1544–53. doi: 10.1016/j.bone.2007.02.012

82. Hamrick MW. Increased bone mineral density in the femora of GDF8 knockout mice. *Anat Rec A Discovery Mol Cell Evol Biol* (2003) 272(1):388–91. doi: 10.1002/ar.a.10044

83. Elkasrawy MN, Hamrick MW. Myostatin (GDF-8) as a key factor linking muscle mass and bone structure. *J Musculoskelet Neuronal Interact* (2010) 10(1):56–63.

84. Dankbar B, Fennen M, Brunert D, Hayer S, Frank S, Wehmeyer C, et al. Myostatin is a direct regulator of osteoclast differentiation and its inhibition reduces inflammatory joint destruction in mice. *Nat Med* (2015) 21(9):1085–90. doi: 10.1038/nm.3917

85. Bataille S, Chauveau P, Fouque D, Aparicio M, Koppe L. Myostatin and muscle atrophy during chronic kidney disease. *Nephrol Dial Transplant* (2021) 36(11):1986–93. doi: 10.1093/ndt/gfaa129

86. Rooks D, Praestgaard J, Hariry S, Laurent D, Petricoul O, Perry RG, et al. Treatment of sarcopenia with bimagrumab: Results from a phase II, randomized, controlled, proof-of-Concept study. *J Am Geriatr Soc* (2017) 65(9):1988–95. doi: 10.1111/jgs.14927

87. Becker C, Lord SR, Studenski SA, Warden SJ, Fielding RA, Recknor CP, et al. Myostatin antibody (LY2495655) in older weak fallers: a proof-of-concept, randomised, phase 2 trial. *Lancet Diabetes Endocrinol* (2015) 3(12):948–57. doi: 10.1016/S2213-8587(15)00298-3

88. Woodhouse L, Gandhi R, Warden SJ, Poiraudeau S, Myers SL, Benson CT, et al. A phase 2 randomized study investigating the efficacy and safety of myostatin antibody LY2495655 versus placebo in patients undergoing elective total hip arthroplasty. *J Frailty Aging* (2016) 5(1):62–70. doi: 10.14283/jfa.2016.81

89. Bostrom P, Wu J, Jedrychowski MP, Korde A, Ye L, Lo JC, et al. A PGC1-alpha-dependent myokine that drives brown-fat-like development of white fat and thermogenesis. *Nature* (2012) 481(7382):463–8. doi: 10.1038/nature10777

90. Huh JY, Dincer F, Mesfum E, Mantzoros CS. Irisin stimulates muscle growth-related genes and regulates adipocyte differentiation and metabolism in humans. *Int J Obes (Lond)* (2014) 38(12):1538–44. doi: 10.1038/ijo.2014.42

91. Reza MM, Subramaniyam N, Sim CM, Ge X, Sathiakumar D, McFarlane C, et al. Irisin is a pro-myogenic factor that induces skeletal muscle hypertrophy and rescues denervation-induced atrophy. *Nat Commun* (2017) 8(1):1104. doi: 10.1038/s41467-017-01131-0

92. Colaianni G, Cuscito C, Mongelli T, Pignataro P, Buccoliero C, Liu P, et al. The myokine irisin increases cortical bone mass. *Proc Natl Acad Sci U S A* (2015) 112(39):12157–62. doi: 10.1073/pnas.1516622112

93. Anastasilakis AD, Polyzos SA, Makras P, Gkiomisi A, Bisbinas I, Katsarou A, et al. Circulating irisin is associated with osteoporotic fractures in postmenopausal women with low bone mass but is not affected by either teriparatide or denosumab treatment for 3 months. *Osteoporos Int* (2014) 25(5):1633–42. doi: 10.1007/s00198-014-2673-x

94. Wen MS, Wang CY, Lin SL, Hung KC. Decrease in irisin in patients with chronic kidney disease. *PloS One* (2013) 8(5):e64025. doi: 10.1371/journal.pone.0064025

95. Kawao N, Kawaguchi M, Ohira T, Ehara H, Mizukami Y, Takafuji Y, et al. Renal failure suppresses muscle irisin expression, and irisin blunts cortical bone loss in mice. *J Cachexia Sarcopenia Muscle* (2022) 13(1):758–71. doi: 10.1002/jcsm.12892

96. Munoz-Canoves P, Scheele C, Pedersen BK, Serrano AL. Interleukin-6 myokine signaling in skeletal muscle: a double-edged sword? *FEBS J* (2013) 280(17):4131–48. doi: 10.1111/febs.12338

97. Liu H, Feng W, Yimin, Cui J, Lv S, Hasegawa T, et al. Histological evidence of increased osteoclast cell number and asymmetric bone resorption activity in the tibiae of interleukin-6-Deficient mice. *J Histochem Cytochem* (2014) 62(8):556–64. doi: 10.1369/0022155414537830

98. Mihai S, Codrici E, Popescu ID, Enciu AM, Albulescu L, Necula LG, et al. Inflammation-related mechanisms in chronic kidney disease prediction, progression, and outcome. *J Immunol Res* (2018) 2018:2180373. doi: 10.1155/2018/2180373

99. Honda H, Qureshi AR, Heimburger O, Barany P, Wang K, Pecoits-Filho R, et al. Serum albumin, c-reactive protein, interleukin 6, and fetuin a as predictors of malnutrition, cardiovascular disease, and mortality in patients with ESRD. *Am J Kidney Dis* (2006) 47(1):139–48. doi: 10.1053/j.ajkd.2005.09.014

100. Avesani CM, Carrero JJ, Axelsson J, Qureshi AR, Lindholm B, Stenvinkel P. Inflammation and wasting in chronic kidney disease: Partners in crime. *Kidney Int* (2006) 70:S8–13. doi: 10.1038/sj.ki.5001969

101. Hu L, Klein JD, Hassounah F, Cai H, Zhang C, Xu P, et al. Low-frequency electrical stimulation attenuates muscle atrophy in CKD–a potential treatment strategy. *J Am Soc Nephrol* (2015) 26(3):626–35. doi: 10.1681/ASN.2014020144

102. Raj DS, Moseley P, Dominic EA, Onime A, Tzamaloukas AH, Boyd A, et al. Interleukin-6 modulates hepatic and muscle protein synthesis during hemodialysis. *Kidney Int* (2008) 73(9):1054–61. doi: 10.1038/ki.2008.21

103. Djaafar S, Pierroz DD, Chicheportiche R, Zheng XX, Ferrari SL, Ferrari-Lacraz S. Inhibition of T cell-dependent and RANKL-dependent osteoclastogenic processes associated with high levels of bone mass in interleukin-15 receptor-deficient mice. *Arthritis Rheumatol* (2010) 62(11):3300–10. doi: 10.1002/art.27645

104. Takeda H, Kikuchi T, Soboku K, Okabe I, Mizutani H, Mitani A, et al. Effect of IL-15 and natural killer cells on osteoclasts and osteoblasts in a mouse coculture. *Inflammation* (2014) 37(3):657–69. doi: 10.1007/s10753-013-9782-0

105. Quinn LS, Anderson BG, Strait-Bodey L, Stroud AM, Argiles JM. Oversecretion of interleukin-15 from skeletal muscle reduces adiposity. *Am J Physiol Endocrinol Metab* (2009) 296(1):E191–202. doi: 10.1152/ajpendo.90506.2008

106. Hamrick MW. The skeletal muscle secretome: an emerging player in muscle-bone crosstalk. *Bonekey Rep* (2012) 1:60. doi: 10.1038/bonekey.2012.60

107. Adhikary S, Choudhary D, Tripathi AK, Karvande A, Ahmad N, Kothari P, et al. FGF-2 targets sclerostin in bone and myostatin in skeletal muscle to mitigate the deleterious effects of glucocorticoid on musculoskeletal degradation. *Life Sci* (2019) 229:261–76. doi: 10.1016/j.lfs.2019.05.022

108. Bozic M, Betriu A, Bermudez-Lopez M, Ortiz A, Fernandez E, Valdivielso JM, et al. Association of FGF-2 concentrations with atheroma progression in chronic kidney disease patients. *Clin J Am Soc Nephrol* (2018) 13(4):577–84. doi: 10.2215/CJN.07980717

109. Velasquez-Mao AJ, Velasquez MA, Hui Z, Armas-Ayon D, Wang J, Vandsburger MH. Hemodialysis exacerbates proteolytic imbalance and pro-fibrotic platelet dysfunction. *Sci Rep* (2021) 11(1):11764. doi: 10.1038/s41598-021-91416-8

110. Johansen KL, Chertow GM, Ng AV, Mulligan K, Carey S, Schoenfeld PY, et al. Physical activity levels in patients on hemodialysis and healthy sedentary controls. *Kidney Int* (2000) 57(6):2564–70. doi: 10.1046/j.1523-1755.2000.00116.x

111. Segura-Orti E, Gordon PL, Doyle JW, Johansen KL. Correlates of physical functioning and performance across the spectrum of kidney function. *Clin Nurs Res* (2018) 27(5):579–96. doi: 10.1177/1054773816689282

112. Avesani CM, Trolonge S, Deleaval P, Baria F, Mafra D, Faxen-Irving G, et al. Physical activity and energy expenditure in haemodialysis patients: an international survey. *Nephrol Dial Transplant* (2012) 27(6):2430–4. doi: 10.1093/ndt/gfr692

113. Torres A, Tennant B, Ribeiro-Lucas I, Vaux-Bjerke A, Piercy K, Bloodgood B. Umbrella and systematic review methodology to support the 2018 physical activity guidelines advisory committee. *J Phys Act Health* (2018) 15(11):805–10. doi: 10.1123/jpah.2018-0372

114. Kuo CP, Tsai MT, Lee KH, Lin YP, Huang SS, Huang CC, et al. Dose-response effects of physical activity on all-cause mortality and major cardiorenal outcomes in chronic kidney disease. *Eur J Prev Cardiol* (2022) 29(3):452–61. doi: 10.1093/eurjpc/zwaa162

115. Alghadir AH, Gabr SA, Al-Eisa ES, Alghadir MH. Correlation between bone mineral density and serum trace elements in response to supervised aerobic training in older adults. *Clin Interv Aging* (2016) 11:265–73. doi: 10.2147/CIA.S100566

116. Marinho SM, Moraes C, Barbosa JE, Carraro Eduardo JC, Fouque D, Pelletier S, et al. Exercise training alters the bone mineral density of hemodialysis patients. *J Strength Cond Res* (2016) 30(10):2918–23. doi: 10.1519/JSC.0000000000001374

117. Adami S, Gatti D, Viapiana O, Fiore CE, Nuti R, Luisetto G, et al. Physical activity and bone turnover markers: a cross-sectional and a longitudinal study. *Calcif Tissue Int* (2008) 83(6):388–92. doi: 10.1007/s00223-008-9184-8

118. Pedersen BK, Febbraio MA. Muscles, exercise and obesity: skeletal muscle as a secretory organ. *Nat Rev Endocrinol* (2012) 8(8):457–65. doi: 10.1038/nrendo.2012.49

119. Leal DV, Ferreira A, Watson EL, Wilund KR, Viana JL. Muscle-bone crosstalk in chronic kidney disease: The potential modulatory effects of exercise. *Calcif Tissue Int* (2021) 108(4):461–75. doi: 10.1007/s00223-020-00782-4

120. Hittel DS, Axelson M, Sarna N, Shearer J, Huffman KM, Kraus WE. Myostatin decreases with aerobic exercise and associates with insulin resistance. *Med Sci Sports Exerc* (2010) 42(11):2023–9. doi: 10.1249/MSS.0b013e3181e0b9a8

121. Ryan AS, Ivey FM, Prior S, Li G, Hafer-Macko C. Skeletal muscle hypertrophy and muscle myostatin reduction after resistive training in stroke survivors. *Stroke* (2011) 42(2):416–20. doi: 10.1161/STROKEAHA.110.602441

122. Gomes TS, Aoike DT, Baria F, Graciolli FG, Moyses RMA, Cuppari L. Effect of aerobic exercise on markers of bone metabolism of overweight and obese patients with chronic kidney disease. *J Ren Nutr* (2017) 27(5):364–71. doi: 10.1053/j.jrn.2017.04.009

123. Moraes C, Leal VO, Marinho SM, Barroso SG, Rocha GS, Boaventura GT, et al. Resistance exercise training does not affect plasma irisin levels of hemodialysis patients. *Horm Metab Res* (2013) 45(12):900–4. doi: 10.1055/s-0033-1354402

124. Marinho SM, Carraro Eduardo JC, Mafra D. Effect of a resistance exercise training program on bone markers in hemodialysis patients. *Sci Sports* (2017) 32:99–105. doi: 10.1016/j.scispo.2017.01.003

125. Zhou Y, Hellberg M, Hellmark T, Hoglund P, Clyne N. Muscle mass and plasma myostatin after exercise training: a substudy of renal exercise (RENEXC)-a randomized controlled trial. *Nephrol Dial Transplant* (2021) 36(1):95–103. doi: 10.1093/ndt/gfz210

126. Cardoso DF, Marques EA, Leal DV, Ferreira A, Baker LA, Smith AC, et al. Impact of physical activity and exercise on bone health in patients with chronic kidney disease: a systematic review of observational and experimental studies. *BMC Nephrol* (2020) 21(1):334. doi: 10.1186/s12882-020-01999-z

127. Castillo G, Presseau J, Wilson M, Cook C, Field B, Garg AX, et al. Addressing feasibility challenges to delivering intradialytic exercise interventions: a theory-informed qualitative study. *Nephrol Dial Transplant* (2022) 37(3):558–74. doi: 10.1093/ndt/gfab228

frontiers | Frontiers in Endocrinology

TYPE Systematic Review
PUBLISHED 22 November 2023
DOI 10.3389/fendo.2023.1282675

OPEN ACCESS

EDITED BY
Seerapani Gopaluni,
University of Cambridge, United Kingdom

REVIEWED BY
Amirmohammad Khalaji,
Tehran University of Medical Sciences, Iran
Amir Hossein Behnoush,
Tehran University of Medical Sciences, Iran

*CORRESPONDENCE
Ping-Hsun Feng
fengbenson@gmail.com

†These authors have contributed equally to this work

RECEIVED 24 August 2023
ACCEPTED 09 November 2023
PUBLISHED 22 November 2023

CITATION
Chang W–T, Liu C-C, Huang Y-T, Wu J-Y, Tsai W-W, Hung K–C, Chen I–W and Feng P-H (2023) Diagnostic efficacy of the triglyceride–glucose index in the prediction of contrast-induced nephropathy following percutaneous coronary intervention.
Front. Endocrinol. 14:1282675.
doi: 10.3389/fendo.2023.1282675

Diagnostic efficacy of the triglyceride–glucose index in the prediction of contrast-induced nephropathy following percutaneous coronary intervention

Wei–Ting Chang[1,2,3], Chien-Cheng Liu[4,5,6], Yen-Ta Huang[7], Jheng-Yan Wu[8], Wen-Wen Tsai[9], Kuo–Chuan Hung[10,11], I–Wen Chen[12†] and Ping-Hsun Feng[12*†]

[1]School of Medicine and Doctoral Program of Clinical and Experimental Medicine, College of Medicine and Center of Excellence for Metabolic Associated Fatty Liver Disease, National Sun Yat-sen University, Kaohsiung, Taiwan, [2]Division of Cardiology, Department of Internal Medicine, Chi-Mei Medical Center, Tainan, Taiwan, [3]Department of Biotechnology, Southern Taiwan University of Science and Technology, Tainan, Taiwan, [4]Department of Anesthesiology, E-Da Hospital, I-Shou University, Kaohsiung, Taiwan, [5]Department of Nursing, College of Medicine, I-Shou University, Kaohsiung, Taiwan, [6]School of Medicine, I-Shou University, Kaohsiung, Taiwan, [7]Department of Surgery, National Cheng Kung University Hospital, College of Medicine, National Cheng Kung University, Tainan, Taiwan, [8]Department of Nutrition, Chi Mei Medical Center, Tainan, Taiwan, [9]Department of Neurology, Chi-Mei Medical Center, Tainan, Taiwan, [10]Department of Anesthesiology, Chi Mei Medical Center, Tainan, Taiwan, [11]School of Medicine, College of Medicine, National Sun Yat-sen University, Kaohsiung, Taiwan, [12]Department of Anesthesiology, Chi Mei Medical Center, Liouying, Tainan, Taiwan

Introduction: Contrast-induced nephropathy (CIN) is a common complication of percutaneous coronary intervention (PCI). Identifying patients at high CIN risk remains challenging. The triglyceride-glucose (TyG) index may help predict CIN but evidence is limited. We conducted a meta-analysis to evaluate the diagnostic value of TyG index for CIN after PCI.

Methods: A systematic literature search was performed in MEDLINE, Cochrane, and EMBASE until August 2023 (PROSPERO registration: CRD42023452257). Observational studies examining TyG index for predicting CIN risk in PCI patients were included. This diagnostic meta-analysis aimed to evaluate the accuracy of the TyG index in predicting the likelihood of CIN. Secondary outcomes aimed to assess the pooled incidence of CIN and the association between an elevated TyG index and the risk of CIN.

Results: Five studies (Turkey, n=2; China, n=3) with 3518 patients (age range: 57.6 to 68.22 years) were included. The pooled incidence of CIN was 15.3% [95% confidence interval (CI) 11-20.8%]. A high TyG index associated with increased CIN risk (odds ratio: 2.25, 95% CI 1.82-2.77). Pooled sensitivity and specificity were 0.77 (95% CI 0.59-0.88) and 0.55 (95% CI 0.43-0.68) respectively. Analysis of the summary receiver operating characteristic (sROC) curve revealed an area under the curve of 0.69 (95% CI 0.65-0.73). There was a low risk of publication bias (p = 0.81).

Conclusion: The TyG index displayed a noteworthy correlation with the risk of CIN subsequent to PCI. However, its overall diagnostic accuracy was found to be moderate in nature. While promising, the TyG index should not be used in isolation for CIN screening given the heterogeneity between studies. In addition, the findings cannot be considered conclusive given the scarcity of data. Further large-scale studies are warranted to validate TyG cutoffs and determine how to optimally incorporate it into current risk prediction models.

Systematic Review Registration: https://www.crd.york.ac.uk/prospero/display_record.php?ID=CRD42023452257, identifier CRD42023452257.

KEYWORDS

contrast-induced nephropathy, triglyceride-glucose index, meta-analysis, insulin resistance, cardiovascular disease

1 Introduction

Contrast-induced nephropathy (CIN), characterized by rapidly declining renal function following the administration of iodinated contrast agents, is the most commonly encountered dilemma during percutaneous coronary intervention (PCI) (1–4). CIN is associated with poor clinical outcomes including long-term deterioration in kidney function and increased mortality risk (5–7). Therefore, identifying patients at high risk of CIN is crucial to optimize prevention strategies and clinical management. Predicting CIN involved assessing risk factors and identifying high-risk patients, which remains challenging (1, 3, 8). To date, although pre-existing kidney disease, diabetes, advanced age, hypertension, and heart failure are reported as risk factors of CIN, whether other index also contribute to the development of CIN is still largely unknown (1, 2, 8).

Research interest has recently focused on exploring whether certain metabolic markers could further refine CIN risk stratification. The triglyceride–glucose (TyG) index, which is determined by fasting triglyceride and glucose levels, has been regarded as a marker representing insulin resistance and metabolic status (9–11). TyG index was calculated as the Ln [fasting triglycerides(mg/dl) × fasting glucose (mg/dL)/2]. Studies have suggested that the TyG index could serve as a predictive marker for cardiovascular risk such as coronary artery disease, heart attack, and stroke (9, 10, 12). In addition, some studies have explored the potential connection between the TyG index and nephropathy, particularly in diabetic nephropathy (13–17). A higher TyG index, indicative of insulin resistance, can contribute to inflammation, oxidative stress, and vascular dysfunction (9, 15, 18). In addition, the TyG index exhibits a positive correlation with a high risk of developing diabetic nephropathy and other renal-related complications (15, 17).

Emerging evidence suggests that the TyG index may predict the risk of CIN (13, 14). For instance, Aktas et al. found that the TyG index was an independent predictor of CIN in 272 patients without diabetes who were undergoing PCI for non-ST elevation myocardial infarction (13). In another study of 350 patients without diabetes who were undergoing PCI for acute coronary syndrome, Gursoy and Baydar observed that the incidence of CIN was significantly higher in those with high TyG indices (≥8.65) than in those with lower indices (<8.65) (14). Importantly, the predictive value of the TyG index for CIN appears to be present even after adjusting for potential confounders such as diabetes status (13, 14). While promising, research on the TyG index and CIN risk remains limited. Only a few studies, mainly from China and Turkey, with relatively small sample sizes, have examined this association (13–17). Moreover, the diagnostic accuracy of the TyG index remains unclear. Further investigation through meta-analyses could help synthesize the current evidence regarding the utility of the TyG index as a predictor of CIN in patients undergoing PCI. Thus, in this diagnostic meta-analysis, we aimed to investigate whether the TyG index could be used to predict the likelihood of CIN in patients receiving PCI.

2 Methods

2.1 Protocol registration

This report was presented in compliance with the PRISMA guidelines and registered in PROSPERO (CRD42023452257).

2.2 Literature search

Potentially relevant articles were identified following searches of electronic databases such as MEDLINE, Cochrane Library, and EMBASE, spanning from their inception to August 3, 2023. The search was conducted using relevant keywords: ("PCI" or "Left Main Disease" or "Coronary Angiograph*" or "coronary artery disease" or "Percutaneous Coronary Intervention" or "Myocardial infarction" or "MI") and ("Triglyceride–Glucose Index" or "Triglyceride–Glucose Indices" or "TyG" or "insulin resistance"), and ("CI-AKI" or "CA-AKI" or "Contrast-induced acute kidney

injury" or "Contrast-Associated Acute Kidney Injury" or "Contrast-Induced Nephropathy" or "Contrast-Associated Nephropathy" or "Acute Renal Insufficiency" or "Acute Kidney Insufficiency" or "Renal Insufficienc*" or "Kidney insufficienc*" or "Acute kidney injury" or "AKI" or "Nephropathy"). Using a comprehensive approach, controlled vocabulary search terms were used alongside keyword searches to enhance the breadth of the literature exploration. Furthermore, the reference lists from the acquired studies were manually checked to find potentially suitable articles. The search was comprehensive and was not limited by country or language of publication. Supplementary Table 1 provides detailed information of the search strategies.

2.3 Inclusion and exclusion criteria

In this meta-analysis, the selection of studies for inclusion adhered to predefined criteria: (1) the studies encompassed patients with coronary disease who had undergone coronary angiography or PCI, (2) the studies employed the TyG index as a predictive measure for CIN risk, and (3) these studies furnished comprehensive data concerning sensitivity, specificity, and count of patients with CIN. Randomized controlled trials or retrospective study designs (e.g., case–control studies) were deemed suitable for this meta-analysis.

Studies were excluded if (1) they were exclusively presented as conference papers, case series, abstracts, or review articles; (2) they concentrating on outcomes other than CIN; and (3) they did not provide full-text versions.

2.4 Data retrieval

Two team members extracted information separately from the individual research papers, and any differences were resolved through discussion. To gather any missing details, efforts were made to communicate with the corresponding author of the studies. The extracted data for each study included the country of origin, author's details, sample size, study setting, age, sex, information on specificity/sensitivity values, details related to the TyG index, and count of patients with CIN.

2.5 Outcomes

This diagnostic meta-analysis was conducted to appraise the precision of the TyG index in anticipating the probability of CIN, as per the definitions employed in individual studies. Secondary outcomes sought to appraise the combined incidence of CIN and the relationship between a high TyG index and the risk of CIN.

2.6 Quality assessment

The Quality Assessment for Diagnostic Accuracy Studies-2 (QUADAS-2) tool was used to assess the risk of bias (19). Four main domains including patient selection, index test, reference standard, and flow and timing were systematically examined to identify sources of bias. Two authors conducted a subjective review of all eligible studies to establish consistency. By using the QUADAS-2 tool, the authors assigned each domain to one of three categories: 'low risk,' 'some concerns,' or 'high risk. Discussions were held to resolve discrepancies.

2.7 Statistical analysis

For all statistical analyses, Stata version 15.0 and RevMan version 5.4 were used. The sensitivity and specificity were extracted from each study and pooled. Heterogeneity was assessed using the I^2 statistic, where an I^2 >50% signifies significant heterogeneity. Publication bias was evaluated through Deeks' funnel plot asymmetry test. To summarize the diagnostic accuracy, a hierarchical summary receiver operating characteristic curve was constructed, and the area under the curve (AUC) was calculated. Fagan's nomogram was utilized to estimate post-test probability based on likelihood ratios (LRs) (20). A positive LR in the range of 2–5 slightly increase the likelihood of disease presence following the test, whereas ratios ranging from 5 to 10 moderately enhance the likelihood; ratios >10 significantly amplify the probability of having the disease (21). The predictive utility of the TyG index was assessed by examining how the post-test probability changed from the pre-test probability. Two-sided tests in all statistical analyses were conducted at a significance level of 0.05.

3 Results

3.1 Database searching and study characteristics

Through a search on four electronic databases, 890 records were discovered (Figure 1). By eliminating duplicate studies (n = 130) and carrying out initial title and abstract examination (n = 760), 15 articles emerged as potentially aligned with the predefined inclusion criteria. Subsequent full-text reading led to the exclusion of 10 studies. Ultimately, five studies met the predetermined requirements and were included in the meta-analysis (13–17).

The characteristics of studies involving 3518 patients are summarized in Table 1. All studies were conducted in two countries, including Turkey (n = 2) (13, 14) and China (n = 3) (15–17). In these studies, the age range of the patients fell between 57.6 and 68.22 years. The number of participants varied across the studies, ranging from 272 to 1108, with male proportions ranging from 52.3% to 79.4%. Among the five studies, two on patients without diabetes mellitus (DM) (13, 14), while two targeted patients with DM (15, 17). However, one study did not explicitly specify this information (16). Regarding the definition of CIN, three studies adopted the same criteria, defining CIN as either a 25% increase or a 0.5 mg/dL increase in serum creatinine (Scr) levels from baseline within the first 48–72 h (13, 14, 16). In another study, CIN was defined as a 50% increase or a ≥0.3 mg/dL increase in Scr levels from baseline within 1 week (15). However, one study did not specify the criteria used to define CIN (17). The AUC, which reflects the accuracy of the predictive models,

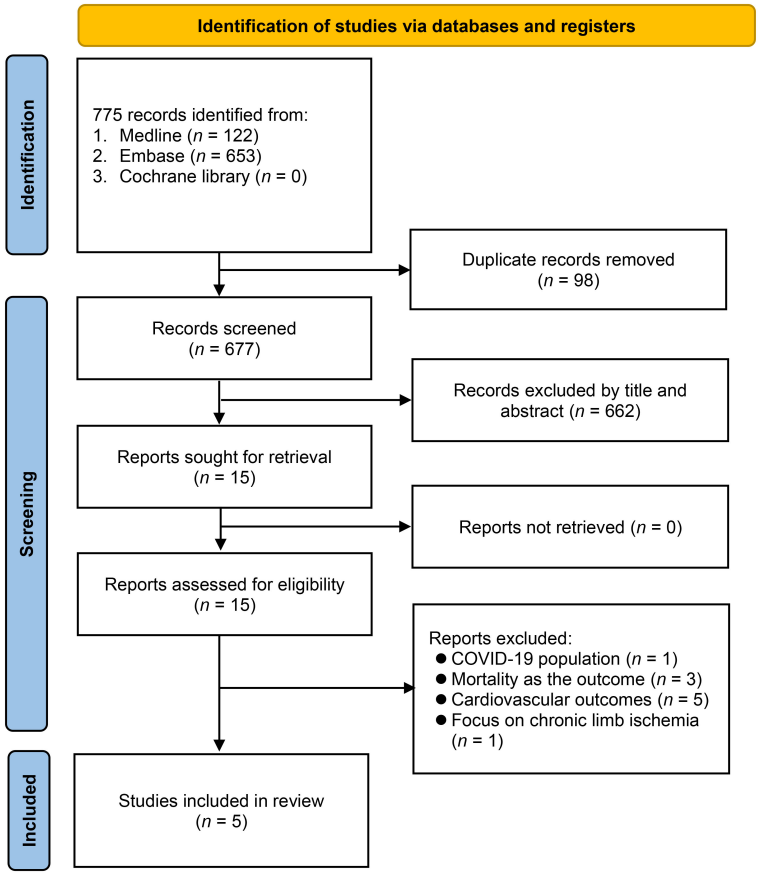

FIGURE 1
Flow chart for study selection.

ranged from 0.662 to 0.811. The sensitivity varied between 59.3% and 94.9%, while the specificity ranged between 31.7% and 72%. Four studies (13, 14, 16, 17) reported cutoff values to predict CIN occurrence, with the range being 8.69–9.17, while one study did not provide this information (15).

3.2 Risk of bias

The risk of bias and applicability concerns for the five included studies are shown in Figure 2. Overall, the majority of studies displayed a low risk of bias across the assessed domains. The primary areas of concern were related to the measurement of the TyG index in one study (15) and the definition of CIN in another (17). Apart from these issues, patient selection, index tests, reference standards, and flow/timing exhibited a low risk of bias in the included studies.

3.3 Outcomes

3.3.1 Pooled incidence of CIN

The incidence of CIN varied among studies, with the lowest being 6.6% in a study from Turkey (13), and the highest reaching 21.2% in a study conducted in China (17). After pooling data from a total of 3518 patients, the combined incidence of CIN was 15.3% (95% confidence interval [CI] 11% to 20.8%) (Figure 3).

3.3.2 Association between the TyG index and CIN risk

Five studies consistently demonstrated a positive relationship between the TyG index and CIN risk. Upon calculation, a high TyG index was associated with an increased risk of CIN, with an odds ratio of 2.25 (95% CI 1.82–2.77, $p < 0.00001$) (Figure 4). The level of heterogeneity across these studies was moderate ($I^2 = 35\%$).

3.3.3 Diagnostic efficacy of the TyG index for CIN

In relation to the diagnostic effectiveness of the TyG index, the combined sensitivity and specificity values were 0.77 (95% CI 0.59–0.88) and 0.55 (95% CI 0.43–0.68), respectively, accompanied by I^2 values of 95.1% for sensitivity and 98.29% for specificity (Figure 5). The aggregated AUC was 0.69 (95% CI 0.65–0.73) (Figure 6). Fagan's nomogram plot, presented in Figure 7, provides a visualization of post-test probabilities derived from the LRs. Specifically, an LR of 2 translates to a marginal increment in the probability of a positive outcome, while an LR of 0.42 signifies a minor reduction in the likelihood of a negative outcome. Notably, Deek's funnel plot asymmetry test demonstrated a low susceptibility to publication bias ($p = 0.81$) (Figure 8).

10.3389/fendo.2023.1282675

TABLE 1 Characteristics of studies (n = 5).

Parameters	Aktas 2023	Cursoy 2023	Hu 2022	Li 2022	Qin 2021
Age (years)	60.47 ± 12.25	57.6 vs 56.5	65 (56-71)	66.4 ± 10.4	68.22 ± 10.6
Male (%)	79.4%	52.3%	62.4%	62.5%	68.7%
BMI (kg/m^2) or weight (kg)	27.2 ± 3.3	76 vs. 76	24.5 (23-26.8)	24.9 ± 3.2	25.0 ± 3.7
N	272	350	860	1108	928
Population	Non-DM patients with NSTEMI	Non-DM patients with NSTEMI	DM patients with ACS	Patients with NSTE-ACS	DM patients with MI
CIN %	6.6%	16%	19.9%	15.1%	21.2%
Definition of CIN	A 25% or 0.5 mg/dL increase in Scr from baseline within the first 48-72 hours.	A 25% or 0.5 mg/dL increase in Scr from baseline within the first 48-72 hours.	A 50% or ≥0.3 mg/dL increase in Scr from baseline within one week	A 25% or 0.5 mg/dL increase in Scr from baseline within the first 48-72 hours.	Based on the preoperative and postoperative Scr, as measured within one week
AUC	0.712	0.666	0.811	0.662	0.728
Sensitivity	61%	71.4%	77.9%	59.3%	94.9%
Specificity	72%	55.1%	31.7%	66.1%	51.3%
Cut-off values for TyG index	9.17	8.69	NA	9.043	8.88
Country	Turkey	Turkey	China	China	China

Scr, serum creatinine; CIN, contrast-induced nephropathy; TyG, triglyceride-glucose; BMI, body mass index; AUC, area under curve; DM, diabetes mellitus.

4 Discussion

On five studies involving 3518 patients with or without DM, patients with a high TyG index were prone to CIN than those with a low index. Regarding the diagnostic efficacy of TyG, the pooled AUC was 0.69, and the pooled sensitivity and specificity were 0.77 and 0.55, respectively. Although several risk factors correlated with CIN development, such as pre-existing kidney disease, diabetes, and heart failure (22–24), whether insulin resistance-associated index could predict CIN following PCI remains unknown. Hereby, this

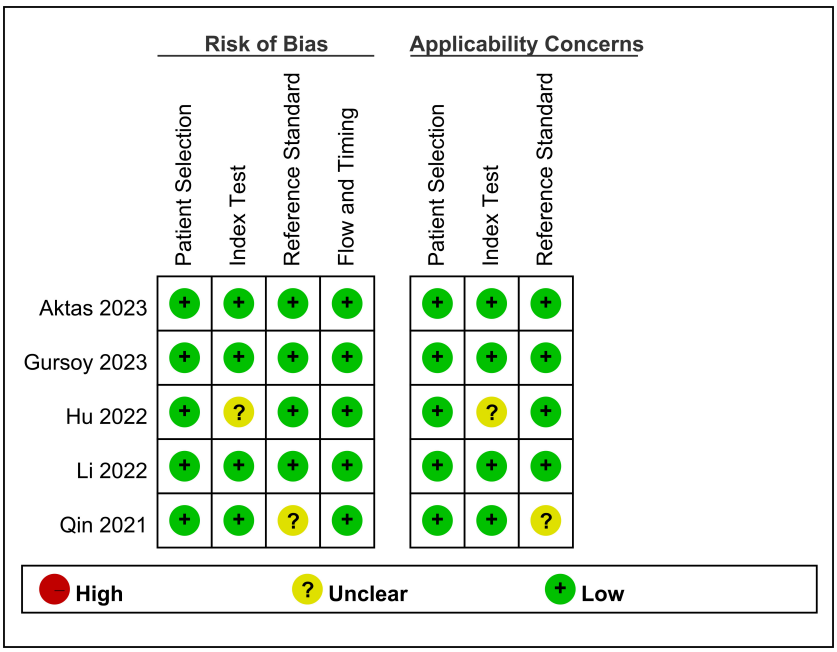

FIGURE 2
Methodological quality summary of included studies.

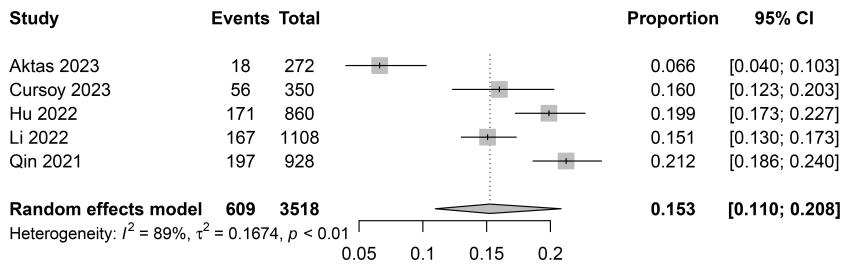

FIGURE 3
Pooled incidence of contrast-induced nephropathy (CIN).

diagnostic meta-analysis highlighted that the TyG index could be a marker that reflects the risk of CIN development in patients receiving PCI.

To date, several risk scores have been established to predict CIN development. For instance, the Mehran contrast nephropathy risk score including hypotension, intra-aortic balloon pump (IABP), heart failure, chronic renal failure, diabetes, old age (>75 years), anemia, and contrast volume, was reported to sensitively predict CIN post-PCI (22). In another study of CIN in patients with ST-segment elevation myocardial infarction who received primary PCI, Koowattanatianchai et al. attempted to set up a simpler predictive model than the Mehran risk score (23). They found that three final predictors, which were ejection fraction of <40%, triple-vessel disease, and use of IABP were the most powerful predictors for the risk stratification of CIN (23). Upon reviewing 16 studies, including 12 prediction models, Silver et al. identified pre-existing chronic kidney disease, age, diabetes, heart failure or impaired ejection fraction, and shock as risk factors for CIN (24). In another meta-analysis, Yin et al. observed that the Maioli score had the best discrimination for CIN occurrence (25, 26). Nevertheless, most studies were based on single-center setting and lacked external validations (25). Thus, a comprehensive review including multiple institutes are necessary to evaluate and discover novel predictive markers for the risk stratification of CIN.

In a study of 1108 patients undergoing PCI for non-ST elevation acute coronary syndrome, the TyG index was identified as an independent predictor of CIN in the multivariate analysis, with a J-shaped association observed between the TyG index and the CIN risk after adjusting for confounders such as DM and kidney function (16). Our pooled meta-analysis also confirmed a significant association between the TyG index and CIN risk (odds ratio: 2.25; I^2: 35%). However, our meta-analysis, which encompasses five studies with a total of 3518 patients, provides a more substantial evidence base compared to the single study involving 1108 patients (16). This larger pooled dataset enhances the generalizability of the observed association and allows for a more robust analysis of the TyG index's predictive capacity for CIN. Compared with the TyG index, a recent meta-analysis of four studies involving 1346 patients found that gamma-glutamyl transferase (GGT) levels could potentially predict CIN in patients undergoing cardiac catheterization, showing a significantly higher GGT levels in patients with CIN (odds ratio: 3.21; I^2:91.93%) (27). In our previous meta-analysis, patients with a low prognostic nutritional index (PNI) demonstrated a higher risk of CIN than those with a high PNI, with an odds ratio of 3.362 (I^2 = 89.6%) (28). Although both GGT levels and PNI appear to have a stronger relationship with CIN than the TyG index, the relatively low heterogeneity in the current meta-analysis highlighted that the TyG index may be a reliable predictor of CIN.

Our meta-analysis found that the TyG index had the modest diagnostic accuracy based on the pooled sensitivity of 0.77 and specificity of 0.55. These results may be attributed to the complex, multifactorial mechanisms driving CIN, which are not yet fully elucidated. Proposed pathways for CIN include renal ischemia and hypoxia from altered hemodynamics, direct tubular cytotoxicity, and inflammation/oxidative stress (4, 29, 30). More specifically, contrast agents can reduce renal blood flow through the effects on vasoactive mediators such as nitric oxide and endothelin-1, leading to ischemic injury (4). Contrast media may directly induce tubular epithelial cell damage by increasing intracellular calcium levels, disrupting the mitochondria, and generating reactive oxygen species (29). In addition, the high osmolality and viscosity of some agents can impair tubular cell function and morphology

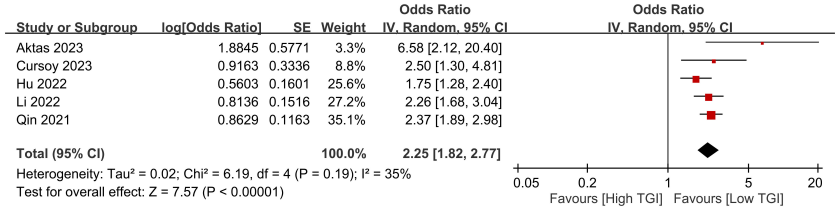

FIGURE 4
Forest plot showing a positive relationship between a high triglyceride–glucose (TyG) index and the risk of contrast-induced nephropathy.

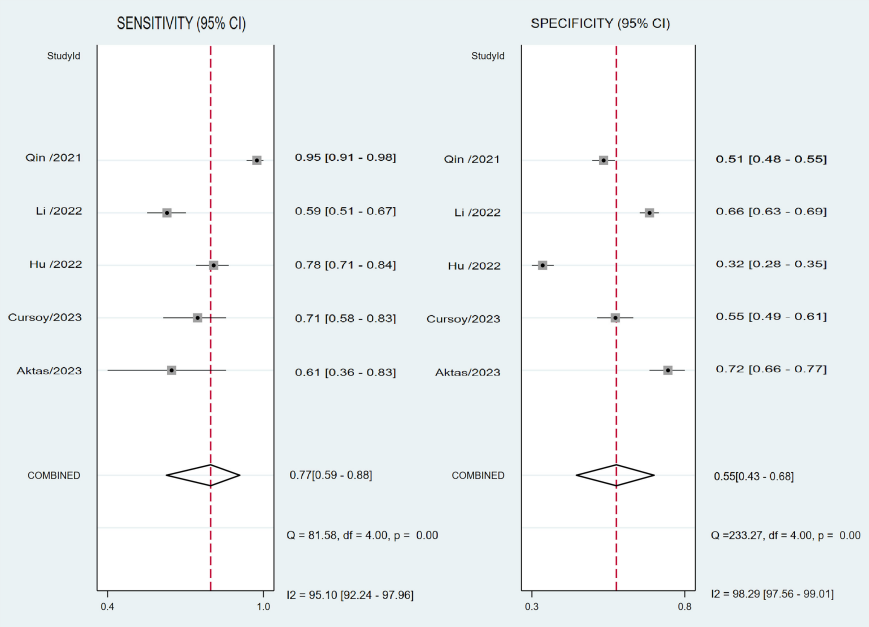

FIGURE 5
Forest plot depicting the combined sensitivity and specificity of the triglyceride–glucose (TyG) index in predicting contrast-induced nephropathy.

(29). Finally, contrast-mediated CIN may involve free radical formation that damages cell membranes and activation of inflammatory and immunologic cascades (30). Consistently, the observed moderate diagnostic efficacy of the TyG index in predicting CIN might be attributed to the presence of multifactorial mechanisms contributing to CIN. Although the TyG index may not be used in isolation for screening, it may be a supplemental predictor to improve CIN detection.

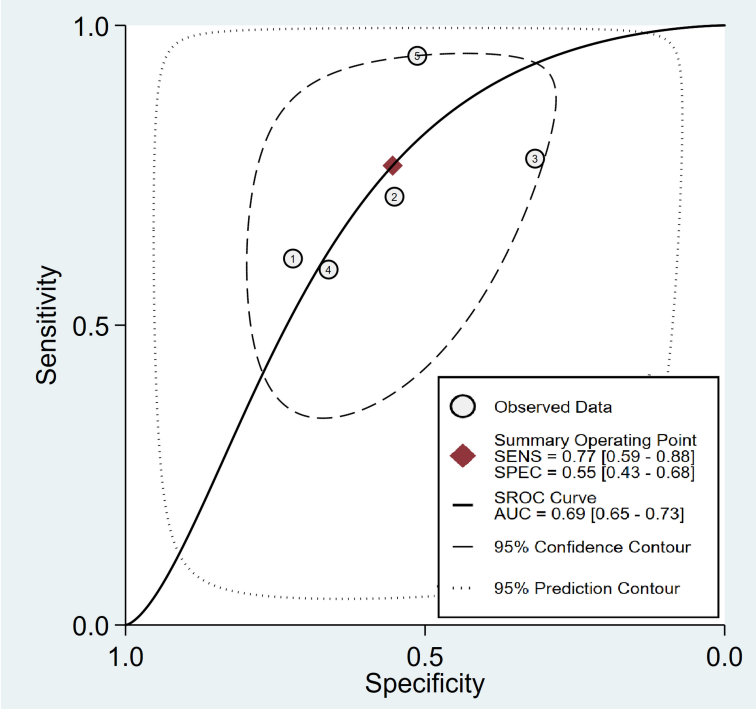

FIGURE 6
Analysis on summary receiver operating characteristic (sROC) curve demonstrating the predictive effectiveness of the triglyceride–glucose Index concerning contrast-induced nephropathy.

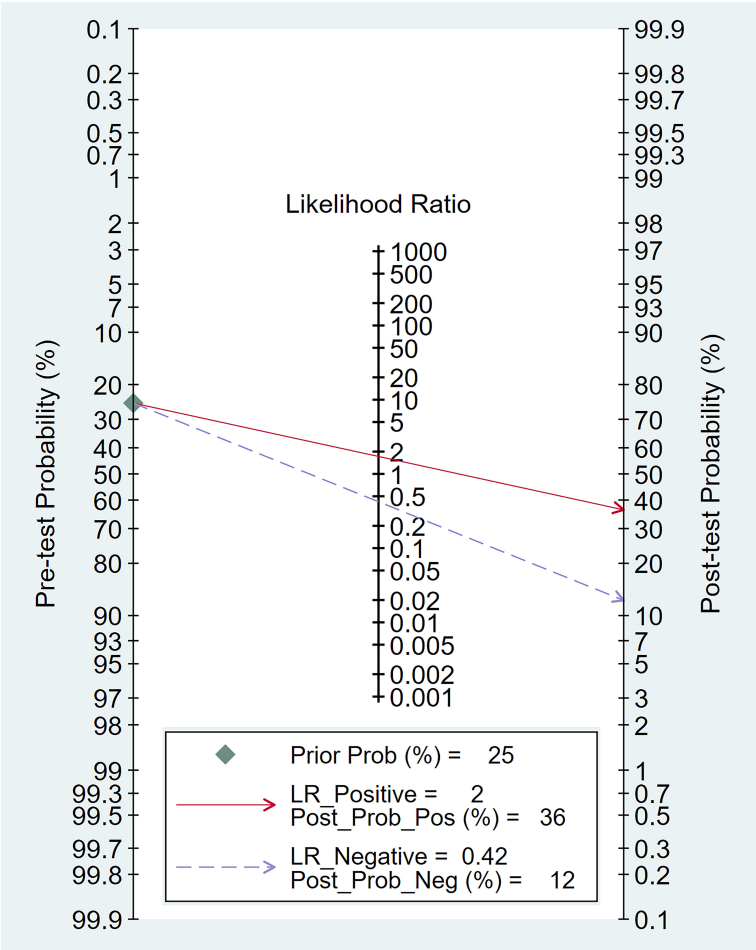

FIGURE 7
The clinical applicability of the triglyceride–glucose (TyG) index in forecasting the occurrence of contrast-induced nephropathy illustrated through Fagan's nomogram plot.

In current meta-analysis, while studies adjusted for potential confounders such as diabetes and kidney function, other factors like contrast volume and hemodynamic instability were not consistently adjusted for across studies included. Failure to control for all potential mediating and moderating variables may weaken the observed TyG-CIN association. In addition, the heterogeneity between studies regarding patient characteristics, TyG cutoffs, and CIN definitions may have reduced the predictive value of the TyG index. Future studies should focus on optimally adjusting for possible confounders to elucidate the independent contribution of the TyG index to CIN occurrence.

Regarding the pathophysiological link between the TyG index and the risk of CIN, while our study did not directly investigate the underlying mechanisms, we can speculate based on existing literature. Metabolic syndrome, which is characterized by a cluster of conditions including insulin resistance, hypertension, dyslipidemia, and obesity, has been reported in several studies to be a stronger predictor of CIN (31, 32). Given that the TyG index is a recognized surrogate marker for insulin resistance and has been associated with metabolic syndrome (33, 34), it is plausible to consider the TyG index as a potential predictive marker for CIN.

The TyG index has garnered attention because of its potential clinical applications, particularly in the assessment of insulin resistance (9, 12). High TyG index levels are linked to reduced insulin sensitivity (9). This metric can be an initial screening tool for identifying individuals at risk of insulin resistance (9). Furthermore, the TyG index allows for monitoring alterations in insulin resistance and metabolic well-being in response to interventions such as lifestyle modification and medications (9, 12). A low TyG index could indicate enhanced insulin sensitivity and an improved metabolic status (35). The homeostasis model assessment of insulin resistance (HOMA-IR) is another commonly used marker of insulin resistance (36). However, the TyG index has some potential advantages over HOMA-IR. The TyG index requires only fasting glucose and triglyceride levels, which are routinely measured in clinical practice. In contrast, HOMA-IR calculation requires fasting insulin levels, which may not be routinely available. The simpler calculation and widespread availability of the components make the TyG index easily applicable. Furthermore, recent research highlights the TyG index as a superior alternative to HOMA-IR for predicting metabolic syndrome or type 2 diabetes, emphasizing its enhanced efficacy as a surrogate marker of insulin resistance (37, 38).

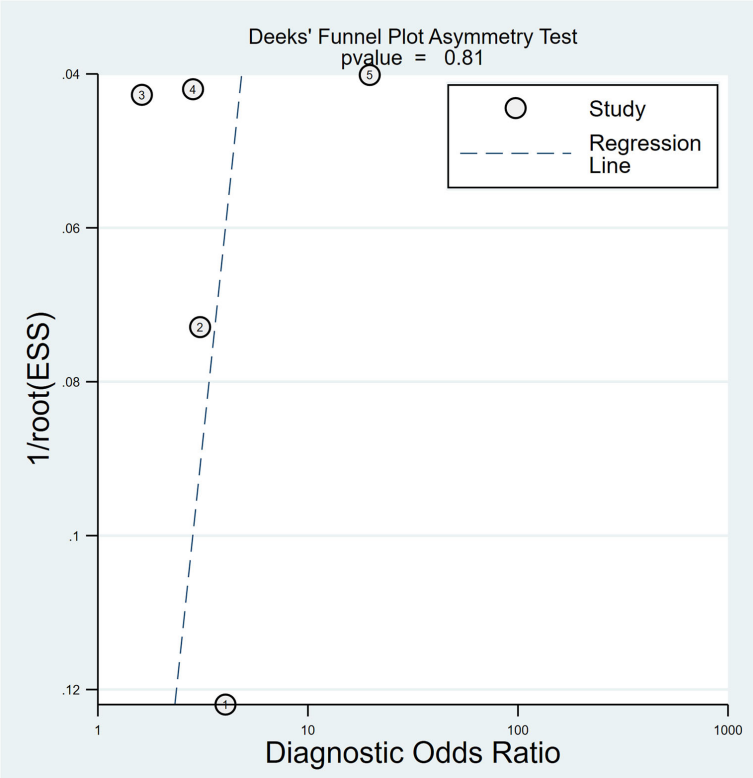

FIGURE 8
Utilizing Deek's funnel plot asymmetry test, the probability of publication bias was deemed minimal (p = 0.81).

Several systematic reviews and meta-analyses have examined the relationship between the TyG index and cardiovascular diseases (39–41). A recent meta-analysis of seven studies, contrasting the highest-TyG group with the lowest-TyG group, revealed a notable rise in the risk of heart failure for the higher-TyG group (i.e., HR: 1.21) (39). Another meta-analysis reported that individuals with elevated TyG index levels face an increased risk of cardiovascular disease [i.e., odds ratio: 1.94], more pronounced coronary artery lesions [odds ratio: 3.49], and a less favorable prognosis than those with lower TyG index levels (40). These studies highlight the growing evidence linking the TyG index to increased risks of various cardiovascular diseases. In addition, studies have explored the potential link between the TyG index and nephropathy, particularly in the context of diabetic nephropathy (23, 25, 26). Thus, while the TyG index holds promise across various clinical applications, our meta-analysis suggested that it should not be solely relied upon as a diagnostic tool. Its interpretation should be complemented with other clinical data, including patient history, physical examinations, and supplementary laboratory tests.

Compared with other metabolic predictors, the TyG index had better diagnostic performance for predicting CIN compared with HbA1c, fasting glucose, or triglycerides alone based on the AUC analysis (16). However, the ideal approach for integrating the TyG index into CIN prediction remains unclear, as our meta-analysis relied on aggregate study-level data. A previous study found that adding TyG to the Mehran risk score increased its predictive accuracy from 62.3% to 71.2% and incorporating TyG improved risk reclassification compared with adding fasting blood glucose alone (16). This suggests that the TyG index may have incremental value when combined with established risk factors or prediction models.

This meta-analysis is the first to specifically assess and quantify the TyG index's overall diagnostic accuracy in predicting the risk of CIN in patients undergoing PCI. While previous research has primarily concentrated on the TyG index's relationship with diabetic nephropathy, our meta-analysis extends the scope by focusing on its utility in predicting CIN post-PCI. We provide pooled estimates for the sensitivity and specificity of the TyG index, offering a comprehensive view of its diagnostic performance as a predictor for CIN. This meta-analysis not only yields a more accurate assessment of the link between a heightened TyG index and the risk of CIN but also underscores the need for more extensive studies to determine optimal TyG thresholds and to confirm its predictive value across diverse populations.

This meta-analysis has several limitations. First, while showing promise, the evidence base remains limited to just a handful of studies conducted mainly in two countries. Larger scale and more geographically diverse studies are needed to confirm the association between the TyG index and CIN risk. Second, as our meta-analysis found significant heterogeneity between studies, optimal TyG index cutoff values for predicting CIN risk may differ based on patient population characteristics. Careful calibration is necessary before applying proposed cutoffs such as 8.69–9.17 from these studies. Third, this study only investigated the predictive utility of baseline

or pre-procedural TyG index. Changes in the TyG index during hospitalization may also correlate with CIN but were not examined here. Finally, the lack of individual patient data precluded more detailed assessment of how the TyG index could enhance existing CIN prediction models. Future pooled analyses should focus on optimally incorporating the TyG index into the risk stratification.

5 Conclusion

The results of this meta-analysis showed that patients who received PCI with a higher TyG index were at an increased risk to develop CIN than those with a low index. In addition to the conventional risk factors, the TyG index may be used as an additional predictor of CIN. Nevertheless, CIN can stem from various factors. Therefore, clinical practitioners must take into account all potential risks holistically and evaluate each patient's situation individually. In addition, the small number of studies identified makes the results preliminary and precludes definitive conclusions. Larger studies are needed to validate the utility of the TyG index and determine appropriate cutoffs.

Data availability statement

The original contributions presented in the study are included in the article/Supplementary Material. Further inquiries can be directed to the corresponding author.

Author contributions

W-TC: Conceptualization, Writing – original draft, Writing – review & editing. C-CL: Conceptualization, Investigation, Writing – original draft. Y-TH: Data curation, Formal Analysis, Investigation, Software, Writing – original draft. J-YW: Formal Analysis, Methodology, Software, Writing – original draft. W-WT: Investigation, Methodology, Resources, Writing – original draft. K-CH: Writing – original draft, Writing – review & editing. I-WC: Supervision, Writing – original draft, Writing – review & editing. P-HF: Supervision, Writing – original draft, Writing – review & editing.

Funding

The author(s) declare financial support was received for the research, authorship, and/or publication of this article. This research was funded by Chi Mei Medical Center, Tainan, Taiwan, grant number CMOR11203. This work was supported by Chi Mei Medical Center, Liouying branch.

Conflict of interest

The authors declare that the research was conducted in the absence of any commercial or financial relationships that could be construed as a potential conflict of interest.

Publisher's note

Supplementary material

The Supplementary Material for this article can be found online at: https://www.frontiersin.org/articles/10.3389/fendo.2023.1282675/full#supplementary-material

References

1. Basta G, Chatzianagnostou K, Paradossi U, Botto N, Del Turco S, Taddei A, et al. The prognostic impact of objective nutritional indices in elderly patients with ST-elevation myocardial infarction undergoing primary coronary intervention. *Int J Cardiol* (2016) 221:987–92. doi: 10.1016/j.ijcard.2016.07.039

2. Kusirisin P, Chattipakorn SC, Chattipakorn N. Contrast-induced nephropathy and oxidative stress: mechanistic insights for better interventional approaches. *J Transl Med* (2020) 18:400. doi: 10.1186/s12967-020-02574-8

3. Wi J, Ko YG, Kim JS, Kim BK, Choi D, Ha JW, et al. Impact of contrast-induced acute kidney injury with transient or persistent renal dysfunction on long-term outcomes of patients with acute myocardial infarction undergoing percutaneous coronary intervention. *Heart* (2011) 97:1753–7. doi: 10.1136/hrt.2010.218677

4. McCullough PA, Choi JP, Feghali GA, Schussler JM, Stoler RM, Vallabahn RC, et al. Contrast-induced acute kidney injury. *J Am Coll Cardiol* (2016) 68:1465–73. doi: 10.1016/j.jacc.2016.05.099

5. James MT, Ghali WA, Tonelli M, Faris P, Knudtson ML, Pannu N, et al. Acute kidney injury following coronary angiography is associated with a long-term decline in kidney function. *Kidney Int* (2010) 78:803–9. doi: 10.1038/ki.2010.258

6. Ebert N, Schneider A, Huscher D, Mielke N, Balabanova Y, Brobert G, et al. Incidence of hospital-acquired acute kidney injury and trajectories of glomerular filtration rate in older adults. *BMC Nephrol* (2023) 24:226. doi: 10.1186/s12882-023-03272-5

7. Sun G, Chen P, Wang K, Li H, Chen S, Liu J, et al. Contrast-induced nephropathy and long-term mortality after percutaneous coronary intervention in patients with acute myocardial infarction. *Angiology* (2019) 70:621–6. doi: 10.1177/0003319718803677

8. Wu X, Ma C, Sun D, Zhang G, Wang J, Zhang E. Inflammatory indicators and hematological indices in contrast-induced nephropathy among patients receiving coronary intervention: A systematic review and meta-analysis. *Angiology* (2021) 72:867–77. doi: 10.1177/00033197211000492

9. Anto EO, Frimpong J, Boadu WIO, Korsah EE, Tamakloe V, Ansah E, et al. Cardiometabolic syndrome among general adult population in Ghana: The role of lipid accumulation product, waist circumference-triglyceride index, and triglyceride-glucose index as surrogate indicators. *Health Sci Rep* (2023) 6:e1419. doi: 10.1002/hsr2.1419

10. Boshen Y, Yuankang Z, Xinjie Z, Taixi L, Kaifan N, Zhixiang W, et al. Triglyceride-glucose index is associated with the occurrence and prognosis of cardiac arrest: a multicenter retrospective observational study. *Cardiovasc Diabetol* (2023) 22:190. doi: 10.1186/s12933-023-01918-0

11. Guerrero-Romero F, Simental-Mendía LE, González-Ortiz M, Martínez-Abundis E, Ramos-Zavala MG, Hernández-González SO, et al. The product of triglycerides and glucose, a simple measure of insulin sensitivity. Comparison with the euglycemic-hyperinsulinemic clamp. *J Clin Endocrinol Metab* (2010) 95:3347–51. doi: 10.1210/jc.2010-0288

12. Cai XL, Xiang YF, Chen XF, Lin XQ, Lin BT, Zhou GY, et al. Prognostic value of triglyceride glucose index in population at high cardiovascular disease risk. *Cardiovasc Diabetol* (2023) 22:198. doi: 10.1186/s12933-023-01924-2

13. Aktas H, Inci S, Gul M, Gencer S, Yildirim O. Increased triglyceride-glucose index predicts contrast-induced nephropathy in non-diabetic NSTEMI patients: A prospective study. *J Investig Med* (2023) 71(8):838–44. doi: 10.1177/10815589231182317

14. Gursoy E, Baydar O. The triglyceride-glucose index and contrast-induced nephropathy in non-ST elevation myocardial infarction patients undergoing percutaneous coronary intervention. *Med (Baltimore)* (2023) 102:e32629. doi: 10.1097/MD.0000000000032629

15. Hu Y, Wang X, Xiao S, Sun N, Huan C, Wu H, et al. A clinical nomogram based on the triglyceride-glucose index to predict contrast-induced acute kidney injury after percutaneous intervention in patients with acute coronary syndrome with diabetes mellitus. *Cardiovasc Ther* (2022) 2022:5443880. doi: 10.1155/2022/5443880

16. Li M, Li L, Qin Y, Luo E, Wang D, Qiao Y, et al. Elevated TyG index predicts incidence of contrast-induced nephropathy: A retrospective cohort study in NSTE-ACS patients implanted with DESs. *Front Endocrinol (Lausanne)* (2022) 13:817176. doi: 10.3389/fendo.2022.817176

17. Qin Y, Tang H, Yan G, Wang D, Qiao Y, Luo E, et al. A high triglyceride-glucose index is associated with contrast-induced acute kidney injury in Chinese patients with type 2 diabetes mellitus. *Front Endocrinol (Lausanne)* (2020) 11:522883. doi: 10.3389/fendo.2020.522883

18. Lin HY, Zhang XJ, Liu YM, Geng LY, Guan LY, Li XH. Comparison of the triglyceride glucose index and blood leukocyte indices as predictors of metabolic syndrome in healthy Chinese population. *Sci Rep* (2021) 11:10036. doi: 10.1038/s41598-021-89494-9

19. Whiting PF, Rutjes AW, Westwood ME, Mallett S, Deeks JJ, Reitsma JB, et al. QUADAS-2: a revised tool for the quality assessment of diagnostic accuracy studies. *Ann Internal Med* (2011) 155:529–36. doi: 10.7326/0003-4819-155-8-201110180-00009

20. Tsai WW, Hung KC, Huang YT, Yu CH, Lin CH, Chen IW, et al. Diagnostic efficacy of sonographic measurement of laryngeal air column width difference for predicting the risk of post-extubation stridor: A meta-analysis of observational studies. *Front Med* (2023) 10:1109681. doi: 10.3389/fmed.2023.1109681

21. Grimes DA, Schulz KF. Refining clinical diagnosis with likelihood ratios. *Lancet (London England)* (2005) 365:1500–5. doi: 10.1016/S0140-6736(05)66422-7

22. Mehran R, Aymong ED, Nikolsky E, Lasic Z, Iakovou I, Fahy M, et al. A simple risk score for prediction of contrast-induced nephropathy after percutaneous coronary intervention: development and initial validation. *J Am Coll Cardiol* (2004) 44:1393–9. doi: 10.1016/j.jacc.2004.06.068

23. Koowattanatianchai S, Chantadansuwan T, Kaladee A, Phinyo P, Patumanond J. Practical risk stratification score for prediction of contrast-induced nephropathy after primary percutaneous coronary intervention in patients with acute ST-segment elevation myocardial infarction. *Cardiol Res* (2019) 10:350–7. doi: 10.14740/cr939

24. Silver SA, Shah PM, Chertow GM, Harel S, Wald R, Harel Z. Risk prediction models for contrast induced nephropathy: systematic review. *BMJ* (2015) 351:h4395. doi: 10.1136/bmj.h4395

25. Yin W, Zhou G, Zhou L, Liu M, Xie Y, Wang J, et al. Validation of pre-operative risk scores of contrast-induced acute kidney injury in a Chinese cohort. *BMC Nephrol* (2020) 21:45. doi: 10.1186/s12882-020-1700-8

26. Maioli M, Toso A, Gallopin M, Leoncini M, Tedeschi D, Micheletti C, et al. Preprocedural score for risk of contrast-induced nephropathy in elective coronary angiography and intervention. *J Cardiovasc Med (Hagerstown)* (2010) 11:444–9. doi: 10.2459/JCM.0b013e328335227c

27. Javid M, Mirdamadi A, Javid M, Amini-Salehi E, Vakilpour A, Keivanlou MH, et al. Gamma glutamyl transferase as a biomarker to predict contrast-induced nephropathy among patients with acute coronary syndrome undergoing coronary interventions: a meta-analysis. *Ann Med Surg* (2023) 85:4033–40. doi: 10.1097/MS9.0000000000000967

28. Chang WT, Sun CK, Wu JY, Huang PY, Liu TH, Chang YJ, et al. Association of prognostic nutritional index with risk of contrast induced nephropathy: A meta-analysis. *Front Nutr* (2023) 10:1154409. doi: 10.3389/fnut.2023.1154409

29. Andreucci M, Faga T, Pisani A, Sabbatini M, Michael A. Acute kidney injury by radiographic contrast media: pathogenesis and prevention. *BioMed Res Int* (2014) 2014:362725. doi: 10.1155/2014/362725

30. Romano G, Briguori C, Quintavalle C, Zanca C, Rivera NV, Colombo A, et al. Contrast agents and renal cell apoptosis. *Eur Heart J* (2008) 29:2569–76. doi: 10.1093/eurheartj/ehn197

31. Amiri A, Ghanavati R, Riahi Beni H, Sezavar SH, Sheykhvatan M, Arab M. Metabolic syndrome and the iodine-dose/creatinine clearance ratio as determinants of contrast-induced acute kidney injury. *Cardiorenal Med* (2018) 8:217–27. doi: 10.1159/000488374

32. Ozcan OU, Adanir Er H, Gulec S, Ustun EE, Gerede DM, Goksuluk H, et al. Impact of metabolic syndrome on development of contrast-induced nephropathy after elective percutaneous coronary intervention among nondiabetic patients. *Clin Cardiol* (2015) 38:150–6. doi: 10.1002/clc.22364

33. Couto AN, Pohl HH, Bauer ME, Schwanke CHA. Accuracy of the triglyceride-glucose index as a surrogate marker for identifying metabolic syndrome in non-diabetic individuals. *Nutr (Burbank Los Angeles County Calif)* (2023) 109:111978. doi: 10.1016/j.nut.2023.111978

34. Raimi TH, Dele-Ojo BF, Dada SA, Fadare JO, Ajayi DD, Ajayi EA, et al. Triglyceride-glucose index and related parameters predicted metabolic syndrome in Nigerians. *Metab syndrome related Disord* (2021) 19:76–82. doi: 10.1089/met.2020.0092

35. Sanchez-Garcia A, Rodriguez-Gutierrez R, Mancillas-Adame L, Gonzalez-Nava V, Diaz Gonzalez-Colmenero A, Solis RC, et al. Diagnostic accuracy of the triglyceride and glucose index for insulin resistance: A systematic review. *Int J Endocrinol* (2020) 2020:4678526. doi: 10.1155/2020/4678526

36. Matthews DR, Hosker JP, Rudenski AS, Naylor BA, Treacher DF, Turner RC. Homeostasis model assessment: insulin resistance and beta-cell function from fasting plasma glucose and insulin concentrations in man. *Diabetologia* (1985) 28:412–9. doi: 10.1007/BF00280883

37. Park HM, Lee HS, Lee YJ, Lee JH. The triglyceride-glucose index is a more powerful surrogate marker for predicting the prevalence and incidence of type 2 diabetes mellitus than the homeostatic model assessment of insulin resistance. *Diabetes Res Clin practice* (2021) 180:109042. doi: 10.1016/j.diabres.2021.109042

38. Son DH, Lee HS, Lee YJ, Lee JH, Han JH. Comparison of triglyceride-glucose index and HOMA-IR for predicting prevalence and incidence of metabolic syndrome. *Nutrition metabolism Cardiovasc diseases: NMCD.* (2022) 32:596–604. doi: 10.1016/j.numecd.2021.11.017

39. Khalaji A, Behnoush AH, Khanmohammadi S, Ghanbari Mardasi K, Sharifkashani S, Sahebkar A, et al. Triglyceride-glucose index and heart failure: a systematic review and meta-analysis. *Cardiovasc Diabetol* (2023) 22:244. doi: 10.1186/s12933-023-01973-7

40. Liang S, Wang C, Zhang J, Liu Z, Bai Y, Chen Z, et al. Triglyceride-glucose index and coronary artery disease: a systematic review and meta-analysis of risk, severity, and prognosis. *Cardiovasc Diabetol* (2023) 22:170. doi: 10.1186/s12933-023-01906-4

41. Ding X, Wang X, Wu J, Zhang M, Cui M. Triglyceride-glucose index and the incidence of atherosclerotic cardiovascular diseases: a meta-analysis of cohort studies. *Cardiovasc Diabetol* (2021) 20:76. doi: 10.1186/s12933-021-01268-9

frontiers | Frontiers in Endocrinology

TYPE Review
PUBLISHED 20 December 2023
DOI 10.3389/fendo.2023.1320603

OPEN ACCESS

EDITED BY
Federica Mescia,
University of Brescia, Italy

REVIEWED BY
Karoline Schousboe,
Odense University Hospital, Denmark
Bertram Pitt,
University of Michigan, United States

*CORRESPONDENCE
Tianbiao Zhou
zhoutb@aliyun.com

RECEIVED 12 October 2023
ACCEPTED 04 December 2023
PUBLISHED 20 December 2023

CITATION
Chen W, Zheng L, Wang J, Lin Y and Zhou T (2023) Overview of the safety, efficiency, and potential mechanisms of finerenone for diabetic kidney diseases.
Front. Endocrinol. 14:1320603.
doi: 10.3389/fendo.2023.1320603

Overview of the safety, efficiency, and potential mechanisms of finerenone for diabetic kidney diseases

Wenmin Chen, Lingqian Zheng, Jiali Wang, Yongda Lin and Tianbiao Zhou*

Department of Nephrology, The Second Affiliated Hospital of Shantou University Medical College, Shantou, China

Diabetic kidney disease (DKD) is a common disorder with numerous severe clinical implications. Due to a high level of fibrosis and inflammation that contributes to renal and cardiovascular disease (CVD), existing treatments have not effectively mitigated residual risk for patients with DKD. Excess activation of mineralocorticoid receptors (MRs) plays a significant role in the progression of renal and CVD, mostly by stimulating fibrosis and inflammation. However, the application of traditional steroidal MR antagonists (MRAs) to DKD has been limited by adverse events. Finerenone (FIN), a third-generation non-steroidal selective MRA, has revealed anti-fibrotic and anti-inflammatory effects in pre-clinical studies. Current clinical trials, such as FIDELIO-DKD and FIGARO-DKD and their combined analysis FIDELITY, have elucidated that FIN reduces the kidney and CV composite outcomes and risk of hyperkalemia compared to traditional steroidal MRAs in patients with DKD. As a result, FIN should be regarded as one of the mainstays of treatment for patients with DKD. In this review, the safety, efficiency, and potential mechanisms of FIN treatment on the renal system in patients with DKD is reviewed.

KEYWORDS

finerenone, chronic kidney disease, type 2 diabetes, diabetic kidney disease, cardiovascular disease, non-steroidal mineralocorticoid receptor antagonist, hyperkalemia, reactive oxygen species

1 Introduction

Chronic kidney disease (CKD) is a significant global public health challenge characterized by persistent abnormalities in kidney structure or function such as albuminuria, abnormal urinary sediment and decreased estimated glomerular filtration rate (eGFR) for at least three months, with associated symptomology (1, 2). It is a major contributor to morbidity and mortality on a world scale, with a reported

prevalence of 9.1% in 2017 (3). CKD is anticipated to rank as the fifth-leading cause of death around the world by 2040 and the second-cause of death before the end of the century in countries with extended life expectancies (4). Over 850 million individuals worldwide have CKD, acute kidney injury (AKI), and are receiving renal replacement therapy (5). The prevalence has been increasing with serious and significant implications for public health and society attributed to disease burden, complications leading to cardiovascular (CV) morbidity, excess mortality, and costs associated with managing kidney failure (3).

Among a broad range of etiologies, diabetes has emerged as the primary cause of CKD globally, with an grown risk of disease progression, CV events, and mortality (6, 7). About 40% of individuals diagnosed with type 2 diabetes (T2D) are susceptible to the development of diabetic kidney disease (DKD), a condition that may progress to end-stage kidney disease (ESKD) and subsequently contribute to the burden of CV disease (CVD) (8–13). The mortality rate of DKD exceeds that of diabetes alone or CKD without diabetes by more than two-fold (14, 15). The coexistence of diabetes and CKD has been demonstrated to shorten the average life expectancy by about 16 years, representing a major challenge for society and public health systems all over the world (14). Therefore, new strategies that not only protect the kidney but also reduce the risk of CV events development should be imperatively taken into account in patients with DKD.

The development and progression of CKD in individuals with T2D are influenced by various factors, including hemodynamic factors, metabolic factors, and mineralocorticoid receptor (MR) overactivation (9, 16). In the kidney, MR is expressed in the distal tubules, collecting ducts, podocytes, fibroblasts, and mesangial cells (17). Upregulation of MR is evident in several clinical conditions such as hyperglycemia, CKD, albuminuria, cardiac disease, and high salt (HS) intake (18–24). MR overarousal promotes oxidative stress, inflammation, and fibrosis, resulting in renal alterations such as changes in the sodium-potassium ATPase in the distal convoluted tubule, sodium retention, elevated blood pressure (BP), glomerular hypertrophy, glomerulosclerosis, mesangial proliferation, and tubulointerstitial fibrosis, and ultimately contributing to the progression of CKD and CV complication (13, 17, 25–33). Hence, early intervention and intensive treatment are essential to mitigate renal and CV complications in individuals with DKD (34).

While renin-angiotensin system (RAS) blockers (e.g., angiotensin-converting enzyme inhibitors (ACEI), angiotensin receptor blockers (ARB)) and sodium-glucose co-transporters-2 inhibitors (SGLT2i) have shown beneficial renal and CV effects in DKD patients by targeting hemodynamic and metabolic drivers of CKD progression (35–40), they inadequately address the inflammation and fibrosis driven by MR overactivation, leading to a persistent high residual risk of CKD progression and CV events development, even in response to combined treatment by these two therapies (9, 13, 37, 38, 41). Therefore, a comprehensive approach is imperative to address the broader pathogenesis of DKD patients, including increased fibrosis and inflammation (25, 32, 42–44). Given this context, it is evident that MR antagonists (MRAs) play a pivotal role in the prevention of fibrosis and inflammation in both the renal and CV systems.

At the renal level, MR blockage significantly reduces albuminuria and promotes the preservation of renal function (32, 45–47). In the past years, classical steroidal MRAs like first-generation spironolactone and second-generation eplerenone, while potentially beneficial for nephroprotection and cardioprotection, are hindered by the risk of hyperkalemia and other progestogenic and antiandrogenic adverse effects (AEs) such as breast tenderness, gynecomastia, erectile dysfunction in men, and menstrual irregularities in premenopausal women, particularly in patients with DKD (48–55). The risk of hyperkalemia can escalate up to 8-fold in patients with moderate-to-severe CKD using steroidal MRAs (53, 56). While these AEs are not typically life-threatening, they can undermine treatment adherence and persistence, with roughly half of the patients discontinuing MRAs and 10% of patients continuing at reduced dose due to hyperkalemia (54). The conundrum of possessing effective therapies but not employing them due to safety concerns has prompted substantial efforts over the past two decades to develop novel MRAs with improved safety profiles.

Now, the emergence of the nonsteroidal MRAs (NS-MRAs) with an improved benefit-risk profile, exemplified by finerenone (FIN), offers a new opportunity for MRAs in DKD (57). To overcome the inherent limitations of steroidal MRAs by achieving high MR specificity and a balanced distribution between cardiac and renal tissues, FIN, a novel, nonsteroidal, selective, and potent third-generation MRA with enhanced antifibrotic and anti-inflammatory properties and a reduced incidence of hyperkalemia compared to traditional MRAs, is currently the most studied and has received approved for the treatment of DKD (58–61). An array of preclinical and clinical studies has substantiated the efficacy and safety of FIN in conferring renal and CV benefits.

On these grounds, this review aims to elucidate the molecular mechanisms of FIN and provide insights into its efficacy and safety across the spectrum of DKD patients, including those with and without a history of CVD.

2 Physiological and pathophysiological roles of MR in the kidney

The primary physiological role of the MR, found in the epithelial cells of the kidney and colon, is to regulate water and electrolyte balance (62). However, MR is also present in non-epithelial cells within the kidney and various extrarenal tissues, including the heart and vasculature (63). Upregulation of MR in these non-epithelial cells in the heart and kidney leads to increased transcription of profibrotic genes such as transforming growth factor-β-1 (TGF-β1), connective tissue growth factor, plasminogen activator inhibitor-1 (PAI-1), and various extracellular matrix proteins including fibronectin and collagens, all of which are associated with renal and cardiac fibrosis (33). Additionally, there is a positive correlation between elevated levels of serum aldosterone and an increased susceptibility to renal

failure in both diabetic and non-diabetic individuals (64). Accumulating evidence indicates that the activation of MR is linked to injury in podocytes through various mechanisms. These mechanisms include the involvement of Ras-related C3 botulinum toxin substrate 1 (Rac1), the reduction of autophagy which is crucial for podocyte maintenance, and an increase in NADPH oxidases (NOX) activity resulting in oxidative stress and further leads to the upregulation of a cascade of proinflammatory cytokines and profibrotic proteins (65). Subsequently, development of albuminuria, reduced renal blood flow, and AKI lead to the progression of chronic renal interstitial inflammation and fibrosis (65, 66). Thus, MRAs may potentially delay the progression of CKD irrespective of its underlying cause (64). Accordingly, although blocking MR in non-epithelial cells has a positive impact, blockade of MR in epithelial cells increases the risk of hyperkalemia. The contrasting roles of MR in physiological and pathobiological processes need careful consideration of their interplay when implementing medication.

3 Effect of FIN on renal reactive oxygen species, inflammation and fibrosis

3.1 Renal ROS

In the renal context, the overactivation of MR leads to an increased presence of ROS through the upregulation of NOX (67–69). These superoxide radicals have the potential to disrupt the normal functioning of both the renal vasculature and tubules. Additionally, hydrogen peroxide, another byproduct of this process, contributes to dysfunction, particularly in the preglomerular region (67–69). Nitric oxide (NO) bioavailability and increased oxidant damage are linked to ischemia in renal IR injury-inducing AKI (70). The generation of oxidative stress is decreased by the pharmacologic use of FIN or the genetic removal of MR in smooth muscle cells (SMCs) (71). In both mice (71) and rats (72), FIN has been demonstrated to suppress the expression of markers of tubular injury in the kidney, such as kidney injury molecule 1 (KIM-1) and neutrophil gelatinase-associated lipocalin (NGAL) (Table 1). It has also been shown that after renal IR damage, FIN normalizes pathophysiologic elevations in the oxidative stress markers like malondialdehyde and 8-hydroxyguanosine (Figure 1) (72).

3.2 Renal inflammation

In a murine knockout model of glomerulonephritis, it was observed that signaling of the MR in myeloid cells contributes to the progression of renal injury (29). One possible protective effect of MR knockout on myeloid cells against renal damage is a reduction in the recruitment of neutrophils and macrophages (29). The decrease in leukocytes was associated with the downregulation of pro-inflammatory markers' gene expression, such as tumor necrosis factor-α (TNF-α), matrix metalloproteinase (MMP)-12, inducible NO synthase, and C-C motif chemokine ligand 2 (CCL-2) (29). Recruitment of macrophages is crucial during both the injury and repair phases after a kidney ischemia event (74). Activation of MR in monocytes tends to polarize macrophages toward an "inflammatory M1" phenotype (75). The rationale for utilizing MRAs to impede the progression from AKI to CKD is supported by the fact that MR inhibition via FIN promotes increased expression of interleukin (IL)-4 receptor in murine kidney IR models, subsequently facilitating the polarization of macrophage toward an M2 phenotype (27). This shift is accompanied by decreased macrophage mRNA expression of the pro-inflammatory cytokine TNF-α and the M1 macrophage marker IL-1β (27). Additionally, there is a reduction in the inflammatory population of $CD11b^{+}$, $F4/80^{+}$, and $Ly6C^{high}$ macrophages (27). In uninephrectomized (UNX) DOCA-treated mice, the downregulation of kidney retinoid-related orphan receptor (ROR) gamma t-positive T-cells, along with a significant reduction in UACR, demonstrates significant renal protection in response to FIN treatment (76). Notably, MR antagonism by FIN can modulate inflammation as indicated by its ability to reduce proinflammatory cytokines like IL-6 and IL-1ß following renal ischemic damage (27). Furthermore, FIN has been shown to lower the expression of renal NGAL (71, 72), which is released during systemic inflammation by neutrophils and in response to tubular injury by renal tubular cells (71, 72). The pro-inflammatory cytokine monocyte chemoattractant protein-1 (MCP-1) is also reduced by FIN in the DOCA-salt model of cardiorenal end-organ damage (77). Both NGAL and MCP-1 play significant roles in the progression of human CKD (78, 79). Renal osteopontin (OPN) expression was also decreased in a DOCA-salt rat CKD model following FIN treatment (77). OPN is believed to regulate various aspects of renal fibrogenesis, including fibroblast proliferation, macrophage activation and infiltration, cytokine secretion, and extracellular matrix production. It is associated with CKD progression, with elevated plasma levels detected in the early stages of CKD (80). FIN also offers protection against podocyte damage in a murine model of CKD progression in T2D (UNX mice with T2D fed a HS diet), as indicated by reduced production of fibronectin and inflammatory markers such as MCP-1 and PAI-1 in glomeruli (Figure 1) (81).

3.3 Renal fibrosis

The development of kidney fibrosis is a critical factor in the progression of CKD and eventual renal failure, as it disrupts the structural integrity of renal tubules and adjacent blood vessels. Studies conducted on individuals with kidney diseases have identified pro-fibrotic cytokines like TGF-β, MCP-1, and MMP-2 as potential biomarkers for fibrosis development, which have been correlated with worsening renal function (WRF) (82). Additionally, plasma levels of PAI-1 have showed moderate correlations with fibrosis observed in biopsies (82). To investigate the role of MR in fibrosis development and CKD progression, as well as the effectiveness of FIN in mitigating renal fibrosis, various preclinical models have been employed. In the DOCA-salt rat model of CKD, FIN treatment led to a reduction in renal mRNA expression of the pro-fibrotic marker PAI-1 and a decrease in

TABLE 1 Efficacy of FIN for renal protection in animal experiments.

Author, Year	Animal Species	Modeling Type	Research Results
Kolkhof et al., 2014 (62)	Sprague-Dawley rats and Wistar rats	A rat model of DOCA/Salt-induced Heart and Kidney Injury	FIN ↓: proteinuria, glomerular tubular and vascular damage, risk of electrolyte disturbances, cardiac hypertrophy, BNP, renal expression of pro-inflammatory and pro-fibrotic markers (PAI-1, MCP-1, OPN, and MMP-2); FIN ↑: end-organ protection, systolic and diastolic left ventricular function
Barrera-Chimal et al., 2017 (65)	Male C57Bl/6 mice and Large White pig	Model of AKI induced by IR	FIN ↓: renal injury induced by IR through effects on Rac1-mediated MR signaling; renal mRNA levels of NGAL and Kim-1; oxidative stress production
Lattenist et al., 2017 (64)	Male Wistar rats	A rat model of AKI to CKD	FIN ↓: inflammatory factors; fibrogenic markers; oxidative stress markers; deposition of perinephric macrophages and collagen; proteinuria; tubulointerstitial fibrosis; acute injury induced by IR and the chronic and progressive deterioration of kidney function and structure
Barrera-Chimal et al., 2018 (27)	Male C57Bl/6 mice	A mice model of bilateral IR-induced CKD	FIN ↓: inflammatory population of CD11bD, F4/80D, Ly6Chigh macrophages; proinflammatory cytokines IL-6 and IL-1ß; subsequent chronic dysfunction and fibrosis induced by IR; FIN ↑: M2-antiinflamatory markers, IL-4 receptor.
González-Blázquez et al., 2018 (45)	Male Wistar and MWF rats	A genetic model of CKD	FIN ↓: albuminuria, endothelial dysfunction, superoxide anion levels; FIN ↑: NO bioavailability, SOD activity
Gil-Ortega et al., 2020 (46)	Male Wistar and MWF rats	A genetic model of CKD	FIN ↓: albuminuria, plasma MMP-2 and MMP-9 activities, superoxide anion levels, intrinsic (mesenteric) arterial stiffness; FIN ↑: plasma pro-MMP-2 activity, NO bioavailability
Droebner et al., 2021 (73)	C57BL/6J mice	2 relevant mouse kidney fibrosis models: unilateral ureter obstruction and sub-chronic IR injury	FIN has direct anti-fibrotic properties resulting in reduced myofibroblast and collagen deposition accompanied by a reduction in renal PAI-1 and NKD2 expression in mouse models of progressive kidney fibrosis at BP-independent dosages
Hirohama et al., 2021 (66)	Mice	Uninephrectomized T2M db/db mice fed a HS diet (DKD with hypertension model)	FIN ↓: Salt-induced activation of Rac1-MR pathway associated with Sgk1 upregulation and subsequent increased expressions of cleaved α-ENaC and phosphorylated NCC in distal tubules and glomeruli. FIN ↓: fibronectin; inflammatory markers (MCP-1 and PAI-1)
Kolkhof et al., 2021 (73)	Transgenic (mRen2) 27 rats	A rat model of hypertension-induced end-organ damage	Combination of FIN and empagliflozin at low dosages effectively reduces cardiac and renal lesions, proteinuria, BP, creatinine, uric acid and mortality. FIN reduced renal fibrosis and the renal expression of pro-fibrotic COL1A1
Luettges et al., 2022 (63)	Male C57BL6/J mice	UNX DOCA-salt model	FIN protects against functional and morphological renal damage and exerts antihypertensive actions. FIN reduces renal IL-17 producing RORγt γδ T cells
Lima-Posada et al., 2023 (67)	ZSF1 rats	A model of DN associated with cardiac dysfunction	FIN did not impact kidney function but ↓ renal hypertrophy

renal fibrosis as evaluated through histopathology (77). The study revealed that the administration of FIN had a dose-dependent effect in diminishing the upregulation of mRNA expression of MMP-2, which serves as a significant indicator of tissue remodeling (77). In a rat model of hypertensive cardiorenal disease, FIN also attenuated renal fibrosis and reduced the production of pro-fibrotic collagen type I α 1 chain (COL1A1) in the kidney (83). Moreover, FIN dose-dependently suppressed pathologic myofibroblast accumulation and collagen deposition in a mouse model of renal fibrosis, irrespective of changes in systemic blood pressure or inflammatory markers (84). The levels of the fibrotic biomarkers PAI-1 and naked cuticle homolog 2 (NKD2) were concomitantly decreased in the kidneys (84), with recent reports identifying NKD2 as a specific marker for myofibroblasts in human renal fibrosis (85). In a chronic CKD rat model characterized by renal dysfunction, elevated proteinuria, and extensive tubule-interstitial fibrosis, treatment with FIN effectively limited collagen deposition and fibrosis in the kidney, as confirmed through histopathological assessments (72). FIN also inhibited the upregulation of the pro-fibrotic cytokine TGF-β and collagen-I expression in the kidneys (72). Likewise, in a mouse CKD model featuring unilateral, IR-induced tubulo-interstitial fibrosis, FIN administration resulted in a significant reduction in the severity of renal fibrosis (27) (Figure 1 and Table 1).

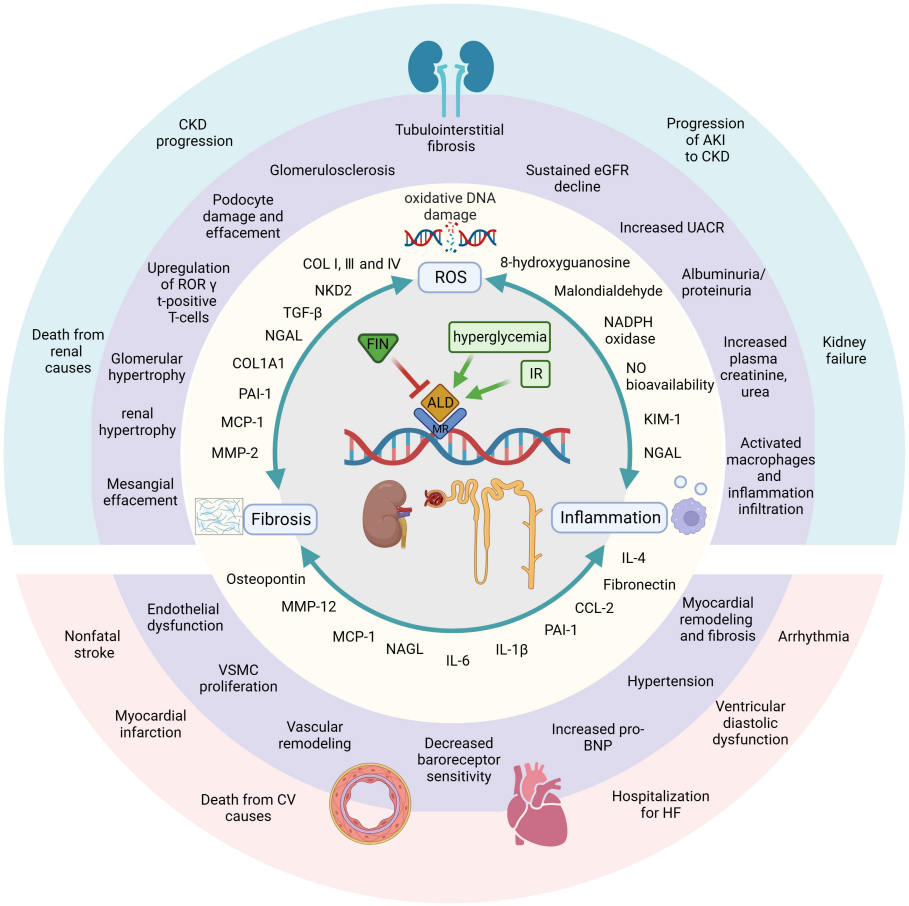

FIGURE 1
FIN displays beneficial effects against DKD and renal IR damage by different mechanisms of action in kidney. Diabetic and ischemic environment induce hyperactivation of MR and trigger three pathways, which can start a great variety of molecular, cellular, tissue and subsequently organ responses. On contrast, MRA FIN blocks the binding of aldosterone and MR, then blocks and attenuates those pathophysiological progressions. First, FIN alleviate oxidative stress by attenuating oxidative DNA damage and reducing the production of ROSs. The second major mechanism, FIN reduce the upregulation of pro-inflammatory mediators, leading to reduced inflammation. FIN also leads to reduced fibrosis by downregulating fibrotic biomarkers. In these ways, FIN shows renal-cardiovascular protective effect. Created by BioRender.com.

4 Renal protection of FIN in animal models

The efficacy of FIN for renal protection in animal experiments has been evaluated in recent years (Table 1). Kolkhof et al. (77) found that FIN consistently protects from functional as well as structural end-organ damage in kidneys with a reduced risk of electrolyte disturbances in the 10-week rat deoxycorticosterone acetate (DOCA)/salt model in a dose-dependent manner, with the most significant effect at 10 mg/kg·d. Histological analyses indicated that when compared at equinatriuretic doses, FIN outperformed eplerenone in reducing proteinuria and alleviating glomerular, tubular, and vascular damage (77). Similarly, Luettges et al. (76) conducted experiments highlighting FIN's protective effects against functional and morphological renal damage and its ability to exert antihypertensive actions in mice subjected to the DOCA-Salt model. In a rodent model transitioning from AKI to CKD, FIN demonstrated efficacy in preventing AKI induced by ischemia-reperfusion (IR) and the subsequent chronic and progressive deterioration of kidney function and structure (27, 71, 72). These long-term protective effects of FIN were also observed in a preclinical model involving large white pigs (71). Furthermore, prophylactic FIN administration efficiently prevented increased plasma creatinine, urea, and proteinuria (27, 71, 72). Current investigations have unveiled the favorable impact of FIN on both arterial distensibility and albuminuria in the munich Wistar frömter (MWF) CKD model (45, 46). In uninephretomized db/db mice fed a HS diet, Hirohama et al. (81) reported that FIN ameliorated albuminuria, associated with reduced BP and glomerular injury. Nevertheless, in ZSF1 rats with diabetes, the administration of FIN did not significantly affect kidney function but did reduce renal hypertrophy (86).

5 Renal protection of FIN in clinic

The efficacy and safety profiles of FIN were evaluated in 4 phase II trials in patients with CVD and kidney disease within the ARTS

program and 2 phase III trials in patients with DKD (Table 2) (Figure 2) (87–92).

5.1 Clinical efficacy of FIN treatment for patients with CKD and T2D

The Mineralocorticoid Receptor Antagonist Tolerability Study–Diabetic Nephropathy (ARTS-DN), a pioneering multicenter, phase II clinical trial investigating the use of FIN in combination with a RAS inhibitor in individuals with DKD exhibited significant reductions in albuminuria and enhancements in the urine albumin-creatinine ratio (UACR) after 90 days of treatment with FIN (7.5–20 mg/day) in comparison to a placebo (91). The results of the ARTS-DN Japan trial, which included 96 Japanese patients with DKD receiving a RAS inhibitor, support those of ARTS-DN (92). Detailed dose–exposure–response modeling and simulation, encompassing an analysis of both ARTS-DN and ARTS-DN Japan, suggested that the effects of FIN were predominantly saturated at a dosage of 20 mg, with both 10 mg and 20 mg administered once daily proving to be safe and effective in reducing albuminuria (93). Furthermore, there were no discernible differences in the incidence of a 30% decrease in eGFR between the treatment groups (91).

Certainly, the most comprehensive insights into the advantages of FIN in individuals with DKD have been garnered through pivotal phase III clinical trials: FIDELIO-DKD (Finerenone in Reducing Kidney Failure and Disease Progression in Diabetic Kidney Disease) (88); FIGARO-DKD (Finerenone in Reducing Cardiovascular Mortality and Morbidity in Diabetic Kidney Disease) (87); and the predefined combined analysis known as FIDELITY (Combined FIDELIO-DKD and FIGARO-DKD Trial program analysis) (94).

FIDELIO-DKD, a multicenter, double-blind randomized controlled trial (RCT), has furnished the initial clinical evidence affirming that MR blockade yields improvements in kidney outcomes for patients with DKD (88). This study included 5734 adults with DKD who were already receiving the maximum tolerated doses of an ACEI or ARB and maintained a serum potassium concentration of 4.8 mmol/L (88). Eligible patients had a UACR 30–<300 mg/g, an eGFR of 25–<60 ml/min/1.73 m^2, and diabetic retinopathy, or they had a UACR of 300–5000 mg/g and an eGFR of 25–<75 ml/min/1.73 m^2 (88). Following a median follow-up of 2.6 years, the results of the FIDELIO-DKD study exhibited a significantly lower incidence of the primary composite outcome, encompassing kidney failure, a sustained eGFR decline of ≥40% from baseline, or death from renal causes in the FIN group compared to the placebo group (17.8% vs. 21.1%) (88). At the 4-month post-treatment mark, UACR demonstrated a 31% reduction compared to the placebo group, with this difference persisting throughout the trial (88). A secondary model-based analysis of FIDELIO-DKD showed that the early UACR effect of FIN was predictive of its long-term impact on eGFR decline, and these effects were found to be independent of the concurrent use of SGLT2i (95). Furthermore, FIN achieved a placebo-subtracted reduction of 14% in the crucial secondary composite outcome, encompassing CV death, nonfatal myocardial infarction (MI), nonfatal stroke, or hospitalization for heart failure (HF) (88). In a secondary analysis of the FIDELIO-DKD trial, FIN was shown to reduce the risk of newly diagnosed atrial fibrillation/flutter compared to placebo, irrespective of a history of atrial arrhythmias at baseline (3.2% vs. 4.5%) (96).

Similarly, in the next major phase III FIGARO-DKD clinical trial (87), which enrolled 7437 adults with DKD across a wider range of CKD stages (a UACR of 30–<300 mg/g and an eGFR of 25–90 mL/min/1.73 m^2 or a UACR of 300–5000 mg/g and an eGFR of≥60 ml/min/1.73 m^2) already treated with maximum tolerated doses of an ACEI or ARB and maintaining a serum potassium concentration less than 4.8 mmol/L, a notable 13% reduction in the composite primary outcome, comprising CV death, nonfatal stroke, nonfatal MI, or hospitalization for HF, was observed after a mean follow-up of 3.4 years (87). While a lower incidence rate for the eGFR ≥40% kidney composite endpoint was noted with FIN compared to placebo, it did not reach statistical significance (P = 0.069). Nevertheless, a greater treatment effect was noted on the eGFR ≥57% kidney composite endpoint, with a 36% relative risk reduction for ESKD (P = 0.041) (87). FIN achieved a 32% greater reduction in UACR from baseline to 4 months compared to placebo (87), and its impact on kidney outcomes was particularly pronounced in patients with significantly elevated albuminuria as opposed to those with moderately increased albuminuria (97). An analysis derived from the FIGARO-DKD study emphasizes the importance of albuminuria screening in T2D patients, as early initiation of treatment effectively mitigated the risk of CV events and albuminuria progression in individuals with moderately elevated albuminuria (98).

The outcomes of the FIDELITY study, which pooled data from FIDELIO-DKD and FIGARO-DKD involving over 13,000 patients, revealed significant reductions associated with FIN, including a 23% reduction in the risk of kidney composite events (renal failure, >57% eGFR reduction, and renal disease-related death), a 20% reduction in dialysis initiation, a 32% reduction in UACR from baseline to 4 months, a 14% reduction in the primary composite CV outcome, and a 22% reduction in HF hospitalizations compared to placebo (94). Moreover, it's worth emphasizing that FIN induced a modest reduction in mean systolic BP at 4 months (3.2mmHg vs. 0.5 mmHg increase with placebo) in the FIDELITY pooled analysis (94). While it did not exhibit significant differences between groups in the whole population from both FIDELIO-DKD and FIGARO-DKD, a FIDELITY *post hoc* analysis of a subgroup of patients with treatment-resistant hypertension showed a significant differences of the least squares mean change in office systolic BP between FIN and placebo groups during the first 4 months (−7.1 mmHg vs. −1.3 mmHg, respectively) (P <.0001) (99). Meanwhile, the cardiorenal effects of FIN do not seem to be primarily mediated by its antihypertensive properties, as the impact on BP was minimal compared to spironolactone (94, 99). There is no evidence suggesting a correlation between the antialbuminuric effects of FIN and changes in BP.

Further analyses demonstrate that FIN provides robust renal and CV efficacy and safety benefits across the spectrum of DKD (100, 101). FIN consistently showed improvements in indicators of kidney injury, as evidenced by a reduction in UACR and function, with better preservation of eGFR in the chronic phase, compared to placebo in patients with stage 4 CKD (101). However, the effect of FIN on the composite kidney outcome in patients with stage 4 CKD exhibited inconsistencies between early and late years of follow-up,

TABLE 2 Efficacy of FIN for renal protection in clinic.

Trial, Auther, Year	Research Type	Phase	Race	Country	Sample Size	Patient's Condition	Intervention	Duration	Change in End Indicators	Safety Evaluation
ARTS, Pitt et al., 2013 (70)	Randomized control study	IIa	/	Multi-center	part A, n = 65; part B, n = 392	HFrEF (NYHA II-III, LVEF≤40%) and mild or moderate CKD (eGFR 60–90 mL/min/ 1.73 m^2 in the safety assessment [part A], or 30–60 mL/ min/1.73 m^2 in the efficacy assessment [part B])	FIN (2.5, 5, or 10 mg QD [parts A & B], or 5 mg BID [part B]) Open-label spironolactone (25 or 50 mg/day [part B]) Placebo (parts A & B)	28 days (parts A & B)	FIN vs. spironolactone: equivalent or greater reductions in albuminuria and N-terminal pro-BNP levels; smaller decrease in eGFR	FIN vs. spironolactone: smaller increases in serum potassium concentration; lower incidences of hyperkalemia and WRF
ARTS-DN, Bakris et al., 2015 (72)	Randomized control study	IIb	White, Black or African American, Asian, Multiple, Not reported, Hispanic or Latino	Multi-center	823	DKD receiving RAS inhibitors (UACR ≥30 mg/g and eGFR >30 mL/min/1.73 m^2)	FIN (1.25–20 mg/ day; 7 doses assessed) Placebo	90 days	Reduction in UACR: dose dependent at the 4 highest doses of FIN vs. placebo; 38% UACR reduction with FIN 20 mg/ day; Only a modest reduction in BP at the highest dosage of FIN	Hyperkalemia leading to discontinuation: not observed in the placebo and FIN 10 mg/ day groups; incidences in the FIN 7.5-20 mg/day groups were low (1.7%–3.2%). No differences in the incidence of an eGFR decrease of ≥30% or in incidences of AEs and serious AEs between the placebo and FIN groups
ARTS-HF, Filippatos et al., 2016 (71)	Randomized control study	IIb	Europe, North America, Asia, Other	Multi-center	1066	HFrEF and T2D and/ or CKD (eGFR >30 mL/min/ 1.73 m^2 in patients with diabetes or 30–60 mL/ min/1.73 m^2 in those without diabetes)	FIN (2.5–15 mg/ day, uptitrated to 5-20 mg on day 30) Eplerenone (25 mg every other day, increased to 25 mg/day and 50 mg/day on days 30 and 60, respectively)	90 days	FIN vs. eplerenone: similar effects on N-terminal pro-BNP levels and BP; greater reduction of composite clinical outcome of all-cause death, CV hospitalization, or emergency presentation due to worsening HF	FIN vs. eplerenone: smaller increases in serum potassium concentration; similar incidence of hyperkalemic events and TEAEs
ARTS-DN Japan, Katayama et al., 2017 (74)	Randomized control study	IIb	Japanese	Multi-center	96	Japanese patients with DKD receiving a RAS blocker	FIN or placebo	90 days	The UACR at day 90 relative to baseline for each FIN treatment group was numerically reduced compared with placebo	No serious AEs or deaths were reported and no patients experienced TEAEs resulting in discontinuation of study drug. Small mean increases in serum potassium level in FIN vs. Placebo. No patients developed hyperkalemia
FIDELIO-DKD, Bakris et al., 2020 (69)	Randomized control study	III	White, Black/ African American,	Multi-center	5734	DKD receiving RAS inhibitors First set: UACR 30 to <300 mg/ g, eGFR 25 to <60 mL/ min/1.73 m^2, and	FIN (10–20 mg/ day). Placebo	2.6 years (median follow up)	Key primary composite outcome events: significantly less with FIN vs. placebo. Key secondary composite outcome events: significantly less with FIN vs.	Frequency of AEs: overall similar with FIN vs. placebo. Incidence of serum potassium levels >5.5 mmol/l: FIN (21.7%) vs. placebo (9.8%); The incidence of hyperkalemia-related

(Continued)

10.3389/fendo.2023.1320603

TABLE 2 Continued

Trial, Auther, Year	Research Type	Phase	Race	Country	Sample Size	Patient's Condition	Intervention	Duration	Change in End Indicators	Safety Evaluation
			Asian, Other			history of diabetic retinopathy. Second set: UACR 300–5000 mg/g, eGFR 25 to <75 mL/ min/1.73 m^2			placebo. FIN was associated with a 31% reduction in the UACR from baseline to 4 months, and a lower UACR was maintained throughout the remainder of the trial.	AEs: FIN (18.3%) vs. placebo (9.0%); Hyperkalemia leading to discontinuation: FIN (2.3%) vs. placebo (0.9%); Serious hyperkalemia related AEs requiring hospitalization: FIN (1.4%) vs. placebo (0.3%); No report of any mortal event directly attributable to hyperkalemia
FIGARO-DKD, Pitt et al., 2021 (68)	Randomized control study	III	White, Black/ African American, Asian, Other	Multi-center	7437	DKD receiving RAS inhibitors. First set: UACR 30 to <300 mg/g, eGFR 25–90 mL/ min/1.73 m^2. Second set: UACR 300-5000 mg/g, eGFR ≥60 mL/ min/1.73 m^2	FIN (10–20 mg/ day). Placebo	3.4 years (median follow up)	Key primary composite outcome events: significantly less with FIN vs. placebo; Key secondary composite outcome events: similar with FIN vs. placebo.	Frequency of AEs: overall similar with FIN vs. placebo; Hyperkalemia leading to discontinuation: higher with FIN than with placebo (1.2% vs. 0.4%)
FIDELITY, Agarwal et al., 2022 (76)	FIDELITY prespecified pooled analysis of FIDELIO-DKD and FIGARO-DKD	III	White, Black/ African American, Asian, Other	Multi-center	13026	DKD	standard therapy + FIN or placebo	interquartile range 2.3–3.8 years	Significant reductions of 14% for the endpoint CV outcome; 23% for risk of kidney composite events; and 20% for dialysis initiation with a 20% reduction in ESKD and a 22% reduction in HF hospitalizations; and significantly reduced UACR by 32% compared to placebo.	AEs related to treatment: FIN (18.5%) vs. placebo (13.3%); AEs leading to treatment discontinuation FIN (6.4%) vs. placebo (5.4%); hyperkalemia: FIN (14%) vs. placebo (6.9%); Hospitalizations due to hyperkalemia FIN (0.9%) vs. placebo (0.2%); Hyperkalemia leading to permanent treatment discontinuation FIN (1.7%) vs. placebo (0.6%); No hyperkalemia-related AEs were fatal; The incidence of TEAE is similar in the FIN and placebo groups, with no increase in sex hormone-related AEs compared to the placebo group

10.3389/fendo.2023.1320603

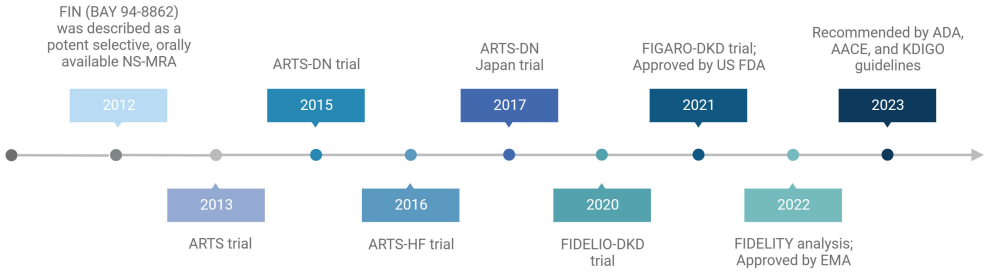

FIGURE 2
Summary of the milestones and main trials of finerenone. Created by BioRender.com.

with a notable loss of precision over time (101). A recent study included nine patients with advanced DKD with an eGFR below 25 mL/min/1.73 m^2 revealed that FIN caused a significantly slower decline in eGFR in patients with advanced DKD, thus providing initial evidence that FIN is effective across a wide range of renal functions (102). As such, further large-scale investigation will be necessary to confirm the efficacy and safety of FIN in DKD patients with an eGFR below 25 mL/min/1.73 m^2.

Furthermore, some FIDELITY analyses emphasize the benefits of early treatment initiation and co-administration of potassium-binding agents to maximize the protective effects of FIN in individuals with DKD (100, 103). FIN improved cardiorenal outcome in patients with DKD, regardless of baseline HbA1c (94, 104, 105), HbA1c variability (104), diabetes duration (104), baseline insulin use (104, 105), baseline HF history (106, 107), prevalent atherosclerotic CVD (108), and history of atrial fibrillation/flutter at baseline (96). Additionally, it is worth noting that the antihypertensive effect of adding FIN to a maximally tolerated dose of ACEI or ARB was relatively modest (87, 88).

In conclusion, these results suggest that in patients with DKD, FIN may be an effective treatment for kidney and CV protection. In fact, FIN has been approved by the U.S. Food and Drug Administration (FDA) in 2021 to reduce the risk of sustained eGFR decline, ESKD, nonfatal MI, hospitalization for HF, and CV death in adults with DKD (109). In addition, the European Medicines Agency (EMA) authorized the marketing of FIN for routine clinical use in patients with DKD on 16 February 2022 (110). Recently published guidelines from the American Diabetes Association (ADA) (111–113), the American Association of Clinical Endocrinology (AACE) (114) and the updated Kidney Disease: Improving Global Outcomes (KDIGO) Diabetes Work Group (112, 115) recommend the addition of the oral NS-MRAs FIN to standard treatment in patients with DKD (Figure 2).

5.2 Clinical efficacy of FIN treatment for patients with CVD and kidney disease

The phase IIa study known as Mineralocorticoid Receptor Antagonist Tolerability Study (ARTS) (89) represents the inaugural RCT of FIN. It encompassed both a double-blind placebo group and an open-label spironolactone comparison group and targeted individuals with heart failure with reduced ejection fraction (HFrEF) along with mild or moderate CKD. This study established safe dosing of FIN and demonstrated that FIN exhibited equivalent or greater reductions in albuminuria and N-terminal pro-B-type natri (89) uretic peptide (pro-BNP) levels compared to spironolactone. The study results indicated that individuals receiving FIN (10 mg q.d.) showed a significant smaller decrease in eGFR than those receiving spironolactone at visit 7 (day 29 + 2) (-2.69 vs. -6.70 ml/min/1.73 m^2) (P ¼ 0.0002–0.0133) (89).

In the phase IIb ARTS-Heart Failure (ARTS-HF) study (90), which included 1066 patients diagnosed with HFrEF and T2D and/or CKD, there was a notable indication of benefit associated with FIN. Specifically, there was a significant reduction in the composite clinical outcome, which included events such as all-cause mortality, CV hospitalization, or emergency admissions due to worsening HF, among patients treated with FIN in comparison to those receiving eplerenone. A recent prespecified analysis of FIGARO-DKD indicated that FIN reduced the risk of developing HF independent of a history of HF (107). These findings suggest that FIN may offer valuable prospects as a treatment option for patients with heart failure with preserved ejection fraction (HFpEF), particularly those who also have T2D and/or CKD.

6 The safety of FIN treatment

Even though FIN has beneficial effects on renal outcomes, the safety of FIN therapy is important and is an essential precondition for clinical application. AEs associated with using FIN include the risk of hyperkalemia, renal insufficiency and sex hormone-associated AEs.

The safety profile of FIN underwent thorough investigation within an extensive phase II clinical trial program, encompassing over 2000 patients who had HFrEF, CKD, and/or T2D or with DKD (Table 2) (89–91). In the ARTS study, it was evident that the mean rise in serum potassium levels over a 28-day period was significantly lower in all four dosage groups of FIN when compared to the spironolactone group (0.04 to 0.30 vs. 0.45 mmol/L, respectively) and there was lower incidence of hyperkalemia with FIN vs spironolactone (5.3% vs 12.7%, p = 0.048) (89). In the ARTS-HF study, the mean increase in serum potassium from baseline to Day

90 was greater in the eplerenone group than in the FIN groups (90). Hyperkalemia, defined as a serum potassium elevation exceeding 5.6 mmol/L, was observed in 4.3% of patients, with the incidence of hyperkalemic events and treatment-emergent AEs (TEAEs) being similar in both the FIN and eplerenone groups (90). Within the ARTS-DN trial, permanent discontinuation of the medication due to hyperkalemia was not reported in the placebo group or the FIN 10 mg/day group. However, it occurred in 2.1%, 3.2%, and 1.7% of patients randomized to the FIN 7.5 mg/day, 15 mg/day, and 20 mg/day groups, respectively (91). Secondary safety outcomes, including a decline in eGFR of ≥30% and the incidence of other serious AEs, did not exhibit significant differences between the various treatment groups (91). In summary, these phase II trials collectively demonstrate that hyperkalemia does not serve as a substantial impediment to the utilization of FIN for renal protection (89–91).

With respect to the safety profile in the FIDELIO-DKD phase III trial (88), it is noteworthy that FIN treatment was generally well-tolerated, and the distribution of AEs was comparable between the FIN and placebo groups. It is worth mentioning that the incidence of serum potassium levels exceeding 5.5 mmol/L was higher in the FIN group compared to the placebo group (21.7% vs. 9.8%), and hyperkalemia-related AEs occurred at a double rate in FIN-treated patients compared to those receiving placebo (18.3% vs. 9.0%). However, it's important to highlight that severe hyperkalemia-related AEs necessitating hospitalization were infrequent (1.4% vs. 0.3%), and there were no reported fatalities directly attributed to hyperkalemia. Permanent discontinuation of the medication was observed in 2.3% of patients in the FIN group and 0.9% in the placebo group. A secondary model-based analysis of FIDELIO-DKD revealed that higher FIN doses were linked to lower serum potassium levels and reduced incidences of hyperkalemia, guided by serum potassium-based dose adjustments (116). Additionally, FIN exhibited a lower risk of AEs related to sex hormones (117). In the FIGARO-DKD trial (87), the incidence of overall AEs and the risk of serious AEs leading to discontinuation were similar between the FIN and placebo groups. Although the occurrence of severe hyperkalemia was slightly higher with FIN than placebo (0.7% vs. 0.1%), it is noteworthy that no fatal hyperkalemia events were reported. The discontinuation rate due to hyperkalemia was also higher with FIN compared to placebo (1.2% vs. 0.4%, respectively). However, none of the hyperkalemia-related AEs resulted in fatalities. In the FIDELITY pooled analysis (94), 18.5% of patients who got FIN experienced treatment-related AEs, compared to 13.3% of patients who received a placebo, with AEs leading to treatment discontinuation occurring in 6.4% vs. 5.4% of patients, respectively. Hyperkalemia was more common with FIN than with placebo (14% vs. 6.9%). Hospitalizations due to hyperkalemia (0.9% and 0.2%, respectively) were minimal, and the incidence of hyperkalemia leading to permanent treatment discontinuation was low across study arms but occurred more frequently with FIN (1.7%) than with placebo (0.6%). However, no hyperkalemia-related AEs were fatal. The incidence of TEAEs was comparable between the FIN and placebo groups, and there were no notable increases in AEs related to sex hormones or AKI compared to the placebo group. Regarding patients with CKD stage 4, the safety profile of FIN in individuals with T2D remained consistent with that of CKD stages 1 to 3. A FIDELITY *post hoc* analysis showed that FIN was related to a lower risk of hyperkalemia compared with spironolactone with/without a potassium-binding agent (99).

In conclusion, FIN appeared safe and effective in most clinical studies (Table 2). Nevertheless, baseline eGFR and serum potassium levels should be evaluated before initiation of FIN, and periodic measurement of serum potassium should still be performed during treatment with FIN, and the dose adjusted as needed. Additionally, implementing dietary interventions, avoiding agents that have the potential to induce hyperkalemia (118), correcting metabolic acidosis, and using potassium-lowering drugs (119) are effective strategies for preventing hyperkalemia.

7 Combination treatment with ACEI/ARB and SGLT2i/glucagon-like peptide-1 receptor agonists

A subgroup analysis, based on various MRAs, indicates that the relative risk of hyperkalemia when combining ACEI/ARB with FIN is lower compared to eplerenone or spironolactone (120).

Additionally, the combination of FIN with a SGLT2i like empagliflozin at low dose provides renal protection effect and effectively reduces proteinuria, plasma creatinine, uric acid, BP, cardiac and renal lesions, and mortality in a nondiabetic hypertensive cardiorenal disease model (50). However, multiple clinical studies, including FIDELIGO-DKD, have illustrated that FIN alone reduces UACR independently of SGLT2i (121). In the FIDELITY analyses, FIN outperformed placebo in terms of cardiorenal outcomes in individuals with DKD, regardless of SGLT2i usage (73, 94). In other words, SGLT2i did not alter the effects of FIN on the primary endpoint. However, as for the safety, MRAs increase serum potassium concentration and the risk of hyperkalemia while SGLT2is reduce the risk of hyperkalemia (122, 123), which makes the combination of SGLT2i with MRAs an attractive treatment option from a safety perspective. Analysis from the FIDELIO-DKD trial reveals that when combined with FIN, treatment with an SGLT2i may offer protection from hyperkalemia events despite low number of hyperkalemia events was observed (73, 117). Moreover, it should be pointed out that in several trials, the SGLT2i dapagliflozin and MRA eplerenone reduce albuminuria and the incidence of hyperkalemia was significantly less during treatment with dapagliflozin-eplerenone compared with eplerenone alone (124, 125). These findings offer a convincing reason for evaluating the long-term efficacy and safety of combined SGLT2i and MRA treatment and may make eplerenone, a second-generation MRA, combined with SGLT2i, a second option for patients who can't tolerate FIN or can't afford such an expensive drug price of FIN.

Regarding GLP-1RAs, a *post hoc* exploratory analysis of the FIDELIO-DKD and FIGARO-DKD trials found that FIN reduces UACR in patients, irrespective of whether they were using GLP-1RAs use at the beginning of the study. The effects on kidney and CV outcomes remain consistent regardless of GLP-1RA usage, with no obvious safety signals associated with the combination treatment (126, 127).

In summary, the results from clinical studies comparing combination therapy to monotherapy vary. Understanding the molecular mechanisms and potential interactions between FIN, ACEI/ARB, and SGLT2i/GLP-1RA agents remains unclear. Consequently, further clinical trials and in-depth mechanistic research are essential to provide conclusive evidence.

8 Ongoing trials

So far, clinical investigation into the kidney and CV disease outcomes associated with FIN have primarily focused on individuals with DKD. However, it's essential to emphasize that the FIDELIO-DKD and FIGARO-DKD trials specifically enrolled participants with DKD, characterized by an eGFR of ≥25 mL/min/1.73 m^2, normal serum potassium levels, and albuminuria. Consequently, the current approval of FIN cannot be generalized to the entire population of individuals with DKD. Hence, further research is needed to clarify this aspect. Ongoing studies are exploring the role of triple therapy, consisting of RAS blockade, SGLT2i, and FIN, in individuals with DKD (CONFIDENCE study, NCT05254002) (128). Additionally, there are investigations into the efficacy and safety of FIN in subjects with CKD who do not have diabetes (FIND-CKD study, NCT05047263) (129), as well as an examination of treatment patterns in patients with DKD treated with FIN in routine clinical practice, including safety assessments (FINE-REAL study, NCT05348733) (130).

The CONFIDENCE trial is an ongoing phase II randomized controlled trial designed to investigate the combination of FIN and empagliflozin compared with each drug alone in 807 participants with T2D, stage 2–3 CKD and UACR ranging from ≥300 to <5000 mg/g (128). This trial is estimated to be completed by 2024 and will comprehensively evaluate the cumulative efficacy, safety, and tolerability of dual therapy (128). The study will primarily focus on endpoints related to UACR, change in eGFR, and the incidence of hyperkalemia (128). However, as of this writing, no prospective clinical trials were planned to judge the combination of FIN and GLP-1RAs in patients with DKD.

Initiated in September 2021, the FIND-CKD trial includes non-diabetic CKD patients with an eGFR ranging from 25–90 mL/min/1.73 m^2 and a UACR between ≥200 to ≤3500 mg/gCr (129). The primary objective of this study is to assess the change in eGFR from baseline to 32 months in both the placebo and FIN groups.

The ongoing FINE-REAL study (130) aims to demonstrate treatment patterns in patients with DKD receiving FIN in routine clinical practice and assess the safety of FIN. FINE-REAL will provide meaningful insights into DKD patients treated with FIN, capturing AEs, specifically hyperkalemia, and identifying how they are handled in routine clinical care. The FINE-REAL study will aid to inform decision-making about initiating FIN in individuals with DKD and also shed light on the dynamics of adoption of new therapies in different regions and health systems, providing conducive perspectives for international guidance and implementation.

9 Conclusion and future advancement

FIN is a third-generation, selective and potent NS-MRA that has been illustrated in clinical trials to slow CKD progression, reduce the risk of CV events development and hyperkalemia compared to traditional steroidal MRAs in patients with DKD through specific impacts on inflammatory and fibrotic pathways. As such, FIN is a valuable addition to the treatment landscape for managing DKD. However, more clinical trials and deep mechanism research are needed to provide conclusive evidence for the combination treatment of FIN with ACEI/ARB and SGLT2i/GLP-1RAs. Additionally, further large-scale investigations are supposed to confirm the efficacy and safety of FIN in DKD with an eGFR below 25 mL/min/1.73 m^2 and assess the clinical usage of FIN in patients with CKD but without diabetes. Besides, few studies have assessed whether this novel NS-MRA retain their beneficial effects across various kidney diseases as those observed with extant steroidal MRA, and there is no evidence for use in other settings like resistant hypertension, ascites due to cirrhosis, or primary hyperaldosteronism as compared to the first- and second-generation MRAs spironolactone or eplerenone. In addition, whether MR blockade alleviates IR injury in kidney transplantation is an intriguing topic. To justify these usages, comparative studies will need to be conducted for these specific conditions.

Author contributions

WC: Investigation, Methodology, Visualization, Writing – original draft. LZ: Investigation, Methodology, Validation, Writing – review & editing. JW: Investigation, Methodology, Visualization, Writing – review & editing. YL: Investigation, Methodology, Supervision, Visualization, Writing – review & editing. TZ: Investigation, Methodology, Project administration, Supervision, Validation, Visualization, Writing – review & editing.

Conflict of interest

The authors declare that the research was conducted in the absence of any commercial or financial relationships that could be construed as a potential conflict of interest.

Publisher's note

References

1. Romagnani P, Remuzzi G, Glassock R, Levin A, Jager KJ, Tonelli M, et al. Chronic kidney disease. *Nat Rev Dis Primers* (2017) 3:17088. doi: 10.1038/nrdp.2017.88

2. Levey AS, de Jong PE, Coresh J, El Nahas M, Astor BC, Matsushita K, et al. The definition, classification, and prognosis of chronic kidney disease: a KDIGO Controversies Conference report. *Kidney Int* (2011) 80(1):17–28. doi: 10.1038/ki.2010.483

3. GBD Chronic Kidney Disease Collaboration. Global, regional, and national burden of chronic kidney disease, 1990-2017: a systematic analysis for the Global Burden of Disease Study 2017. *Lancet* (2020) 395(10225):709–33. doi: 10.1016/S0140-6736(19)32977-0

4. Ortiz AAsociación Información Enfermedades Renales Genéticas (AIRG-E), European Kidney Patients' Federation (EKPF), Federación Nacional de Asociaciones para la Lucha Contra las Enfermedades del Riñón (ALCER), Fundación Renal Íñigo Álvarez de Toledo (FRIAT) and Red de Investigación Renal (REDINREN), et al. RICORS2040: the need for collaborative research in chronic kidney disease. *Clin Kidney J* (2022) 15(3):372–87. doi: 10.1093/ckj/sfab170

5. Jager KJ, Kovesdy C, Langham R, Rosenberg M, Jha V, Zoccali C. A single number for advocacy and communication-worldwide more than 850 million individuals have kidney diseases. *Nephrol Dial Transpl* (2019) 34(11):1803–5. doi: 10.1093/ndt/gfz174

6. Gansevoort RT, Correa-Rotter R, Hemmelgarn BR, Jafar TH, Heerspink HJL, Mann JF, et al. Chronic kidney disease and cardiovascular risk: epidemiology, mechanisms, and prevention. *Lancet* (2013) 382(9889):339–52. doi: 10.1016/S0140-6736(13)60595-4

7. Doshi SM, Friedman AN. Diagnosis and management of type 2 diabetic kidney disease. *Clin J Am Soc Nephrol* (2017) 12(8):1366–73. doi: 10.2215/CJN.11111016

8. Li H, Lu W, Wang A, Jiang H, Lyu J. Changing epidemiology of chronic kidney disease as a result of type 2 diabetes mellitus from 1990 to 2017: Estimates from Global Burden of Disease 2017. *J Diabetes Investig* (2021) 12(3):346–56. doi: 10.1111/jdi.13355

9. Alicic RZ, Rooney MT, Tuttle KR. Diabetic kidney disease: challenges, progress, and possibilities. *Clin J Am Soc Nephrol* (2017) 12(12):2032–45. doi: 10.2215/CJN.11491116

10. Rangaswami J, Bhalla V, de Boer IH, Staruschenko A, Sharp JA, Singh RR, et al. Cardiorenal protection with the newer antidiabetic agents in patients with diabetes and chronic kidney disease: A scientific statement from the American heart association. *Circulation* (2020) 142(17):e265–86. doi: 10.1161/CIR.0000000000000920

11. Narres M, Claessen H, Droste S, Kvitkina T, Koch M, Kuss O, et al. The incidence of end-stage renal disease in the diabetic (Compared to the non-diabetic) population: A systematic review. *PloS One* (2016) 11(1):e0147329. doi: 10.1371/journal.pone.0147329

12. Nichols GA, Déruaz-Luyet A, Hauske SJ, Brodovicz KG. The association between estimated glomerular filtration rate, albuminuria, and risk of cardiovascular hospitalizations and all-cause mortality among patients with type 2 diabetes. *J Diabetes Complications* (2018) 32(3):291–7. doi: 10.1016/j.jdiacomp.2017.12.003

13. Chaudhuri A, Ghanim H, Arora P. Improving the residual risk of renal and cardiovascular outcomes in diabetic kidney disease: A review of pathophysiology, mechanisms, and evidence from recent trials. *Diabetes Obes Metab* (2022) 24(3):365–76. doi: 10.1111/dom.14601

14. Wen CP, Chang CH, Tsai MK, Lee JH, Lu PJ, Tsai SP, et al. Diabetes with early kidney involvement may shorten life expectancy by 16 years. *Kidney Int* (2017) 92 (2):388–96. doi: 10.1016/j.kint.2017.01.030

15. Afkarian M, Sachs MC, Kestenbaum B, Hirsch IB, Tuttle KR, Himmelfarb J, et al. Kidney disease and increased mortality risk in type 2 diabetes. *J Am Soc Nephrol* (2013) 24(2):302–8. doi: 10.1681/ASN.2012070718

16. Zoccali C, Vanholder R, Massy ZA, Ortiz A, Sarafidis P, Dekker FW, et al. The systemic nature of CKD. *Nat Rev Nephrol* (2017) 13(6):344–58. doi: 10.1038/nrneph.2017.52

17. Bertocchio JP, Warnock DG, Jaisser F. Mineralocorticoid receptor activation and blockade: an emerging paradigm in chronic kidney disease. *Kidney Int* (2011) 79 (10):1051–60. doi: 10.1038/ki.2011.48

18. Shibata S, Nagase M, Yoshida S, Kawarazaki W, Kurihara H, Tanaka H, et al. Modification of mineralocorticoid receptor function by Rac1 GTPase: implication in proteinuric kidney disease. *Nat Med* (2008) 14(12):1370–6. doi: 10.1038/nm.1879

19. Quinkler M, Zehnder D, Eardley KS, Lepenies J, Howie AJ, Hughes SV, et al. Increased expression of mineralocorticoid effector mechanisms in kidney biopsies of patients with heavy proteinuria. *Circulation* (2005) 112(10):1435–43. doi: 10.1161/CIRCULATIONAHA.105.539122

20. Bădilă E. The expanding class of mineralocorticoid receptor modulators: New ligands for kidney, cardiac, vascular, systemic and behavioral selective actions. *Acta Endocrinol (Buchar)* (2020) 16(4):487–96. doi: 10.4183/aeb.2020.487

21. Kawarazaki W, Nagase M, Yoshida S, Takeuchi M, Ishizawa K, Ayuzawa N, et al. Angiotensin II- and salt-induced kidney injury through Rac1-mediated mineralocorticoid receptor activation. *J Am Soc Nephrol* (2012) 23(6):997–1007. doi: 10.1681/ASN.2011070734

22. Kawarazaki W, Fujita T. The role of aldosterone in obesity-related hypertension. *Am J Hypertens* (2016) 29(4):415–23. doi: 10.1093/ajh/hpw003

23. Jaques DA, Wuerzner G, Ponte B. Sodium intake as a cardiovascular risk factor: A narrative review. *Nutrients* (2021) 13(9):3177. doi: 10.3390/nu13093177

24. Shibata S, Mu S, Kawarazaki H, Muraoka K, Ishizawa K, Yoshida S, et al. Rac1 GTPase in rodent kidneys is essential for salt-sensitive hypertension via a mineralocorticoid receptor-dependent pathway. *J Clin Invest* (2011) 121(8):3233–43. doi: 10.1172/JCI43124

25. Epstein M. Aldosterone and mineralocorticoid receptor signaling as determinants of cardiovascular and renal injury: from Hans Selye to the present. *Am J Nephrol* (2021) 52(3):209–16. doi: 10.1159/000515622

26. Barrera-Chimal J, Girerd S, Jaisser F. Mineralocorticoid receptor antagonists and kidney diseases: pathophysiological basis. *Kidney Int* (2019) 96(2):302–19. doi: 10.1016/j.kint.2019.02.030

27. Barrera-Chimal J, Estrela GR, Lechner SM, Giraud S, El Moghrabi S, Kaaki S, et al. The myeloid mineralocorticoid receptor controls inflammatory and fibrotic responses after renal injury via macrophage interleukin-4 receptor signaling. *Kidney Int* (2018) 93(6):1344–55. doi: 10.1016/j.kint.2017.12.016

28. Erraez S, López-Mesa M, Gómez-Fernández P. Mineralcorticoid receptor blockers in chronic kidney disease. *Nefrologia (Engl Ed)* (2021) 41(3):258–75. doi: 10.1016/j.nefroe.2021.08.001

29. Huang LL, Nikolic-Paterson DJ, Han Y, Ozols E, Ma FY, Young MJ, et al. Myeloid mineralocorticoid receptor activation contributes to progressive kidney disease. *J Am Soc Nephrol* (2014) 25(10):2231–40. doi: 10.1681/ASN.2012111094

30. Brown NJ. Contribution of aldosterone to cardiovascular and renal inflammation and fibrosis. *Nat Rev Nephrol* (2013) 9(8):459–69. doi: 10.1038/nrneph.2013.110

31. Remuzzi G, Cattaneo D, Perico N. The aggravating mechanisms of aldosterone on kidney fibrosis. *J Am Soc Nephrol* (2008) 19(8):1459–62. doi: 10.1681/ASN.2007101079

32. Barrera-Chimal J, Lima-Posada I, Bakris GL, Jaisser F. Mineralocorticoid receptor antagonists in diabetic kidney disease - mechanistic and therapeutic effects. *Nat Rev Nephrol* (2022) 18(1):56–70. doi: 10.1038/s41581-021-00490-8

33. Tesch GH, Young MJ. Mineralocorticoid receptor signaling as a therapeutic target for renal and cardiac fibrosis. *Front Pharmacol* (2017) 8:313. doi: 10.3389/fphar.2017.00313

34. Handelsman Y, Butler J, Bakris GL, DeFronzo RA, Fonarow GC, Green JB, et al. Early intervention and intensive management of patients with diabetes, cardiorenal, and metabolic diseases. *J Diabetes Complications* (2023) 37(2):108389. doi: 10.1016/j.jdiacomp.2022.108389

35. Brenner BM, Cooper ME, de Zeeuw D, Keane WF, Mitch WE, Parving HH, et al. Effects of losartan on renal and cardiovascular outcomes in patients with type 2 diabetes and nephropathy. *N Engl J Med* (2001) 345(12):861–9. doi: 10.1056/NEJMoa011161

36. Lewis EJ, Hunsicker LG, Clarke WR, Berl T, Pohl MA, Lewis JB, et al. Renoprotective effect of the angiotensin-receptor antagonist irbesartan in patients with nephropathy due to type 2 diabetes. *N Engl J Med* (2001) 345(12):851–60. doi: 10.1056/NEJMoa011303

37. Sarafidis P, Ferro CJ, Morales E, Ortiz A, Malyszko J, Hojs R, et al. SGLT-2 inhibitors and GLP-1 receptor agonists for nephroprotection and cardioprotection in patients with diabetes mellitus and chronic kidney disease. A consensus statement by the EURECA-m and the DIABESITY working groups of the ERA-EDTA. *Nephrol Dial Transpl* (2019) 34(2):208–30. doi: 10.1093/ndt/gfy407

38. Perkovic V, Jardine MJ, Neal B, Bompoint S, Heerspink HJL, Charytan DM, et al. Canagliflozin and renal outcomes in type 2 diabetes and nephropathy. *N Engl J Med* (2019) 380(24):2295–306. doi: 10.1056/NEJMoa1811744

39. Heerspink HJL, Stefánsson BV, Correa-Rotter R, Chertow GM, Greene T, Hou FF, et al. Dapagliflozin in patients with chronic kidney disease. *N Engl J Med* (2020) 383 (15):1436–46. doi: 10.1056/NEJMoa2024816

40. Lewis EJ, Hunsicker LG, Bain RP, Rohde RD. The effect of angiotensin-converting-enzyme inhibition on diabetic nephropathy. The Collaborative Study Group. *N Engl J Med* (1993) 329(20):1456–62. doi: 10.1056/NEJM199311113292004

41. Terpening CM. Prevention of cardiovascular events in patients with chronic kidney disease. *Ann Pharmacother* (2023) 57(12):1425–35. doi: 10.1177/10600280231165774

42. D'Marco L, PuChades MJ, Gandía L, Forquet C, Giménez-Civera E, Panizo N, et al. Finerenone: A potential treatment for patients with chronic kidney disease and type 2 diabetes mellitus. *touchREV Endocrinol* (2021) 17(2):84–7. doi: 10.17925/EE.2021.17.2.84

43. DuPont JJ, Jaffe IZ. 30 YEARS OF THE MINERALOCORTICOID RECEPTOR: The role of the mineralocorticoid receptor in the vasculature. *J Endocrinol* (2017) 234 (1):T67–82. doi: 10.1530/JOE-17-0009

44. Alicic RZ, Johnson EJ, Tuttle KR. Inflammatory mechanisms as new biomarkers and therapeutic targets for diabetic kidney disease. *Adv Chronic Kidney Dis* (2018) 25 (2):181–91. doi: 10.1053/j.ackd.2017.12.002

45. González-Blázquez R, Somoza B, Gil-Ortega M, Martín Ramos M, Ramiro-Cortijo D, Vega-Martín E, et al. Finerenone attenuates endothelial dysfunction and

albuminuria in a chronic kidney disease model by a reduction in oxidative stress. *Front Pharmacol* (2018) 9:1131. doi: 10.3389/fphar.2018.01131

46. Gil-Ortega M, Vega-Martín E, Martín-Ramos M, González-Blázquez R, Pulido-Olmo H, Ruiz-Hurtado G, et al. Finerenone reduces intrinsic arterial stiffness in Munich Wistar Frömter rats, a genetic model of chronic kidney disease. *Am J Nephrol* (2020) 51(4):294–303. doi: 10.1159/000506275

47. Dutzmann J, Musmann RJ, Haertlé M, Daniel JM, Sonnenschein K, Schäfer A, et al. The novel mineralocorticoid receptor antagonist finerenone attenuates neointima formation after vascular injury. *PLoS One* (2017) 12(9):e0184888. doi: 10.1371/journal.pone.0184888

48. Ng KP, Arnold J, Sharif A, Gill P, Townend JN, Ferro CJ. Cardiovascular actions of mineralocorticoid receptor antagonists in patients with chronic kidney disease: A systematic review and meta-analysis of randomized trials. *J Renin Angiotensin Aldosterone Syst* (2015) 16(3):599–613. doi: 10.1177/1470320315575849

49. Currie G, Taylor AHM, Fujita T, Ohtsu H, Lindhardt M, Rossing P, et al. Effect of mineralocorticoid receptor antagonists on proteinuria and progression of chronic kidney disease: a systematic review and meta-analysis. *BMC Nephrol* (2016) 17(1):127. doi: 10.1186/s12882-016-0337-0

50. Sarafidis PA, Memmos E, Alexandrou ME, Papagianni A. Mineralocorticoid receptor antagonists for nephroprotection: current evidence and future perspectives. *Curr Pharm Des* (2018) 24(46):5528–36. doi: 10.2174/1381612825666190306162658

51. Ai Dhaybi O, Bakris GL. Renal targeted therapies of antihypertensive and cardiovascular drugs for patients with stages 3 through 5d kidney disease. *Clin Pharmacol Ther* (2017) 102(3):450–8. doi: 10.1002/cpt.758

52. Pitt B, Rossignol P. The safety of mineralocorticoid receptor antagonists (MRAs) in patients with heart failure. *Expert Opin Drug Saf* (2016) 15(5):659–65. doi: 10.1517/14740338.2016.1163335

53. Bolignano D, Palmer SC, Navaneethan SD, Strippoli GFM. Aldosterone antagonists for preventing the progression of chronic kidney disease. *Cochrane Database Syst Rev* (2014) 4:CD007004. doi: 10.1002/14651858.CD007004.pub3

54. Trevisan M, de Deco P, Xu H, Evans M, Lindholm B, Bellocco R, et al. Incidence, predictors and clinical management of hyperkalaemia in new users of mineralocorticoid receptor antagonists. *Eur J Heart Fail* (2018) 20(8):1217–26. doi: 10.1002/ejhf.1199

55. Kolkhof P, Bärfacker L. 30 YEARS OF THE MINERALOCORTICOID RECEPTOR: Mineralocorticoid receptor antagonists: 60 years of research and development. *J Endocrinol* (2017) 234(1):T125–40. doi: 10.1530/JOE-16-0600

56. Lazich I, Bakris GL. Prediction and management of hyperkalemia across the spectrum of chronic kidney disease. *Semin Nephrol* (2014) 34(3):333–9. doi: 10.1016/j.semnephrol.2014.04.008

57. Kolkhof P, Joseph A, Kintscher U. Nonsteroidal mineralocorticoid receptor antagonism for cardiovascular and renal disorders - New perspectives for combination therapy. *Pharmacol Res* (2021) 172:105859. doi: 10.1016/j.phrs.2021.105859

58. Bärfacker L, Kuhl A, Hillisch A, Grosser R, Figueroa-Pérez S, Heckroth H, et al. Discovery of BAY 94-8862: a nonsteroidal antagonist of the mineralocorticoid receptor for the treatment of cardiorenal diseases. *ChemMedChem* (2012) 7(8):1385–403. doi: 10.1002/cmdc.201200081

59. Kintscher U, Bakris GL, Kolkhof P. Novel non-steroidal mineralocorticoid receptor antagonists in cardiorenal disease. *Br J Pharmacol* (2022) 179(13):3220–34. doi: 10.1111/bph.15747

60. Lorente-Ros M, Aguilar-Gallardo JS, Shah A, Narasimhan B, Aronow WS. An overview of mineralocorticoid receptor antagonists as a treatment option for patients with heart failure: the current state-of-the-art and future outlook. *Expert Opin Pharmacother* (2022) 23(15):1737–51. doi: 10.1080/14656566.2022.2138744

61. Heinig R, Kimmeskamp-Kirschbaum N, Halabi A, Lentini S. Pharmacokinetics of the novel nonsteroidal mineralocorticoid receptor antagonist finerenone (BAY 94-8862) in individuals with renal impairment. *Clin Pharmacol Drug Dev* (2016) 5(6):488–501. doi: 10.1002/cpdd.263

62. Shibata S. 30 YEARS OF THE MINERALOCORTICOID RECEPTOR: Mineralocorticoid receptor and NaCl transport mechanisms in the renal distal nephron. *J Endocrinol* (2017) 234(1):T35–47. doi: 10.1530/JOE-16-0669

63. Lother A, Jaisser F, Wenzel UO. Emerging fields for therapeutic targeting of the aldosterone-mineralocorticoid receptor signaling pathway. *Br J Pharmacol* (2022) 179(13):3099–102. doi: 10.1111/bph.15808

64. Verma A, Vaidya A, Subudhi S, Waikar SS. Aldosterone in chronic kidney disease and renal outcomes. *Eur Heart J* (2022) 43(38):3781–91. doi: 10.1093/eurheartj/ehac352

65. Bauersachs J, Jaisser F, Toto R. Mineralocorticoid receptor activation and mineralocorticoid receptor antagonist treatment in cardiac and renal diseases. *Hypertension* (2015) 65(2):257–63. doi: 10.1161/HYPERTENSIONAHA.114.04488

66. Jaisser F, Farman N. Emerging roles of the mineralocorticoid receptor in pathology: toward new paradigms in clinical pharmacology. *Pharmacol Rev* (2016) 68(1):49–75. doi: 10.1124/pr.115.011106

67. Iyer A, Chan V, Brown L. The DOCA-salt hypertensive rat as a model of cardiovascular oxidative and inflammatory stress. *Curr Cardiol Rev* (2010) 6(4):291–7. doi: 10.2174/157340310793566109

68. Araujo M, Wilcox CS. Oxidative stress in hypertension: role of the kidney. *Antioxid Redox Signal* (2014) 20(1):74–101. doi: 10.1089/ars.2013.5259

69. Nishiyama A, Yao L, Nagai Y, Miyata K, Yoshizumi M, Kagami S, et al. Possible contributions of reactive oxygen species and mitogen-activated protein kinase to renal injury in aldosterone/salt-induced hypertensive rats. *Hypertension* (2004) 43(4):841–8. doi: 10.1161/01.HYP.0000118519.66430.22

70. Barrera-Chimal J, Prince S, Fadel F, El Moghrabi S, Warnock DG, Kolkhof P, et al. Sulfenic acid modification of endothelin B receptor is responsible for the benefit of a nonsteroidal mineralocorticoid receptor antagonist in renal ischemia. *J Am Soc Nephrol* (2016) 27(2):398–404. doi: 10.1681/ASN.2014121216

71. Barrera-Chimal J, André-Grégoire G, Nguyen Dinh Cat A, Lechner SM, Cau J, Prince S, et al. Benefit of mineralocorticoid receptor antagonism in AKI: role of vascular smooth muscle Rac1. *J Am Soc Nephrol* (2017) 28(4):1216–26. doi: 10.1681/ASN.2016040477

72. Lattenist L, Lechner SM, Messaoudi S, Le Mercier A, El Moghrabi S, Prince S, et al. Nonsteroidal mineralocorticoid receptor antagonist finerenone protects against acute kidney injury-mediated chronic kidney disease: role of oxidative stress. *Hypertension* (2017) 69(5):870–8. doi: 10.1161/HYPERTENSIONAHA.116.08526

73. Rossing P, Anker SD, Filippatos G, Pitt B, Ruilope LM, Birkenfeld AL, et al. Finerenone in patients with chronic kidney disease and type 2 diabetes by sodium-glucose cotransporter 2 inhibitor treatment: the FIDELITY analysis. *Diabetes Care* (2022) 45(12):2991–8. doi: 10.2337/dc22-0294

74. Huen SC, Cantley LG. Macrophage-mediated injury and repair after ischemic kidney injury. *Pediatr Nephrol* (2015) 30(2):199–209. doi: 10.1007/s00467-013-2726-y

75. van der Heijden CDCC, Deinum J, Joosten LAB, Netea MG, Riksen NP. The mineralocorticoid receptor as a modulator of innate immunity and atherosclerosis. *Cardiovasc Res* (2018) 114(7):944–53. doi: 10.1093/cvr/cvy092

76. Luettges K, Bode M, Diemer JN, Schwanbeck J, Wirth EK, Klopfleisch R, et al. Finerenone reduces renal RORγt γδ T cells and protects against cardiorenal damage. *Am J Nephrol* (2022) 53(7):552–64. doi: 10.1159/000524940

77. Kolkhof P, Delbeck M, Kretschmer A, Steinke W, Hartmann E, Bärfacker L, et al. Finerenone, a novel selective nonsteroidal mineralocorticoid receptor antagonist protects from rat cardiorenal injury. *J Cardiovasc Pharmacol* (2014) 64(1):69–78. doi: 10.1097/FJC.0000000000000091

78. Murea M, Register TC, Divers J, Bowden DW, Carr JJ, Hightower CR, et al. Relationships between serum MCP-1 and subclinical kidney disease: African American-Diabetes Heart Study. *BMC Nephrol* (2012) 13:148. doi: 10.1186/1471-2369-13-148

79. Bolignano D, Lacquaniti A, Coppolino G, Donato V, Campo S, Fazio MR, et al. Neutrophil gelatinase-associated lipocalin (NGAL) and progression of chronic kidney disease. *Clin J Am Soc Nephrol* (2009) 4(2):337–44. doi: 10.2215/CJN.03530708

80. Steinbrenner I, Sekula P, Kotsis F, von Cube M, Cheng Y, Nadal J, et al. Association of osteopontin with kidney function and kidney failure in chronic kidney disease patients: the GCKD study. *Nephrol Dial Transpl* (2023) 38(6):1430–8. doi: 10.1093/ndt/gfac173

81. Hirohama D, Nishimoto M, Ayuzawa N, Kawarazaki W, Fujii W, Oba S, et al. Activation of rac1-mineralocorticoid receptor pathway contributes to renal injury in salt-loaded db/db mice. *Hypertension* (2021) 78(1):82–93. doi: 10.1161/HYPERTENSIONAHA.121.17263

82. Mansour SG, Puthumana J, Coca SG, Gentry M, Parikh CR. Biomarkers for the detection of renal fibrosis and prediction of renal outcomes: a systematic review. *BMC Nephrol* (2017) 18(1):72. doi: 10.1186/s12882-017-0490-0

83. Kolkhof P, Hartmann E, Freyberger A, Pavkovic M, Mathar I, Sandner P, et al. Effects of finerenone combined with empagliflozin in a model of hypertension-induced end-organ damage. *Am J Nephrol* (2021) 52(8):642–52. doi: 10.1159/000516213

84. Droebner K, Pavkovic M, Grundmann M, Hartmann E, Goea L, Nordlohne J, et al. Direct blood pressure-independent anti-fibrotic effects by the selective nonsteroidal mineralocorticoid receptor antagonist finerenone in progressive models of kidney fibrosis. *Am J Nephrol* (2021) 52(7):588–601. doi: 10.1159/000518254

85. Kuppe C, Ibrahim MM, Kranz J, Zhang X, Ziegler S, Perales-Patón J, et al. Decoding myofibroblast origins in human kidney fibrosis. *Nature* (2021) 589(7841):281–6. doi: 10.1038/s41586-020-2941-1

86. Lima-Posada I, Stephan Y, Soulié M, Palacios-Ramirez R, Bonnard B, Nicol L, et al. Benefits of the non-steroidal mineralocorticoid receptor antagonist finerenone in metabolic syndrome-related heart failure with preserved ejection fraction. *Int J Mol Sci* (2023) 24(3):2536. doi: 10.3390/ijms24032536

87. Pitt B, Filippatos G, Agarwal R, Anker SD, Bakris GL, Rossing P, et al. Cardiovascular events with finerenone in kidney disease and type 2 diabetes. *N Engl J Med* (2021) 385(24):2252–63. doi: 10.1056/NEJMoa2110956

88. Bakris GL, Agarwal R, Anker SD, Pitt B, Ruilope LM, Rossing P, et al. Effect of finerenone on chronic kidney disease outcomes in type 2 diabetes. *N Engl J Med* (2020) 383(23):2219–29. doi: 10.1056/NEJMoa2025845

89. Pitt B, Kober L, Ponikowski P, Gheorghiade M, Filippatos G, Krum H, et al. Safety and tolerability of the novel non-steroidal mineralocorticoid receptor antagonist BAY 94-8862 in patients with chronic heart failure and mild or moderate chronic kidney disease: a randomized, double-blind trial. *Eur Heart J* (2013) 34(31):2453–63. doi: 10.1093/eurheartj/eht187

90. Filippatos G, Anker SD, Böhm M, Gheorghiade M, Køber L, Krum H, et al. A randomized controlled study of finerenone vs. eplerenone in patients with worsening chronic heart failure and diabetes mellitus and/or chronic kidney disease. *Eur Heart J* (2016) 37(27):2105–14. doi: 10.1093/eurheartj/ehw132

91. Bakris GL, Agarwal R, Chan JC, Cooper ME, Gansevoort RT, Haller H, et al. Effect of finerenone on albuminuria in patients with diabetic nephropathy: A randomized clinical trial. *JAMA* (2015) 314(9):884–94. doi: 10.1001/jama.2015.10081

92. Katayama S, Yamada D, Nakayama M, Yamada T, Myoishi M, Kato M, et al. A randomized controlled study of finerenone versus placebo in Japanese patients with type 2 diabetes mellitus and diabetic nephropathy. *J Diabetes Complications* (2017) 31 (4):758–65. doi: 10.1016/j.jdiacomp.2016.11.021

93. Snelder N, Heinig R, Drenth HJ, Joseph A, Kolkhof P, Lippert J, et al. Population pharmacokinetic and exposure-response analysis of finerenone: insights based on phase IIb data and simulations to support dose selection for pivotal trials in type 2 diabetes with chronic kidney disease. *Clin Pharmacokinet* (2020) 59(3):359–70. doi: 10.1007/s40262-019-00820-x

94. Agarwal R, Filippatos G, Pitt B, Anker SD, Rossing P, Joseph A, et al. Cardiovascular and kidney outcomes with finerenone in patients with type 2 diabetes and chronic kidney disease: the FIDELITY pooled analysis. *Eur Heart J* (2022) 43(6):474–84. doi: 10.1093/eurheartj/ehab777

95. Goulooze SC, Heerspink HJL, van Noort M, Snelder N, Brinker M, Lippert J, et al. Dose-exposure-response analysis of the nonsteroidal mineralocorticoid receptor antagonist finerenone on UACR and eGFR: an analysis from FIDELIO-DKD. *Clin Pharmacokinet* (2022) 61(7):1013–25. doi: 10.1007/s40262-022-01124-3

96. Filippatos G, Bakris GL, Pitt B, Agarwal R, Rossing P, Ruilope LM, et al. Finerenone reduces new-onset atrial fibrillation in patients with chronic kidney disease and type 2 diabetes. *J Am Coll Cardiol* (2021) 78(2):142–52. doi: 10.1016/j.jacc.2021.04.079

97. Mende CW, Samarakoon R, Higgins PJ. Mineralocorticoid receptor-associated mechanisms in diabetic kidney disease and clinical significance of mineralocorticoid receptor antagonists. *Am J Nephrol* (2023) 54(1–2):50–61. doi: 10.1159/000528783

98. Ruilope LM, Pitt B, Anker SD, Rossing P, Kovesdy CP, Pecoits-Filho R, et al. Kidney outcomes with finerenone: an analysis from the FIGARO-DKD study. *Nephrol Dial Transpl* (2023) 38(2):372–83. doi: 10.1093/ndt/gfac157

99. Agarwal R, Pitt B, Palmer BF, Kovesdy CP, Burgess E, Filippatos G, et al. A comparative *post hoc* analysis of finerenone and spironolactone in resistant hypertension in moderate-to-advanced chronic kidney disease. *Clin Kidney J* (2023) 16(2):293–302. doi: 10.1093/ckj/sfac234

100. Bakris GL, Ruilope LM, Anker SD, Filippatos G, Pitt B, Rossing P, et al. A prespecified exploratory analysis from FIDELITY examined finerenone use and kidney outcomes in patients with chronic kidney disease and type 2 diabetes. *Kidney Int* (2023) 103(1):196–206. doi: 10.1016/j.kint.2022.08.040

101. Sarafidis P, Agarwal R, Pitt B, Wanner C, Filippatos G, Boletis J, et al. Outcomes with finerenone in participants with stage 4 CKD and type 2 diabetes: A FIDELITY subgroup analysis. *Clin J Am Soc Nephrol* (2023) 18(5):602–12. doi: 10.2215/CJN.0000000000000149

102. Mima A, Lee R, Murakami A, Gotoda H, Akai R, Kidooka S, et al. Effect of finerenone on diabetic kidney disease outcomes with estimated glomerular filtration rate below 25 mL/min/1. *73 m2. Metabol Open* (2023) 19:100251. doi: 10.1016/j.metop.2023.100251

103. Filippatos G, Anker SD, August P, Coats AJS, Januzzi JL, Mankovsky B, et al. Finerenone and effects on mortality in chronic kidney disease and type 2 diabetes: a FIDELITY analysis. *Eur Heart J Cardiovasc Pharmacother* (2023) 9(2):183–91. doi: 10.1093/ehjcvp/pvad001

104. McGill JB, Agarwal R, Anker SD, Bakris GL, Filippatos G, Pitt B, et al. Effects of finerenone in people with chronic kidney disease and type 2 diabetes are independent of HbA1c at baseline, HbA1c variability, diabetes duration and insulin use at baseline. *Diabetes Obes Metab* (2023) 25(6):1512–22. doi: 10.1111/dom.14999

105. Rossing P, Burgess E, Agarwal R, Anker SD, Filippatos G, Pitt B, et al. Finerenone in patients with chronic kidney disease and type 2 diabetes according to baseline HbA1c and insulin use: an analysis from the FIDELIO-DKD study. *Diabetes Care* (2022) 45(4):888–97. doi: 10.2337/dc21-1944

106. Filippatos G, Pitt B, Agarwal R, Farmakis D, Ruilope LM, Rossing P, et al. Finerenone in patients with chronic kidney disease and type 2 diabetes with and without heart failure: a prespecified subgroup analysis of the FIDELIO-DKD trial. *Eur J Heart Fail* (2022) 24(6):996–1005. doi: 10.1002/ejhf.2469

107. Filippatos G, Anker SD, Agarwal R, Ruilope LM, Rossing P, Bakris GL, et al. Finerenone reduces risk of incident heart failure in patients with chronic kidney disease and type 2 diabetes: analyses from the FIGARO-DKD trial. *Circulation* (2022) 145 (6):437–47. doi: 10.1161/CIRCULATIONAHA.121.057983

108. Filippatos G, Anker SD, Pitt B, McGuire DK, Rossing P, Ruilope LM, et al. Finerenone efficacy in patients with chronic kidney disease, type 2 diabetes and atherosclerotic cardiovascular disease. *Eur Heart J Cardiovasc Pharmacother* (2022) 9 (1):85–93. doi: 10.1093/ehjcvp/pvac054

109. Finerenone (Kerendia) for chronic kidney disease. *Med Lett Drugs Ther* (2021) 63(1631):131–2.

110. Vizcaya D, Kovesdy CP, Reyes A, Pessina E, Pujol P, James G, et al. Characteristics of patients with chronic kidney disease and Type 2 diabetes initiating finerenone in the USA: a multi-database, cross-sectional study. *J Comp Eff Res* (2023) 12 (8):e230076. doi: 10.57264/cer-2023-0076

111. ElSayed NA, Aleppo G, Aroda VR, Bannuru RR, Brown FM, Bruemmer D, et al. 10. Cardiovascular disease and risk management: standards of care in diabetes-2023. *Diabetes Care* (2023) 46(Suppl 1):S158–90. doi: 10.2337/dc23-S010

112. de Boer IH, Khunti K, Sadusky T, Tuttle KR, Neumiller JJ, Rhee CM, et al. Diabetes management in chronic kidney disease: A consensus report by the American diabetes association (ADA) and kidney disease: improving global outcomes (KDIGO). *Diabetes Care* (2022) 45(12):3075–90. doi: 10.2337/dci22-0027

113. American Diabetes Association Professional Practice Committee. 11. Chronic kidney disease and risk management: standards of medical care in diabetes-2022. *Diabetes Care* (2022) 45(Suppl 1):S175–84. doi: 10.2337/dc22-S011

114. Blonde L, Umpierrez GE, Reddy SS, McGill JB, Berga SL, Bush M, et al. American association of clinical endocrinology clinical practice guideline: developing a diabetes mellitus comprehensive care plan-2022 update. *Endocr Pract* (2022) 28 (10):923–1049. doi: 10.1016/j.eprac.2022.08.002

115. Kidney Disease: Improving Global Outcomes (KDIGO) Diabetes Work Group. KDIGO 2022 clinical practice guideline for diabetes management in chronic kidney disease. *Kidney Int* (2022) 102(5S):S1–127. doi: 10.1016/j.kint.2022.06.008

116. Goulooze SC, Snelder N, Seelmann A, Horvat-Broecker A, Brinker M, Joseph A, et al. Finerenone dose-exposure-serum potassium response analysis of FIDELIO-DKD phase III: the role of dosing, titration, and inclusion criteria. *Clin Pharmacokinet* (2022) 61(3):451–62. doi: 10.1007/s40262-021-01083-1

117. Agarwal R, Joseph A, Anker SD, Filippatos G, Rossing P, Ruilope LM, et al. Hyperkalemia risk with finerenone: results from the FIDELIO-DKD trial. *J Am Soc Nephrol* (2022) 33(1):225–37. doi: 10.1681/ASN.2021070942

118. Leon SJ, Whitlock R, Rigatto C, Komenda P, Bohm C, Sucha E, et al. Hyperkalemia-related discontinuation of renin-angiotensin-aldosterone system inhibitors and clinical outcomes in CKD: A population-based cohort study. *Am J Kidney Dis* (2022) 80(2):164–73.e1. doi: 10.1053/j.ajkd.2022.01.002

119. Natale P, Palmer SC, Ruospo M, Saglimbene VM, Strippoli GF. Potassium binders for chronic hyperkalaemia in people with chronic kidney disease. *Cochrane Database Syst Rev* (2020) 6(6):CD013165. doi: 10.1002/14651858.CD013165.pub2

120. Zuo C, Xu G. Efficacy and safety of mineralocorticoid receptor antagonists with ACEI/ARB treatment for diabetic nephropathy: A meta-analysis. *Int J Clin Pract* (2019) 29:e13413. doi: 10.1111/ijcp.13413

121. Vaduganathan M, Docherty KF, Claggett BL, Jhund PS, de Boer RA, Hernandez AF, et al. SGLT-2 inhibitors in patients with heart failure: a comprehensive meta-analysis of five randomised controlled trials. *Lancet* (2022) 400(10354):757–67. doi: 10.1016/S0140-6736(22)01429-5

122. Neuen BL, Oshima M, Perkovic V, Agarwal R, Arnott C, Bakris G, et al. Effects of canagliflozin on serum potassium in people with diabetes and chronic kidney disease: the CREDENCE trial. *Eur Heart J* (2021) 42(48):4891–901. doi: 10.1093/eurheartj/ehab497

123. Neuen BL, Oshima M, Agarwal R, Arnott C, Cherney DZ, Edwards R, et al. Sodium-glucose cotransporter 2 inhibitors and risk of hyperkalemia in people with type 2 diabetes: A meta-analysis of individual participant data from randomized, controlled trials. *Circulation* (2022) 145(19):1460–70. doi: 10.1161/CIRCULATIONAHA.121.057736

124. Provenzano M, Jongs N, Vart P, Stefánsson BV, Chertow GM, Langkilde AM, et al. The kidney protective effects of the sodium-glucose cotransporter-2 inhibitor, Dapagliflozin, are present in patients with CKD treated with mineralocorticoid receptor antagonists. *Kidney Int Rep* (2022) 7(3):436–43. doi: 10.1016/j.ekir.2021.12.013

125. Provenzano M, PuChades MJ, Garofalo C, Jongs N, D'Marco L, Andreucci M, et al. Albuminuria-lowering effect of dapagliflozin, eplerenone, and their combination in patients with chronic kidney disease: A randomized crossover clinical trial. *J Am Soc Nephrol* (2022) 33(8):1569–80. doi: 10.1681/ASN.2022020207

126. Rossing P, Agarwal R, Anker SD, Filippatos G, Pitt B, Ruilope LM, et al. Efficacy and safety of finerenone in patients with chronic kidney disease and type 2 diabetes by GLP-1RA treatment: A subgroup analysis from the FIDELIO-DKD trial. *Diabetes Obes Metab* (2022) 24(1):125–34. doi: 10.1111/dom.14558

127. Rossing P, Agarwal R, Anker SD, Filippatos G, Pitt B, Ruilope LM, et al. Finerenone in patients across the spectrum of chronic kidney disease and type 2 diabetes by glucagon-like peptide-1 receptor agonist use. *Diabetes Obes Metab* (2023) 25(2):407–16. doi: 10.1111/dom.14883

128. Green JB, Mottl AK, Bakris G, Heerspink HJL, Mann JFE, McGill JB, et al. Design of the COmbinatioN effect of FInerenone anD EmpagliflozIN in participants with chronic kidney disease and type 2 diabetes using a UACR Endpoint study (CONFIDENCE). *Nephrol Dial Transpl* (2023) 38(4):894–903. doi: 10.1093/ndt/gfac198

129. *A Trial to Learn How Well Finerenone Works and How Safe it is in Adult Participants with Non-diabetic Chronic Kidney Disease*. Available at: https://clinicaltrials.gov/ct2/show/NCT05047263 (Accessed 27 February 2023).

130. Desai NR, Navaneethan SD, Nicholas SB, Pantalone KM, Wanner C, Hamacher S, et al. Design and rationale of FINE-REAL: A prospective study of finerenone in clinical practice. *J Diabetes Complications* (2023) 37(4):108411. doi: 10.1016/j.jdiacomp.2023.108411

10.3389/fendo.2023.1320603

Glossary

DKD	diabetic kidney disease
CKD	chronic kidney disease
T2D	type 2 diabetes
CV	cardiovascular
MRs	mineralocorticoid receptors
MRAs	MR antagonists
FIN	finerenone
CVD	CV disease
eGFR	estimated glomerular filtration rate
AKI	acute kidney injury
ESKD	end-stage kidney disease
BP	blood pressure
RAS	renin-angiotensin system
ACEi	angiotensin-converting enzyme inhibitors
ARB	angiotensin receptor blockers
SGLT2i	sodium-glucose co-transporters-2 inhibitors
NS-MRAs	nonsteroidal MRAs
DOCA	deoxycorticosterone acetate
IR	ischemia-reperfusion
MWF	munich Wistar frömter
HS	high salt
UACR	urine albumin-creatinine ratio
ARTS-DN	Mineralocorticoid Receptor Antagonist Tolerability Study–Diabetic Nephropathy
FIDELIO-DKD	Finerenone in Reducing Kidney Failure and Disease Progression in Diabetic Kidney Disease
FIGARO-DKD	Finerenone in Reducing Cardiovascular Mortality and Morbidity in Diabetic Kidney Disease
RCT	randomized controlled trial
MI	myocardial infarction
HF	heart failure
FDA	Food and Drug Administration
EMA	European Medicines Agency
ADA	American Diabetes Association
AACE	American Association of Clinical Endocrinology
KDIGO	Kidney Disease: Improving Global Outcomes
ARTS	Mineralocorticoid Receptor Antagonist Tolerability Study
HFrEF	heart failure with reduced ejection fraction
pro-BNP	pro-B-type natriuretic peptide
WRF	worsening renal function
ARTS-HF	ARTS-Heart Failure
HFpEF	heart failure with preserved ejection fraction
AEs	adverse effects
TEAEs	treatment-emergent AEs
GLP-1RAs	glucagon-like peptide-1 receptor agonist
TGF-β1	transforming growth factor-β-1
PAI-1	plasminogen activator inhibitor-1
Rac1	Ras-related C3 botulinum toxin substrate 1
NOX	NADPH oxidases
ROS	reactive oxygen species
NO	Nitric oxide
SMCs	smooth muscle cells
KIM-1	kidney injury molecule 1
NGAL	neutrophil gelatinase-associated lipocalin
TNF-α	tumor necrosis factor-α
MMP	matrix metalloproteinase
CCL-2	C-C motif chemokine ligand 2
IL	interleukin
ROR	retinoid-related orphan receptor
MCP-1	monocyte chemoattractant protein-1
OPN	osteopontin
COL1A1	collagen type I α 1 chain
NKD2	naked cuticle homolog 2
VSMC	vascular smooth muscle cell
SOD	superoxide dismutase
ENaC	epithelial sodium channel
NCC	thiazide-sensitive sodium chloride cotransporter
UNX	Uninephrectomized

(Continued)

Continued

frontiers | Frontiers in Endocrinology

TYPE Original Research
PUBLISHED 22 February 2024
DOI 10.3389/fendo.2024.1329256

OPEN ACCESS

EDITED BY
Seerapani Gopaluni,
University of Cambridge, United Kingdom

REVIEWED BY
Maria Cannoletta,
Royal Brompton Hospital, United Kingdom
Nguyen Quoc Khanh Le,
Taipei Medical University, Taiwan

*CORRESPONDENCE
Hongyang Xu
xuhongyangCN@163.com

†These authors have contributed equally to this work

RECEIVED 28 October 2023
ACCEPTED 05 February 2024
PUBLISHED 22 February 2024

CITATION
Li X, Cui L and Xu H (2024) Association between systemic inflammation response index and chronic kidney disease: a population-based study.
Front. Endocrinol. 15:1329256.
doi: 10.3389/fendo.2024.1329256

Association between systemic inflammation response index and chronic kidney disease: a population-based study

Xiaowan Li†, Lan Cui† and Hongyang Xu*

Department of Critical Care Medicine, The Affiliated Wuxi People's Hospital of Nanjing Medical University, Wuxi, China

Introduction: Our objective was to explore the potential link between systemic inflammation response index (SIRI) and chronic kidney disease (CKD).

Methods: The data used in this study came from the National Health and Nutrition Examination Survey (NHANES), which gathers data between 1999 and 2020. CKD was diagnosed based on the low estimated glomerular filtration rate (eGFR) of less than 60 mL/min/1.73 m^2 or albuminuria (urinary albumin-to-creatinine ratio (ACR) of more than 30 mg/g). Using generalized additive models and weighted multivariable logistic regression, the independent relationships between SIRI and other inflammatory biomarkers (systemic immune-inflammation index (SII), monocyte/high-density lipoprotein ratio (MHR), neutrophil/high-density lipoprotein ratio (NHR), platelet/high-density lipoprotein ratio (PHR), and lymphocyte/high-density lipoprotein ratio (LHR)) with CKD, albuminuria, and low-eGFR were examined.

Results: Among the recruited 41,089 participants, males accounted for 49.77% of the total. Low-eGFR, albuminuria, and CKD were prevalent in 8.30%, 12.16%, and 17.68% of people, respectively. SIRI and CKD were shown to be positively correlated in the study (OR = 1.24; 95% CI: 1.19, 1.30). Furthermore, a nonlinear correlation was discovered between SIRI and CKD. SIRI and CKD are both positively correlated on the two sides of the breakpoint (SIRI = 2.04). Moreover, increased SIRI levels were associated with greater prevalences of low-eGFR and albuminuria (albuminuria: OR = 1.27; 95% CI: 1.21, 1.32; low-eGFR: OR = 1.11; 95% CI: 1.05, 1.18). ROC analysis demonstrated that, compared to other inflammatory indices (SII, NHR, LHR, MHR, and PHR), SIRI exhibited superior discriminative ability and accuracy in predicting CKD, albuminuria, and low-eGFR.

Discussion: When predicting CKD, albuminuria, and low-eGFR, SIRI may show up as a superior inflammatory biomarker when compared to other inflammatory biomarkers (SII, NHR, LHR, MHR, and PHR). American adults with elevated levels of SIRI, SII, NHR, MHR, and PHR should be attentive to the potential risks to their kidney health.

KEYWORDS

systemic inflammation response index, chronic kidney disease, albuminuria, estimated glomerular filtration rate, cross-sectional study

1 Introduction

An estimated 10% of the global population has chronic kidney disease (CKD), which is associated with a major economic and public health burden (1). The United States (US) continues to have one of the highest rates of end-stage renal disease (ESRD) worldwide (2). The optimal management of CKD and its prevention have emerged as crucial public health issues due to its high prevalence, prevalence, and healthcare costs. Inflammation, obesity, diabetes, hypertension, and cardiovascular diseases (CVD) are all risk factors for CKD (3). Inflammation, as an increasingly prominent modifiable risk factor, plays a vital role in establishing effective treatment strategies to prevent the onset and progression of CKD in clinical practice.

One new inflammatory biomarker that is predictive for a number of diseases is the systemic inflammation response index (SIRI), which is derived from counts of neutrophils, monocytes, and lymphocytes. Previous studies have found that SIRI can predict the severity and development of acute pancreatitis (AP) (4). For hepatocellular carcinoma (HCC) patients undergoing systemic therapy, SIRI is a standalone prognostic factor (5). The study by Xia et al. concentrated on the positive correlation between SIRI with cardiovascular mortality and all-cause mortality in American people (6).

Prior research has indicated a close relationship between inflammation and CKD. An association was shown between elevated albuminuria prevalence and elevated values of the systemic immune inflammation index (SII) by Qin et al. (7). One biomarker that helps forecast how CKD will progress is the neutrophil-to-lymphocyte ratio (NLR) (8). Monocyte-to-lymphocyte ratio (MLR) and the risk of 90-day all-cause death in patients with type 2 diabetes (T2DM) and diabetic kidney disease (DKD) were found to be significantly correlated by Qiu's research (9). Monocyte/high-density lipoprotein ratio (MHR) may be a biomarker for predicting DKD (10). However, there has been no previous research investigating the association between SIRI and CKD.

Determining the relationship between SIRI and CKD is the goal of this study, which uses data from the National Health and Nutrition Examination Survey (NHANES).

2 Materials and methods

2.1 Survey description

To get a representative sample of the non-institutionalized, civilian U.S. population, NHANES was conducted twice a year in the country. The US population's health and nutritional condition were tracked over time by the NHANES using a sophisticated, multistage probability sampling design. The National Center for Health Statistics (NCHS) Ethics Review Board approved the study, and everyone who participated in NHANES gave their informed consent. NHANES was carried out by the Centers for Disease Control and Prevention (CDC).

2.2 Study population

NHANES 1999-2020 individuals were gathered for this investigation. We concluded that 41,089 people were suitable after excluding patients with cancer (n = 1,285), age < 20 (n = 48,975), or pregnancy (n = 220), as well as those without the albumin-to-creatinine ratio (ACR) (n = 8,506), estimated glomerular filtration rate (eGFR) (n = 16,013), and SIRI (n = 1,125) (Figure 1).

2.3 Definition of SIRI and CKD

Blood cell count measurements were conducted using the Beckman Coulter MAXM automated analytical instrument (Beckman Coulter Inc.). Counts for lymphocytes, neutrophils, monocytes, and platelets were expressed in units of $\times 10^3$ cells/μl. In our study, SIRI was considered as the primary exposure variable. Neutrophil count × monocyte count/lymphocyte count is how SIRI is computed (11). To further explore the connection between SIRI and CKD, we also examined the link between other inflammatory biomarkers and renal function. These additional inflammation biomarkers included SII, MHR, neutrophil/high-density lipoprotein ratio (NHR), platelet/high-density lipoprotein ratio (PHR), and lymphocyte/high-density lipoprotein ratio (LHR). SII = platelet counts × neutrophil counts/lymphocyte counts, NHR = neutrophil counts/high-density lipoprotein cholesterol (HDL-C) (mmol/L), MHR = monocyte counts/HDL-C, LHR = lymphocyte counts/HDL-C, and PHR = platelet counts/HDL-C are the formulas for these inflammatory indicators (12). To measure HDL-C levels, chemical analyzers Roche Cobas 6000 and Roche modular P were utilized.

To diagnose CKD, one of two conditions must exist albuminuria or an eGFR of less than 60 mL/min/1.73 m^2 (13). In 2009, the equation for standardized creatinine developed by the Chronic Kidney Disease Epidemiology Collaboration (CKD-EPI) was used to determine eGFR (14). ACR ≥ 30 mg/g was utilized to characterize albuminuria. In our investigation, the outcome variables were albuminuria, low-eGFR, and CKD.

2.4 Selection of covariates

Our study employed a set of covariates to control for potential confounding factors. These confounders included age, race, sex, marital status, family income to poverty ratio (PIR), and educational level, among other demographic factors. We also included a number of laboratory and anthropometric factors, including CVD, alcohol consumption, smoking status, total cholesterol (TC), triglycerides, aspartate aminotransferase (AST), alanine aminotransferase (ALT), blood uric acid, serum phosphorus, and body mass index (BMI) (7, 15–17).

The word "hypertension" in this study refers to three different things. At first, respondents self-reported having high blood pressure in response to the survey question "Ever told you had hypertension." Examining if average blood pressure surpassed

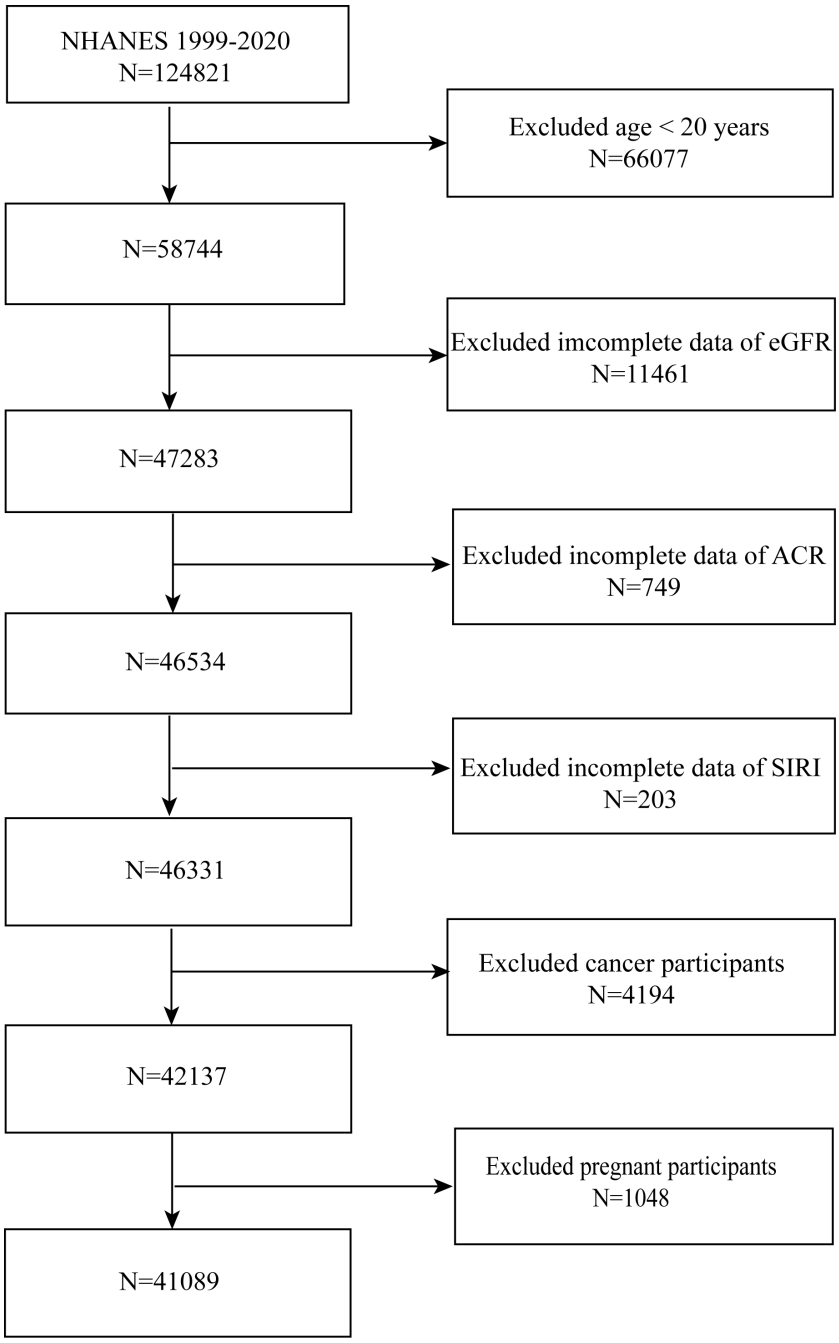

FIGURE 1
Flowchart of the sample selection from NHANES 1999–2020.

130/80 mmHg diastolic or systolic values was the second component (18). The last phase used the item "taking hypertension prescription" program to identify people who had hypertension. Likewise, this study's definition of diabetes is divided into three sections. Diabetes self-reporting is covered in the first section, and using insulin or prescription drugs is covered in the second. Lastly, hemoglobin A1c (HbA1c) (%) > 6.5 and fasting blood sugar levels (mmol/l) ≥ 7.0 were used to identify those with diabetes. Visit the website www.cdc.gov/nchs/nhanes/ for further information.

2.5 Statistical analysis

When doing the statistical analyses, which took into account intricate multistage cluster surveys and made use of the proper NHANES sampling weights, the CDC guidelines were adhered to. When presenting categorical variables by proportions, standard error (SE) were used to represent continuous variables. To analyze the differences between participants categorized by SIRI tertiles, either a weighted Student's t-test or a weighted chi-square test was used (for continuous variables). The correlation between SIRI and

CKD was examined in three distinct models using multivariable logistic regression. Covariates were not adjusted in Model 1. Race, age, and sex were adjusted in Model 2. The variables sex, age, race, education level, BMI, alcohol consumption, smoking status, TC, triglycerides, AST, ALT, PIR, CVD, blood uric acid, serum phosphorus, marital status, diabetes, and hypertension were all adjusted for in Model 3. We tested the robustness of our results by doing a sensitivity analysis using SIRI converted from a continuous variable to a categorical variable (tertiles). Nonlinear relationships were addressed using generalized additive models (GAM) and smooth curve fitting. Utilizing the log-likelihood ratio test, we compared the segmented regression model—a two-segment linear regression model fitted to each interval—against the non-segmented model, or a one-line model. This allowed us to further investigate threshold effects. To locate breakpoints, we used a two-step recursive technique. Subgroup analyses were conducted using stratified multivariable logistic regression models, with stratification based on sex, age, BMI, hypertension, CVD, and diabetes (7, 19). These stratification factors were considered potential effect modifiers to assess heterogeneity in the correlations between subgroups. Additionally, the predictive efficacy of NLR and other inflammatory biomarkers (SII, NHR, LHR, MHR, and PHR) was assessed through the examination of area under the curve (AUC) values and the use of receiver operating characteristic (ROC) curves (20, 21). For categorical variables, mode imputation was utilized to resolve missing values, whereas median imputation was applied to continuous variables. For all of our statistical analyses, we utilized the Empower software suite and R version 4.1.3. A two-tailed p-value < 0.05 was used to determine statistical significance.

3 Results

3.1 Participants characteristics at baseline

Among the 41,089 participants in our analysis, 48.26% of them were men and 51.74% of them were women. Mexican Americans make up 17.78% of the population. 37.00% of the population is between the ages of 20 and 40. The prevalences of low-eGFR, CKD, and albuminuria were 8.30%, 17.68%, and 12.16%, respectively, with an average SIRI of 1.20 ± 0.86. As shown in Table 1, the prevalence of low-eGFR, albuminuria, and CKD was significantly greater among people in the higher SIRI tertiles (all $p < 0.05$).

Numerous variables, such as sex, age, race, education level, BMI, smoking status, alcohol consumption, blood uric acid, serum phosphorus, hypertension, diabetes, TC, triglycerides, ALT, AST, PIR, CVD, marital status, ACR, eGFR, SII, NHR, LHR, MHR, and PHR, showed significant differences across SIRI tertiles (all $p < 0.05$).

3.2 Association between SIRI and CKD

Table 2 displays the correlations between SIRI and other inflammatory biomarkers with CKD. According to the findings of our study, there is a positive link between SIRI, SII, NHR, and MHR with CKD in Models 1 and 2. After fully adjusting for covariates (Model 3), SIRI, SII, NHR, and MHR remain positively correlated with CKD (SIRI: OR = 1.24; 95% CI: 1.19, 1.30; SII: OR = 1.01; 95% CI: 1.01, 1.02; NHR: OR = 1.09; 95% CI: 1.06, 1.11; MHR: OR = 1.22; 95% CI: 1.03, 1.44). This implies that the prevalence of CKD rises by 24%, 1%, 9%, and 22%, respectively, with every unit increase in SIRI, SII, NHR, and MHR. In order to perform a sensitivity analysis, SIRI and other inflammatory biomarkers were divided into tertiles. People in the higher tertile of SIRI, SII, and NHR had a greater prevalence of CKD in Model 3 compared to participants in the lower tertile (all p for trend < 0.05).

Smooth curve fitting and GAM indicated that the relationships between SIRI, SII, NHR, LHR, and PHR with CKD were nonlinear (Figure 2). After full adjustment, breakpoints (K) were found to be 2.04, 2105.48, 3.37, 1.2, and 113.14, respectively (all logarithmic likelihood ratio test P-value <0.05). SIRI and CKD are both positively correlated on the two sides of the breakpoint (Table 3).

3.3 Association between SIRI and albuminuria

Additionally, we discovered that the prevalence of albuminuria rises along with levels of SIRI, SII, NHR, MHR, and PHR. For every unit increase in SIRI, SII, NHR, MHR, and PHR, the prevalences of albuminuria increase by 27%, 1%, 8%, 21%, and 1% in Model 3 (SIRI: OR = 1.27; 95% CI: 1.21, 1.32; SII: OR = 1.01; 95% CI: 1.01, 1.02; NHR: OR = 1.08; 95% CI: 1.06, 1.11; MHR: OR = 1.21; 95% CI: 1.03, 1.44; PHR: OR = 1.01; 95% CI: 1.00, 1.01). There are still substantial correlations even once these inflammatory biomarkers are divided into tertiles. As compared to those in the lower tertile, the higher tertiles of SIRI, SII, and NHR persons in Model 3 demonstrated a higher prevalence of albuminuria (Table 2).

SIRI, SII, NHR, MHR, LHR, and PHR showed nonlinear associations with albuminuria, according to the GAM and smooth curve fitting. Breakpoints after complete adjustment were discovered to be 2.18, 1924.3, 5.96, 0.87, 1.19, and 153.3, respectively. SIRI and albuminuria are positively correlated on the two sides of the breakpoint (Table 3).

3.4 Association between SIRI and low-eGFR

We also assessed the relationships between SIRI and other inflammatory biomarkers with low-eGFR using three different models (Table 2). In the fully adjusted model, low-eGFR was strongly correlated with SIRI and SII (SIRI: OR = 1.11; 95% CI: 1.05, 1.18; SII: OR = 1.01; 95% CI: 1.01, 1.02). Those in the tertiles with the highest SIRI had the highest prevalence of low-eGFR, as compared to those in the lowest tertiles (p for trend < 0.05).

GAM and smooth curve fitting indicated that the relationships between SIRI, SII, NHR, and LHR with low-eGFR were nonlinear (Figure 2). Breakpoints after complete adjustment were discovered to be 1.85, 682.5, 3.31, and 1.88, respectively. In the nonlinear

10.3389/fendo.2024.1329256

TABLE 1 Baseline characteristics according to SIRI tertiles.

SIRI	Overall	Tertile 1	Tertile 2	Tertile 3	*P*-value
		(0.06–0.79)	(0.79–1.27)	(1.27–24.60)	
N	41089	13650	13737	13702	
SIRI	1.20 ± 0.86	0.55 ± 0.15	1.01 ± 0.14	2.04 ± 1.01	<0.001
SII	537.07 ± 364.05	332.66 ± 146.24	493.21 ± 186.29	784.68 ± 486.29	<0.001
NHR	3.44 ± 2.03	2.31 ± 1.11	3.34 ± 1.42	4.67 ± 2.52	<0.001
MHR	0.45 ± 0.24	0.33 ± 0.20	0.44 ± 0.18	0.58 ± 0.26	<0.001
LHR	1.76 ± 1.07	1.82 ± 1.38	1.79 ± 0.86	1.68 ± 0.86	<0.001
PHR	200.85 ± 82.35	187.56 ± 74.02	201.83 ± 80.02	213.11 ± 90.19	<0.001
Age, years					<0.001
20-40	15203 (37.00%)	5422 (39.72%)	5222 (38.01%)	4559 (33.27%)	
41-60	14252 (34.69%)	5054 (37.03%)	4860 (35.38%)	4338 (31.66%)	
> 60	11634 (28.31%)	3174 (23.25%)	3655 (26.61%)	4805 (35.07%)	
Sex, n (%)					<0.001
Male	20451 (49.77%)	5913 (43.32%)	6764 (49.24%)	7774 (56.74%)	
Female	20638 (50.23%)	7737 (56.68%)	6973 (50.76%)	5928 (43.26%)	
Race, n (%)					<0.001
Mexican American	7307 (17.78%)	2316 (16.97%)	2602 (18.94%)	2389 (17.44%)	
Other Hispanic	3850 (9.37%)	1241 (9.09%)	1395 (10.16%)	1214 (8.86%)	
Non-Hispanic White	16678 (40.59%)	3726 (27.30%)	5904 (42.98%)	7048 (51.44%)	
Non-Hispanic Black	8915 (21.70%)	4623 (33.87%)	2382 (17.34%)	1910 (13.94%)	
Other Races	4339 (10.56%)	1744 (12.78%)	1454 (10.58%)	1141 (8.33%)	
Education level, n (%)					<0.001
Less than high school	10828 (26.35%)	3504 (25.67%)	3617 (26.33%)	3707 (27.05%)	
High school or GED	9512 (23.15%)	2959 (21.68%)	3105 (22.60%)	3448 (25.16%)	
Above high school	20707 (50.40%)	7175 (52.56%)	6998 (50.94%)	6534 (47.69%)	
Others	42 (0.10%)	12 (0.09%)	17 (0.12%)	13 (0.09%)	
Marital status, n (%)					<0.001
Married	17747 (52.46%)	5798 (52.10%)	6175 (54.05%)	5774 (51.21%)	
Never married	6287 (18.59%)	2233 (20.07%)	2012 (17.61%)	2042 (18.11%)	
Living with a partner	2606 (7.70%)	907 (8.15%)	881 (7.71%)	818 (7.25%)	
Others	7188 (21.25%)	2190 (19.68%)	2356 (20.62%)	2642 (23.43%)	
BMI, n (%)					<0.001
Normal weight	11879 (29.20%)	4347 (32.11%)	3871 (28.41%)	3661 (27.08%)	
Overweight	13566 (33.35%)	4570 (33.76%)	4627 (33.95%)	4369 (32.32%)	
Obese	15236 (37.45%)	4620 (34.13%)	5129 (37.64%)	5487 (40.59%)	
Smoking status, n (%)					< 0.001
≥100 cigarettes lifetime	18238 (44.42%)	5195 (38.09%)	5973 (43.50%)	7070 (51.65%)	
< 100 cigarettes lifetime	22820 (55.58%)	8444 (61.91%)	7759 (56.50%)	6617 (48.35%)	
PIR, n (%)					<0.001

(Continued)

TABLE 1 Continued

SIRI	Overall	Tertile 1	Tertile 2	Tertile 3	*P*-value
Low income	13801 (37.04%)	4467 (36.08%)	4492 (36.15%)	4842 (38.87%)	
Medium income	12010 (32.23%)	3957 (31.96%)	3965 (31.91%)	4088 (32.82%)	
High income	11451 (30.73%)	3957 (31.96%)	3968 (31.94%)	3526 (28.31%)	
CVD, n (%)	3161 (7.69%)	640 (4.69%)	894 (6.51%)	1627 (11.87%)	< 0.001
Alcohol consumption, n (%)					<0.001
yes	25777 (78.67%)	8426 (79.78%)	8709 (79.41%)	8642 (76.91%)	
no	6988 (21.33%)	2135 (20.22%)	2258 (20.59%)	2595 (23.09%)	
Hypertension, n (%)	21512 (52.35%)	6527 (47.82%)	7005 (50.99%)	7980 (58.24%)	< 0.001
Diabetes, n (%)	6482 (15.78%)	1877 (13.75%)	1988 (14.47%)	2617 (19.10%)	< 0.001
TC, mg/dL	193.79 ± 41.36	195.23 ± 41.65	195.13 ± 40.66	191.01 ± 41.63	<0.001
ALT, U/L	25.45 ± 23.66	24.55 ± 17.38	25.64 ± 18.94	26.15 ± 31.89	<0.001
AST, U/L	25.36 ± 19.69	25.14 ± 15.03	25.11 ± 14.16	25.82 ± 27.14	0.004
Triglyceride, mg/dL	149.39 ± 119.98	138.11 ± 119.50	152.67 ± 117.86	157.34 ± 121.72	<0.001
Blood uric acid, mg/dL	5.44 ± 1.44	5.24 ± 1.37	5.43 ± 1.40	5.65 ± 1.52	<0.001
Serum phosphorus, mg/dL	3.69 ± 0.56	3.71 ± 0.55	3.69 ± 0.56	3.67 ± 0.57	<0.001
ACR, mg/g	48.01 ± 378.40	30.45 ± 263.45	38.80 ± 299.76	74.74 ± 518.73	<0.001
eGFR, mL/min/1.73 m2	92.32 ± 26.70	95.73 ± 25.54	92.45 ± 25.69	88.79 ± 28.32	<0.001
Low-eGFR, n (%)	3410 (8.30%)	683 (5.00%)	1019 (7.42%)	1708 (12.47%)	< 0.001
Albuminuria, n (%)	4997 (12.16%)	1293 (9.47%)	1458 (10.61%)	2246 (16.39%)	< 0.001
CKD, n (%)	7265 (17.68%)	1794 (13.14%)	2184 (15.90%)	3287 (23.99%)	< 0.001

SIRI, systemic inflammation response index; SII, systemic immune-inflammation index; NHR, neutrophil/high-density lipoprotein ratio; MHR, monocyte/high-density lipoprotein ratio; LHR, lymphocyte/high-density lipoprotein ratio; PHR, platelet/high-density lipoprotein ratio; GED, general educational development; BMI, body mass index; PIR, family income to poverty ratio; CVD, cardiovascular diseases; TC, total cholesterol; ALT, alanine aminotransferase; AST, aspartate aminotransferase; ACR, albumin-to-creatinine ratio; eGFR, estimated glomerular filtration rate; CKD, chronic kidney disease.

relationship between SIRI and low-eGFR, we also noticed a saturation effect. SIRI and the prevalence of low-eGFR are positively correlated when SIRI is less than 1.85 (OR = 1.29; 95% CI: 1.14, 1.47). The two do not significantly correlate on the right side of the breakpoint (OR = 1.03; 95% CI: 0.95, 1.11) (Table 3).

3.5 Subgroup analysis

Subgroup analysis showed that SIRI and CKD were positively correlated in all groupings (Figure 3). The relationships between SIRI and MHR with CKD were not substantially associated in the interaction tests for the different strata, suggesting that this positive association was the same across populations(all p for interaction > 0.05).

An analysis of the interaction test revealed that no stratum showed a significant effect of sex, BMI, diabetes, or hypertension on the relationships between SIRI and albuminuria (Figure 3). The association between MHR and albuminuria showed a dependence on CVD status, which may be applicable to CVD patients. The association between PHR and albuminuria showed a dependence on diabetes and may apply to a non-diabetic US population.

Per the interaction test, age, BMI, diabetes, or CVD subgroups did not substantially affect the relationship between SIRI and low-eGFR (p for interaction > 0.05). The association of NHR with low-eGFR showed dependence on hypertension status and may apply to non-hypertension populations. The association of PHR with albuminuria showed dependence on sex and may apply to female populations (Figure 3).

3.6 ROC analysis

To evaluate SIRI's predictive power for CKD, albuminuria, and low-eGFR against other inflammatory biomarkers (SII, NHR, LHR, MHR, and PHR), we computed the AUC values (Figure 4). Our results show that SIRI had higher AUC values than the other five inflammatory biomarkers in terms of predicting CKD, albuminuria, and low-eGFR. Additionally, Table 4 demonstrates that AUC values for SIRI and the other inflammatory biomarkers differed statistically significantly (all $p < 0.05$). These results indicate that, in comparison to other inflammatory biomarkers (SII, NHR, LHR, MHR, and PHR), SIRI has the best discriminative ability and accuracy in predicting CKD, albuminuria, and low-eGFR.

10.3389/fendo.2024.1329256

TABLE 2 Associations between SIRI and other inflammatory biomarkers with CKD, albuminuria, and low-eGFR.

Index	Outcome	Continuous or categories	Model 1[3]		Model 2[4]		Model 3[5]	
			OR[1] (95%CI[2])	*P*- value	OR (95%CI)	*P*- value	OR (95%CI)	*P*- value
SIRI	**CKD**	SIRI as continuous variable	1.42 (1.38, 1.46)	<0.0001	1.33 (1.29, 1.37)	<0.0001	1.24 (1.19, 1.30)	<0.0001
		Tertile 1	Reference		Reference		Reference	
		Tertile 2	1.25 (1.17, 1.34)	<0.0001	1.24 (1.15, 1.33)	<0.0001	1.15 (1.03, 1.27)	0.0089
		Tertile 3	2.09 (1.96, 2.22)	<0.0001	1.88 (1.75, 2.02)	<0.0001	1.61 (1.45, 1.78)	<0.0001
		P for trend	<0.0001		<0.0001		<0.0001	
	Albuminuria	SIRI as continuous variable	1.34 (1.30, 1.38)	<0.0001	1.31 (1.27, 1.36)	<0.0001	1.27 (1.21, 1.32)	<0.0001
		Tertile 1	Reference		Reference		Reference	
		Tertile 2	1.13 (1.05, 1.23)	<0.0001	1.20 (1.11, 1.30)	<0.0001	1.16 (1.04, 1.30)	0.0109
		Tertile 3	1.87 (1.74, 2.02)	<0.0001	1.89 (1.75, 2.05)	<0.0001	1.73 (1.55, 1.94)	<0.0001
		P for trend	<0.0001		<0.0001		<0.0001	
	Low-eGFR	SIRI as continuous variable	1.44 (1.39, 1.48)	<0.0001	1.24 (1.20, 1.29)	<0.0001	1.11 (1.05, 1.18)	0.0003
		Tertile 1	Reference		Reference		Reference	
		Tertile 2	1.52 (1.38, 1.68)	0.0072	1.33 (1.19, 1.49)	<0.0001	1.11 (0.95, 1.30)	0.1898
		Tertile 3	2.70 (2.47, 2.96)	<0.0001	1.85 (1.66, 2.05)	<0.0001	1.34 (1.15, 1.56)	0.0002
		P for trend	<0.0001		<0.0001		<0.0001	
SII	**CKD**	SII as continuous variable	1.01 (1.01, 1.02)	<0.0001	1.01 (1.01, 1.02)	<0.0001	1.01 (1.01, 1.02)	<0.0001
		Tertile 1	Reference		Reference		Reference	
		Tertile 2	1.15 (1.08, 1.23)	<0.0001	1.22 (1.14, 1.31)	<0.0001	1.21 (1.10, 1.34)	0.0001
		Tertile 3	1.58 (1.48, 1.68)	<0.0001	1.66 (1.55, 1.77)	<0.0001	1.62 (1.47, 1.78)	<0.0001
		P for trend	<0.0001		<0.0001		<0.0001	
	Albuminuria	SII as continuous variable	1.01 (1.00, 1.01)	<0.0001	1.01 (1.01, 1.02)	<0.0001	1.01 (1.01, 1.02)	<0.0001
		Tertile 1	Reference		Reference		Reference	
		Tertile 2	1.11 (1.03, 1.20)	<0.0001	1.21 (1.12, 1.31)	<0.0001	1.24 (1.11, 1.39)	0.0001
		Tertile 3	1.58 (1.47, 1.70)	<0.0001	1.75 (1.62, 1.89)	<0.0001	1.74 (1.56, 1.93)	<0.0001
		P for trend	<0.0001		<0.0001		<0.0001	
	Low-eGFR	SII as continuous variable	1.01 (1.00, 1.01)	<0.0001	1.01 (1.01, 1.02)	<0.0001	1.01 (1.01, 1.02)	0.0028
		Tertile 1	Reference		Reference		Reference	
		Tertile 2	1.21 (1.10, 1.32)	<0.0001	1.22 (1.10, 1.35)	0.0001	1.19 (1.03, 1.38)	0.0178
		Tertile 3	1.58 (1.45, 1.72)	<0.0001	1.46 (1.32, 1.60)	<0.0001	1.34 (1.16, 1.54)	<0.0001
		P for trend	<0.0001		<0.0001		<0.0001	
NHR	**CKD**	NHR as continuous variable	1.10 (1.09, 1.12)	<0.0001	1.19 (1.17, 1.21)	<0.0001	1.09 (1.06, 1.11)	<0.0001
		Tertile 1	Reference		Reference		Reference	
		Tertile 2	1.28 (1.20, 1.36)	<0.0001	1.44 (1.35, 1.55)	<0.0001	1.23 (1.12, 1.36)	<0.0001
		Tertile 3	1.57 (1.47, 1.67)	<0.0001	2.14 (1.99, 2.30)	<0.0001	1.47 (1.32, 1.63)	<0.0001
		P for trend	<0.0001		<0.0001		<0.0001	
	Albuminuria	NHR as continuous variable	1.12 (1.10, 1.14)	<0.0001	1.18 (1.16, 1.20)	<0.0001	1.08 (1.06, 1.11)	<0.0001
		Tertile 1	Reference		Reference		Reference	

(Continued)

10.3389/fendo.2024.1329256

TABLE 2 Continued

Index	Outcome	Continuous or categories	Model 1[3]		Model 2[4]		Model 3[5]	
			OR[1] (95%CI[2])	*P*- value	OR (95%CI)	*P*- value	OR (95%CI)	*P*- value
		Tertile 2	1.26 (1.16, 1.36)	<0.0001	1.39 (1.28, 1.50)	<0.0001	1.22 (1.09, 1.37)	0.0007
		Tertile 3	1.68 (1.56, 1.81)	<0.0001	2.12 (1.96, 2.30)	<0.0001	1.55 (1.37, 1.75)	<0.0001
		P for trend	<0.0001		<0.0001		<0.0001	
	Low-eGFR	NHR as continuous variable	1.07 (1.05, 1.08)	<0.0001	1.16 (1.14, 1.19)	<0.0001	1.02 (0.99, 1.06)	0.1082
		Tertile 1	Reference		Reference		Reference	
		Tertile 2	1.42 (1.29, 1.55)	<0.0001	1.61 (1.46, 1.78)	<0.0001	1.28 (1.11, 1.49)	0.0009
		Tertile 3	1.52 (1.40, 1.67)	<0.0001	2.20 (1.98, 2.43)	<0.0001	1.35 (1.14, 1.58)	0.0003
		P for trend	<0.0001		<0.0001		0.0012	
MHR	**CKD**	MHR as continuous variable	1.99 (1.79, 2.21)	<0.0001	2.63 (2.34, 2.97)	<0.0001	1.22 (1.03, 1.44)	0.0248
		Tertile 1	Reference		Reference		Reference	
		Tertile 2	1.15 (1.08, 1.23)	<0.0001	1.26 (1.17, 1.35)	<0.0001	1.03 (0.93, 1.14)	0.5635
		Tertile 3	1.47 (1.38, 1.56)	<0.0001	1.73 (1.61, 1.85)	<0.0001	1.12 (1.01, 1.25)	0.0357
		P for trend	<0.0001		<0.0001		0.0273	
	Albuminuria	MHR as continuous variable	1.85 (1.65, 2.08)	0.0071	2.22 (1.95, 2.52)	0.0073	1.21 (1.03, 1.44)	0.0239
		Tertile 1	Reference		Reference		Reference	
		Tertile 2	1.11 (1.03, 1.19)	0.0092	1.17 (1.08, 1.27)	<0.0001	0.98 (0.88, 1.09)	0.7032
		Tertile 3	1.44 (1.34, 1.55)	<0.0001	1.61 (1.49, 1.75)	<0.0001	1.12 (1.00, 1.26)	0.0548
		P for trend	<0.0001		<0.0001		0.0250	
	Low-eGFR	MHR as continuous variable	2.18 (1.91, 2.49)	<0.0001	2.74 (2.33, 3.22)	<0.0001	1.09 (0.88, 1.35)	0.4275
		Tertile 1	Reference		Reference		Reference	
		Tertile 2	1.25 (1.14, 1.37)	<0.0001	1.35 (1.22, 1.49)	<0.0001	1.07 (0.93, 1.24)	0.3427
		Tertile 3	1.63 (1.49, 1.78)	<0.0001	1.90 (1.72, 2.11)	<0.0001	1.09 (0.93, 1.28)	0.2773
		P for trend	<0.0001		<0.0001		0.3224	
LHR	**CKD**	LHR as continuous variable	0.97 (0.95, 1.00)	0.0505	1.10 (1.07, 1.13)	<0.0001	0.97 (0.94, 1.01)	0.1485
		Tertile 1	Reference		Reference		Reference	
		Tertile 2	0.79 (0.75, 0.84)	<0.0001	1.02 (0.96, 1.09)	0.4973	0.87 (0.79, 0.96)	0.0047
		Tertile 3	0.84 (0.79, 0.90)	<0.0001	1.29 (1.21, 1.39)	<0.0001	0.83 (0.75, 0.93)	0.0008
		P for trend	<0.0001		<0.0001		0.0014	
	Albuminuria	LHR as continuous variable	1.01 (0.98, 1.03)	0.6697	1.06 (1.03, 1.09)	<0.0001	0.95 (0.91, 1.01)	0.0507
		Tertile 1	Reference		Reference		Reference	
		Tertile 2	0.84 (0.78, 0.91)	<0.0001	0.98 (0.91, 1.06)	0.6055	0.83 (0.74, 0.92)	0.0006
		Tertile 3	0.98 (0.91, 1.05)	0.5255	1.25 (1.16, 1.35)	<0.0001	0.82 (0.73, 0.93)	0.0012
		P for trend	0.9622		<0.0001		0.0031	
	Low-eGFR	LHR as continuous variable	0.87 (0.84, 0.91)	<0.0001	1.07 (1.03, 1.11)	0.0002	0.98 (0.95, 1.02)	0.4164
		Tertile 1	Reference		Reference		Reference	
		Tertile 2	0.70 (0.65, 0.77)	<0.0001	1.05 (0.96, 1.15)	0.3173	0.91 (0.79, 1.04)	0.1514
		Tertile 3	0.65 (0.60, 0.71)	<0.0001	1.30 (1.18, 1.43)	<0.0001	0.82 (0.71, 0.96)	0.0144

(Continued)

TABLE 2 Continued

Index	Outcome	Continuous or categories	Model 1[3]		Model 2[4]		Model 3[5]	
			OR[1] (95%CI[2])	*P*- value	OR (95%CI)	*P*- value	OR (95%CI)	*P*- value
		P for trend	<0.0001		<0.0001		0.0150	
PHR	**CKD**	PHR as continuous variable	1.00 (0.98, 1.01)	0.8444	1.01 (1.00, 1.01)	<0.0001	1.01 (1.00, 1.01)	0.0373
		Tertile 1	Reference		Reference		Reference	
		Tertile 2	0.88 (0.83, 0.94)	0.0001	1.08 (1.01, 1.16)	0.0219	0.97 (0.89, 1.07)	0.5930
		Tertile 3	0.96 (0.90, 1.02)	0.2206	1.49 (1.39, 1.59)	<0.0001	1.06 (0.95, 1.17)	0.3037
		P for trend	0.3859		<0.0001		0.2480	
	Albuminuria	PHR as continuous variable	1.01 (1.00, 1.01)	<0.0001	1.01 (1.00, 1.01)	<0.0001	1.01 (1.00, 1.01)	0.0031
		Tertile 1	Reference		Reference		Reference	
		Tertile 2	0.90 (0.84, 0.97)	0.0054	1.03 (0.95, 1.11)	0.4857	0.91 (0.81, 1.01)	0.0723
		Tertile 3	1.13 (1.05, 1.21)	0.0011	1.49 (1.39, 1.61)	<0.0001	1.09 (0.97, 1.22)	0.1377
		P for trend	0.0001		<0.0001		0.0618	
	Low-eGFR	PHR as continuous variable	0.99 (0.98, 0.99)	<0.0001	1.01 (1.00, 1.01)	<0.0001	0.99 (0.99, 1.01)	0.4689
		Tertile 1	Reference		Reference		Reference	
		Tertile 2	0.87 (0.80, 0.95)	0.0014	1.20 (1.09, 1.31)	0.2229	1.09 (0.95, 1.25)	0.2236
		Tertile 3	0.76 (0.69, 0.82)	<0.0001	1.47 (1.33, 1.62)	<0.0001	0.99 (0.85, 1.15)	0.8986
		P for trend	<0.0001		<0.0001		0.8323	

In sensitivity analysis, SIRI, SII, NHR, MHR, LHR, and PHR were converted from continuous variables to categorical variables (tertiles).
[1]OR: Odd ratio.
[2]95% CI: 95% confidence interval.
[3]Model 1: No covariates were adjusted.
[4]Model 2: Adjusted for age, sex, and race.
[5]Model 3: Adjusted for sex, age, race, education level, BMI, smoking status, alcohol consumption, blood uric acid, serum phosphorus, TC, triglycerides, AST, ALT, PIR, CVD, marital status, diabetes, and hypertension.

4 Discussion

This cross-sectional study of 41,089 adult participants revealed a positive correlation between the prevalence of CKD and SIRI. Using smooth curve fitting, we also found a nonlinear connection between SIRI and CKD, with breakpoints set at 2.04. Additionally, it was discovered that low-eGFR and albuminuria have positive and nonlinear correlations with SIRI, with breakpoints at 1.85 and 2.18, respectively. Subgroup studies and interaction testing revealed no statistically significant variation in the relationship between SIRI and CKD between the groups. Additional inflammatory biomarkers and CKD were linked, as we also saw. There were correlations between greater levels of SII, NHR, MHR, and PHR with a higher prevalence of CKD. When SIRI is compared against SII, NHR, LHR, MHR, and PHR, among other inflammatory biomarkers, ROC analysis indicates that SIRI might be a more accurate indicator of low-eGFR, CKD, and albuminuria. Finally, given the significance of the high SIRI values in evaluating kidney health in adult Americans, it is important to emphasize them.

The primary focus of our research was the association between renal function and other inflammatory indicators and SIRI. According to our research, high levels of MHR and NHR are linked to higher prevalences of CKD and albuminuria. This association can be attributed to the fact that these inflammatory biomarkers are novel biomarkers related to whole blood cells and HDL-C. Inflammation can lead to changes in whole blood cells, including neutrophils, monocytes, and platelets. In addition to its function in transporting cholesterol, HDL-C has a number of anti-infection, anti-inflammatory, antioxidant, and anti-thrombotic characteristics (22). Similar to our study, Prior studies have discovered predictive significance for MHR and NHR in conditions such as peripheral arterial disease (PAD), acute myocardial infarction, and schizophrenia with concomitant bipolar affective disorder (23–25). In earlier research, the relationship between SII and renal function was also examined. SII and albuminuria have been shown to be positively correlated, according to Qin et al.'s cross-sectional research of 36,463 adult Americans (7). In Chinese CKD patients, Lai et al. discovered that SII is an independent risk factor for all-cause, cardiovascular, and cancer-related death (26). Our study found that for every unit rise in SII, the prevalence of CKD, albuminuria, and low-eGFR increased by 1%. Because of this, SII, a novel inflammation biomarker that integrates platelets, neutrophils, and lymphocytes, can forecast kidney function in adult Americans. These inflammatory biomarkers (SII, NHR, and MHR) were not the best biomarkers for predicting kidney function, according to ROC analysis, as they

10.3389/fendo.2024.1329256

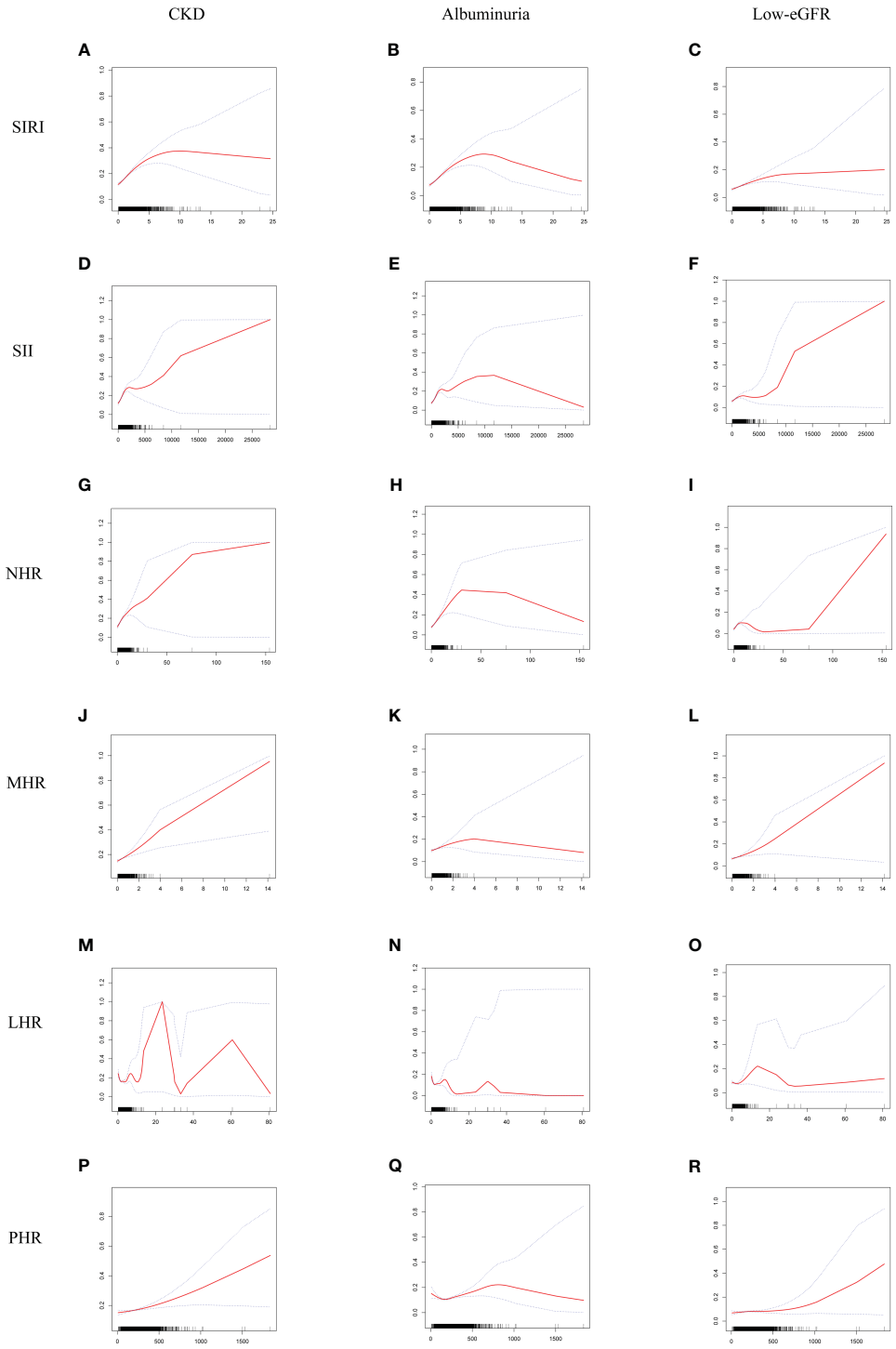

FIGURE 2
Smooth curve fitting for SIRI and other inflammatory biomarkers with CKD, albuminuria, and low-eGFR. **(A)** SIRI and CKD; **(B)** SIRI and albuminuria; **(C)** SIRI and low-eGFR; **(D)** SII and CKD; **(E)** SII and albuminuria; **(F)** SII and low-eGFR; **(G)** NHR and CKD; **(H)** NHR and albuminuria; **(I)** NHR and low-eGFR; **(J)** MHR and CKD; **(K)** MHR and albuminuria; **(L)** MHR and low-eGFR; **(M)** LHR and CKD; **(N)** LHR and albuminuria; **(O)** LHR and low-eGFR; **(P)** PHR and CKD; **(Q)** PHR and albuminuria; **(R)** PHR and low-eGFR.

had significantly lower AUC values. To support our conclusions, more prospective research is required.

The key conclusion of this study, which to our knowledge is the first to examine the connection between SIRI and CKD, is that there is a positive correlation. In earlier studies, the relationship between SIRI and other illnesses was mainly examined. The sickness severity of acute pancreatitis (AP) and development of acute kidney damage (AKI) have both been found to be predicted by SIRI (4). The all-cause and CVD deaths in adult Americans have also been strongly correlated with it (6). Preoperative SIRI, according to Lv et al.'s

10.3389/fendo.2024.1329256

TABLE 3 Threshold effect analysis of SIRI and other inflammatory biomarkers on CKD, albuminuria, and low-eGFR using a two-piecewise linear regression model in Model 3.

	CKD		Albuminuria		Low-eGFR	
	OR[1] (95%CI[2])	*P*- value	OR (95%CI)	*P*- value	OR (95%CI)	*P*- value
SIRI						
Fitting by standard linear model	1.24 (1.19, 1.30)	<0.0001	1.27 (1.21, 1.32)	<0.0001	1.11 (1.05, 1.18)	0.0003
Fitting by two-piecewise linear model						
Breakpoint (K)	2.04		2.18		1.85	
OR1(< K)	1.47 (1.36, 1.60)	<0.0001	1.55 (1.43, 1.68)	<0.0001	1.29 (1.14, 1.47)	0.0001
OR2(> K)	1.09 (1.01, 1.16)	0.0174	1.08 (1.01, 1.16)	0.0188	1.03 (0.95, 1.11)	0.4401
OR2/OR1	0.74 (0.65, 0.83)	<0.0001	0.70 (0.62, 0.79)	<0.0001	0.80 (0.67, 0.95)	0.0099
Logarithmic likelihood ratio test P-value	<0.001		<0.001		0.011	
SII						
Fitting by standard linear model	1.01 (1.01, 1.02)	<0.0001	1.01 (1.01, 1.02)	<0.0001	1.01 (1.01, 1.02)	0.0028
Fitting by two-piecewise linear model						
Breakpoint (K)	2105.48		1924.3		682.5	
OR1(< K)	1.01 (1.00, 1.02)	<0.0001	1.01 (1.01, 1.02)	<0.0001	1.01 (1.00, 1.02)	<0.0001
OR2(> K)	0.99 (0.99, 1.01)	0.7294	0.99 (0.98, 1.01)	0.3143	0.99 (0.98, 1.01)	0.6353
OR2/OR1	1.01 (1.00, 1.02)	<0.0001	1.01 (1.01, 1.02)	<0.0001	1.00 (1.00, 1.01)	0.0008
Logarithmic likelihood ratio test P-value	<0.001		<0.001		0.001	
NHR						
Fitting by standard linear model	1.09 (1.06, 1.11)	<0.0001	1.08 (1.06, 1.11)	<0.0001	1.02 (0.99, 1.06)	0.1082
Fitting by two-piecewise linear model						
Breakpoint (K)	3.37		5.96		3.31	
OR1(< K)	1.19 (1.12, 1.27)	<0.0001	1.16 (1.12, 1.20)	<0.0001	1.22 (1.11, 1.35)	<0.0001
OR2(> K)	1.06 (1.03, 1.09)	<0.0001	1.01 (0.99, 1.03)	0.3451	1.00 (0.98, 1.02)	0.9676
OR2/OR1	0.89 (0.83, 0.96)	0.0029	0.87 (0.84, 0.91)	<0.0001	0.82 (0.74, 0.90)	<0.0001
Logarithmic likelihood ratio test P-value	0.003		<0.001		<0.001	
MHR						
Fitting by standard linear model	1.22 (1.03, 1.44)	0.0248	1.21 (1.03, 1.44)	0.0239	1.09 (0.88, 1.35)	0.4275
Fitting by two-piecewise linear model						
Breakpoint (K)	0.25		0.87		0.19	
OR1(< K)	0.65 (0.12, 3.59)	0.6231	1.48 (1.15, 1.92)	0.0027	0.02 (0.01, 2.04)	0.0899
OR2(> K)	1.24 (1.04, 1.48)	0.0195	0.99 (0.74, 1.33)	0.9495	1.12 (0.90, 1.40)	0.3212
OR2/OR1	1.90 (0.33, 10.91)	0.4716	0.67 (0.44, 1.03)	0.0651	109.75 (0.53, 226.05)	0.0840
Logarithmic likelihood ratio test P-value	0.473		0.047		0.092	
LHR						
Fitting by standard linear model	0.97 (0.94, 1.01)	0.1485	0.95 (0.91, 1.01)	0.0507	0.98 (0.95, 1.02)	0.4164

(Continued)

10.3389/fendo.2024.1329256

TABLE 3 Continued

	CKD		Albuminuria		Low-eGFR	
	OR[1] (95%CI[2])	*P*- value	OR (95%CI)	*P*- value	OR (95%CI)	*P*- value
Fitting by two-piecewise linear model						
Breakpoint (K)	1.2		1.19		1.88	
OR1(< K)	0.55 (0.43, 0.68)	<0.0001	0.48 (0.37, 0.62)	<0.0001	0.79 (0.68, 0.91)	0.0016
OR2(> K)	1.00 (0.97, 1.03)	0.9485	0.99 (0.96, 1.03)	0.7460	1.01 (0.97, 1.04)	0.7245
OR2/OR1	1.83 (1.45, 2.32)	<0.0001	2.07 (1.58, 2.71)	<0.0001	1.27 (1.09, 1.49)	0.0022
Logarithmic likelihood ratio test P-value	<0.001		<0.001		0.002	
PHR						
Fitting by standard linear model	1.01 (1.00, 1.01)	0.0373	1.01 (1.00, 1.01)	0.0031	0.99 (0.99, 1.01)	0.4689
Fitting by two-piecewise linear model						
Breakpoint (K)	113.14		153.3		178.07	
OR1(< K)	0.99 (0.99, 1.00)	0.0229	0.98 (0.98, 0.99)	0.0010	1.00 (0.99, 1.01)	0.2149
OR2(> K)	1.00 (1.00, 1.01)	0.0055	1.00 (1.00, 1.01)	<0.0001	1.00 (0.99, 1.01)	0.1211
OR2/OR1	1.01 (1.00, 1.01)	0.0119	1.00 (1.00, 1.01)	<0.0001	0.99 (0.99, 1.01)	0.1089
Logarithmic likelihood ratio test P-value	0.013		<0.001		0.107	

Adjusted for sex, age, race, education level, BMI, smoking status, alcohol consumption, blood uric acid, serum phosphorus, TC, triglycerides, AST, ALT, PIR, CVD, marital status, diabetes, and hypertension.
[1]OR: Odd ratio.
[2]95% CI: 95% confidence interval.

research, is a reliable indicator of postoperative prognosis in patients with renal cell carcinoma and inferior vena cava tumor thrombus (RCC-IVCTT) (27). The prevalence of CKD rose by 24% in our sample, with each unit rising in SIRI. We also identified a nonlinear association between SIRI and CKD. SIRI exhibited the positive connections with CKD in the two sides of the breakpoint (SIRI = 2.04). This means that the higher the SIRI level, the greater the threat to kidney health. The prevalence of albuminuria and low-eGFR were also observed to be positively correlated with an increase in SIRI. Additionally, there were nonlinear connections between SIRI with albuminuria and low-eGFR, with breakpoints at 2.18 and 1.85, respectively. In conclusion, adult Americans' renal function is significantly impacted negatively by SIRI.

The association between the two may be attributed to the fact that SIRI is a novel systemic inflammatory biomarker based on the counts of neutrophils, monocytes, and lymphocytes in peripheral blood. Monocytes can contribute to this inflammatory response by releasing pro-inflammatory cytokines and interacting with other immune cells such as lymphocytes and neutrophils. Renal fibrosis has also been linked to dysregulation of the monocyte-derived transforming growth factor-beta (TGF-β) (28, 29). Through the release of several pro-inflammatory mediators and the production of reactive oxygen species (ROS), neutrophils have a role in the pathophysiology of CKD (30). A substantial correlation has been discovered between lymphocytes, particularly the decline of CD4 T lymphocytes, and worsening kidney function (31). The superiority of SIRI in predicting other diseases has also been investigated in earlier research. The highest AUC value was achieved by SIRI in the prediction of peripheral arterial disease (PAD) in patients with T2DM when compared to AISI, SII, NHR, MHR, and PHR (25). In the context of cervical cancer prognostic prediction, SIRI demonstrated superior accuracy in comparison to NLR, PLR, and MLR (32). SIRI beat NLR, PLR, lymphocyte-to-monocyte ratio (LMR), and red blood cell distribution width (RDW) for predicting the prognosis of stroke (33). Furthermore, in comparison to other inflammation biomarkers (SII, NHR, LHR, MHR, and PHR), our research shows that SIRI may have a better discriminative capacity and accuracy in predicting CKD, albuminuria, and low-eGFR. Because of its cost-effectiveness and accessibility, SIRI can be seen as a more accurate and complete inflammatory biomarker. The ability of SIRI to evaluate kidney health in adult Americans has enormous potential, to sum up.

CKD has a number of important risk factors, including CVD (3). This opinion is backed up by our research. This is supported by our study, where subgroup analyses showed that the prevalence of CKD was higher in the CVD population than in the non-CVD population for each unit increase in SIRI. Subgroup analysis also reveals that obese people are more likely to develop CKD than normal-weight or overweight people, probably as a result of obesity's impact on the kidneys through inflammation and insulin resistance (34). Furthermore, our results show that age, sex, BMI, hypertension, diabetes, and CVD had no appreciable influence on the association between SIRI with CKD. These study findings add to the body of evidence demonstrating SIRI's detrimental impact on renal health.

10.3389/fendo.2024.1329256

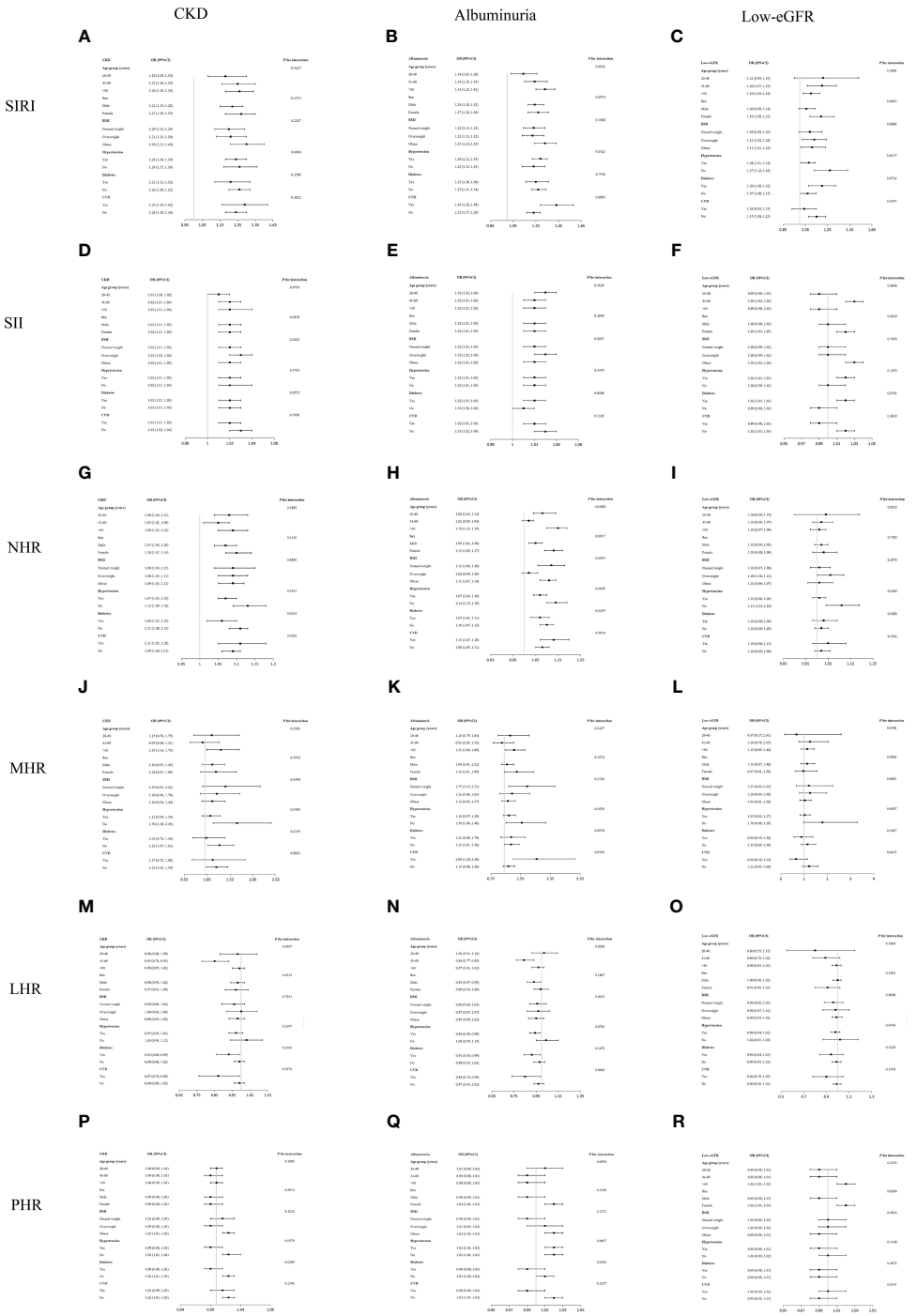

FIGURE 3
Subgroup analysis for the association of SIRI and other inflammatory biomarkers with CKD, albuminuria, and low-eGFR. **(A)** SIRI and CKD; **(B)** SIRI and albuminuria; **(C)** SIRI and low-eGFR; **(D)** SII and CKD; **(E)** SII and albuminuria; **(F)** SII and low-eGFR; **(G)** NHR and CKD; **(H)** NHR and albuminuria; **(I)** NHR and low-eGFR; **(J)** MHR and CKD; **(K)** MHR and albuminuria; **(L)** MHR and low-eGFR; **(M)** LHR and CKD; **(N)** LHR and albuminuria; **(O)** LHR and low-eGFR; **(P)** PHR and CKD; **(Q)** PHR and albuminuria; **(R)** PHR and low-eGFR.

It is still unknown what the underlying mechanisms are that connect SIRI to CKD. A number of tubular toxins, such as ROS, are produced in response to systemic or intrarenal inflammation. These toxins lead to tubular damage, nephron dropout, and the start of chronic kidney disease. Proinflammatory cytokines in circulation activate leukocytes and endothelial cells found in intrarenal microvessels, leading to a localized rise in proinflammatory factors and ROS. These mechanisms induce disruptions in the glycocalyx layer and affect the cell-surface adhesion molecules. Receptor-mediated vasoreactivity, endothelial barrier function, and the activation of the coagulation system are also compromised. These inflammatory-induced alterations may result in irreversible tubular damage and nephron failure (35, 36).

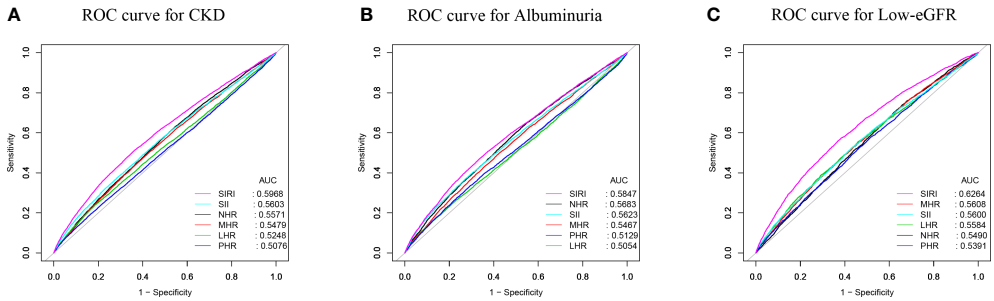

FIGURE 4
ROC curves and the AUC values of the six inflammatory biomarkers (SIRI, SII, NHR, PHR, MHR, and LHR) in diagnosing CKD, albuminuria and low-eGFR. **(A)** Six obesity indicators were assessed to identify CKD. **(B)** Six obesity indicators were assessed to identify albuminuria. **(C)** Six obesity indicators were assessed to identify low-eGFR.

There are advantages to our study. Firstly, the sample selection was representative, with a sufficiently large sample size. Second, in order to get more accurate results, we also made adjustments for confounders. But because of a number of restrictions, the study's findings should be regarded cautiously. In the first place, we were unable to determine causal linkages because of the cross-sectional study design. Therefore, to clarify causality, prospective research with bigger sample numbers is still required. Second, even after adjusting for a few potential factors, the impacts of additional potential confounders could not be fully ruled out. Thirdly, Median imputation, which is unaffected by outliers, can better maintain the overall trend and distribution pattern of the data, but cannot fully

TABLE 4 Comparison of AUC values between SIRI and other inflammatory biomarkers.

Test	AUC[1]	95%CI[2] low	95%CI upp	Best threshold	Specificity	Sensitivity	*P* for different in AUC
CKD							
SIRI	0.5968	0.5894	0.6041	1.1741	0.6382	0.5120	Reference
SII	0.5603	0.5528	0.5678	606.0263	0.7167	0.3747	<0.0001
NHR	0.5571	0.5498	0.5644	2.8219	0.4539	0.6312	<0.0001
MHR	0.5479	0.5405	0.5552	0.4336	0.5718	0.5026	<0.0001
LHR	0.5173	0.5324	1.0537	0.8141	0.2399	0.5173	<0.0001
PHR	0.5076	0.5001	0.5151	129.1092	0.8350	0.1937	<0.0001
Albuminuria							
SIRI	0.5847	0.5760	0.5934	1.2465	0.6688	0.4659	Reference
SII	0.5623	0.5535	0.5711	620.0719	0.7285	0.3696	<0.0001
NHR	0.5683	0.5597	0.5769	3.0242	0.5045	0.5980	<0.0001
MHR	0.5467	0.5380	0.5554	0.4399	0.5842	0.4905	<0.0001
LHR	0.5054	0.4965	0.5143	0.9246	0.8746	0.1594	<0.0001
PHR	0.5129	0.5040	0.5219	228.7314	0.7059	0.3361	<0.0001
Low-eGFR							
SIRI	0.6264	0.6165	0.6364	1.1771	0.6305	0.5601	Reference
SII	0.5600	0.5497	0.5704	501.7929	0.5668	0.5270	<0.0001
NHR	0.5490	0.5391	0.5588	2.4417	0.3417	0.7397	<0.0001
MHR	0.5608	0.5507	0.5710	0.4592	0.6184	0.4736	<0.0001
LHR	0.5584	0.5480	0.5688	1.2411	0.7055	0.3908	<0.0001
PHR	0.5391	0.5289	0.5493	190.5980	0.4868	0.5748	<0.0001

[1]AUC, area under the curve.
[2]95% CI, 95% confidence interval.

utilize all the information in the data set. Though it is a good approximation of the ground truth, mode imputation—especially for skewed distributions—can add bias by substituting the most common value for missing values (37, 38). In conclusion, our study presents important strengths but is not without limitations. Careful consideration of these limitations is necessary when interpreting our findings. Further research, particularly prospective studies with diverse populations, is needed to confirm and expand upon our results.

5 Conclusions

When predicting CKD, albuminuria, and low-eGFR, SIRI may show up as a superior inflammatory biomarker when compared to other inflammatory biomarkers (SII, NHR, LHR, MHR, and PHR). American adults with elevated levels of SIRI, SII, NHR, MHR, and PHR should be attentive to the potential risks to their kidney health.

Data availability statement

Publicly available datasets were analyzed in this study. This data can be found here: https://www.cdc.gov/nchs/nhanes.

Ethics statement

The studies involving humans were approved by The National Center for Health Statistics Ethics Review Board. The studies were conducted in accordance with the local legislation and institutional requirements. Written informed consent for participation was not required from the participants or the participants' legal guardians/next of kin in accordance with the national legislation and institutional requirements. Written informed consent was obtained from the individual(s) for the publication of any potentially identifiable images or data included in this article.

Author contributions

XL: Writing – original draft. LC: Writing – review & editing. HX: Conceptualization, Writing – review & editing.

Funding

The author(s) declare that no financial support was received for the research, authorship, and/or publication of this article. This research did not receive any specific grant from funding agencies in the public, commercial, or not-for-profit sectors.

Acknowledgments

We thank the National Health and Nutrition Examination Surveys for providing the data.

Conflict of interest

The authors declare that the research was conducted in the absence of any commercial or financial relationships that could be construed as a potential conflict of interest.

Publisher's note

References

1. GBD Chronic Kidney Disease Collaboration. Global, regional, and national burden of chronic kidney disease, 1990-2017: a systematic analysis for the Global Burden of Disease Study 2017. *Lancet* (2020) 395:709–33. doi: 10.1016/S0140-6736(20)30045-3

2. Johansen KL, Chertow GM, Foley RN, Gilbertson DT, Herzog CA, Ishani A, et al. US renal data system 2020 annual data report: epidemiology of kidney disease in the United States. *Am J Kidney Dis* (2021) 77:A7–8. doi: 10.1053/j.ajkd.2021.01.002

3. Brennan E, Kantharidis P, Cooper ME, Godson C. Pro-resolving lipid mediators: regulators of inflammation, metabolism and kidney function. *Nat Rev Nephrol* (2021) 17:725–39. doi: 10.1038/s41581-021-00454-y

4. Biyik M, Biyik Z, Asil M, Keskin M. Systemic inflammation response index and systemic immune inflammation index are associated with clinical outcomes in patients with acute pancreatitis? J. *Invest. Surg* (2022) 35:1613–20. doi: 10.1080/08941939.2022.2084187

5. Zhao M, Duan X, Mi L, Shi J, Li N, Yin X, et al. Prognosis of hepatocellular carcinoma and its association with immune cells using systemic inflammatory response index. *Future Oncol* (2022) 18:2269–88. doi: 10.2217/fon-2021-1087

6. Xia Y, Xia C, Wu L, Li Z, Li H, Zhang J. Systemic immune inflammation index (SII), system inflammation response index (SIRI) and risk of all-cause mortality and cardiovascular mortality: A 20-year follow-up cohort study of 42,875 US adults. *J Clin Med* (2023) 12(3):1128. doi: 10.3390/jcm12031128

7. Qin Z, Li H, Wang L, Geng J, Yang Q, Su B, et al. Systemic immune-inflammation index is associated with increased urinary albumin excretion: A population-based study. *Front Immunol* (2022) 13:863640. doi: 10.3389/fimmu.2022.863640

8. Kim J, Song SH, Oh TR, Suh SH, Choi HS, Kim CS, et al. Prognostic role of the neutrophil-to-lymphocyte ratio in patients with chronic kidney disease. *Korean J Intern Med* (2023) 38:725–33. doi: 10.3904/kjim.2023.171

9. Qiu C, Liu S, Li X, Li W, Hu G, Liu F. Prognostic value of monocyte-to-lymphocyte ratio for 90-day all-cause mortality in type 2 diabetes mellitus patients with chronic kidney disease. *Sci Rep* (2023) 13:13136. doi: 10.1038/s41598-023-40429-6

10. Karatas A, Turkmen E, Erdem E, Dugeroglu H, Kaya Y. Monocyte to high-density lipoprotein cholesterol ratio in patients with diabetes mellitus and diabetic nephropathy. *biomark Med* (2018) 12:953–9. doi: 10.2217/bmm-2018-0048

11. Qi X, Li Y, Fang C, Jia Y, Chen M, Chen X, et al. The associations between dietary fibers intake and systemic immune and inflammatory biomarkers, a multi-cycle study of NHANES 2015-2020. *Front Nutr* (2023) 10:1242115. doi: 10.3389/fnut.2023.1242115

12. Wang L, Dong J, Xu M, Li L, Yang N, Qian G. Association between monocyte to high-density lipoprotein cholesterol ratio and risk of non-alcoholic fatty liver disease: A cross-sectional study. *Front Med (Lausanne)* (2022) 9:898931. doi: 10.3389/fmed.2022.898931

13. Chapter 1: definition and classification of CKD. *Kidney Int Suppl (2011)* (2013) 3:19–62. doi: 10.1038/kisup.2012.64

14. Levey AS, Stevens LA, Schmid CH, Zhang YL, Castro AR, Feldman HI, et al. A new equation to estimate glomerular filtration rate. *Ann Intern Med* (2009) 150:604–12. doi: 10.7326/0003-4819-150-9-200905050-00006

15. Li X, Wang L, Liu M, Zhou H, Xu H. Association between neutrophil-to-lymphocyte ratio and diabetic kidney disease in type 2 diabetes mellitus patients: a cross-sectional study. *Front Endocrinol (Lausanne)* (2023) 14:1285509. doi: 10.3389/fendo.2023.1285509

16. Yan LJ, Zhang FR, Ma CS, Zheng Y. Higher dietary inflammatory index is associated with increased all-cause mortality in adults with chronic kidney disease. *Front Nutr* (2022) 9:883838. doi: 10.3389/fnut.2022.883838

17. Guo W, Song Y, Sun Y, Du H, Cai Y, You Q, et al. Systemic immune-inflammation index is associated with diabetic kidney disease in Type 2 diabetes mellitus patients: Evidence from NHANES 2011-2018. *Front Endocrinol (Lausanne)* (2022) 13:1071465. doi: 10.3389/fendo.2022.1071465

18. Whelton PK, Carey RM, Aronow WS, Casey DJ, Collins KJ, Dennison HC, et al. 2017 ACC/AHA/AAPA/ABC/ACPM/AGS/APhA/ASH/ASPC/NMA/PCNA guideline for the prevention, detection, evaluation, and management of high blood pressure in adults: A report of the American college of cardiology/American heart association task force on clinical practice guidelines. *Hypertension* (2018) 71:e13–e115. doi: 10.1161/HYP.0000000000000065

19. Qin Z, Chen X, Sun J, Jiang L. The association between visceral adiposity index and decreased renal function: A population-based study. *Front Nutr* (2023) 10:1076301. doi: 10.3389/fnut.2023.1076301

20. Le VH, Minh T, Kha QH, Le NQK. A transfer learning approach on MRI-based radiomics signature for overall survival prediction of low-grade and high-grade gliomas. *Med Biol Eng. Comput* (2023) 61:2699–712. doi: 10.1007/s11517-023-02875-2

21. Le VH, Kha QH, Minh T, Nguyen VH, Le VL, Le NQK. Development and validation of CT-based radiomics signature for overall survival prediction in multi-organ cancer. *J Digit. Imaging* (2023) 36:911–22. doi: 10.1007/s10278-023-00778-0

22. Tanaka S, Couret D, Tran-Dinh A, Duranteau J, Montravers P, Schwendeman A, et al. High-density lipoproteins during sepsis: from bench to bedside. *Crit Care* (2020) 24:134. doi: 10.1186/s13054-020-02860-3

23. Huang JB, Chen YS, Ji HY, Xie WM, Jiang J, Ran LS, et al. Neutrophil to high-density lipoprotein ratio has a superior prognostic value in elderly patients with acute myocardial infarction: a comparison study. *Lipids Health Dis* (2020) 19:59. doi: 10.1186/s12944-020-01238-2

24. Wei Y, Wang T, Li G, Feng J, Deng L, Xu H, et al. Investigation of systemic immune-inflammation index, neutrophil/high-density lipoprotein ratio, lymphocyte/high-density lipoprotein ratio, and monocyte/high-density lipoprotein ratio as indicators of inflammation in patients with schizophrenia and bipolar disorder. *Front Psychiatry* (2022) 13:941728. doi: 10.3389/fpsyt.2022.941728

25. Song Y, Zhao Y, Shu Y, Zhang L, Cheng W, Wang L, et al. Combination model of neutrophil to high-density lipoprotein ratio and system inflammation response index is more valuable for predicting peripheral arterial disease in type 2 diabetic patients: A cross-sectional study. *Front Endocrinol (Lausanne)* (2023) 14:1100453. doi: 10.3389/fendo.2023.1100453

26. Lai W, Xie Y, Zhao X, Xu X, Yu S, Lu H, et al. Elevated systemic immune inflammation level increases the risk of total and cause-specific mortality among patients with chronic kidney disease: a large multi-center longitudinal study. *Inflamm Res* (2023) 72:149–58. doi: 10.1007/s00011-022-01659-y

27. Lv Z, Feng HY, Wang T, Ma X, Zhang X. Preoperative systemic inflammation response index indicates poor prognosis in patients treated with resection of renal cell carcinoma with inferior vena cava tumor thrombus. *Urol Oncol* (2022) 40:167–9. doi: 10.1016/j.urolonc.2021.11.030

28. Lee SB, Kalluri R. Mechanistic connection between inflammation and fibrosis. *Kidney Int Suppl* (2010) 119):S22–6. doi: 10.1038/ki.2010.418

29. Feng C, Jiang H, Yang X, Cong H, Li L, Feng J. GLUT1 mediates the metabolic reprogramming and inflammation of CCR2$^+$ Monocytes/macrophages from patients with DCM. *Front Biosci (Landmark Ed)* (2023) 28:223. doi: 10.31083/j.fbl2809223

30. Kouhpayeh H. Clinical features predicting COVID-19 mortality risk. *Eur J Transl Myol* (2022) 32(2):10268. doi: 10.4081/ejtm.2022.10268

31. Van Laecke S, Kerre T, Nagler EV, Maes B, Caluwe R, Schepers E, et al. Hereditary polycystic kidney disease is characterized by lymphopenia across all stages of kidney dysfunction: an observational study. *Nephrol Dial Transplant* (2018) 33:489–96. doi: 10.1093/ndt/gfx040

32. Chao B, Ju X, Zhang L, Xu X, Zhao Y. A novel prognostic marker systemic inflammation response index (SIRI) for operable cervical cancer patients. *Front Oncol* (2020) 10:766. doi: 10.3389/fonc.2020.00766

33. Zhang Y, Xing Z, Zhou K, Jiang S. The predictive role of systemic inflammation response index (SIRI) in the prognosis of stroke patients. *Clin Interv Aging* (2021) 16:1997–2007. doi: 10.2147/CIA.S339221

34. Li X, Wang L, Zhou H, Xu H. Association between weight-adjusted-waist index and chronic kidney disease: a cross-sectional study. *BMC Nephrol* (2023) 24:266. doi: 10.1186/s12882-023-03316-w

35. Qian Q. Inflammation: A key contributor to the genesis and progression of chronic kidney disease. *Contrib. Nephrol* (2017) 191:72–83. doi: 10.1159/000479257

36. Mihai S, Codrici E, Popescu ID, Enciu AM, Albulescu L, Necula LG, et al. Inflammation-related mechanisms in chronic kidney disease prediction, progression, and outcome. *J Immunol Res* (2018) 2018:2180373. doi: 10.1155/2018/2180373

37. Xu X, Xia L, Zhang Q, Wu S, Wu M, Liu H. The ability of different imputation methods for missing values in mental measurement questionnaires. *BMC Med Res Methodol* (2020) 20:42. doi: 10.1186/s12874-020-00932-0

38. Zhang Z. Missing data imputation: focusing on single imputation. *Ann Transl Med* (2016) 4:9. doi: 10.3978/j.issn.2305-5839.2015.12.38

frontiers | Frontiers in Endocrinology

TYPE Original Research
PUBLISHED 22 March 2024
DOI 10.3389/fendo.2024.1253492

OPEN ACCESS

EDITED BY
Federica Mescia,
University of Brescia, Italy

REVIEWED BY
Sebastjan Bevc,
Maribor University Medical Centre, Slovenia
Gianmarco Lugli,
University of Brescia, Italy

*CORRESPONDENCE
Camilla Sammut-Powell
camilla.sammut@outlook.com

RECEIVED 05 July 2023
ACCEPTED 19 February 2024
PUBLISHED 22 March 2024

CITATION
Sammut-Powell C, Sisk R, Silva-Tinoco R, de la Pena G, Almeda-Valdes P, Juarez Comboni SC, Goncalves S and Cameron R (2024) External validation of a minimal-resource model to predict reduced estimated glomerular filtration rate in people with type 2 diabetes without diagnosis of chronic kidney disease in Mexico: a comparison between country-level and regional performance.
Front. Endocrinol. 15:1253492.
doi: 10.3389/fendo.2024.1253492

External validation of a minimal-resource model to predict reduced estimated glomerular filtration rate in people with type 2 diabetes without diagnosis of chronic kidney disease in Mexico: a comparison between country-level and regional performance

Camilla Sammut-Powell[1*], Rose Sisk[1], Ruben Silva-Tinoco[2], Gustavo de la Pena[3], Paloma Almeda-Valdes[3,4], Sonia Citlali Juarez Comboni[5], Susana Goncalves[6] and Rory Cameron[1]

[1]Gendius Ltd, Alderley Edge, United Kingdom, [2]Clinic Specialized in the Diabetes Management of the Mexico City Government, Public Health Services of the Mexico City Government, Mexico, City, Mexico, [3]Department of Endocrinology and Metabolism, Instituto Nacional de Ciencias Médicas y Nutrición Salvador Zubirán (INCMNSZ), Mexico City, Mexico, [4]Metabolic Diseases Research, Instituto Nacional de Ciencias Médicas y Nutrición Salvador Zubirán, Mexico City, Mexico, [5]AstraZeneca, Mexico City, Mexico, [6]International Region, AstraZeneca, Buenos Aires, Argentina

Background: Patients with type 2 diabetes are at an increased risk of chronic kidney disease (CKD) hence it is recommended that they receive annual CKD screening. The huge burden of diabetes in Mexico and limited screening resource mean that CKD screening is underperformed. Consequently, patients often have a late diagnosis of CKD. A regional minimal-resource model to support risk-tailored CKD screening in patients with type 2 diabetes has been developed and globally validated. However, population heath and care services between countries within a region are expected to differ. The aim of this study was to evaluate the performance of the model within Mexico and compare this with the performance demonstrated within the Americas in the global validation.

Methods: We performed a retrospective observational study with data from primary care (Clinic Specialized in Diabetes Management in Mexico City), tertiary care (Instituto Nacional de Ciencias Médicas y Nutrición Salvador Zubirán) and the Mexican national survey of health and nutrition (ENSANUT-MC 2016). We applied the minimal-resource model across the datasets and evaluated model performance metrics, with the primary interest in the sensitivity and increase in the positive predictive value (PPV) compared to a screen-everyone approach.

Results: The model was evaluated on 2510 patients from Mexico (primary care: 1358, tertiary care: 735, ENSANUT-MC: 417). Across the Mexico data, the

sensitivity was 0.730 (95% CI: 0.689 – 0.779) and the relative increase in PPV was 61.0% (95% CI: 52.1% - 70.8%). These were not statistically different to the regional performance metrics for the Americas (sensitivity: p=0.964; relative improvement: p=0.132), however considerable variability was observed across the data sources.

Conclusion: The minimal-resource model performs consistently in a representative Mexican population sample compared with the Americas regional performance. In primary care settings where screening is underperformed and access to laboratory testing is limited, the model can act as a risk-tailored CKD screening solution, directing screening resources to patients who are at highest risk.

KEYWORDS

type 2 diabetes, chronic kidney disease, screening, risk stratification, clinical prediction model, low-and-middle-income countries

1 Introduction

Diabetes is a leading cause of kidney disease and with the rising prevalence of type 2 diabetes (1), the burden of chronic kidney disease (CKD) is also expected to increase (2). The burden of CKD in Mexico is growing at an exponential rate (3), yet, the majority of patients with CKD do not receive a timely diagnosis nor treatment (4). The Kidney Early Evaluation Program (KEEP) Mexico currently supports the early detection of CKD amongst adults with risk factors, such as diabetes, but its outreach remains low (8858 individuals screened between 2008 and 2017) (5). Therefore, a targeted approach to screening that can be implemented within health care services may offer a larger-scale solution to the early detection of CKD.

A minimal resource model to predict a reduced estimated glomerular filtration rate (eGFR below 60 ml/min/1.73m^2) in patients with type 2 diabetes has been previously developed and globally validated (6–8). The model uses age, sex, duration of diabetes, body mass index and blood pressure to predict the probability that the patient's eGFR is below 60, potentially indicating undiagnosed CKD. If the probability is 11.5% or higher, the patient is deemed 'high risk' and it is recommended that the patient is prioritized for CKD screening. This threshold was selected to achieve on average a sensitivity of 80%, whilst simultaneously improving the positive predictive value (PPV) compared to a screen-everyone approach, where only 10-20% have an eGFR below 60. The purpose of the model is to support earlier identification of CKD by understanding which patients are at highest risk and using this information to strategically allocate CKD screening resource to those most in need. The global validation used AstraZeneca's global registry data (iCaReMe and DISCOVER) and demonstrated promising potential to refine the population to those at highest risk, whilst retaining a high detection rate: overall, a relative improvement of 50% was observed in the PPV, whilst retaining a sensitivity of 80%. However, the validation focused on global and regional performance, using the World Health Organization (WHO) classification of region. Most contributing countries had small samples; for the Americas, the total sample size was 1430 patients made up from 7 countries (Canada and Latin America), each contributing between 28 and 296 patients. Therefore, the results may not be generalizable to individual country-level performance.

Healthcare systems and patient populations vary considerably across Latin America (9). For example, in Brazil the population is made up of a higher proportion of Afro-descendants, whereas Mexico has a higher proportion of indigenous people, and the Mexican population was shown to be three times more likely to present with complications of diabetes (10). Consequently, the regional performance may not be representative of its performance within Mexico. Therefore, we aimed to perform a country-level validation of the minimal-resource model in Mexico and compare it against the regional performance for the Americas.

2 Materials and methods

2.1 Design and data sources

This was a retrospective, observational study using data collected from: the DIABEMPIC programme within the Clinic Specialized in Diabetes Management in Mexico City, consisting of data collected from patients with continuous medical care in 32 public primary care units between 2nd January 2017 and 8th December 2022; Instituto Nacional de Ciencias Médicas y Nutrición Salvador Zubirán (INCMNSZ), consisting of data from

patients attending a tertiary care center for specialized care, located in Mexico City, collected between 20th September 2020 and 10th November 2022; and the Encuesta Nacional de SAlud y NUTricion 2016 (ENSANUT-MC 2016), i.e. the Mexican National Survey of Health and Nutrition (11).

Ethical approval was obtained on a clinic-by-clinic basis, adhering to policy within each clinic. All adults (aged 18 and over) with a diagnosis of type 2 diabetes were included. Patients with a disease diagnosis code (e.g. ICD-10 code) of CKD stage 3-5 were excluded.

2.2 Prediction model

We implemented the minimal-resource CKD pre-screening model developed by Gendius, described in Sammut-Powell et al. (6). The model uses age, gender, body mass index, time since diagnosis of diabetes and blood pressure to predict the probability that a patient's eGFR is below 60 ml/min/1.73m^2, herein referred to as the predicted probability. A pre-determined threshold of 11.5% (derived during model development) was used to categorize patients as high risk or not, i.e. if the risk was 11.5% or higher, the patient was categorized as 'high risk'.

2.3 Primary outcome

The primary outcome was an indicator of whether the eGFR was below 60 ml/min/1.73m^2 or not, consistent with the definition in the model. The eGFRs were provided directly from the clinics. However, for the survey data, only the serum creatinine was available, therefore we calculated the eGFR using the 2009 CKD-EPI formula (12).

2.4 Missing data

All demographic data for patients with corresponding outcome data were complete.

2.5 Statistical methods

Population summary statistics were evaluated to compare the populations within the clinics. T-tests and Wilcoxon rank-sum tests were performed to determine statistical differences between patient demographics that had a normal and non-normal distribution, respectively.

2.5.1 Model performance

The model was applied to the data and the distribution of the predicted risks were visualized by data source. The sensitivity and the relative improvement in the positive predictive value (PPV) were the primary performance metrics. Relative improvement in the PPV is defined as the improvement over a screen-everyone approach, where the PPV of a screen-everyone approach is equal to the prevalence of eGFR below 60 ml/min/1.73m^2.

Secondary performance metrics included the specificity, negative predictive value, and the C-statistic. Binomial regression and Poisson tests were used to compare the sensitivity and relative improvement in PPV estimates, respectively, with the estimates previously obtained during the global registry validation for the Americas. The 95% bootstrap confidence intervals (CI) were obtained using 200 samples. Calibration was assessed visually.

2.5.2 Sample size requirements

A total of 220 positive cases from the Americas were included in global validation. Consequently, an additional 321 positive cases from Mexico corresponds to an 80% power for a 5% significance level to detect a reduction of 10% in the sensitivity, using a Normal approximation and the sensitivity estimate of 0.732 for the Americas, as previously observed.

All analyses were performed in R.

3 Results

There were 2510 patients identified as aged 18 or above, diagnosed with type 2 diabetes and no previous diagnosis of CKD stage 3-5, with a serum creatinine or eGFR and no missing data (primary care: 1358, tertiary care: 735, ENSANUT-MC: 417). The prevalence of an eGFR below 60ml/min/1.73m^2 was 11.7% and 20.1%, in the primary and tertiary clinics, respectively (Table 1). The tertiary clinic population consisted of older patients with a longer duration of type 2 diabetes, compared to the primary care (age: $p<0.001$, duration: $p<0.001$) and survey (age: $p<0.001$, duration: $p<0.001$) populations (Figure 1). Overall, the Mexico population sample was statistically significantly different across the majority of demographics but not clinically different in age and BMI.

The overall sensitivity averaged across all the data from Mexico (0.730, 95% CI: 0.689 – 0.779) was not statistically different to that previously reported for the Americas in a global registry validation ($p=0.964$). However, considerable variability was observed in the sensitivity estimates across the data sources within Mexico (Primary clinics: 0.592; ENSANUT-MC survey: 0.733; Tertiary clinic: 0.872; Table 2). No statistical difference was observed between the sensitivity observed in the survey data and the Americas registry data, but the sensitivity was statistically lower in the primary clinics ($p=0.006$) and higher in the tertiary clinic ($p=0.001$) compared to the sensitivity obtained for the Americas (Figure 2).

For the primary care and survey populations, most patients with an eGFR of 60 ml/min/1.73m^2 and above had a predicted probability that was below the cut-off (Figure 2); the specificity remained between 0.671 and 0.700 within the regional, primary care and survey populations. However, it was significantly reduced in the tertiary care clinic, evidencing the trade-off from achieving a high sensitivity. Despite this, the negative predictive value remained above 0.9 across all populations, likely due to the low prevalence of patients with an eGFR below 60 ml/min/1.73m^2.

10.3389/fendo.2024.1253492

TABLE 1 Baseline demographics of patients across primary and tertiary care services in Mexico City and a representative population sample from a nutritional survey (ENSANUT-MC).

	Americas, Global Validation (registry)	Mexico Validation				
		Total		Primary Clinics	ENSANUT-MC (survey)	Tertiary Clinic
	n = 1430	n = 2510	p-value	n = 1358	n = 417	n = 735
Gender, n (%)						
Female	685 (47.9%)	1390 (55.4%)	<0.001	825 (60.8%)	117 (28.1%)	448 (61%)
Male	745 (52.1%)	1120 (44.6%)		533 (39.2%)	300 (71.9%)	287 (39%)
Age (years), mean (SD)	58.7 (12.1)	57.6 (12.3)	0.009	54.1 (11.6)	58.1 (11.9)	63.8 (11.5)
Body mass index (kg/m^2), mean (SD)	30.6 (5.7)	29.2 (5.8)	<0.001	29.7 (6.0)	29.7 (5.6)	28.1 (5.1)
Time since diagnosis of diabetes (years), median (LQ-UQ)	5.2 (2.2-10.4)	12 (5-20)	<0.001	10 (4-16)	7 (3-14)	20 (13-26)
Diastolic blood pressure (mmHg), mean (SD)	79.3 (10.9)	74.2 (10.4)	<0.001	74.3 (10.3)	74.7 (11.7)	73.5 (9.5)
Systolic blood pressure (mmHg), mean (SD)	130.7 (17.1)	125.3 (19.6)	<0.001	124.7 (20.0)	131.4 (22.1)	122.9 (16.6)
eGFR (ml/min/1.73m^2), median (LQ-UQ)	87.5 (69.9-101.2)	93.5 (73-105.5)	<0.001	94.2 (76.6-104.9)	103.5 (85.4-118)	89 (63-99)
eGFR below 60, n (%)	220 (15.4%)	352 (14%)	0.263	159 (11.7%)	45 (10.8%)	148 (20.1%)
CKD G-stage, n (%)						
Stage G0-1	664 (46.4%)	1433 (57.1%)	<0.001	779 (57.4%)	293 (70.3%)	361 (49.1%)
Stage G2	546 (38.2%)	725 (28.9%)		420 (30.9%)	79 (18.9%)	226 (30.7%)
Stage G3	174 (12.2%)	304 (12.1%)		151 (11.1%)	39 (9.4%)	114 (15.5%)
Stage G4-5	46 (3.2%)	48 (1.9%)		8 (0.6%)	6 (1.4%)	34 (4.6%)

Statistical tests between the Americas population and combined Mexico population data were performed to determine statistical differences in the populations; a p-value of below 0.05 was considered significant. SD, standard deviation; LQ, lower quartile; UQ, upper quartile; eGFR, estimated glomerular filtration rate.

The average relative improvement in the PPV was not statistically different in the Mexico data compared to that previously demonstrated for the Americas (p=0.132), despite the estimate being heavily discounted by the performance in the tertiary care clinic whose individual performance was statistically lower (p<0.001). The primary care and survey data relative improvements in PPV were not statistically different to that estimated for the Americas (primary clinic: p=0.748; survey: p=0.770).

The discrimination was good (C-statistic above 0.7) across all data sources (Table 2). The model remained well-calibrated in the Mexico data within those with a predicted probability below 0.2 (Figure 3). For larger probabilities, the model was observed to overestimate the risk. For both the primary care and survey populations, the proportion of patients predicted as high risk was below 40%, indicating a large reduction in the population by selecting only patients that are high risk.

4 Discussion

We have demonstrated that the regional performance was consistent with the average performance using a large sample from Mexico; the minimal-resource model reduced the screening population to significantly increase the positive predictive value, whilst retaining an adequate sensitivity. However, performance across data sources varied. Therefore, care must be taken when anticipating how the model will perform in various clinical settings, and establishing whether use of the model in a particular setting is appropriate or supported by sufficient performance estimates.

Differences in populations and performance estimates between the care services can be partly explained by the care system in Mexico. Unlike other healthcare services such as UK primary care, the primary care service in Mexico does not serve all patients. Instead, the population is split across primary, secondary, and

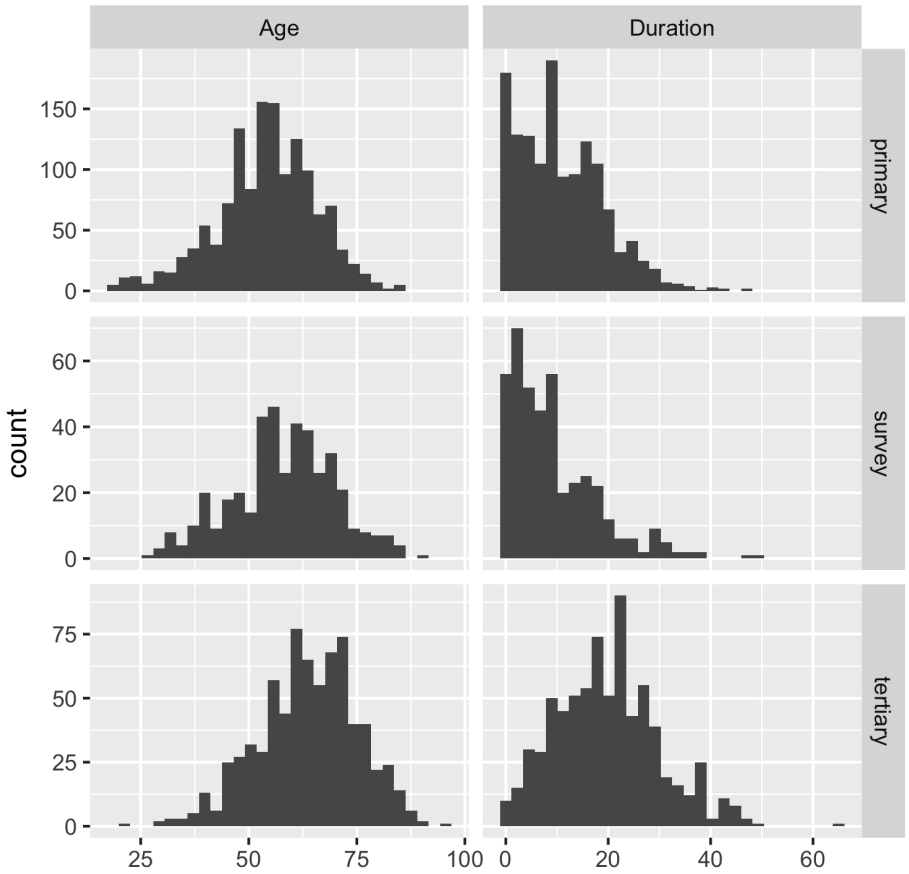

FIGURE 1
Histograms of the age of the patients and duration (time since diagnosis) of type 2 diabetes in years across the Mexican data sources (primary = primary care clinics; tertiary = tertiary care clinic; survey = ENSANUT-MC 2016).

TABLE 2 Estimates and 95% bootstrap confidence intervals of performance metrics.

	Global Validation (Americas)	Mexico Validation				
		Total		Primary Clinics	ENSANUT-MC (survey)	Tertiary Clinic
	n = 1430	n = 2510	p-value	n = 1358	n = 417	n = 735
Prevalence	0.154 (0.136 - 0.173)	0.140 (0.127 - 0.155)	0.263	0.117 (0.099 - 0.134)	0.108 (0.079 - 0.132)	0.201 (0.175 - 0.226)
Positive Predictive Value (PPV)	0.288 (0.256 - 0.326)	0.226 (0.204 - 0.252)	0.005	0.209 (0.171 - 0.245)	0.214 (0.164 - 0.277)	0.244 (0.211 - 0.287)
Relative improvement in PPV	0.872 (0.735 - 1.052)	0.610 (0.521 - 0.708)	0.132	0.783 (0.543 - 1.006)	0.986 (0.703 - 1.394)	0.211 (0.144 - 0.284)
Sensitivity	0.732 (0.683 - 0.792)	0.730 (0.689 - 0.779)	0.964	0.597 (0.520 - 0.667)	0.733 (0.622 - 0.865)	0.872 (0.820 - 0.926)
Specificity	0.671 (0.646 - 0.698)	0.592 (0.573 - 0.613)	<0.001	0.700 (0.674 - 0.727)	0.675 (0.628 - 0.723)	0.319 (0.289 - 0.361)

(Continued)

10.3389/fendo.2024.1253492

TABLE 2 Continued

	Global Validation (Americas)	Mexico Validation				
		Total		Primary Clinics	ENSANUT-MC (survey)	Tertiary Clinic
	n = 1430	n = 2510	p-value	n = 1358	n = 417	n = 735
Negative Predictive Value (NPV)	0.932 (0.915 - 0.950)	0.931 (0.918 - 0.943)	0.891	0.929 (0.912 - 0.943)	0.954 (0.932 - 0.981)	0.908 (0.869 - 0.945)
C-statistic	0.768 (0.738 - 0.805)	0.733 (0.711 - 0.761)	0.113	0.718 (0.675 - 0.760)	0.779 (0.722 - 0.848)	0.706 (0.659 - 0.750)
Proportion predicted high risk	0.391 (0.367 - 0.417)	0.453 (0.436 - 0.474)	<0.001	0.335 (0.311 - 0.359)	0.369 (0.328 - 0.415)	0.720 (0.687 - 0.750)

P-values to test for statistical differences between the Americas population sample and the Mexico population sample are presented.

tertiary care. Therefore, data from a single service are not representative of the whole population. To get an overall estimate of the performance across the population, population study data or a collection of data from all care services with a population weighting is required. Therefore, comparing performances between the regional and the survey data is likely to attenuate selection bias. Additionally, the Americas population primarily consisted of patients from the DISCOVER study (n=933/1430) which enrolled patients at initiation of second-line glucose-lowering therapy and therefore may explain differences in baseline demographics and performance metrics within single-service populations.

Whilst the sensitivity of the model was below the desirable threshold in the primary care clinics, the sensitivity within the tertiary care clinic surpassed the minimum required performance. Therefore, the model appears to be more conservative to ruling-out patients that may have a worse overall health, likely due to confounding with age. This aligns with current clinical practice to remain risk-averse in comorbid patients with severe health conditions; in tertiary clinics, risk factor monitoring of patients is routinely performed across all patients, regardless of symptoms. The inherent trade-off between sensitivity and specificity was evident, with a much lower specificity observed within the tertiary care clinic. Therefore, the application of the model may be most beneficial in primary and secondary care services where screening is not routinely performed. When adopting only within these services, expectations of the model's performance should be adjusted to accommodate the change in the overarching population.

The Mexican National Health and Nutritional Survey data has been widely used amongst researchers and is considered to be a representative sample of the Mexican population (13–15), however it is difficult to assert conclusively that the samples of patients in the primary and tertiary clinics are representative of the entire country, particularly because they are from an urban population. Therefore, the survey data provides a more comparable population performance within Mexico. The performance within this subgroup was most similar to the performance previously estimated for the Americas region. However, the survey data is subject to limitations. Firstly, the sample size was small, meaning that these estimates may not be reliable. Secondly, the only way to

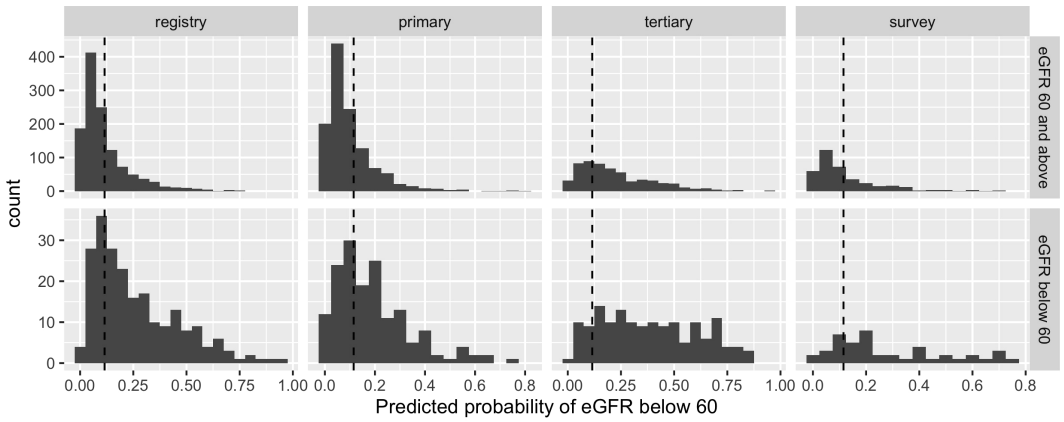

FIGURE 2
Histograms of predicted probabilities of eGFR below 60ml/min/1.73m^2 by data source (registry = Americas, Global Validation; primary = primary care clinics; tertiary = tertiary care clinics; survey = ENSANUT-MC 2016) and observed eGFR below 60ml/min/1.73m^2 or not. The cut-off for categorising a patient as high risk is indicated by a dashed line; probabilities to the right of the line are high risk.

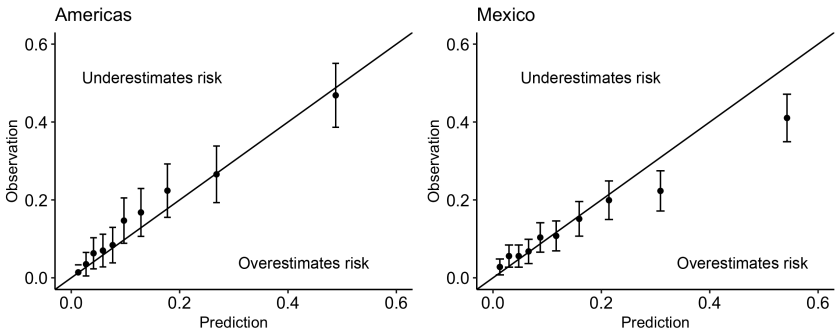

FIGURE 3
Calibration plots for the minimal-resource model when applied to (left): the Americas registry data used in the Global Validation and (right): the combined primary care, tertiary care and survey data from Mexico. Above the line indicates that the risk was underestimated by the model; below the line indicates that the risk was overestimated by the model.

identify a previous CKD diagnosis was through a patient self-reporting that they had been told they have kidney failure. In contrast, the clinics were able to determine whether a patient has a CKD diagnosis code and therefore the patient selection within the survey population may not be consistent with the clinic data. Thirdly, the data are taken from 2016 and therefore may not be representative of the current population, given temporal changes to population health and care practices.

Intensified multifactorial interventions to control major risk factors, e.g., HbA1c, blood pressure, and lipids, are associated with a reduced risk of CKD incidence or progression and other relevant outcomes in patients with type 2 diabetes mellitus (16, 17). Moreover, clinical trials have demonstrated the effectiveness of the sodium-glucose cotransporter inhibitor 2 (SGLT2i) in delaying progression of CKD (18–20), yet prescribing remains low (21). Given the significant burden of CKD within Mexico (3), it is imperative that there is a strategy to identify and treat patients in a timely fashion. Using the minimal-resource model provides a solution to support identification of high-risk patients enabling targeted screening programs with higher efficiency than standard practice, especially where standard practice is sub-par due to limited available resources. For example, in primary care, patients that are identified as high risk for undiagnosed CKD may be targeted to receive a diagnosis assessment and in those with confirmatory results, a patient may be transitioned to secondary or tertiary care, and new treatments may be initiated to slow the progression of the disease.

Mexico has the world's sixth-highest premature death rate from CKD (22). From 1990 to 2017, the country's age-standardized CKD mortality rate jumped from 28.7 to 58.1 per 100,000 inhabitants (3, 22). This jump represented an increase in the mortality rate of 102.3%, while the increases in the rates of Latin America and the worldwide population were 32.9 and 2.8%, respectively (22, 23). This remarkable increase in the mortality rate is explained by a growing burden of risk factors such as diabetes, restricted access to preventive interventions and resources supporting early management of the disease, and limited availability of renal replacement therapy, primarily among the low-income population (3, 22, 24).

In low- and middle-income countries, like Mexico, barriers to provision and access to diabetes care are compounded by the often-fragmented care pathways for the multiple needs of many people with diabetes. These impact patients' adherence to treatment, diabetes care goals attainment, and the screening of complications (25–27). For example, patients without health insurance (mainly unsalaried workers, the unemployed and the economically inactive population) have no guarantee of adequate medical follow-up and screening for complications related to diabetes (25). As a result, the differences in coverage and access to medical care for patients with CKD have greatly contributed to deepening the health inequities among the Mexican population, with the most unfavourable results occurring among its poorest members.

In Mexico, as in other low- and middle-income countries, routine procedures to detect and diagnose CKD are not sufficiently performed (28, 29). This has resulted in a high rate of undiagnosed and undertreated patients (30). Given that CKD progresses slowly, without pain or discomfort, and irreversibly, patients may not know that they have it for years, especially at primary and secondary levels of the care system. Many patients spend time presenting chronic poor metabolic control with silent deterioration of renal function until very advanced stages, where the only viable treatment option is renal replacement therapy. This illustrates the importance of strengthening primary level care and improving early detection of CKD, particularly for those at high-risk (those who are overweight or obese or have diabetes or hypertension).

Alternative published models to predict diabetic kidney disease are largely prognostic (31–36), i.e. remain focused on predicting future onset of disease as opposed to undiagnosed CKD, or are not specific to the population with type 2 diabetes (15, 37). They often include measurements from invasive testing (33, 38) which may not be available in low-to-middle income countries and therefore are unsuitable for use in such settings. The minimal-resource model removes barriers to application through requiring only readily available information. It can be utilised during a patient consultation or within community care to instantly assess a patient's risk. Where electronic health records are available, the model can be applied using the most recent measurements to risk-

stratify the entire patient group. Upon identifying a patient as high risk, a clinician can prioritize the patient for CKD screening and act with urgency, supporting early detection.

5 Conclusions

The minimal-resource model performs consistently in a representative Mexican population sample compared with the Americas regional performance using registry data. When applying the model within an individual clinic or sector of healthcare, the performance is expected to vary, aligned with the health of the population served by the clinic. In primary care settings where screening is underperformed and access to laboratory testing is limited, the model can act as a risk-tailored CKD screening solution, directing screening resources to patients who are at highest risk. This may enable earlier detection of CKD and an opportunity to intervene at a time when the course of the disease may be changed.

Data availability statement

The primary care and tertiary care datasets presented in this article are not readily available because the patients have not given written consent to share their data publicly. Requests to access the datasets should be directed to ruben_ost@hotmail.com and paloma.almedav@incmnsz.mx respectively. Data from the ENSANUT-MC 2016 are freely available from https://ensanut.insp.mx.

Ethics statement

Ethical approval was not required for the study involving humans in accordance with the local legislation and institutional requirements. Written informed consent to participate in this study was not required from the participants or the participants' legal guardians/next of kin in accordance with the national legislation and the institutional requirements.

Author contributions

CS-P: Conceptualization, Formal analysis, Methodology, Visualization, Writing – original draft, Writing – review & editing. RS: Conceptualization, Writing – review & editing. RS-T: Data curation, Writing – original draft, Writing – review & editing. GD: Data curation, Writing – original draft, Writing – review & editing. PA-V: Data curation, Writing – original draft, Writing – review & editing. SJ: Conceptualization, Writing – review & editing. SG: Conceptualization, Writing – review & editing. RC: Conceptualization, Writing – review & editing.

Funding

The author(s) declare financial support was received for the research, authorship, and/or publication of this article. This study was funded by AstraZeneca.

Conflict of interest

Authors CS-P, RS and RC were employed by the company Gendius Limited. Authors SJ and SG were employed by the company AstraZeneca.

The remaining authors declare that the research was conducted in the absence of any commercial or financial relationships that could be construed as potential conflict of interest.

The authors declare that this study received funding from AstraZeneca. The funder had the following involvement in the study: conceptualization and writing - editing & review.

Publisher's note

References

1. Khan MAB, Hashim MJ, King JK, Govender RD, Mustafa H, Al Kaabi J. Epidemiology of type 2 diabetes – global burden of disease and forecasted trends. *J Epidemiol Glob Health*. (2020) 10:107–11. doi: 10.2991/jegh.k.191028.001

2. Kovesdy CP. Epidemiology of chronic kidney disease: an update 2022. *Kidney Int Suppl*. (2022) 12:7. doi: 10.1016/j.kisu.2021.11.003

3. Agudelo-Botero M, Valdez-Ortiz R, Giraldo-Rodríguez L, González-Robledo MC, Mino-León D, Rosales-Herrera MF, et al. Overview of the burden of chronic kidney disease in Mexico: secondary data analysis based on the Global Burden of Disease Study 2017. *BMJ Open*. (2020) 10:e035285. doi: 10.1136/bmjopen-2019-035285

4. Aguilar-Ramirez D, Alegre-Díaz J, Gnatiuc L, Ramirez-Reyes R, Wade R, Hill M, et al. Changes in the diagnosis and management of diabetes in Mexico City between 1998–2004 and 2015–2019. *Diabetes Care*. (2021) 44:944–51. doi: 10.2337/dc20-2276

5. Obrador Vera G, Villa A, Cuadra M, De Arrigunaga S, Cárdenas C, Bracho M, et al. Longitudinal follow-up of incident chronic kidney disease (CKD) in the KEEP Mexico CKD screening program. *Kidney Int Rep*. (2019) 4:S245. doi: 10.1016/j.ekir.2019.05.610

6. Sammut-Powell C, Sisk R, Budd J, Patel N, Edge M, Cameron R. Development of minimal resource pre-screening tools for chronic kidney disease in people with type 2 diabetes. *Future Healthc J*. (2022) 9(3):305–9. doi: 10.7861/fhj.2022-0020

7. Sisk R, Sammut-Powell C, Budd J, Cameron R, Edge M, Vazquez-Mendez E, et al. Minimal resource pre-screening tools for chronic kidney disease in people with type 2 diabetes: a global validation study. *Diabetologia*. (2022) 65:S374–375. doi: 10.1007/s00125-022-05755-w

8. Sisk R, Sammut-Powell C, Budd J, Cameron R, Edge M, Vazquez-Mendez E, et al. A global validation of a minimal-resource pre-screening model for reduced kidney function in patients with type 2 diabetes. *J Am Soc Nephrol*. (2022) 33:681.

9. Macinko J, Andrade FCD, Nunes BP, Guanais FC. Primary care and multimorbidity in six Latin American and Caribbean countries. *Rev Panam Salud Publica*. (2019) 43:e8. doi: 10.26633/RPSP.2019.8

10. Martins RB, Ordaz-Briseño SA, Flores-Hernández S, Bós ÂJG, Baptista-Rosas RC, Mercado-Sesma AR. Comparison of prevalence of diabetes complications in Brazilian and Mexican adults: a cross-sectional study. *BMC Endocr Disord*. (2021) 21:48. doi: 10.1186/s12902-021-00711-y

11. Ávila MH, Dommarco JR, Levy TS, Nasu LC, Acosta LMG, Pineda EBG, et al. *Encuesta Nacional de Salud y Nutrición de Medio Camino 2016*. (2016). https://ensanut.insp.mx/encuestas/ensanut2016/informes.php.

12. Levey AS, Stevens LA, Schmid CH, Zhang YL, Castro AF 3rd, Feldman HI, et al. A new equation to estimate glomerular filtration rate. *Ann Intern Med*. (2009) 150 (9):604–12. doi: 10.7326/0003-4819-150-9-200905050-00006

13. Campos-Nonato I, Ramírez-Villalobos M, Flores-Coria A, Valdez A, Monterrubio-Flores E. Prevalence of previously diagnosed diabetes and glycemic control strategies in Mexican adults: ENSANUT-2016. *PloS One*. (2020) 15: e0230752. doi: 10.1371/journal.pone.0230752

14. Martínez-Valverde S, Zepeda-Tello R, Castro-Ríos A, Toledano-Toledano F, Reyes-Morales H, Rodríguez-Matías A, et al. Health needs assessment: chronic kidney disease secondary to type 2 diabetes mellitus in a population without social security, Mexico 2016–2032. *Int J Environ Res Public Health*. (2022) 19:9010. doi: 10.3390/ijerph19159010

15. Colli VA, González-Rocha A, Canales D, Hernández-Alcáraz C, Pedroza A, Pérez-Chan M, et al. Chronic kidney disease risk prediction scores assessment and development in Mexican adult population. *Front Med (Lausanne)*. (2022) 9:903090. doi: 10.3389/fmed.2022.903090

16. Sasako T, Yamauchi T, Ueki K. Intensified multifactorial intervention in patients with type 2 diabetes mellitus. *Diabetes Metab J*. (2023) 47:185–97. doi: 10.4093/dmj.2022.0325

17. Gæde P, Vedel P, Larsen N, Jensen GVH, Parving H-H, Pedersen O. Multifactorial intervention and cardiovascular disease in patients with type 2 diabetes. *N Engl J Med*. (2003) 348:383–93. doi: 10.1056/NEJMoa021778

18. Perkovic V, Jardine MJ, Neal B, Bompoint S, Heerspink HJL, Charytan DM, et al. Canagliflozin and renal outcomes in type 2 diabetes and nephropathy. *N Engl J Med*. (2019) 380:2295–306. doi: 10.1056/NEJMoa1811744

19. Heerspink HJL, Stefánsson BV, Correa-Rotter R, Chertow GM, Greene T, Hou F-F, et al. Dapagliflozin in patients with chronic kidney disease. *N Engl J Med*. (2020) 383:1436–46. doi: 10.1056/NEJMoa2024816

20. Wanner C, Inzucchi SE, Lachin JM, Fitchett D, von Eynatten M, Mattheus M, et al. Empagliflozin and progression of kidney disease in type 2 diabetes. *New Engl J Med*. (2016) 375:323–34. doi: 10.1056/NEJMOA1515920

21. Arnold SV, Tang F, Cooper A, Chen H, Gomes MB, Rathmann W, et al. Global use of SGLT2 inhibitors and GLP-1 receptor agonists in type 2 diabetes. *Results DISCOVER BMC Endocr Disord*. (2022) 22:111. doi: 10.1186/s12902-022-01026-2

22. GBD Chronic Kidney Disease Collaboration. Global, regional, and national burden of chronic kidney disease, 1990-2017: a systematic analysis for the Global Burden of Disease Study 2017. *Lancet*. (2020) 395:709–33. doi: 10.1016/S0140-6736(20)30045-3

23. Institute for Health Metrics and Evaluation. GBD Compare. Available at: http://vizhub.healthdata.org/gbd-compare (Accessed 22 Mar 2023).

24. Jha V, Garcia-Garcia G, Iseki K, Li Z, Naicker S, Plattner B, et al. Chronic kidney disease: global dimension and perspectives. *Lancet*. (2013) 382:260–72. doi: 10.1016/S0140-6736(13)60687-X

25. Gómez Dantés O, Sesma S, Becerril VM, Arreola H. *Sistema de salud de México* Vol. 53. Mexico: salud pública de méxico (2011).

26. Silva-Tinoco R, Cuatecontzi-Xochitiotzi T, de la Torre-Saldaña V, León-García E, Serna-Alvarado J, Orea-Tejeda A, et al. Influence of social determinants, diabetes knowledge, health behaviors, and glycemic control in type 2 diabetes: an analysis from real-world evidence. *BMC Endocr Disord*. (2020) 20:130. doi: 10.1186/s12902-020-00604-6

27. Chan JCN, Lim L-L, Wareham NJ, Shaw JE, Orchard TJ, Zhang P, et al. The Lancet Commission on diabetes: using data to transform diabetes care and patient lives. *Lancet*. (2020) 396:2019–82. doi: 10.1016/S0140-6736(20)32374-6

28. Garcia-Garcia G, Jha V. Chronic kidney disease in disadvantaged populations. *Braz J Med Biol Res*. (2015) 48:377–81. doi: 10.1590/1414-431X20144519

29. Stanifer JW, Von Isenburg M, Chertow GM, Anand S. Chronic kidney disease care models in low- and middle-income countries: a systematic review. *BMJ Glob Health*. (2018) 3:e000728. doi: 10.1136/bmjgh-2018-000728

30. Tamayo y Orozco JA, Santiago Lastiri Quirós H. *La enfermedad renal crónica en México. Hacia una política nacional para enfrentarla*. Mexico: Intersistemas, S.A. de C.V. (2016).

31. Allen A, Iqbal Z, Green-Saxena A, Hurtado M, Hoffman J, Mao Q, et al. Prediction of diabetic kidney disease with machine learning algorithms, upon the initial diagnosis of type 2 diabetes mellitus. *BMJ Open Diabetes Res Care*. (2022) 10:e002560. doi: 10.1136/bmjdrc-2021-002560

32. Chauhan K, Nadkarni GN, Fleming F, McCullough J, He CJ, Quackenbush J, et al. Initial validation of a machine learning-derived prognostic test (KidneyIntelX) integrating biomarkers and electronic health record data to predict longitudinal kidney outcomes. *Kidney360*. (2020) 1:731–9. doi: 10.34067/KID.0002252020

33. Gregorich M, Kammer M, Heinzel A, Böger C, Eckardt K-U, Heerspink HL, et al. Development and validation of a prediction model for future estimated glomerular filtration rate in people with type 2 diabetes and chronic kidney disease. *JAMA Netw Open*. (2023) 6:e231870. doi: 10.1001/jamanetworkopen.2023.1870

34. Hui D, Zhang F, Lu Y, Hao H, Tian S, Fan X, et al. A multifactorial risk score system for the prediction of diabetic kidney disease in patients with type 2 diabetes mellitus. *DMSO*. (2023) 16:385–95. doi: 10.2147/DMSO.S391781

35. Lin C-C, Niu MJ, Li C-I, Liu C-S, Lin C-H, Yang S-Y, et al. Development and validation of a risk prediction model for chronic kidney disease among individuals with type 2 diabetes. *Sci Rep*. (2022) 12:4794. doi: 10.1038/s41598-022-08284-z

36. Gurudas S, Nugawela M, Prevost AT, Sathish T, Mathur R, Rafferty JM, et al. Development and validation of resource-driven risk prediction models for incident chronic kidney disease in type 2 diabetes. *Sci Rep*. (2021) 11:1–11. doi: 10.1038/s41598-021-93096-w

37. Bang H, Vupputuri S, Shoham DA, Klemmer PJ, Falk RJ, Mazumdar M, et al. SCreening for occult REnal disease (SCORED): A simple prediction model for chronic kidney disease. *Arch Internal Med*. (2007) 167:374–81. doi: 10.1001/archinte.167.4.374

38. Liu Xz, Duan M, Huang Hd, Zhang Y, Xiang T, Niu W, et al. Predicting diabetic kidney disease for type 2 diabetes mellitus by machine learning in the real world: a multicenter retrospective study. *Front Endocrinol*. (2023) 14. doi: 10.3389/fendo.2023.1184190

frontiers | Frontiers in Endocrinology

TYPE Original Research
PUBLISHED 25 March 2024
DOI 10.3389/fendo.2024.1282564

OPEN ACCESS

EDITED BY
Federica Mescia,
University of Brescia, Italy

REVIEWED BY
Lannie O'Keefe,
Victoria University, Australia
Angelika Buczyńska,
Medical University of Bialystok, Poland

*CORRESPONDENCE
Felicia A. Hanzu
fhanzu@clinic.cat
Gregori Casals
casals@clinic.cat

RECEIVED 24 August 2023
ACCEPTED 06 March 2024
PUBLISHED 25 March 2024

CITATION
Boswell L, Vega-Beyhart A, Blasco M, Quintana LF, Rodríguez G, Díaz-Catalán D, Vilardell C, Claro M, Mora M, Amor AJ, Casals G and Hanzu FA (2024) Hair cortisol and changes in cortisol dynamics in chronic kidney disease. *Front. Endocrinol.* 15:1282564. doi: 10.3389/fendo.2024.1282564

Hair cortisol and changes in cortisol dynamics in chronic kidney disease

Laura Boswell [1,2,3], Arturo Vega-Beyhart [2], Miquel Blasco [4,5,6], Luis F. Quintana [4,5,6], Gabriela Rodríguez [7], Daniela Díaz-Catalán [2], Carme Vilardell [3], María Claro [1], Mireia Mora [1,2,6,8], Antonio J. Amor [1], Gregori Casals [6,7]* and Felicia A. Hanzu [1,2,6,8]*

[1]Endocrinology and Nutrition Department, Hospital Clínic de Barcelona, Barcelona, Spain, [2]Group of Endocrine Disorders, Institut d'Investigacions Biomèdiques August Pi Sunyer (IDIBAPS), Barcelona, Spain, [3]Endocrinology and Nutrition Department, Althaia University Health Network, Manresa, Spain, [4]Group of Nephrology and Transplantation, Institut d'Investigacions Biomèdiques August Pi Sunyer (IDIBAPS), Barcelona, Spain, [5]Nephrology Department, Hospital Clínic de Barcelona, Barcelona, Spain, [6]Department of Medicine, Faculty of Medicine and Health Sciences, University of Barcelona, Barcelona, Spain, [7]Biochemistry and Molecular Genetics Department, Hospital Clínic de Barcelona, Barcelona, Spain, [8]Centro de Investigación Biomédica en Red de Diabetes y Enfermedades Metabo´ licas Asociadas (CIBERDEM), Carlos III Health Institute, Madrid, Spain

Objective: We compared hair cortisol (HC) with classic tests of the hypothalamic–pituitary–adrenal (HPA) axis in chronic kidney disease (CKD) and assessed its association with kidney and cardiometabolic status.

Design and methods: A cross-sectional study of 48 patients with CKD stages I–IV, matched by age, sex, and BMI with 24 healthy controls (CTR) was performed. Metabolic comorbidities, body composition, and HPA axis function were studied.

Results: A total of 72 subjects (age 52.9 ± 12.2 years, 50% women, BMI 26.2 ± 4.1 kg/m^2) were included. Metabolic syndrome features (hypertension, dyslipidaemia, glucose, HOMA-IR, triglycerides, waist circumference) and 24-h urinary proteins increased progressively with worsening kidney function ($p < 0.05$ for all). Reduced cortisol suppression after 1-mg dexamethasone suppression (DST) ($p < 0.001$), a higher noon (12:00 h pm) salivary cortisol ($p = 0.042$), and salivary cortisol AUC ($p = 0.008$) were seen in CKD. 24-h urinary-free cortisol (24-h UFC) decreased in CKD stages III–IV compared with I–II ($p < 0.001$); higher midnight salivary cortisol ($p = 0.015$) and lower suppressibility after 1-mg DST were observed with declining kidney function ($p < 0.001$). Cortisol-after-DST cortisol was >2 mcg/dL in 23% of CKD patients (12.5% in stage III and 56.3% in stage IV); 45% of them had cortisol >2 mcg/dL after low-dose 2-day DST, all in stage IV ($p < 0.001$ for all). Cortisol-after-DST was lineally inversely correlated with eGFR ($p < 0.001$). Cortisol-after-DST (OR 14.9, 95% CI 1.7–103, $p = 0.015$) and glucose (OR 1.3, 95% CI 1.1–1.5, $p = 0.003$) were independently associated with eGFR <30 mL/min/m^2). HC was independently correlated with visceral adipose tissue (VAT) ($p = 0.016$). Cortisol-after-DST ($p = 0.032$) and VAT ($p < 0.001$) were independently correlated with BMI.

Conclusion: Cortisol-after-DST and salivary cortisol rhythm present progressive alterations in CKD patients. Changes in cortisol excretion and HPA dynamics in CKD are not accompanied by significant changes in long-term exposure to cortisol evaluated by HC. The clinical significance and pathophysiological mechanisms explaining the associations between HPA parameters, body composition, and kidney damage warrant further study.

KEYWORDS

hair cortisol, salivary cortisol, dexamethasone suppression test, chronic kidney disease, visceral adipose tissue, cardiovascular risk

1 Introduction

Chronic kidney disease (CKD) is a condition affecting a substantial proportion of the general population; the overall prevalence of CKD stages III–V according to the Kidney Disease Improving Global Outcomes (KDIGO) guidelines ranges from 2% to 17%, with estimates of higher prevalence when including patients in earlier stages (abnormal urinary albumin excretion with preserved estimated glomerular filtration rate [eGFR]) (1). This condition is comorbid with diabetes, hypertension, and other metabolic complications and dramatically increases the risk of cardiovascular disease and premature mortality (2). Although a few studies have described changes in the hypothalamic–pituitary–adrenal (HPA) axis in the presence of CKD, evidence is scarce and previous studies have limitations: they are series with a low number of participants, two only include patients in haemodialysis, and all only performed a partial evaluation of the HPA axis (3–6).

Thus, the effect of CKD on the HPA axis and its mechanisms and possible consequences remain unknown. HPA axis evaluation is complex, and standard biochemical tests have limitations and methodologic difficulties (7). Also, they all have in common the measurement of cortisol in the acute (serum, saliva) or in a very short (24-h urine) timeframe, reflecting acute changes of the HPA axis but not mid- or long-term exposure (8, 9). Considering the changes described above and the unreliability of 24-h-urine cortisol when kidney function is impaired, HPA functional disturbances in CKD present a challenge for the differential diagnosis of pseudo-Cushing states and Cushing's syndrome (CS) in this setting. Hence, new diagnostic strategies are required.

In recent years, the measurement of hair cortisol (HC) concentrations has emerged as a reliable strategy for quantifying long-term exposure to cortisol. As hair in the area of the posterior vertex grows at a relatively constant speed (1 cm/month), exposure to cortisol during the previous months can be estimated by measuring cortisol concentrations in this area (10, 11). Several studies have displayed evidence of its validity, test and retest reliability, and correlation with classical biochemical tests of the HPA axis (12, 13). It is a validated measure in the study of CS, especially in cyclic CS (14–16). There is also evidence that HC increases in acute and chronic stress situations (9), and it is widely used in psychopathology (17). HC is also predictive of metabolic syndrome (18), type 2 diabetes (T2D) and cardiovascular disease (19). Higher levels of HC have been described in some pseudo-Cushing states (alcoholism, obesity, depression). However, no studies have evaluated HC in CKD.

Against this background, we aimed to study HC in the setting of CKD, compare it with the classical biochemical tests of the HPA axis, and investigate its association with kidney function outcomes and cardiometabolic status.

Abbreviations: 11β-HSD-2, 11β-hydroxysteroid-dehydrogenase type 2; 24-h UFC, 24-h urinary free cortisol; ACTH, adrenocorticotropic hormone; ANOVA, analysis of variance; AUC, are under the curve; BMI, body mass index; BP, blood pressure; CBG, cortisol-binding-globulin; CI, confidence interval; CKD, chronic kidney disease; CKD-EPI, Chronic Kidney Disease Epidemiology Collaboration; CS, Cushing's syndrome; CVD, cardiovascular disease; DEXA, dual-energy X-ray absorptiometry; DST, dexamethasone suppression test; eGFR, estimated glomerular filtration rate; ELISA, enzyme-linked immunosorbent assay; HbA_{1c}, glycated haemoglobin; HC, hair cortisol; HDL-c, high-density lipoprotein cholesterol; HOMA-IR, homeostatic model assessment-insulin resistance; HPA, hypothalamus–pituitary–adrenal; hs-CRP, high-sensitivity C-reactive protein; IQR, interquartile range; KDIGO, Kidney Disease Improving Global Outcomes; LDL-c, low-density lipoprotein cholesterol; OR, odds ratio; T2D, type 2 diabetes; VAT, visceral adipose tissue; WC, waist circumference; WHR, waist-to-hip ratio.

2 Methods

2.1 Study design and participants

A cross-sectional, controlled, single-centre study was performed. Patients had to fulfil criteria for chronic kidney disease (CKD): decreased eGFR through the Chronic Kidney Disease Epidemiology Collaboration [CKD-EPI] equation and/or kidney damage as defined by structural or functional abnormalities other than decreased eGFR (p. ex. albuminuria ≥30 mg/g, structural abnormalities detected by imaging) for >3 months according to the

KDIGO guidelines (20). Patients with CKD stages I–II (eGFR >60 mL/min/1.73 m^2), stage III (eGFR 30–60 mL/min/1.73 m^2), and stage IV (eGFR 15–30 mL/min/1.73 m^2) CKD with preserved diuresis were prospectively included and matched with healthy controls by age, sex, and body mass index (BMI). Controls had to fulfil both criteria of normal kidney function: eGFR >60 mL/min/1.73 m^2) and absence of kidney damage markers. The age ranges for CKD patients and healthy controls were similar: 54 (45–61.3) years (median (interquartile range [IQR]) and 23.4–77.4 years (minimum and maximum) for CKD patients and 54.6 (47.9–63.8) years (median [IQR]) and 27.2–69.2 years (minimum and maximum) for control subjects.

CKD subjects were divided according to stages (mild: stages I–II, moderate: III and severe: IV) to be able to describe the differences in HPA axis physiology according to CKD severity. A control group with preserved kidney function and no structural kidney damage was included for a normality reference.

All subjects had preserved diuresis (defined as absence of oliguria or anuria). Subjects with CKD all had a urinary output >1,000 mL/24 h and controls >800 mL/24 h.

Patients were prospectively included from the cohort of CKD patients who visited the Nephrology Department of the Hospital Clínic de Barcelona between December 2019 and June 2022. Controls were selected from among hospital workers or their acquaintances, CKD patients' spouses, and volunteers. Controls were initially selected based on medical records and underwent the same screening and inclusion/exclusion criteria as CKD subjects to ensure they had no kidney damage whatsoever (eGFR >60 mL/min/1.73 m^2) and an absence of kidney damage markers).

The exclusion criteria were active glucocorticoid, immunosuppressive or anti-inflammatory treatment, diabetes mellitus, morbid obesity (BMI ≥40 kg/m^2), drugs interfering with the HPA axis, active malignancy, active Cushing's syndrome, or pseudo-Cushing states such as depression or high-risk alcohol consumption. The rationale behind these exclusion criteria was to rule out any drug interference or physiological or pathophysiological alteration of the HPA axis unrelated to CKD.

The study protocol was conducted according to the principles of the Declaration of Helsinki and approved by the Institution's Research Ethics Committee (reference number: HCB/2019/0845). All participants provided written informed consent.

2.2 Study outline

The subjects underwent clinical and analytical assessment of metabolic comorbidities, body composition analysis using dual-energy X-ray absorptiometry (DEXA), and a thorough evaluation of the HPA axis. On the first appointment, all subjects (both CKD patients and controls) were screened for inclusion and exclusion criteria and signed the informed consent. Then, a thorough clinical and body composition evaluation was performed and the hair sample was collected. Finally, the instructions and material to collect the saliva and 24-h urine samples were handed over. On the second appointment, the subjects had an early-morning blood test and handed over the samples. On the last appointment, the dexamethasone suppression test was performed. The time interval between the first and second appointments was 4 (2–14) days, and that between the second and last appointments was 10 (4–21) days. The study outline is shown in Figure 1.

2.2.1 Clinical and body composition evaluation

At inclusion, all subjects underwent a complete clinical evaluation. Age, sex, smoking status, metabolic comorbidities, and current medical treatment were recorded for all participants. CKD stage, aetiology, duration, and previous treatments were recorded for CKD patients. Both the patients and controls were screened for pseudo-Cushing states. Data regarding hair colour, treatment, and frequency of washing were also recorded. Metabolic comorbidities were defined as follows: hypertension was defined as repeated clinical systolic blood pressure (BP) ≥140 mmHg and/or diastolic BP ≥90 mmHg or active treatment with antihypertensive drugs; dyslipidaemia was defined as LDL-cholesterol (LDL-c) >160 mg/dL, low high-density lipoprotein cholesterol (HDL-c) (<40 mg/dL in men and <45 mg/dL in women), triglycerides ≥150 mg/dL, or active treatment with lipid-lowering drugs (statins, ezetimibe, or fibrates); and prediabetes was defined as fasting plasma glucose 100 mg/dL to 126 mg/dL or HbA_{1c} 5.7% to 6.4% and obesity as a BMI ≥30 kg/m^2). Anthropometric parameters (weight, height, BMI, blood pressure, and waist and hip circumferences) were obtained by physical examination as previously described (21–23).

Body composition (quantification and distribution of fat mass) was studied using DEXA, an indirect and non-invasive technique (*iDEXA, General Electrics*). DEXA was used to measure total fat

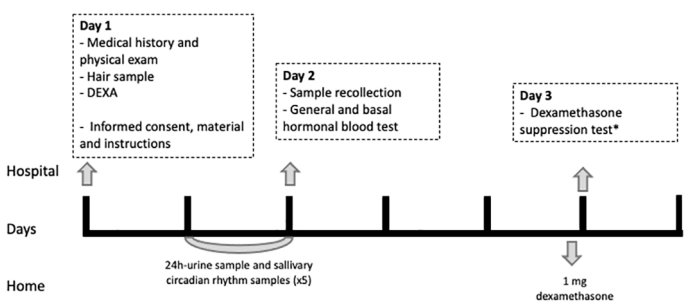

FIGURE 1
Study outline. DEXA, dual-energy X-ray absorptiometry (DEXA). *Those participants with a cortisol after 1-mg DST >2 mcg/dL underwent a low-dose 2-day DST (2 mg/6h).

mass, fat distribution (proportion of android and gynoid fat), subcutaneous adipose tissue, and visceral adipose tissue (VAT).

2.2.2 HPA axis evaluation

2.2.2.1 Chronic exposition to cortisol: hair cortisol concentration

HC was chosen because it is the only available test able to quantify cortisol levels in the mid-long term. Hair samples were processed and analysed for cortisol following the method previously described by Sauvé et al. (24) In the first visit, a hair sample of >1-cm length from the posterior vertex was obtained. As hair in this area grows at a relatively constant speed (1 cm/month), cortisol exposure during previous months can be estimated (10, 11). Once the sample had been cut with metal scissors, as close as possible to the scalp, a thread was tied to the end to signal the external tip. The samples were kept in an envelope, protected from light and at room temperature until the analysis. At the moment of evaluation, they were placed in a container and washed twice with 10 mL isopropanol to eliminate possible contaminants. The proximal 1 cm was cut and analysed as representative of the mean cortisol value in the last month. Prior to the cortisol extraction, the hair was cut into small fragments using surgical scissors and weighed to obtain the hair mass (minimum 25 mg). Cortisol extraction was performed by adding 1 mL of methanol to the glass vial where the hair was weighed and incubated overnight with slow shaking. Then, the supernatant was transferred to an assay tube and evaporated with nitrogen. Finally, the remnant was resuspended with the diluent of the cortisol assay and agitated until complete dissolution. Cortisol was measured by ELISA (Salimetrics LLC, State College, PA, USA). The weighing, extraction, and analysis of the same hair sample collection were performed in duplicate when a sufficient sample was available and the mean coefficient of variation of duplicates was 8%. Interassay coefficient of variation was 7%.

2.2.2.2 Cortisol circadian rhythm and overall cortisol secretion analysis/study

Saliva samples were collected at regular intervals during the day to assess cortisol circadian rhythm and to indirectly estimate cumulative cortisol exposure during the day. Furthermore, evening and late-night cortisol measurements are more appropriate to detect high cortisol exposure when a mild corticoid excess is suspected. Moreover, salivary cortisol measures free biologically active cortisol, which is less altered by binding protein levels than serum cortisol. 24-h UFC was measured to estimate the cortisol excreted in a 24-h period. Basal cortisol and ACTH were measured to establish the cortisol level at its diurnal peak and the central activity of the HPA axis, respectively (25). Cortisol-binding globulin (CBG) and albumin (see section 2.2.3) were measured to assess levels of circulating cortisol-binding proteins.

The subjects collected a 24-h urine sample and five saliva samples (8:00 h am, 12:00 h pm, 4:00 h pm, 8:00 h pm, 12:00 am) from the day before. During the first visit, they systematically received instructions for adequate sample collections to minimise variability in sample collection. If instructions had not been carefully followed, subjects were reinstructed and sample collection was performed once again. Furthermore, adequate 24-h urine recollection was verified through 24-h urinary creatinine levels.

Serum and EDTA plasma samples were obtained in the early morning (8:00 h am) after a 12-h fast to measure basal cortisol and ACTH, respectively, as well as metabolic parameters (see below).

The samples were kept at −80°C until analysis. Hormonal analyses were performed in the Hormonal Laboratory, applying the standard procedures, with the following methods: 24-h UFC by chemiluminescence immunoassay (Liaison; DiaSorin, Saluggia, Italy) after extraction with dichloromethane; serum cortisol was measured by chemiluminescence immunoassay (Atellica IM 1600, Siemens Healthineers, Tarrytown, NY, USA); ACTH was measured using chemiluminescence immunoassay (IMMULITE 2000; Siemens Healthineers, Tarrytown, NY, USA); CBG was measured by radioimmunoassay (DiaSource, Louvain-la-Neuve, Belgium); and salivary cortisol was measured with a specifically validated ELISA (Salimetrics LLC, State College, PA, USA).

2.2.2.3 Dynamic study of the HPA axis: dexamethasone suppression test

The DST was performed to study the HPA axis negative feedback mechanism. We expected a certain degree of resistance after the DST in advancing CKD and an adequate suppression after a low-dose 2-day-DST in all subjects (5). Dexamethasone at the doses given to perform the functional tests has rarely any side effects. Nevertheless, all subjects were questioned for allergy to the active principle in the first evaluation.

The cortisol from the first blood test was used as the basal cortisol. On the first visit, subjects were given a 1-mg dexamethasone pill and instructions on when to take it. The subjects took the dexamethasone pill at 11:00 h pm the night before the second blood test and were instructed to follow a 12-h fast. The following morning (8:00–9:00 h am), a serum sample to measure (post-DST) cortisol was obtained.

Those subjects with cortisol >2 mcg/dL after the DST went through a low-dose 2-day-DST: a blood test for basal (8:00–9:00 h am) cortisol was extracted on the first day, the subject took 0.5 mg every 6 h for 48 h, and on the third day, a blood test for post 2-day-DST cortisol was performed (8:00–9:00 h am).

2.2.3 Metabolic and systemic inflammation evaluation

The basal blood and 24-h urine samples were analysed in the local laboratory using standardised assays. Specifically, glucose, creatinine, sodium, potassium, calcium, magnesium, total cholesterol, HDL-c, triglycerides, and high-sensitive C-reactive protein (hs-CRP) were measured in serum on an Atellica CH930 chemistry analyser (Siemens Healthcare Diagnostics). LDL-c was calculated using the Friedewald formula. Serum and 24-h urinary creatinine, proteins, and albumin were measured on an Atellica CH930 chemistry analyser. Insulin was measured by chemiluminescence immunoassay on an Atellica IM1 600 analyser, and homeostatic model assessment-insulin resistance (HOMA-IR) was calculated using the following formula: glucose

(mmol L^{-1}) × insulin (mIU L^{-1})/22.5. HbA_{1C} was measured on a Tosoh G8 HPLC Analyzer. Leukocyte formula and blood count were measured on an ADVIA 120 haematology system (Siemens Healthcare Diagnostics).

2.3 Statistical analyses

Data are presented as median and 25th and 75th percentiles (IQR), mean ± SD or number (percentage). Normal distribution of continuous variables was evaluated with the Kolmogorov–Smirnov test. Between-group differences in clinical, anthropometric, and laboratory variables were assessed using unpaired Student's t-test, Mann–Whitney test, and chi-square tests as appropriate, for parametric, non-parametric, and categorical values, respectively. Multiple-group analyses were performed using ANOVA or Kruskal–Wallis as appropriate. Bonferroni and Jonckheere–Terpstra were performed to test for multiple comparisons after one-way ANOVA and Kruskal–Wallis, respectively. To examine linear trends, the Mantel–Haenszel test for categorical variables and the linear contrast analysis for continuous variables were used.

Univariate linear regression analyses were performed to evaluate the association of hair cortisol and cortisol after DST with kidney function and cardiometabolic variables (age, waist-to-hip ratio (WHR), eGFR, glucose, and VAT volume). Variables with a significant association were then included in stepwise multiple linear regression models to identify independent parameters related to hair cortisol and cortisol after DST. Multivariate linear regression models were adjusted for age, sex, BMI, and clinical data or conventional lab parameters that resulted in statistical significance when performing the univariate correlation tests: Particularly, the first model included eGFR, cortisol after DST, age, BMI, and smoking; the second model included cortisol after DST, glucose, eGFR, age, BMI, hypertension, CKD duration, LDL-c, and hs-PCR, and the third model included HC, VAT volume, age, BMI, smoking, sex, and eGFR.

Significance level was defined as a p-value <0.05. IBM SPSS Statistics 23.0 (SPSS, Inc; Chicago, Illinois) was used to perform the statistical analysis.

3 Results

3.1 Study population characteristics and cardiometabolic status according to CKD stage

A total of 72 subjects were included: 48 patients with CKD (16 in stages I–II, 16 in stage III, and 16 in stage IV) and 24 paired controls; age 52.9 ± 12.2 years (minimum: 23.4 years, maximum: 77.4 years), 50% women, and BMI 26.2 ± 4.1 kg/m^2 (minimum: 19.3 kg/m^2, maximum: 37.4 kg/m^2).

The aetiology of CKD was the following: 27 (56.3%) polycystic kidney disease, 7 (14.6%) IgA nephropathy, 4 (8.3%) hypertensive nephroangiosclerosis, 4 (8.3%) focal segmental glomerulosclerosis, and 6 (12.5%) other causes. There were no subjects with diabetic CKD or glomerulopathies requiring corticoid treatment (such as lupic nephropathy) in this study, as diabetes and glucocorticoid treatment were both exclusion criteria. Hence, only CKD aetiologies which were compatible (either because of their physiopathology or their treatment) with the study aims and which would not hamper the HPA axis measurements were included. In the general population, diabetic CKD is the main cause of CKD (approximately 30%–50%) and glomerulopathies are infrequent (26).

In CKD patients, a stepped increase in hypertension and dyslipidaemia prevalence, lipid-lowering therapy, and increasing levels of glucose, insulin, HOMA-IR, triglycerides, and 24-h urinary protein excretion were observed with worsening kidney function ($p < 0.05$ for all) whereas no changes were seen in other lipid parameters. Lipid profiles excluding triglycerides were similar despite an increasing prevalence of dyslipidaemia. CKD subjects were much more frequently on lipid-lowering drugs (75% of CKD subjects and 33.3% controls, $p = 0.027$). Moreover, not only were there more subjects receiving these drugs in more advanced kidney stages (p for trend <0.001) but also the proportion of subjects with dyslipidaemia receiving therapy was higher (p for trend = 0.003). No differences were observed regarding hs-CRP, all subjects had low levels.

Moreover, systolic and diastolic BP increased with advancing CKD stage ($p < 0.05$). BP was clinically significantly higher in the stage III and IV groups, which is consistent with a prevalence of hypertension approximately 90% in these subjects.

Visceral fat was assessed through clinical surrogates (such as waist circumference [WC] and WHR) and measured with DEXA. An increased WC was observed in stage III CKD subjects ($p = 0.007$) compared with controls and those in stages I–II; a non-significant trend towards increasing WC with advancing CKD stage was also seen ($p = 0.059$). WHR was high in all groups but significantly higher in stage III ($p = 0.030$). A trend to an increased VAT volume and mass measured with DEXA ($p = 0.073$) was observed with advancing CKD stage.

A significative linear trend for cardiovascular disease (CVD) ($p = 0.042$) was also observed: Three subjects had CVD, all in CKD stages III–IV. Cardiometabolic factors according to CKD stages and controls are presented in Table 1.

3.2 Hair cortisol determinants

Hair cortisol was positively correlated with age (β 0.835, standardised-β 0.279, $p = 0.018$), but this association was lost when adjusting for confounders. No differences in hair cortisol were seen according to sex ($p = 0.287$), smoker status ($p = 0.979$), or smoking index ($p = 0.420$). Hair cortisol was correlated with alcohol consumption (measured as standard drinks, 10 g of alcohol) (β 1.812, standardised-β 0.248, $p = 0.036$). Nevertheless, this finding was not clinically relevant as alcohol consumption was low in all subjects. None had a high-risk alcohol consumption as this was an exclusion criterion of the study. Hair cortisol was unrelated to the frequency of hair washing ($p = 0.579$), hair colour ($p = 0.909$), or hair treatment ($p = 0.346$).

10.3389/fendo.2024.1282564

TABLE 1 Study population characteristics and metabolic changes by CKD stage.

	Controls (n = 24)	Stages I–II (n = 16)	Stage III (n = 16)	Stage IV (n = 16)	p	p for trend
Age (years)	52.7 ± 12.9	47.5 ± 13	53.6 ± 8.8	57.8 ± 11.8	0.121	0.145
Sex (women)	12 (50)	9 (56.3)	8 (50)	7 (43.8)	0.919	0.685
BMI (kg/m^2)	25.6 ± 4.6	24.9 ± 3.2	28.3 ± 4.1	26.2 ± 11.8	0.101	0.213
Summary of key findings						
Hypertension	8 (33.3)	8 (50)	14 (87.5)	15 (93.8)	<0.001	<0.001
Dyslipidaemia	9 (37.5)	3 (18.8)	8 (50)	12 (75)	0.012	0.004
Lipid-lowering therapy* Proportion of the total Proportion of subjects with dyslipidaemia	3 (12.5) 3 (33)	1 (6.3) 1 (33.3)	6 (37.5) 6 (75)	11 (68.8) 11 (91.7)	<0.001 0.024	<0.001 0.003
Glucose (mg/dL)	85 (77-92)	82 (77-87)	82 (78-86)	92 (84-99)	0.027	0.108
Insulin (mU/L)	7.3 (4.9-8.5)	7.3 (4.8-8.6)	10.5 (6.6-18.9)	11.4 (7.7-13.5)	0.004	0.002
HOMA-IR	1.45 (0.92-2.11)	1.48 (0.95-1.85)	2.12 (1.31-4.31)	2.38 (1.6-3.34)	0.007	0.003
Triglycerides (mg/dL)	86 (72-110)	89 (73-109)	111 (88-164)	135 (102-210)	0.005	0.001
Albuminuria (mg/24 h)	0 (0-4)	20 (8-43)	64 (16-216)	520 (38-1066)	<0.001	<0.001
Kidney function						
eGFR (mL/min/m^2)	90 (85-90)	90 (77-90)	37 (34-51)	24 (20-27)	<0.001	<0.001
Diuresis volume (mL/24 h)	1750 (1200-2100)	1900 (1500-2475)	2000 (1725-2275)	2363 (1919-3225)	0.029	<0.001
Urinary creatinine (mg/24 h)	1187 ± 301	1223 ± 461	1163 ± 236	1197 ± 329	0.993	0.001
Metabolic assessment						
Clinical comorbidities						
Active smokers	0 (0)	4 (25)	3 (18.8)	1 (6.3)	0.059	0.452
Number of antihypertensive drugs	1 (1-1.8)	1.5 (1-2)	2 (1-2.3)	1 (1-2)	0.480	0.345
Family history of premature CVD	4 (16.7)	1 (6.3)	2 (12.5)	3 (18.8)	0.735	0.845
CVD	0 (0)	0 (0)	1 (6.3)	2 (12.5)	0.195	0.042
SBP (mmHg)	123 ± 18	127 ± 17	131 ± 11	140 ± 16	0.016	0.002
DBP (mmHg)	79 ± 10	83 ± 6	84 ± 10	85 ± 12	0.194	0.039
Waist circumference (cm)	95 ± 15	94 ± 5	106.5 ± 9	98 ± 9	0.007	0.059
Waist-to-hip ratio	0.97 (0.89-0.99)	0.94 (0.90-0.97)	0.99 (0.95-1.04)	0.97 (0.93-1-.02)	0.030	0.146
Laboratory measures						
HbA1c (%)	5.5 ± 0.4	5.4 ± 0.35	5.4 ± 0.37	5.7 ± 0.46	0.088	0.149
Total cholesterol (mg/dL)	199 ± 36	189 ± 35	198 ± 42	199 ± 41	0.848	0.897
LDL-c (mg/dL)	128 ± 28	116 ± 29	116 ± 31	121 ± 34	0.531	0.387
HDL-c (mg/dL)	53 ± 13	56 ± 11	56 ± 18	49 ± 13	0.472	0.487
hs-CRP (mg/dL)	0.12 (0.04-0.28)	0.11 (0.04-0.30)	0.27 (0.09-0.64)	0.14 (0.07-0.39)	0.285	0.217
Albumin (g/L)	45 (44-46)	44 (43-45)	45 (44-48)	44.5 (42-47)	0.225	0.862
Body composition**						
Total fat mass (%)	32.7 ± 6.5	32.1 ± 10.3	36.5 ± 5.8	33.3 ± 6.1	0.306	0.406

(Continued)

TABLE 1 Continued

	Controls (n = 24)	Stages I–II (n = 16)	Stage III (n = 16)	Stage IV (n = 16)	p	p for trend
Body composition**						
VAT (cm^3)	979.5 (132.5-2222)	663.5 (203-841)	978 (648-1648)	1322 (722-1935)	0.073	0.154
VAT (g)	924 (124.8-2095.8)	626.5 (191.3-794.3)	923 (612-1554)	1248 (681-1827)	0.074	0.157

Values expressed as mean ± SD, median (interquartile range) or number (percentage). p-value according to ANOVA or Kruskal–Wallis are represented.
*Active treatment with statins or ezetimibe.
**Measured with dual-energy X-ray absorptiometry (DEXA).
BMI, body mass index; CVD, cardiovascular disease; DBP, diastolic blood pressure; eGFR, estimated glomerular filtration rate; HDL-c, high-density lipoprotein cholesterol; HOMA-IR, homeostatic model assessment-insulin resistance; LDL-c, low-density lipoprotein cholesterol; SBP, systolic blood pressure; TC, total cholesterol; hs-PCR, high-sensitivity C-reactive protein; VAT, visceral adipose tissue.

3.3 Hypothalamic–pituitary–adrenal axis study

First, changes in the HPA axis of the whole CKD population compared with controls were analysed. A reduced cortisol suppression after DST (1.3 vs. 0.9 μg/dL, p < 0.001), a higher noon (12:00 h pm) salivary cortisol (p = 0.042), and a higher salivary cortisol area under the curve (AUC) (p = 0.008) were seen in patients with CKD compared with controls.

A trend to a lower 24 h UFC was also observed. Hair cortisol, ACTH, cortisol, CBG, and the remaining salivary cortisol rhythm points remained unchanged.

Then, the HPA axis was studied according to CKD severity: 24-h UFC was decreased in stages III–IV compared with CKD stages I–II and controls (p < 0.001), despite an increased 24-h urinary volume.

Higher late-night (12:00 h am) salivary cortisol levels (p = 0.015) and a significative linear trend for salivary cortisol AUC (p = 0.006) were observed with declining kidney function (Figure 2).

A lower suppressibility after a 1-mg DST was observed with declining kidney function (p < 0.001). Among all, 11 (23%) patients with CKD had post-DST cortisol of >2 mcg/dL (none in controls or stages I–II, 2 [12.5%] in CKD stage III, and 9 [56.3%] in the stage IV group, p < 0.001). To further assess resistance to dexamethasone suppression, these subjects underwent a low-dose 2-day DST (2 mg/6 h): 5 (45.5%) still had an unsuppressed cortisol (>1.8 mcg/dL) after the test, all in stage IV. Namely, the two subjects in stage III with an increased cortisol after DST suppressed correctly after a 2-day DST whereas only 4/9 (44.4%) did so in stage IV (p < 0.001 for all) (Figure 3). Thus, negative feedback regulation is progressively impaired with declining kidney function.

Post-DST cortisol was correlated with 08:00 pm salivary cortisol in controls (r = 0.533, p = 0.016) and in patients with CKD stages III (r = 0.469, p = 0.046) and IV (r = 0.811, p < 0.001). However, no correlation was found with late-night (12:00 h am) salivary cortisol in any group. No differences were observed in HC, ACTH, basal serum cortisol, CBG, or salivary cortisol in the remaining time frames (Table 2).

In the whole cohort, eGFR held an independent inverse association with cortisol after DST adjusted for confounders (age, BMI, smoking), which explained 48% of the variance in the serum levels in patients (Table 3). Correlation factors of the remaining clinical and biochemical variables and cortisol after DST can be found on Supplementary Table 2.

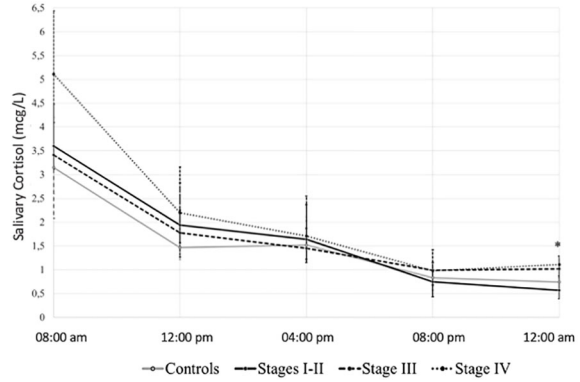

FIGURE 2
Salivary cortisol 24-h rhythm according to study group. *p value <0.05. Salivary cortisol (mcg/L) in median (interquartile range).

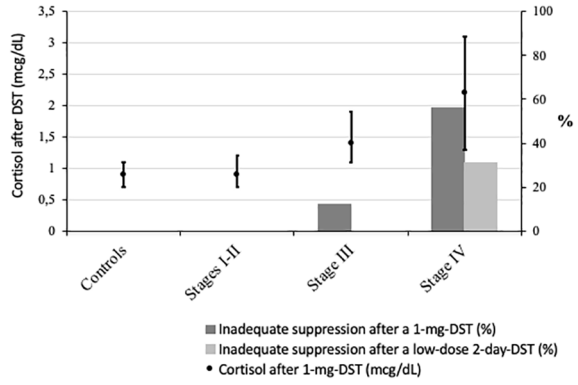

FIGURE 3
Cortisol after dexamethasone suppression test (DST) across study groups. points: cortisol after 1-mg DST (mcg/dL) in median (interquartile range); dark bars: % of subjects with cortisol after 1-mg DST >2 μg/dL; light bars: % of subjects with cortisol after a low-dose 2-day DST (2 mg/6h) >1.8 μg/dL. p value for all <0.001.

TABLE 2 HPA axis changes according to CKD stage.

	Controls (n = 24)	Stages I–II (n = 16)	Stage III (n = 16)	Stage IV (n = 16)	p	p for trend
Chronic exposure to cortisol						
Hair cortisol (pg/mg)	3.95 (2.40-5.08)	2.90 (2.13-3.83)	4 (2.88-5.38)	3.55 (2.78-4.75)	0.263	0.463
Cortisol circadian rhythm						
ACTH (pg/mL)	20 (12.3-28)	21 (18.3-25.6)	23.5 (17.5-29.3)	25 (15-28)	0.525	0.188
Cortisol (mcg/dL)	16 ± 4	18.4 ± 3.5	16.2 ± 4.7	17.3 ± 5.2	0.342	0.350
CBG (mcg/mL)	52.3 ± 9.8	49.3 ± 7	53.3 ± 11.1	52.5 ± 6.9	0.601	0.144
24 h UFC (mcg/24 h)	54.4 (34.8-74.4)	54 (42.3-83.4)	31.8 (24.2-43.3)	30.8 (21-46)	<0.001	<0.001
Diuresis volume (mL/24 h)	1750 (1200-2100)	1900 (1500-2475)	2000 (1725-2275)	2363 (1919-3225)	0.029	<0.001
8:00 am-salivary cortisol (mcg/L)	3.15 (2.59-4.20)	3.60 (3.17-4.48)	3.41 (2.08-4.09)	5.11 (3.11-6.44)	0.130	0.092
12:00 pm-salivary cortisol (mcg/L)	1.47 (1.21-1.96)	1.94 (1.57-2.25)	1.78 (1.47-2.83)	2.20 (1.27-3.16)	0.235	0.070
4:00 pm-salivary cortisol (mcg/L)	1.52 (1.22-2.03)	1.64 (1.15-2.37)	1.45 (1.22-1.87)	1.71 (1.22-2.55)	0.848	0.515
8:00 pm-salivary cortisol (mcg/L)	0.83 (0.57-0.99)	0.75 (0.43-0.99)	0.99 (0.73-1.15)	0.98 (0.68-1.42)	0.131	0.073
12:00 am-salivary cortisol (mcg/L)	0.74 (0.58-0.83)	0.57 (0.39-0.87)	1.02 (0.74-1.29)	1.11 (0.74-1.29)	0.015	0.014
Salivary cortisol AUC (mcg*24h/L)	37.98 ± 8.16	42.19 ± 14.73	44.54 ± 18.55	50.88 ± 15.38	0.138	0.006
Dynamic study of the HPA axis						
Cortisol after DST (µg/dL)	0.9 (0.7-1.1)	0.9 (0.7-1.2)	1.4 (1.1-1.9)	2.2 (1.3-3.1)	<0.001	<0.001
Cortisol after DST >1.8 µg/dL	0 (0)	0 (0)	4 (25)	9 (56.3)	<0.001	<0.001
Cortisol after DST >2 µg/dL	0 (0)	0 (0)	2 (12.5)*	9 (56.3)**	<0.001	<0.001

Values expressed as mean ± SD, median (interquartile range) or number (percentage). p-value according to ANOVA or Kruskal–Wallis are represented.
*100% had a normal response (cortisol ≤1.8 µg/dL) after a low-dose 2-day DST (2 mg/6 h).
**45% had a normal response to a low-dose 2-day DST (2 mg/6 h).
ACTH, adrenocorticotropic hormone; AUC, area under curve; CKD, chronic kidney disease; CBG, cortisol-binding-globulin; DST, 1-mg dexamethasone suppression test; HPA, hypothalamus–pituitary–adrenal; UFC, urinary-free cortisol.

Cortisol after DST (OR 14.9, 95% CI 1.7–130, p = 0.015) and glucose (OR 1.3, 95% CI 1.1–1.5, p = 0.003) were also independently associated with an eGFR <30 mL/min/m^2, adjusted for confounders (age, BMI, hypertension, CKD duration, LDL-c, and hs-PCR) (Supplementary Figure 1).

3.4 Cardiometabolic and body composition status according to HPA changes

In unadjusted regression analyses, HC was linearly correlated with VAT volume (β 78.2, standardised-β 0.316, p = 0.007), WHR (β 13.8, standardised-β 0.258, p = 0.029), and age (see 3.3). Cortisol after DST was correlated with age (β 4.831, standardised-β 0.351, p = 0.004), WHR (β 3.6, standardised-β 0.298, p = 0.014), and glucose (β 3.034, standardised-β 0.266, p = 0.030) but not with VAT volume. Neither HC nor cortisol after DST correlated with BMI.

In multivariate regression analyses, HC (β 54.488, standardised-β 0.22, p = 0.015) was independently correlated with VAT volume, adjusted for age, BMI, smoking, sex, and eGFR (Supplementary Table 1).

Finally, in unadjusted regression analyses, a positive correlation between inflammation markers (neutrophil count and hs-PCR) and ACTH as well as between neutrophils and noon-salivary-cortisol was found, but the relation was lost when adjusted for confounders (data not shown).

4 Discussion

This is the first study to perform a thorough evaluation of the HPA axis including HC concentrations in subjects with CKD stages I to IV. We describe for the first time that chronic exposure to cortisol (through HC concentrations) remains unchanged in CKD, in contrast with changes in the cortisol circadian rhythm and dynamic study of the HPA axis. We describe a resistance to dexamethasone suppression and higher noon-salivary cortisol in CKD subjects compared with healthy controls, as well as increasing midnight-salivary cortisol and cortisol after DST and decreasing 24-h UFC as the kidney function worsens. Additionally, this is the first study to describe an independent association of HC with VAT

TABLE 3 Independent parameters associated with serum cortisol levels after DST.

Parameter	Pearson correlation	Degree of association with cortisol after DST of effect				
		$R^{2\%}$	β	95% CI		p value
				LL	UL	
eGFR (CKD-EPI)	-0.661*	48.1	-0.210	-0.310	-0.011	<0.001
Smoking*	0.566*	14.0	0.020	-0.007	-0.033	0.004
Sex	-0.210	–	-0.466	-1.157	0.226	0.179
BMI	0.021	–	-0.014	-0.041	0.013	0.297
Age	-0.202		-0.147	-0.498	0.009	0.093

*p value <0.05 in univariate testing. R^2% indicates the percent variation in the concentration of cortisol after DST explained by the indicated factor. The β coefficient results from a standardised stepwise model. 95% CI: confidence intervals for coefficient β. p value: after Bonferroni correction to adjust for multiple testing.
BMI, body mass index; DST, 1-mg dexamethasone-suppression test; eGFR, estimated glomerular filtration rate; LL, lower limit; UL, upper limit.

volume. In the light of our findings, more data are needed to support the role of HC in the challenging differential diagnosis when hypercortisolism is suspected in the presence of CKD.

The HPA axis in CKD has seldom been studied. In the 1980s, a small study in end-stage CKD (haemodialysis) described increased free and total plasma cortisol, both at 8:00 h am and after a 1-mg DST as well as increased midnight mean plasma cortisol (3). Three decades later, another study in haemodialysis patients showed a preserved circadian rhythm, albeit with higher midnight nadir (plasmatic and salivary) cortisol and plasmatic ACTH (4). A few studies have studied the HPA axis in earlier stages. One study in CKD stages I–IV described an inverse correlation between midnight-salivary cortisol and eGFR. In this study, 10% had a false positive result after a DST (inadequate suppression), all with eGFR <90 mL/min/1.73 m^2 and a normal response to a 2-day 2-mg DST. There were no changes in dexamethasone absorption or in transport proteins (5). Another study reported an increased concentration of both early morning cortisol and cortisol after DST, with similar ACTH, in patients with adrenal incidentalomas and moderately impaired renal function (eGFR <60 mL/min/1.73 m^2) (6). In addition, a study including CKD stages I–IV described similar basal cortisol and greater ACTH compared with controls. Also, progressive lower morning UFC with decreasing eGFR (especially when eGFR was <29 mL/min) and a normal response to DST (27).

In line with these previous studies (28), in our cohort, a proportional resistance to DST was found with worsening kidney function (increasing cortisol after DST as well as the proportion of patients with inadequate suppression after DST—Figure 3). A previous pharmacokinetic study performed in advanced CKD in haemodialysis subjects revealed that 75% did not suppress after a 1-mg DST and 2-day DST but suppressed adequately after higher doses of oral or iv dexamethasone, suggesting a prolonged cortisol half-life (28).

In our study 45% of subjects with inadequate suppression after a 1-mg DST failed to normally suppress after a 2-day DST, all in stage IV CKD, revealing an even greater resistance to dexamethasone in this group. This contrasts with the study by Cardoso et al. (5) Although the average eGFR across groups was similar in both studies, our cohort included a higher proportion of patients with lower eGFR in the stage IV group. Other unmeasured factors of chronic stress could also explain this difference. Considering these results, the cutoff value for the DST should be revised to avoid false-positive results when eGFR is <60 mL/min/1.73 m^2. Recently, a clinical trial has suggested that 3.2 μg/dL has the best diagnostic accuracy for patients with CKD and eGFR <30 mL/min/1.73 m^2 (https://clinicaltrials.gov/ct2/show/NCT05568602). In our cohort, 100% of subjects with CKD stages I–III and 81.3% in stage IV had cortisol after DST below this cutoff.

Midnight salivary cortisol increased with worsening kidney function suggesting a progressive impairment in the circadian rhythm. This reproduces the findings by Cardoso et al. (5) We observed a tendency toward higher midnight salivary cortisol, a significant increase in noon-salivary cortisol, and an increasing salivary cortisol AUC with advancing CKD, suggesting a global, albeit discrete, increased exposure to cortisol during the 24 h. Previous studies in haemodialysis also described a higher salivary cortisol levels between noon and midnight (4), and a higher mean 24-h plasma cortisol compared with controls (3).

Low eGFR is a well-known condition for a false negative 24-h UFC (8, 27). In our cohort, only patients with preserved diuresis were included. We observed decreasing 24-h UFC with lowering eGFR (especially <60 mL/min/m^2) despite a progressive increase in urinary output. This highlights the unreliability of 24-h UFC even when urinary output is within the normal/high range. Specifically, 24-h UFC is a source of false negative results when evaluating suspected hypercortisolism in CKD patients.

Early-morning cortisol and ACTH remained unchanged in CKD compared with controls. Existing literature is contradictory: In haemodialysis patients, an increase in basal cortisol and ACTH (3) was described in one article and no changes in basal but higher nadir cortisol and ACTH in the other (4). In earlier stages, a higher basal cortisol level was described (6) in one study. Regarding ACTH, one study described greater levels in CKD (27) whereas two studies did not report changes in basal ACTH (5, 6). A hypothesis is that the dynamics of the HPA axis would be progressively impaired with decreasing kidney function: first, night (nadir) levels increase, progressively earlier hours of the day are impaired, whereas basal levels remain the last hurdle. Blunted diurnal decline (higher evening salivary cortisol) seems to appear

parallel to an impaired negative cortisol feedback (resistance to suppression after DST), as post-DST was correlated with 08:00 pm salivary cortisol in most study groups (all but CKD stages I–II). In our study, CBG, albumin and total protein levels were similar between study groups, ruling out a difference in cortisol binding, similar to previous findings (5).

Hair cortisol remained unchanged across CKD stages. This suggests that cumulative exposure to cortisol is not increased in this population, despite the dynamic changes in the HPA axis. This contrasts with a previous study in haemodialysis subjects that suggested an increased cortisol exposure over the day indirectly estimated through serial measurements (serum or salivary cortisol) (4). In case of a minimal degree of hypercortisolism, it may be speculated that a higher amount of excess cortisol is needed to produce a significant accumulation in hair (29). The finding of a progressive increase in salivary cortisol AUC with decreasing kidney function in our study supports this hypothesis. HC is a measurement of mid and long-term exposure to cortisol (1 cm hair = 1 month). Its validity, reliability, and correlation with the classic biochemical tests of the HPA axis have been thoroughly studied in healthy volunteers, CS, and adrenal insufficiency (10–13, 15–17). We observed a correlation of HC with age, which was lost when adjusting for confounders. Previous studies are discordant, some have shown increased levels with increasing age whereas others have not (10, 17). HC does not significantly correlate with sex and smoking but correlated with alcohol consumption, which has also been described (19). Nevertheless, heavy alcohol consumption was an exclusion criterion in the study and the multivariate analyses remained unchanged when alcohol consumption was included.

The mechanisms leading to changes in the HPA axis in CKD remain unknown. On the one hand, an activation of the HPA axis is suggested. Evidence suggests that ACTH may have renoprotective effects, mainly through systemic immunomodulation and anti-inflammatory actions through the melanocortin pathways and protective effects on kidney cells, particularly podocytes, *via* the melanocortin and neurogenic pathways. It has been hypothesised that ACTH would be upregulated in initial phases of CKD, an initial adaptive response which later becomes inadaptative (30). In accordance with this notion, complications of advanced CKD such as metabolic acidosis, low-grade inflammation, and stress related to life with a chronic condition could be drivers for a greater pituitary secretion of ACTH (25). On the other hand, a decreased intracellular inactivation of cortisol by the 11β-hydroxysteroid-dehydrogenase (HSD)-2 with decreasing renal function is hypothesised. This enzyme, which is highly expressed in the kidneys, inactivates cortisol to cortisone and prevents an indiscriminate activation of the mineral corticoid receptor by cortisol. A decrease in 11β-HSD-2 activity would lead to cortisol activating of the mineralocorticoid receptor causing adverse outcomes in the renal and cardiovascular systems and influence the rates of cortisol appearing in the systemic circulation (31). Reduced activity of the 11β-HSD-2 has been described in CKD (including patients on haemodialysis), T2D, advanced age, and inflammation settings (30, 32, 33). Another possible mechanism is an increased half-life of cortisol when kidney function is impaired leading to higher levels of cortisol in circulation, which translates into changes in cortisol rhythm and inadequate DST (28). Finally, little research in haemodialysis subjects suggests an impaired renal clearance of cortisol (accumulation of cortisol metabolites) (34) and a less effective hepatic cortisol metabolism (an accumulation of end products of cortisol hepatic metabolism) (35). Data regarding these mechanisms in earlier CKD stages are lacking.

In our cohort, cortisol after DST was linearly and inversely correlated with eGFR. Moreover, cortisol after DST and glucose were independently associated with an eGFR <30 mL/min/m^2, independently of CKD duration or other cardiovascular risk factors. Olsen et al. found eGFR 30–60 (together with age and adenoma size) to be the main predictor of a cortisol post-DST >1.8 mcg/dL in subjects with adrenal incidentalomas (6). In another study in subjects with T2D, cortisol after DST was negatively correlated with eGFR and positively with CKD markers. Furthermore, higher terciles of cortisol after DST (as early as cortisol post-DST 0.6 mcg/dL) were associated with an increased prevalence of CKD, suggesting an activation of the HPA axis as a risk factor for the development of CKD in T2D (36). One study indirectly assessed the 11β-HSD system, describing a dysregulation toward increased intracellular cortisol in T2D, which was more pronounced in subjects with CKD (31). Finally, a recent study concluded that the 11β-HSD-mediated glucocorticoid activation in T2D is determined by inflammation (higher CRP) and is associated with diabetes and poorer glycaemic control in patients with CKD stages III–V (37). In a study in a cohort with hypertension, serum cortisol (8:00 h am) was negatively associated with eGFR and positively associated with CKD markers and higher cortisol terciles were associated with worse renal function (38).

In our cohort, a stepped increase in cardiometabolic comorbidities with CKD severity was observed (hypertension and dyslipidaemia prevalence, glucose, insulin, HOMA-IR, and triglycerides). A statistically significant linear trend was observed for CVD, although only three subjects had had a cardiovascular event (one in stage III and two in stage IV CKD). This finding suggests a higher cardiovascular risk in moderate and advanced CKD. One previous study found an association between serum cortisol before the dialysis session (8:00 h am–12:00 h pm) with mortality at 20 months in haemodialysis patients. In addition, cortisol correlated with CRP, suggesting a relation with inflammation (39). The sum of 24-h urinary cortisol metabolites was positively associated with systolic BP in a cohort of subjects with CKD stages II–III (40). There are no studies regarding the relation between cortisol and cardiovascular disease or mortality in pre-dialysis CKD.

When analysing the relationship of changes in the HPA axis with metabolic comorbidities, we describe an independent positive correlation between HC and VAT volume. In some studies, increased HC was correlated with features of the metabolic syndrome (especially BMI, abdominal obesity, and HbA_{1c}) (18) whereas others found association only with CVD and T2D but not with BMI, WC, or smoking (19). Higher HC was reported in elderly people admitted for myocardial infarction compared with admissions for other causes; these also had higher BMI and LDL-c and lower HDL-c (34).

Regarding HC and body composition, the results of previous studies are conflicting. Some found a positive association between

HC and BMI in men (18), whereas others found no relationship between HC and BMI in young (41) or elderly subjects (19). No previous studies have assessed HC and body composition in CKD. Our study includes subjects within a wide age range (52.9 ± 12.2 years), including elderly subjects (the eldest 77.4 years old). Both in older age (42) and CKD (37), changes in body composition occur, with an increase in body fat and a decrease in fat-free mass despite a stable BMI. We describe an independent correlation of HC with VAT volume, which better assesses fat mass in CKD (see above). To sum up, it cannot be ruled out that a mild hypercortisolism in CKD could contribute to an enlarged VAT volume, which in turn is associated with an adverse metabolic phenotype and increased cardiovascular burden (43).

Several limitations should be acknowledged. First, its observational design precludes drawing conclusions on causality. Second, the inclusion criteria were strict, so it may not be representative of the general CKD population and hamper generalizability. Third, the study does not include positive controls (CKD patients with hypercortisolism). Fourth, HC measurements were performed by immunoassay, which may present cross-reactivity with other structurally related molecules, such as cortisone. However, the immunoassay used presented adequate limit of quantification for the expected concentrations in hair and the cross-reactivity with other steroids is low, especially with cortisone (0.13%). Finally, while we employed a widely used (9, 14, 16) and well-validated (24, 41) procedure for hair cortisol measurements, enhanced cortisol extraction from hair samples can be achieved by hair grinding in conjunction with sequential and alternating solvents, rather than relying on hair mincing and a single methanol extraction (10). In fact, there is currently an urgent need to standardise procedures for cortisol extraction and quantification in hair, since various factors can impact their reliability including hair characteristics, the methods used for hair sample collection and storage, sample processing, and analytical techniques (10).

Based on our findings, there are several avenues for future research. First, prospective studies monitoring cortisol exposure over time could shed new light on the progression of HPA axis changes and their relation with CKD progression. Likewise, the physiopathological mechanisms underlying HPA axis disruption in CKD and its association with body composition and kidney damage need to be further explored, especially in initial phases. In addition, future trials could explore the effectiveness of interventions aiming to restore normal cortisol homeostasis (such as peripheral glucocorticoid activation blockade) and the impact on CKD progression and vice versa.

In summary, we describe changes in cortisol excretion, circadian rhythm, and dynamic study of the HPA axis: namely, a blunted diurnal decline and an impaired negative feedback regulation, in contrast to unchanged hair cortisol concentrations in subjects with CKD stages I to IV. Hair cortisol was independently associated with VAT volume, whereas cortisol after DST was associated with severe kidney damage. This is the first study to perform a thorough study of the HPA axis in CKD including hair cortisol concentrations and its association with metabolic comorbidities. Nevertheless, further studies are needed to investigate to a greater extent the sensitivity and reliability of hair cortisol as a tool for the diagnosis of Cushing syndrome in patients with impaired kidney function.

Data availability statement

The original contributions presented in the study are included in the article/Supplementary Material. Further inquiries can be directed to the corresponding authors.

Ethics statement

The studies involving humans were approved by CEIM Hospital Clinic Barcelona. The studies were conducted in accordance with the local legislation and institutional requirements. The participants provided their written informed consent to participate in this study.

Author contributions

LB: Conceptualization, Data curation, Formal analysis, Investigation, Methodology, Software, Visualization, Writing – original draft, Writing – review & editing. AV-B: Formal analysis, Methodology, Software, Visualization, Writing – review & editing, Data curation, Investigation. MB: Data curation, Formal analysis, Investigation, Methodology, Writing – review & editing, Validation. LQ: Data curation, Formal analysis, Investigation, Writing – review & editing, Conceptualization, Supervision. GR: Data curation, Formal analysis, Investigation, Writing – review & editing, Methodology, Visualization. DD-C: Data curation, Formal analysis, Investigation, Methodology, Writing – review & editing. CV: Data curation, Formal analysis, Methodology, Writing – review & editing, Conceptualization, Validation. MC: Data curation, Formal analysis, Writing – review & editing, Investigation, Writing – original draft. MM: Formal analysis, Writing – review & editing, Conceptualization, Methodology, Project administration, Validation, Visualization. AA: Formal analysis, Methodology, Validation, Visualization, Writing – review & editing, Investigation, Software, Supervision. GC: Methodology, Software, Supervision, Validation, Visualization, Writing – review & editing, Conceptualization, Data curation, Project administration, Resources. FH: Conceptualization, Methodology, Project administration, Resources, Software, Supervision, Validation, Visualization, Writing – review & editing, Formal analysis, Funding acquisition.

Funding

The author(s) declare that no financial support was received for the research, authorship, and/or publication of this article.

Acknowledgments

The authors would like to thank Irene Halperin for her valuable guidance on the initial study layout. L.B received a research grant (Resident Award "Premi Fi de Residènica Emili Letang" 2019) from Research, Innovation and Education Department at Hospital Clínic de Barcelona and a research grant ("Ajut ACD per la realització del programa de doctorat 2020") from the ACD.

Conflict of interest

The authors declare that the research was conducted in the absence of any commercial or financial relationships that could be construed as a potential conflict of interest.

Publisher's note

Supplementary material

The Supplementary Material for this article can be found online at: https://www.frontiersin.org/articles/10.3389/fendo.2024.1282564/full#supplementary-material

References

1. Murton M, Anna DG, Bobrowska A, Garcia-Sanchez JJ, James G, Wittbrodt E, et al. Burden of chronic kidney disease by KDIGO categories of glomerular filtration rate and albuminuria: A systematic review. *Adv Ther*. (2021) 38(1):180–200. doi: 10.1007/s12325-020-01568-8

2. GBD 2015 Mortality and Causes of Death Collaborators. Global, regional, and national life expectancy, all-cause mortality, and cause-specific mortality for 249 causes of death, 1980-2015: a systematic analysis for the Global Burden of Disease Study 2015. *Lancet (London England)*. (2016) 388:1459–544. doi: 10.1016/S0140-6736(16)31012-1

3. Wallace EZ, Rosman P, Toshav N, Sacerdote A, Balthazar A. Pituitary-adrenocortical function in chronic renal failure: Studies of episodic secretion of cortisol and dexamethasone suppressibility. *J Clin Endocrinol Metab*. (1980) 50:46–51. doi: 10.1210/jcem-50-1-46

4. Raff H, Trivedi H. Circadian rhythm of salivary cortisol, plasma cortisol, and plasma ACTH in end-stage renal disease. *Endocr Connect*. (2012) 2:23–31. doi: 10.1530/ec-12-0058

5. Cardoso EM del L, Arregger AL, Budd D, Zucchini AE, Contreras LN. Dynamics of salivary cortisol in chronic kidney disease patients at stages 1 through 4. *Clin Endocrinol (Oxf)*. (2016) 85:313–9. doi: 10.1111/cen.13023

6. Olsen H, Mjöman M. Moderately impaired renal function increases morning cortisol and cortisol levels at dexamethasone suppression test in patients with incidentally detected adrenal adenomas. *Clin Endocrinol (Oxf)*. (2015) 83:762–7. doi: 10.1111/cen.12823

7. Nieman LK, Biller BMK, Findling JW, Newell-Price J, Savage MO, Stewart PM, et al. The diagnosis of Cushing's syndrome: An endocrine society clinical practice guideline. *J Clin Endocrinol Metab*. (2008) 93:1526–40. doi: 10.1210/jc.2008-0125

8. Bansal V, El Asmar N, Selman WR, Arafah BM. Pitfalls in the diagnosis and management of Cushing's syndrome. *Neurosurg Focus*. (2015) 38:E4. doi: 10.3171/2014.11.FOCUS14704

9. Wester VL, Van Rossum EFC. Clinical applications of cortisol measurements in hair. *Eur J Endocrinol*. (2015) 173:M1–M10. doi: 10.1530/EJE-15-0313

10. Greff MJE, Levine JM, Abuzgaia AM, Elzagallaai AA, Rieder MJ, van Uum SHM. Hair cortisol analysis: An update on methodological considerations and clinical applications. *Clin Biochem*. (2019) 63:1–9. doi: 10.1016/j.clinbiochem.2018.09.010

11. Ibrahim C, Van Uum S. Hair analysis of cortisol levels in adrenal insufficiency. *C Can Med Assoc J = J l'Association Medicale Can*. (2014) 186:1244. doi: 10.1503/cmaj.140407

12. Short SJ, Stalder T, Marceau K, Entringer S, Moog SK, Shirtcliff EA, et al. Correspondence between hair cortisol concentrations and 30-day integrated daily salivary and weekly urinary cortisol measures. *Psychoneuroendocrinology*. (2016) 71:12–8. doi: 10.1016/j.psyneuen.2016.05.007

13. Zhang Q, Chen Z, Chen S, Yu T, Wang J, Wang W, et al. Correlations of hair level with salivary level in cortisol and cortisone. *Life Sci*. (2018) 193:57–63. doi: 10.1016/j.lfs.2017.11.037

14. Thomson S, Koren G, Fraser L-A, Rieder M, Friedman TC, Van Uum SHM. Hair analysis provides a historical record of cortisol levels in Cushing's syndrome. *Exp Clin Endocrinol Diabetes Off J Ger Soc Endocrinol [and] Ger Diabetes Assoc*. (2010) 118:133–8. doi: 10.1055/s-0029-1220771

15. Hodes A, Lodish MB, Tirosh A, Meyer J, Belyavskaya E, Lyssikatos L, et al. Hair cortisol in the evaluation of Cushing syndrome. *Endocrine*. (2017) 56(1):164–74. doi: 10.1007/s12020-017-1231-7

16. Manenschijn L, Koper JW, Van Den Akker ELT, de Heide LJM, Geerdink LJM, de Jong FH, et al. A novel tool in the diagnosis and follow-up of (cyclic) Cushing's syndrome: Measurement of long-term cortisol in scalp hair. *J Clin Endocrinol Metab*. (2012) 97:1836–43. doi: 10.1210/jc.2012-1852

17. Stalder T, Steudte-Schmiedgen S, Alexander N, Klucken T, Vater A, Wichmann S, et al. Stress-related and basic determinants of hair cortisol in humans: A meta-analysis. *Psychoneuroendocrinology*. (2017) 77:261–74. doi: 10.1016/j.psyneuen.2016.12.017

18. Stalder T, Kirschbaum C, Alexander N, Bornstein SR, Gao W, Miller R, et al. Cortisol in hair and the metabolic syndrome. *J Clin Endocrinol Metab*. (2013) 98:2573–80. doi: 10.1210/jc.2013-1056

19. Manenschijn L, Schaap L, Van Schoor NM, van der Pas S, Peeters GMEE, Lips P, et al. High long-term cortisol levels, measured in scalp hair, are associated with a history of cardiovascular disease. *J Clin Endocrinol Metab*. (2013) 98:2078–83. doi: 10.1210/jc.2012-3663

20. Journal O, Society I. KDIGO 2012 clinical practice guideline for the evaluation and management of chronic kidney disease. *J Nephrol*. (2013) 3(1):2013.

21. Boswell L, Serés T, Alex N, Perea V, Pané A, Viñals C. Carotid ultrasonography as a strategy to optimize cardiovascular risk management in type 1 diabetes: a cohort study. *Acta Diabetol*. (2022) 59(12):1563–74. doi: 10.1007/s00592-022-01959-z

22. Vega-beyhart A, Iruarrizaga M, Pané A, García-Eguren G, Giró O, Boswell L, et al. Endogenous cortisol excess confers a unique lipid signature and metabolic network. *J Mol Med (Berl)*. (2021) 99(8):1085–99. doi: 10.1007/s00109-021-02076-0

23. García-Eguren G, González-Ramírez M, Vizán P, Giró O, Vega-Beyhart A, Boswell L, et al. Glucocorticoid-induced fingerprints on visceral adipose tissue transcriptome and epigenome. *J Clin Endocrinol Metab*. (2022) 107:150–66. doi: 10.1210/clinem/dgab662

24. Sauvé B, Koren G, Walsh G, Tokmakejian S, Van Uum SHM. Measurement of cortisol in human hair as a biomarker of systemic exposure. *Clin Invest Med*. (2007) 30:E183–91. doi: 10.25011/cim.v30i5.2894

25. Sagmeister MS, Harper L, Hardy RS. Cortisol excess in chronic kidney disease - A review of changes and impact on mortality. *Front Endocrinol (Lausanne)*. (2022) 13:1075809. doi: 10.3389/fendo.2022.1075809

26. Webster AC, Nagler EV, Morton RL, Masson P. Chronic kidney disease. *Lancet (London England)*. (2017) 389:1238–52. doi: 10.1016/S0140-6736(16)32064-5

27. Oguz Y, Oktenli C, Ozata M, Sanisoglu Y, Yenicesu M, Vural A, et al. The midnight-to-morning urinary cortisol increment method is not reliable for the assessment of hypothalamic-pituitary-adrenal insufficiency in patients with end-stage kidney disease. *J Endocrinol Invest*. (2003) 26:609–15. doi: 10.1007/BF03347016

28. Workman RJ, Vaughn WK, Stone WJ. Dexamethasone suppression testing in chronic renal failure: pharmacokinetics of dexamethasone and demonstration of a normal hypothalamic-pituitary-adrenal axis. *J Clin Endocrinol Metab*. (1986) 63:741–6. doi: 10.1210/jcem-63-3-741

29. Puglisi S, Leporati M, Amante E, Parisi A, Pia AR, Berchialla P, et al. Limited role of hair cortisol and cortisone measurement for detecting cortisol autonomy in patients with adrenal incidentalomas. *Front Endocrinol (Lausanne)*. (2022) 13:833514. doi: 10.3389/fendo.2022.833514

30. Meuwese CL, Carrero JJ. Chronic kidney disease and hypothalamic-pituitary axis dysfunction: The chicken or the egg? *Arch Med Res*. (2013) 44:591–600. doi: 10.1016/j.arcmed.2013.10.009

31. Gant CM, Minovic I, Binnenmars H, de Vries L, Kema I, van Beek A, et al. Lower renal function is associated with derangement of 11-β hydroxysteroid dehydrogenase in type 2 diabetes. *J Endocr Soc*. (2018) 2:609–20. doi: 10.1210/JS.2018-00088

32. Quinkler M, Zehnder D, Lepenies J, Petrelli MD, Moore JS, Hughes SV, et al. Expression of renal 11β-hydroxysteroid dehydrogenase type 2 is decreased in patients with impaired renal function. *Eur J Endocrinol*. (2005) 153:291–9. doi: 10.1530/eje.1.01954

33. Homma M, Tanaka A, Hino K, Hirano T, Oka K, Kanazawa M, et al. Assessing systemic 11beta-hydroxysteroid dehydrogenase with serum cortisone/cortisol ratios in healthy subjects and patients with diabetes mellitus and chronic renal failure. *Metabolism*. (2001) 50:801–4. doi: 10.1053/meta.2001.24213

34. N'Gankam V, Uehlinger D, Dick B, Frey BM, Frey FJ. Increased cortisol metabolites and reduced activity of 11beta-hydroxysteroid dehydrogenase in patients on hemodialysis. *Kidney Int*. (2002) 61:1859–66. doi: 10.1046/j.1523-1755.2002.00308.x

35. Deck KA, Fischer B, Hillen H. Studies on cortisol metabolism during haemodialysis in man. *Eur J Clin Invest*. (1979) 9:203–7. doi: 10.1111/j.1365-2362.1979.tb00924.x

36. Asao T, Oki K, Yoneda M, Tanaka J, Kohno N. Hypothalamic-pituitary-adrenal axis activity is associated with the prevalence of chronic kidney disease in diabetic patients. *Endocr J*. (2016) 63:119–26. doi: 10.1507/endocrj.EJ15-0360

37. Sagmeister MS, Taylor AE, Fenton A, Wall NA, Chanouzas D, Nightingale PG, et al. Glucocorticoid activation by 11β-hydroxysteroid dehydrogenase enzymes in relation to inflammation and glycaemic control in chronic kidney disease: A cross-sectional study. *Clin Endocrinol (Oxf)*. (2019) 90:241–9. doi: 10.1111/cen.13889

38. Li X, Xiang X, Hu J, Goswami R, Yang S, Zhang A, et al. Association between serum cortisol and chronic kidney disease in patients with essential hypertension. *Kidney Blood Press Res*. (2016) 41:384–91. doi: 10.1159/000443435

39. Gracia-Iguacel C, González-Parra E, Egido J, Lindholm B, Mahillo I, Carrero JJ, et al. Cortisol levels are associated with mortality risk in hemodialysis patients. *Clin Nephrol*. (2014) 82:247–56. doi: 10.5414/cn108311

40. Hammer F, Edwards NC, Hughes BA, Steeds RP, Ferro CJ, Townend JN, et al. The effect of spironolactone upon corticosteroid hormone metabolism in patients with early stage chronic kidney disease. *Clin Endocrinol (Oxf)*. (2010) 73:566–72. doi: 10.1111/j.1365-2265.2010.03832.x

41. Manenschijn L, Koper JW, Lamberts SWJ, van Rossum EFC. Evaluation of a method to measure long term cortisol levels. *Steroids*. (2011) 76:1032–6. doi: 10.1016/j.steroids.2011.04.005

42. Gallagher D, Ruts E, Visser M, Heshka S, Baumgartner RN, Wang J, et al. Weight stability masks sarcopenia in elderly men and women. *Am J Physiol Endocrinol Metab*. (2000) 279:E366–75. doi: 10.1152/ajpendo.2000.279.2.E366

43. Navaneethan SD, Kirwan JP, Remer EM, Schneider E, Addeman B, Arrigain S, et al. Adiposity, physical function, and their associations with insulin resistance, inflammation, and adipokines in CKD. *Am J Kidney Dis Off J Natl Kidney Found*. (2021) 77:44–55. doi: 10.1053/j.ajkd.2020.05.028

frontiers | Frontiers in Endocrinology

TYPE Original Research
PUBLISHED 25 June 2024
DOI 10.3389/fendo.2024.1346082

OPEN ACCESS

EDITED BY
Seerapani Gopaluni,
University of Cambridge, United Kingdom

REVIEWED BY
Carolina Dalmasso,
University of Kentucky, United States
Marianna Ranieri,
University of Bari Aldo Moro, Italy

*CORRESPONDENCE
Aderville Cabassi
aderville.cabassi@unipr.it
Alice Bongrani
alice.bongrani@unipr.it

†These authors have contributed equally to this work and share first authorship

‡Deceased

RECEIVED 28 November 2023
ACCEPTED 29 May 2024
PUBLISHED 25 June 2024

CITATION
Calvi A, Bongrani A, Verzicco I, Figus G, Vicini V, Coghi P, Montanari A and Cabassi A (2024) Urinary hyaluronidase activity is closely related to vasopressinergic system following an oral water load in men: a potential role in blood pressure regulation and early stages of hypertension development.
Front. Endocrinol. 15:1346082.
doi: 10.3389/fendo.2024.1346082

Urinary hyaluronidase activity is closely related to vasopressinergic system following an oral water load in men: a potential role in blood pressure regulation and early stages of hypertension development

Anna Calvi[1†], Alice Bongrani[2*†], Ignazio Verzicco[1], Giuliano Figus[1], Vanni Vicini[1], Pietro Coghi[1], Alberto Montanari[2‡] and Aderville Cabassi[1,2*]

[1]Clinica e Terapia Medica, Department of Medicine and Surgery, University Hospital of Parma, Parma, Italy, [2]Cardiorenal and Hypertension Research Unit, Department of Medicine and Surgery, University of Parma, Parma, Italy

Introduction: Blood pressure (BP) regulation is a complex process involving several factors, among which water-sodium balance holds a prominent place. Arginin-vasopressin (AVP), a key player in water metabolism, has been evoked in hypertension development since the 1980s, but, to date, the matter is still controversial. Hyaluronic acid metabolism has been reported to be involved in renal water management, and AVP appears to increase hyaluronidase activity resulting in decreased high-molecular-weight hyaluronan content in the renal interstitium, facilitating water reabsorption in collecting ducts. Hence, our aim was to evaluate urinary hyaluronidase activity in response to an oral water load in hypertensive patients (HT, n=21) compared to normotensive subjects with (NT+, n=36) and without (NT-, n=29) a family history of hypertension, and to study its association with BP and AVP system activation, expressed by serum copeptin levels and urine Aquaporin 2 (AQP2)/creatinine ratio.

Methods: Eighty-six Caucasian men were studied. Water load test consisted in oral administration of 15–20 ml of water/kg body weight over 40–45 min. BP, heart rate, serum copeptin, urine hyaluronidase activity and AQP2 were monitored for 4 hours.

Results: In response to water drinking, BP raised in all groups with a peak at 20–40 min. Baseline levels of serum copeptin, urinary hyaluronidase activity and AQP2/creatinine ratio were similar among groups and all decreased after water load, reaching their nadir at 120 min and then gradually recovering to baseline values. Significantly, a blunted reduction in serum copeptin, urinary hyaluronidase activity and AQP2/creatinine ratio was observed in NT+ compared to NT- subjects. A strong positive correlation was also found

between urinary hyaluronidase activity and AQP2/creatinine ratio, and, although limited to the NT- group, both parameters were positively associated with systolic BP.

Discussion: Our results demonstrate for the first time the existence in men of a close association between urinary hyaluronidase activity and vasopressinergic system and suggest that NT+ subjects have a reduced ability to respond to water loading possibly contributing to the blood volume expansion involved in early-stage hypertension. Considering these data, AVP could play a central role in BP regulation by affecting water metabolism through both hyaluronidase activity and AQP2 channel expression.

KEYWORDS

hyaluronidase, arginin-vasopressin, ADH, hypertension, Aquaporin 2, water metabolism, water load, blood pressure

Introduction

According to the 2023 World Health Organization (WHO) estimates, 1.28 billion adults between 30 and 79 years old suffer from hypertension and about 1 in 5 have it under control (1). Hypertension is currently the most prevalent risk factor for cardiovascular disease and one of the leading causes of premature death worldwide, with the risk being higher the younger the age of hypertension onset (2).

Blood pressure (BP) regulation is extremely complex, and several endocrine, nervous, vascular and immune factors are closely interconnected in hypertension pathogenesis (3). Water and sodium balance is undoubtedly one of them. As early as 1972, Guyton et al. demonstrated the influence of kidney in BP regulation, showing that increasing BP levels were associated with a significant increase in sodium and, consequently, water renal excretion aimed at reducing extracellular volume and restoring normal BP values (4). While sodium contribution to hypertension development has since been extensively and thoroughly studied, the role of water is still poorly defined.

Arginin-vasopressin (AVP), also known as antidiuretic hormone (ADH), is a 9-amino-acid peptide synthetized by the magnocellular neurons located in the supraoptic and paraventricular nuclei of hypothalamus and secreted in response to raised serum tonicity and/or reduced effective circulating arterial blood volume (5). Characteristically, AVP acts as an antidiuretic hormone by activating V2 receptors on the basolateral membrane of the principal cells in the collecting ducts. This is followed by Aquaporin 2 (AQP2) translocation to the luminal membrane and the formation of AQP2 channels, resulting in increased water permeability, water reabsorption and, finally, excretion of hyperosmotic urine (5). A possible role for AVP in hypertension development has been evoked since the 1980s (6–10), but, to date, is still controversial (11–13). Indeed, AVP was first identified as a pressor hormone (14), and, *in vitro*, its vasoconstrictor effect, mediated by V1a receptors on smooth muscle cells, has shown to be greater than that of angiotensin II (15, 16). *In vivo*, however, its importance is presumably limited by the activation of counter-regulatory mechanisms, including the baroreceptor reflex and the modulation of cardiac output by AVP itself (15, 16).

Interestingly, in 1958, Ginetzinsky demonstrated that hyaluronic acid (HA) metabolism in the renal interstitium is closely related to water handling and AVP action (17). Indeed, HA content in renal medullary significantly influences the process of urine concentration and dilution, mainly by altering the interstitial osmotic gradient that draws AVP-induced water reabsorption at the collecting duct level (18, 19). In humans, the degradation of high-molecular-weight HA into low-molecular-weight fragments is catalyzed by six different types of hyaluronidases, of which HYAL1 and HYAL2 are the most highly expressed and actively involved in HA metabolism (20, 21). Their activity is tightly regulated by several factors, including hormones involved in water balance, such as angiotensin II and AVP (22). Notably, AVP seems to accelerate HA catabolism in renal medullary by increasing both hyaluronidase synthesis and activity (23).

As hyaluronidase excretion in the urine has been shown to be inversely correlated to body water balance (19), the aim of our study was to assess urinary hyaluronidase activity and to study its association with BP and vasopressinergic system activation in response to an oral water load. Hypertensive patients were compared to normotensive men with and without a family history of hypertension. Since over 90% of circulating AVP is bound to platelets and its plasma half-life is only 5 to 20 min (24), the urinary AQP2/creatinine ratio, which reflects the shedding phenomenon of AQP2 from the apical luminal membrane of collecting duct principal cells, has been considered as valid surrogate for assessing renal sensitivity to AVP action, based on results obtained in a rat model of essential hypertension (25). To

further confirm our results, we also assessed serum levels of copeptin, the 39-aminoacid C-terminal part of the AVP precursor (pre-proAVP), which is secreted into circulation in equimolar concentration with AVP, thus indicating AVP plasma levels (24).

Materials and methods

Study population

Recruitment of study population took place between 2005 and 2008 as part of the I Demand (Italy Developing Education and awareness on Micro-Albuminuria in patients with hypertensive Disease) Project, a multicenter observational study promoted by the Italian Society of Hypertension. The study was conducted in accordance with the Declaration of Helsinki principles and was approved by the Ethics Committee of the University Hospital of Parma. All participants gave written informed consent.

Included subjects referred to the Hypertension and Cardio-Renal Disease Study Center attached to the Internal Medicine Department of the University Hospital of Parma with a diagnosis of essential hypertension never treated with antihypertensive drugs (HT group, n=21). Secondary hypertension was, however, excluded by history, physical examination, blood and urine hormone tests, and renal artery ultrasound. Controls were untreated normotensive healthy volunteers mainly recruited among healthcare professionals and students. Men with both parents suffering from arterial hypertension were classified as normotensive positive subjects (family history of hypertension, NT+, n=36); otherwise, they were considered normotensive negative controls (NT-, n=29).

All subjects were men of Caucasian ethnicity. Women were excluded to avoid potential bias due to the well-known effects of estrogens on the physiological regulation of water-sodium balance, especially on AVP system activation (26). Other exclusion criteria included:

- Age < 18 years
- Ongoing urinary infection
- Heart failure
- Diabetes mellitus or insipidus
- Oedema
- Liver diseases
- Systemic connective tissue diseases.

Water load test

Oral water load and related analyses were performed in the Day Hospital ward of the Internal Medicine Department at eight o'clock a.m. The water load experimental protocol by Velazquez et al. (27) was applied. Subjects were instructed to follow a 7-day diet containing sodium 153 mEq/day and potassium 75 mEq/day and to abstain from smoking and drinking coffee or tea for at least 12 hours before the test. Sodium and potassium levels were verified in 24-hour urine at both 72 and 24 hours prior to the test: levels above or below 25% of the expected values were considered as a protocol violation and subjects were excluded. A fast from solids starting at midnight the previous evening was also required. Small amounts of water were allowed.

Water load test consisted in oral administration of 15–20 mL of water/kg of body weight over 40–45 minutes, followed by supine rest for at least 4 hours. Systolic and diastolic office blood pressure (SBP and DBP, respectively), as well as heart rate, were assessed by the ward nurse using the cuff method every 20 minutes during the first hour and then every 30 minutes up to 4 hours. Body weight and height, as well as 24h-urine volume, were recorded prior to the water load test.

Biological sampling

Venous blood and urine samples were obtained after three series of BP and heart rate measurements, centrifuged and immediately frozen at -80°C for subsequent analysis.

Blood was drawn prior to the test, after at least 30 minutes of supine rest, and collected into propylene tubes containing 1.5 mg/mL EDTA (ethylenediaminetetraacetic acid) buffer. Plasma sodium, potassium, osmolarity and creatinine levels were assessed using standard techniques. Serum copeptin was measured by a commercial enzyme-linked immunosorbent assay (ELISA) kit according to manufacturer's instructions (Human Copeptin ELISA kit CSB-E121304, Cusabio Biotech, China). Intra-assay and inter-assay coefficients of variation were <8% and <10%, respectively. Analysis was performed in duplicate.

Urine samples were collected at baseline, then every 20 minutes during the first hour, every 30 minutes up to 180 minutes, and finally at 240 minutes.

Hyaluronidase activity and AQP2/creatinine ratio assessment

Hyaluronidase activity was quantified in urine by turbidimetric assay, determining turbidity caused by the high-molecular-mass (>6–8 kDa) residual substrate precipitated with cetyltrimethylammonium bromide. The incubation mixture contained citrate-phosphate buffer (solution A: 0.1 M Na_2HPO_4, 0.1 M NaCl; solution B: 0.1 M citric acid, 0.1 M NaCl; solutions A and B were mixed in the appropriate proportions to achieve a 5.0 pH), 30 µL of BSA solution (0.2 mg/mL in water), 30 µL of HA substrate solution (2 mg/mL in water), 50 µL of H_2O, 10 µL of Me_2SO and 30 µL of enzyme solution. After 30-minute incubation at 37°C, 720 µL of 2.5% (w/v) cetyltrimethylammonium bromide solution (2.5 g of cetyltrimethylammonium bromide dissolved in 100 mL of 0.5M sodium hydroxide solution at pH 12.5) was added in order to precipitate the residual high-molecular-mass substrate and stop the enzymatic reaction. The mixture was then incubated a second time at 25°C for 20 minutes and the turbidity of each sample was determined at 600 nm with a spectrophotometer. The obtained hyaluronidase activity levels were then corrected for urinary

10.3389/fendo.2024.1346082

creatinine concentration. Measurements were performed in triplicates according to Botzki et al. (28).

AQP2 levels were assessed in urine using a commercial ELISA kit (SEA580Hu 96, intra- and inter-assay coefficients of variation <10% and <12%, respectively, Cloud-Clone Corp., Katy, TX77494, USA) and then normalized for urinary creatinine concentration.

All laboratory assays were performed without freeze-thaw cycles of the samples and by investigators blind to clinical data.

Statistical analysis

Results are expressed as mean ±standard deviation (SD).

Prior to analysis, the normal distribution of data was verified with the Shapiro-Wilk and Kolmogorov-Smirnov tests, and, when necessary, the logarithmic transformation was applied. Comparisons among groups were then made using one-way ANOVA followed by Bonferroni's *post-hoc* test or two-way ANOVA with repeated measures followed by Dunnett's *post-hoc* test, as appropriate. As concerns serum copeptin levels, due to the great variability of the values obtained, data were analyzed as percent changes from baseline by employing a mixed-effect model followed by Dunnett's *post-hoc* test. The correlations between SBP and urinary hyaluronidase activity and AQP2/creatinine ratio, respectively, were evaluated by single linear regression.

Statistical analysis was performed using GraphPad Prism software (version 10.0.3, San Diego, CA, USA) and $p<0.05$ was considered the statistical threshold to declare significance.

Results

Anthropometric, clinical and biological features of study population are detailed in Table 1. A total of 86 men aged 20 to 52 years were included. HT patients were older than NT subjects ($p<0.0001$ versus both NT- and NT+) and, as expected, had higher baseline SBP and DBP values ($p<0.0001$ for both). No difference in SBP and DBP was found between NT- and NT+ men. Likewise, baseline heart rate was similar among the groups. Subjects had normal renal function and no electrolyte disturbances. After a follow-up period of 8 to 11 years from the water load test, sustained arterial hypertension was diagnosed in 4 out of 29 (14%) NT- versus 11 out of 36 (30%) NT+ men.

TABLE 1 Anthropometric, clinical and biological characteristics of study population.

	NT- (n=29)	NT+ (n=36)	HT (n=21)
Age (years)	27 ± 4	27 ± 5	44 ± 5****
BMI (kg/m^2)	25.9 ± 2.2	25.8 ± 2.3	26.2 ± 2.8
SBP (mmHg)	121 ± 9	118 ± 8	154 ± 8****
DBP (mmHg)	77 ± 5	76 ± 6	95 ± 5****
Heart Rate (bpm)	74 ± 7	74 ± 8	77 ± 10
24h-Urine Volume (mL)	1660 ± 389	1510 ± 298	1634 ± 382
Creatinine (mg/dL)	0.88 ± 0.12	0.90 ± 0.15	0.92 ± 0.19
Sodium (mmol/L)	138 ± 3	139 ± 4	139 ± 4
Potassium (mmol/L)	4.4 ± 0.6	4.6 ± 0.5	4.3 ± 0.7

The values are expressed as mean ± standard deviation. NT-, Normotensive subjects; NT+, Normotensive subjects with family history of hypertension; HT, Hypertensive subjects; BMI, Body Mass Index; SBP, Systolic Blood Pressure; DBP, Diastolic Blood Pressure.
****$p<0.0001$ vs NT- and NT+ groups, One-way ANOVA followed by Bonferroni *post-hoc* test.

As shown in Figure 1, in response to oral water loading, SBP and DBP increased rapidly, with peak values at 20–40 min, and then reverted to basal or even lower levels. Although HT patients maintained higher BP values throughout the test ($p<0.0001$ versus normotensive subjects), this trend was similar in the three groups. By contrast, except for an early increase in NT+ men, heart rate was

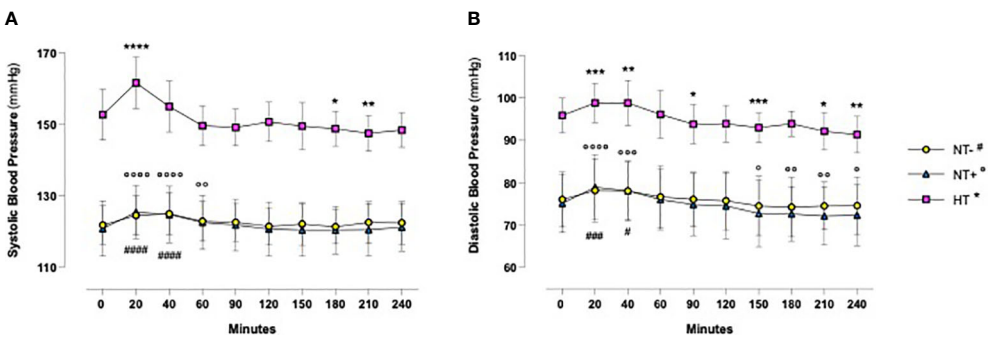

FIGURE 1
Blood pressure time course in response to oral water loading. In response to oral water loading, systolic **(A)** and diastolic **(B)** blood pressure increased rapidly with maximum values at 20 to 60 minutes and then reverted to basal or lower levels. Although hypertensive patients (HT) maintained higher BP values throughout the test ($p<0.0001$), this trend was similar in the three groups. *$p<0.05$, **$p<0.01$, ***$p<0.001$, ****$p<0.0001$ versus T0 for HT group; °$p<0.05$, °°$p<0.01$, °°°$p<0.001$, °°°°$p<0.0001$ versus T0 for normotensive subjects with family history of hypertension (NT+); #$p<0.05$, ###$p<0.001$, ####$p<0.0001$ versus T0 for the normotensive group (NT-); two-way ANOVA with repeated measures followed by Dunnett's *post-hoc* test.

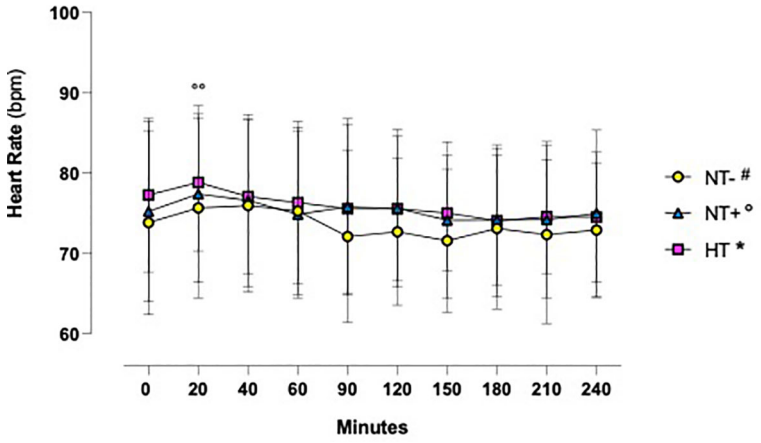

FIGURE 2
Heart rate time course in response to oral water loading. Heart Rate was not significantly influenced by oral water loading, except for a modest increase at 20 minutes in normotensive subjects with a family history of hypertension (NT+). °°p<0.01 versus T0 for NT+ group; two-way ANOVA with repeated measures followed by Dunnett's *post-hoc* test. NT-, normotensive subjects; HT, hypertensive patients.

not significantly affected by the oral water load (Figure 2). No differences in baseline plasma osmolarity, as well as serum copeptin levels, were observed among the groups. However, as expected, water load resulted in a significant reduction in both parameters ($p<0.001$ compared to baseline for all groups, Figures 3A, B). Notably, at 120 minutes, while plasma osmolarity was similar among groups, NT+ subjects showed a blunted decrease in serum copeptin levels ($p<0.05$ versus NT- group).

Similarly, as illustrated in Figure 4, in all groups, urinary hyaluronidase activity was significantly reduced by water load, reaching the lowest levels at 120 min ($p<0.0001$ versus baseline for all groups) and then gradually recovering to baseline values ($p<0.01$ versus baseline for HT patients, $p<0.001$ for NT- and NT+ subjects). In addition, while the trends over time of NT- and HT groups were overlapping, NT+ men showed significantly higher values at both 60 and 120 min after water loading ($p<0.0001$ versus NT-).

Assessing the AQP2/creatinine ratio in urine, we observed a similar time course (Figure 5). Indeed, after water drinking, the AQP2/creatinine ratio rapidly decreased from 20 min onward to reach minimum values at 90–120 min ($p<0.0001$ for all groups at both times). Again, trends over time were comparable among groups, but NT+ and HT subjects had higher values than the NT- ones, especially in the first 2 hours of the test.

In light of these findings, the association between urinary hyaluronidase activity and the AQP2/creatinine ratio was studied. As depicted in Figure 6, including all men, we found significant positive correlations at any time point, especially between 60 and 180 min after water load (Figures 6B–D). Interestingly, when we carried out regression analyses by groups, we observed globally consistent results, confirming the data obtained on the entire cohort (Table 2).

When evaluating the associations between SBP and hyaluronidase activity, as well as AQP2/creatinine ratio, significant

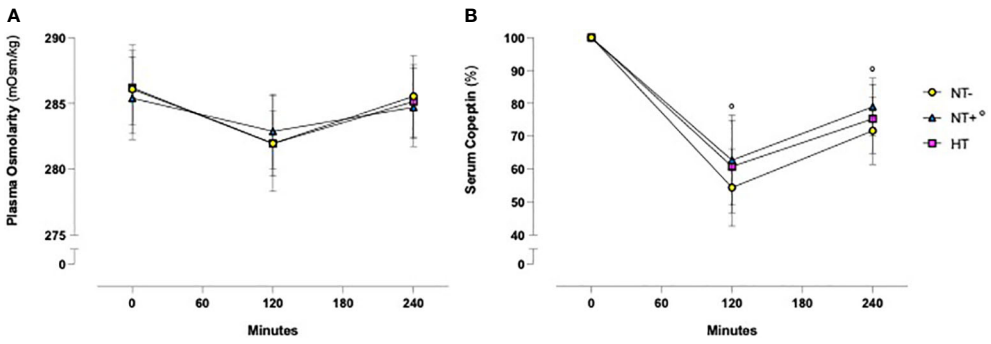

FIGURE 3
Time course of plasma osmolarity and serum copeptin levels in response to an oral water load. Oral water load resulted in a significant decrease in both plasma osmolarity **(A)** and serum copeptin **(B)** levels ($p<0.0001$ compared to baseline for all groups). No differences in plasma osmolarity were observed among the groups. By contrast, at 120 minutes the water load-induced reduction in serum copeptin, expressed as a percent change from baseline, was significantly lower in subjects with a family history of hypertension (NT+). °$p<0.05$ versus NT- group; two-way ANOVA **(A)** and mixed-effect model **(B)** with repeated measures followed by Dunnett's *post-hoc* test. NT-, normotensive subjects; HT, hypertensive patients.

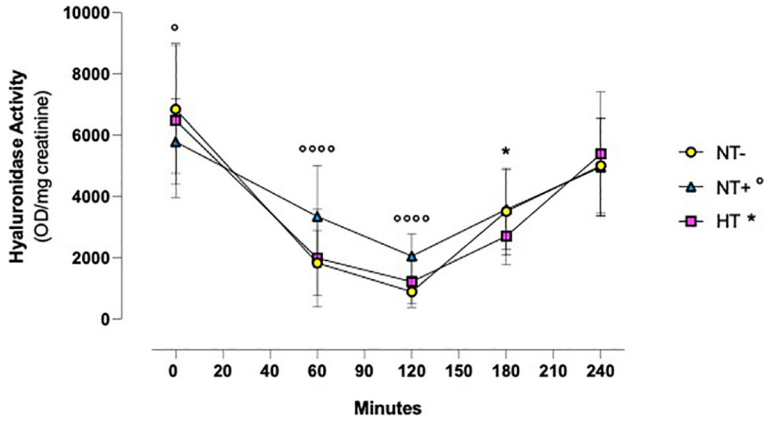

FIGURE 4
Urinary hyaluronidase activity following oral water loading. Urinary hyaluronidase activity, assessed by turbidimetric assay, was significantly reduced by water drinking, with minimal levels at 120 minutes ($p<0.0001$ compared to baseline for all groups) and then gradually recovered to baseline values (compared to baseline, $p<0.01$ for hypertensive patients (HT), $p<0.001$ for normotensive subjects). Although lower at T0, at 60 and 120 minutes, hyaluronidase activity levels were higher in normotensive subjects with family history of hypertension (NT+) compared to the normotensive ones (NT-). *$p<0.05$, HT versus NT- subjects; °$p<0.05$, °°°°$p<0.0001$, NT+ versus NT- subjects; two-way ANOVA with repeated measures followed by Dunnett's *post-hoc* test.

correlations were found only in the NT- group (Tables 3, 4, respectively). In particular, while SBP was positively correlated with urinary hyaluronidase activity at baseline and at the end of the test ($p<0.01$ at 0 and $p<0.05$ at 240 min, Table 3), a significant positive correlation with the AQP2/creatinine ratio was detected at T0 and 40 min after water drinking ($p<0.05$ and $p<0.01$, respectively, Table 4), which corresponded to peak SBP levels (Figure 1).

Discussion

In our study, we first demonstrated that urinary hyaluronidase activity markedly decreases in response to an oral water load, reaching its lowest levels after 120 min. Notably, at this time, NT + subjects showed significantly higher values than both NT- and HT men. Interestingly, the time course of serum copeptin levels and urine AQP2/creatinine ratio followed that of hyaluronidase activity with a close direct correlation. These data, along with the positive associations observed between SBP and both urinary hyaluronidase activity and AQP2/creatinine ratio, support the existence of a close relationship between renal hyaluronidases and vasopressinergic system activation, which could affect water metabolism under both normotensive and sustained hypertensive conditions.

Acute oral water intake is known to increase BP in several animal species (29) as well as in patients with orthostatic hypotension symptoms due to autonomic failure (30). In our

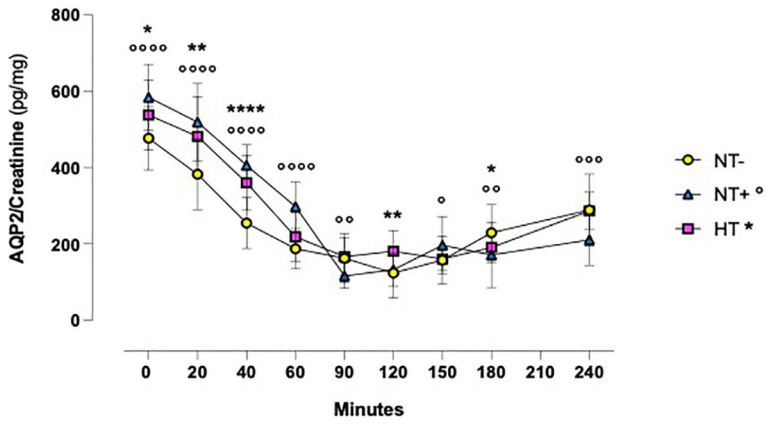

FIGURE 5
Aquaporln2 (AQP2)/creatinine ratio in response to oral water loading. After water drinking, the AQP2/creatinine ratio rapidly decreased to reach minimum values at 90 and 120 minutes ($p<0.0001$ for all groups at both times). Trends over time were comparable between groups, but hypertensive patients (HT) and normotensive subjects with family history of hypertension (NT+) maintained higher values than the normotensive group (NT-). *$p<0.05$, **$p<0.01$, ****$p<0.0001$, HT versus NT- subjects; °$p<0.05$, °°$p<0.01$, °°°$p<0.001$, °°°°$p<0.0001$, NT+ versus NT- subjects; two-way ANOVA with repeated measures followed by Dunnett's *post-hoc* test.

10.3389/fendo.2024.1346082

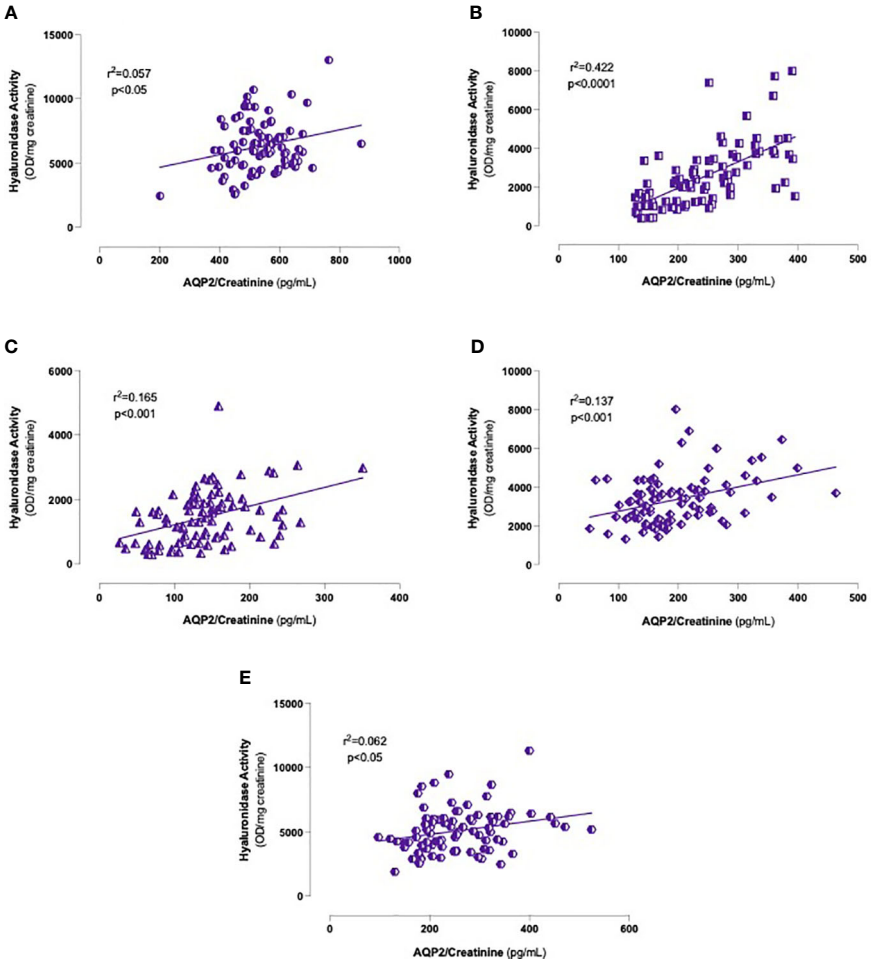

FIGURE 6
Correlations between urinary hyaluronidase activity and AQP2/Creatinine ratio levels. Onset **(A)**, 60 **(B)**, 120 **(C)**, 180 **(D)** and 240 **(E)** minutes after oral water loading. Simple linear regression.

cohort, we observed a significant and early increase in SBP and, to a lesser extent, DBP levels, which reached their highest values about 20 min after the oral water load. These findings, largely consistent with most of the literature (29, 31–34), have been reported to be associated with increased plasma norepinephrine levels, muscle sympathetic nerve activity and peripheral vascular resistance, which would be counterbalanced by vagal modulation and baroreflex activation (29, 32). In accordance with this, in response to the oral water load, we found no significant changes in heart rate, except for a modest increase in NT+ subjects at 20 min. Interestingly, SBP levels increased by 8.9 +/- 0.3 mmHg in HT group versus 4.6 +/- 0.3 mmHg and 2.7 +/- 0.3 mmHg in NT+ and NT- men, respectively, suggesting a greater sympathetic response to water drinking in HT patients. These data, confirming the results of Velasquez et al. (27), are in agreement with the finding of higher basal muscle sympathetic nerve activity in subjects with mild hypertension compared to the normotensive ones (32). In previous studies, no changes were detected in plasma volume, plasma renin activity and sodium balance (32). Furthermore, the pressor effect of drinking water did not appear to be related to water temperature or gastric distension (29) and was not obtained when pure water was replaced by salt water (32) or administered via intravenous infusion (29). Drinking water would rather activate postganglionic sympathetic neurons directly (33) or, alternatively, through a gastro-pressor reflex mediated by the osmoreceptors in the proximal gut and portal system (35, 36), triggering both

TABLE 2 Correlations between urinary hyaluronidase activity and AQP2/creatinine ratio.

Minutes	NT- (n=29)	NT+ (n=36)	HT (n=21)
0	r^2 = 0.137*	r^2 = 0.070	r^2 = 0.332**
60	r^2 = 0.341***	r^2 = 0.291***	r^2 = 0.354**
120	r^2 = 0.326**	r^2 = 0.471****	r^2 = 0.438**
180	r^2 = 0248**	r^2 = 0.150*	r^2 = 0.051
240	r^2 = 0.106	r^2 = 0.059	r^2 = 0.125

Hyaluronidase activity and AQP2/creatinine ratio were measured in urine every 60 minutes after water loading test by turbidimetric assay and ELISA, respectively. All correlations are positive. AQP2, Aquaporin 2; NT-, Normotensive subjects; NT+, Normotensive subjects with family history of hypertension; HT, Hypertensive subjects.
*p<0.05, **p<0.01, ***p<0.001, ****p<0.0001, Simple Linear Regression.

10.3389/fendo.2024.1346082

TABLE 3 Correlations between SBP and urinary hyaluronidase activity.

Minutes	NT- (n=29)	NT+ (n=36)	HT (n=21)
0	r^2 = 0.308 (pos)**	r^2 = 0.002 (neg)	r^2 = 0.010 (pos)
60	r^2 = 0.003 (neg)	r^2 = 0.017 (neg)	r^2 = 0.003 (neg)
120	r^2 = 0.04 (neg)	r^2 = 0.004 (pos)	r^2 = 0.000
180	r^2 = 0.018 (neg)	r^2 = 0.022 (neg)	r^2 = 0.004 (neg)
240	r^2 = 0.166 (pos)*	r^2 = 0.004 (pos)	r^2 = 0.013 (neg)

SBP and urinary hyaluronidase activity by turbidimetric assay were assessed every 60 minutes after water loading test. SBP, Systolic Blood Pressure; NT-, Normotensive subjects; NT+, Normotensive subjects with family history of hypertension; HT, Hypertensive subjects.
*p<0.05, **p<0.01, Simple Linear Regression.

TABLE 4 Correlations between SBP and urinary AQP2/creatinine ratio.

Minutes	NT- (n=29)	NT+ (n=36)	HT (n=21)
0	r^2 = 0.175 (pos)*	r^2 = 0.000	r^2 = 0.044 (neg)
20	r^2 = 0.103 (pos)	r^2 = 0.004 (neg)	r^2 = 0.018 (neg)
40	r^2 = 0.241 (pos)**	r^2 = 0.005 (neg)	r^2 = 0.018 (neg)
60	r^2 = 0.109 (pos)	r^2 = 0.013 (neg)	r^2 = 0.028 (neg)
120	r^2 = 0.047 (neg)	r^2 = 0.022 (neg)	r^2 = 0.018 (neg)
180	r^2 = 0.036 (neg)	r^2 = 0.070 (neg)	r^2 = 0.003 (pos)
240	r^2 = 0.054 (pos)	r^2 = 0.000	r^2 = 0.077 (neg)

SBP and urinary AQP2/creatinine ratio were assessed every 20 minutes during the 1st hour, then every 60 minutes until 240 minutes after water loading test. AQP2, Aquaporin 2; NT-, Normotensive subjects; NT+, Normotensive subjects with no familial history hypertension; HT, Hypertensive subjects.
*p<0.05, **p<0.01, Simple Linear Regression.

sympathetic activation and reflex inhibition of AVP secretion (31). Indeed, whereas in response to oral water loading, Velasquez et al. did not show any difference in plasma AVP levels (27), Geelen et al. demonstrated a rapid decrease followed by a long-lasting inhibition of AVP secretion which was not accompanied by changes in the renin-angiotensin-aldosterone system (RAAS) (31).

Similar to what we observed in normotensive and hypertensive rats (data under submission), oral water load induced a significant decrease in urinary hyaluronidase activity with a nadir at 120 min, followed by an almost complete restoration to baseline physiological values within 4 hours. Meaningfully, NT+ men, despite having lower hyaluronidase activity prior to the test, maintained significantly higher levels than NT- subjects at both 60 and 120 minutes after water load. As far as we know, this is the first time that such a result has been described. Indeed, the effects of oral water load on hyaluronidase activity have at present been studied essentially *in vitro* (37–39) or in animal models (19, 23, 40, 41). In particular, in rats, Stridh et al. (41) demonstrated that, upon continuous hydration, medullary HA levels increased with a peak after about 2 hours and returned to control values after about 4 hours (41).

Although the inverse relationship between the renal excretion of hyaluronidase and body hydration has been known since 1958 (17, 37), the mechanism through which hyaluronidase activity influences water metabolism has not yet been fully elucidated. HA is a negatively charged, ubiquitously distributed linear glycosaminoglycan with a unique water-binding ability (42) that largely depends on its molecular weight. Indeed, when high-molecular-weight HA is above 0.2 mg/mL, inter- and intra-molecular interactions occur such that the volume occupied by HA increases, excluding other large molecules (19). This "steric exclusion" phenomenon might antagonize further water reabsorption and influence the osmotic activity in the intercellular matrix (43). Interestingly, in the kidney, the HA content is considerably higher in the inner medulla than in the cortex, where 80% of the filtered water is reabsorbed (19) and depends mainly on renal medullary interstitial cell (RMICs) activity, which is influenced by both medium osmolality and oxygen tension (38). In particular, high-molecular-weight HA, internalized in RMICs via the CD44-receptor, undergoes degradation by HYAL1 and HYAL2, which seems to be the main regulatory step determining HA content in the interstitial matrix (37, 38). A decrease in hyaluronidase activity thus results in an increase in high-molecular-weight HA content in the renal medullary, which would interfere with the urinary concentration process by modifying the kidneys' ability to excrete or reabsorb adequate amounts of water. In addition to the "steric exclusion" effect, two other mechanisms have been proposed to explain this phenomenon. First, modification of the physicochemical characteristics of the interstitial matrix due to HA accumulation could compromise the medullary osmotic gradient. Alternatively, or complementarily, the functional oedema accompanying the increase in high-molecular-weight HA might widen the diffusion distances between tubules and blood vessels and hinder water reabsorption from the collecting ducts (18). In light of these considerations, the higher hyaluronidase activity found in NT+ subjects strongly suggests that men predisposed to develop hypertension have a lower diuretic response to water load, possibly resulting in blood volume expansion and ultimately, hypertension development.

In our study, the changes in hyaluronidase activity were accompanied by broadly comparable variations over time in serum copeptin levels and urinary AQP2/creatinine ratio, which we have previously shown to reliably reflect body water balance and vasopressinergic system activation (24, 25). Moreover, a positive correlation between urinary hyaluronidase activity and AQP2/creatinine ratio was found at any time point of the test, when analyzing both the entire cohort and each subject group separately, indicating the existence of a close relationship between hyaluronidase activity and AVP. The presence of vasopressinergic V1 (44) and V2 receptors (45) has been demonstrated in RMICs and AVP has been found to enhance both the expression and synthesis of hyaluronidases. In addition, it increases sodium and urea concentration to levels optimal for hyaluronidases activity (23) by inducing the expression of the epithelial sodium channel ENaC and the urea transporter UT-

A1, respectively (5). Interestingly, with regard to animal models, the Brattleboro rats, which genetically lack AVP, show higher HA content in the renal interstitium associated with exaggerated diuresis (23), while gerbils, having 4 times higher AVP levels than rats, have 37% lower papillary HA content which could facilitate water reabsorption to ensure water conservation (40).

Significantly, prior to oral water load and 4 hours after, that is under physiological conditions in the context of a sodium- and potassium-controlled diet, urinary hyaluronidase activity was positively correlated with SBP levels, which, in turn, were positively associated with the urinary AQP2/creatinine ratio at 0 and 40 min, corresponding to BP rise in response to the oral water load. As mentioned above, the role of AVP in hypertension development has long been debated. Although patients suffering from syndrome of inappropriate ADH secretion (SIADH) have normal BP levels (11) and some authors have found no differences in plasma AVP between normotensive and hypertensive subjects (12), others have shown that individuals with hypertension have significantly higher levels of urinary and circulating AVP, which positively correlate with DBP (7, 8, 14, 27). In addition, in a variety of rat models of hypertension, including spontaneously hypertensive and DOCA-salt sensitive rats, higher levels of AVP in urine and plasma, as well as increased pressor responsiveness to AVP, have been described (6). Notably, in these animals, the antidiuretic effect of AVP appears to be necessary to make possible the expansion of circulating volume upon which these hypertensive forms depend (6). In particular, according to Share and Crofton, for AVP to contribute to hypertension, the pressor responsiveness to it must be sufficiently high, which implies both increased vascular smooth muscle cell reactivity and impaired baroreceptor activity (6).

Thus, both the higher hyaluronidase activity levels and the increased AQP2 urinary shedding indicate that in men with a family history of hypertension, the kidneys' ability to excrete water in response to an oral load is reduced and/or impaired. In the long-term, this altered vasopressinergic response could lead to the blood volume expansion that contributes to hypertension development in its early stages, before the sodium and RAAS contribution becomes predominant. The lack of a positive linear correlation between SBP and hyaluronidase activity, or AQP2/creatinine ratio, observed in NT+ and HT men, could be consistent with the loss of the appropriate vasopressinergic system regulation. The resulting alterations in water balance might influence BP through two distinct pathways. Indeed, as previously proposed (18, 39), AVP could act in the renal medullary either by regulating the permeability of the apical membrane of the collecting duct principal cells through AQP2 translocation via V2 receptors, or by modifying the HA content in the interstitial matrix via V1 receptors. In particular, while the role of hyaluronidase activity would be primarily to provide conditions facilitating water flow, AQP2 channels could be recruited when higher water volumes need to be moved to rapidly restore water balance (Figure 7).

Despite the novel and innovative findings, our study has some limitations. First, we do not currently have measurements of plasma AVP levels, urine osmolarity, or urine sodium and potassium concentrations during the water load test, which could have been important for a more complete explanation of our results. Second, hyaluronidase activity was not assessed between 0 and 60 min after the oral water load, when BP increased and the AQP2/creatinine ratio began to drop. Third, women were excluded from our study, limiting the generalization of our findings. It is, however, well-known that the incidence and severity of hypertension are lower in females than in age-matched males due to the protective effects of estrogens, which beside acting on cardiovascular and renal systems, regulate the expression and secretion of AVP by the hypothalamic paraventricular nuclei (46). Recent data obtained in rats also demonstrate that estradiol prevents salt-dependent hypertension by suppressing salt-induced GABA-ergic excitation in AVP-secreting neurons, resulting in AVP secretion that plays a crucial role in the development and maintenance of hypertension in these animals (47). To avoid any potential misleading interpretation of our results, we thus decided to exclude women, including those of postmenopausal age. Indeed, as study subjects were young men aged 20 to 52 years, the inclusion of postmenopausal women would have introduced an additional potentially confounding factor related to age. Further, our sample size is quite limited, but to the best of our knowledge, our study is the first to assess hyaluronidase activity under hyperhydration conditions in men and to evaluate its relationship with BP regulation not only in hypertensive patients, but also in normotensive subjects with a family history of hypertension. In this regard, it is noteworthy that after a follow-up period of 8–11 years from the water load test, 30% of NT+ men were diagnosed as hypertensive compared to 14% of NT- men. This does not mean that all NT+ subjects will necessarily develop this disease during their lifetime. However, since the men's age at the follow-up ranged from 28 to 47 years, having both parents suffering from sustained hypertension is confirmed as a strong predisposing factor for the early development of arterial hypertension. Finally, since this is a noninterventional study, the associations we have pointed out allow us only to speculate about the potential role of AVP in BP regulation, but not to establish a causality link between the AVP-induced changes in HA metabolism and the predisposition to hypertension. Further confirmation of our hypotheses may come from data obtained under water deprivation conditions, which are currently being processed.

In conclusion, in our study we demonstrated for the first time the existence in men of a close association between urinary hyaluronidase activity and vasopressinergic system activation, expressed by serum copeptin levels and urinary AQP2/creatinine ratio. These findings confirm that HA handling is highly involved in renal water metabolism under the influence of AVP, which could play a key role

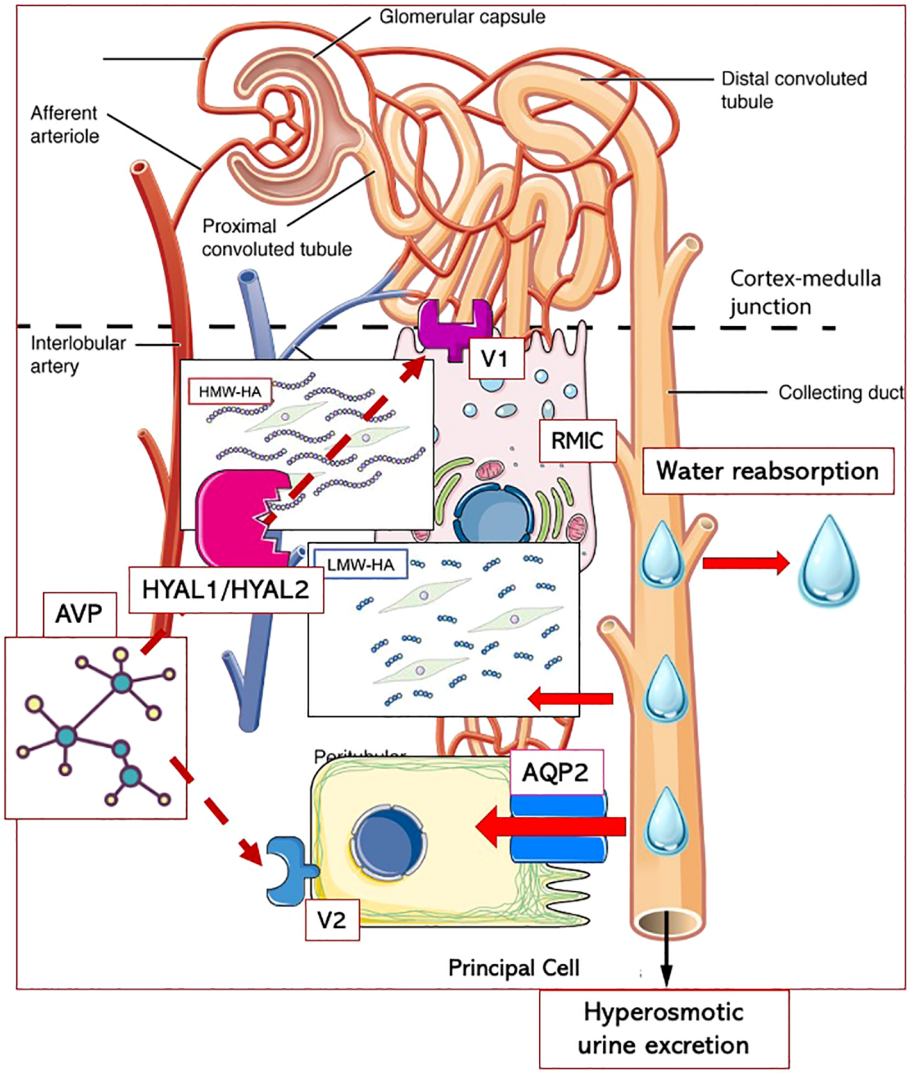

FIGURE 7
Putative interplay between AVP and hyaluronic acid metabolism in renal medullary interstitium. Arginin-Vasopressin (AVP) could act in the renal medullary through two distinct pathways: either by regulating the permeability of the apical membrane of the collecting duct principal cells through Aquaporin 2 (AQP2) translocation via V2 receptors, or by enhancing the activity of hyaluronidases (HYAL1/HYAL2) resulting in decreased content of high-molecular-weight hyaluronic acid (HMW-HA) in the interstitial matrix via V1 receptors. The degradation of HMW-HA into low-molecular-weight fragments (LMW-HA) would be essential to allow water diffusion from the tubules to the interstitium and, ultimately, to blood vessels. While hyaluronidase activity would primarily provide conditions facilitating water flow, AQP2 channels could be recruited when higher water volumes need to be moved to rapidly restore water balance. RMICs, renal medullary interstitial cells.

in BP regulation under both physiological and water-load conditions by alternatively targeting hyaluronidase activity and the AQP2 channel system. With the reservation of being confirmed in larger samples, our results contribute to shed light on the complex interactions involved in the endocrine regulation of BP and highlight some pathophysiological aspects that may be deeply implicated in hypertension susceptibility, paving the way for novel potential target to act upon in the early stages of hypertension development.

Data availability statement

The raw data supporting the conclusions of this article will be made available by the authors, without undue reservation.

Ethics statement

The studies involving humans were approved by Ethics Committee of University Hospital of Parma. The studies were conducted in accordance with the local legislation and institutional requirements. The participants provided their written informed consent to participate in this study.

Author contributions

AnC: Data curation, Investigation, Software, Writing – original draft, Writing – review & editing. AB: Conceptualization,

Datacuration, Writing – original draft, Writing – review & editing, Methodology, Software. IV: Conceptualization, Data curation, Investigation, Writing – review & editing. GF: Data curation, Investigation, Writing – original draft. VV: Data curation, Investigation, Writing – review & editing. PC: Data curation, Investigation, Writing – review & editing. AM: Conceptualization, Writing – review & editing, Methodology, Project, Resources, Supervision. AdC: Conceptualization, Data curation, Funding acquisition, Investigation, Writing – review & editing, Methodology, Project, Supervision.

Funding

The author(s) declare financial support was received for the research, authorship, and/or publication of this article. The study was supported by the Italian Ministry of University and Scientific Research (COFIN-CV2016_0008) and the P.A.R.I.D.E. Research Project grant (CV04/01-03) from University of Parma (Progetto di Ateneo per la Ricerca Scientifica Intra-Universitaria di Eccellenza). No other financial support was received for publication.

Acknowledgments

The authors thank Prof. Alberico Borghetti for the great knowledge given and the financial support provided, as well as the nursing staff of the Day Hospital ward of the Internal Medicine Department for their meticulous work carried out during the water load test.

Conflict of interest

The authors declare that the research was conducted in the absence of any commercial or financial relationships that could be construed as a potential conflict of interest.

Publisher's note

References

1. WHO. *World health organization hypertension* (2023). Available online at: https://www.who.int/news-room/fact-sheets/detail/hypertension.

2. Al Ghorani H, Götzinger F, Böhm M, Mahfoud F. Arterial hypertension - Clinical trials update 2021. *Nutr Metab Cardiovasc Dis*. (2022) 32:21–31. doi: 10.1016/j.numecd.2021.09.007

3. Klimczak D, Jazdzewski K, Kuch M. Regulatory mechanisms in arterial hypertension: role of microRNA in pathophysiology and therapy. *Blood Pressure*. (2017) 26:2–8. doi: 10.3109/08037051.2016.1167355

4. Guyton AC, Coleman TG, Cowley AW, Scheel KW, Manning RD, Norman RA. Arterial pressure regulation. *Am J Med*. (1972) 52:584–94. doi: 10.1016/0002-9343(72)90050-2

5. Warren AM, Grossmann M, Christ-Crain M, Russell N. Syndrome of inappropriate antidiuresis: from pathophysiology to management. *Endocrine Rev*. (2023) 44:819–61. doi: 10.1210/endrev/bnad010

6. Share L, Crofton JT. Contribution of vasopressin to hypertension. *Hypertension*. (1982) 4:III85–92. doi: 10.1161/01.HYP.4.5_Pt_2.III85

7. Cowley AW, Cushman WC, Quillen EW, Skelton MM, Langford HG. Vasopressin elevation in essential hypertension and increased responsiveness to sodium intake. *Hypertension*. (1981) 3:I93–100. doi: 10.1161/01.HYP.3.3_Pt_2.I93

8. Afsar B. Pathophysiology of copeptin in kidney disease and hypertension. *Clin Hypertens*. (2017) 23:13. doi: 10.1186/s40885-017-0068-y

9. Fernandes S, Bruneval P, Hagege A, Heudes D, Ghostine S, Bouby N. Chronic V2 vasopressin receptor stimulation increases basal blood pressure and exacerbates deoxycorticosterone acetate-salt hypertension. *Endocrinology*. (2002) 143:2759–66. doi: 10.1210/endo.143.7.8918

10. Cowley AW, Szczepanska-Sadowska E, Stepniakowski K, Mattson D. Chronic intravenous administration of V1 arginine vasopressin agonist results in sustained hypertension. *Am J Physiol*. (1994) 267:H751–756. doi: 10.1152/ajpheart.1994.267.2.H751

11. Padfield PL, Brown JJ, Lever AF, Morton JJ, Robertson JIS. Blood pressure in acute and chronic vasopressin excess: studies of Malignant hypertension and the syndrome of inappropriate antidiuretic hormone secretion. *N Engl J Med*. (1981) 304:1067–70. doi: 10.1056/NEJM198104303041803

12. Sladek CD, Blair ML, Mangiapane M. Evidence against a pressor role for vasopressin in spontaneous hypertension. *Hypertension*. (1987) 9:332–8. doi: 10.1161/01.HYP.9.4.332

13. Kawano Y. The role of vasopressin in essential hypertension plasma levels and effects of the V1 receptor antagonist OPC-21268 during different dietary sodium intakes. *Am J Hypertension*. (1997) 10:1240–4. doi: 10.1016/S0895-7061(97)00269-0

14. Bankir L, Bichet DG, Bouby N. Vasopressin V2 receptors, ENaC, and sodium reabsorption: a risk factor for hypertension? *Am J Physiol Renal Physiol*. (2010) 299:F917–928. doi: 10.1152/ajprenal.00413.2010

15. Cowley AW, Monos E, Guyton AC. Interaction of vasopressin and the baroreceptor reflex system in the regulation of arterial blood pressure in the dog. *Circ Res*. (1974) 34:505–14. doi: 10.1161/01.RES.34.4.505

16. Montani JP, Liard JF, Schoun J, Möhring J. Hemodynamic effects of exogenous and endogenous vasopressin at low plasma concentrations in conscious dogs. *Circ Res*. (1980) 47:346–55. doi: 10.1161/01.RES.47.3.346

17. Ginetzinsky AG. Role of hyaluronidase in the re-absorption of water in renal tubules: the mechanism of action of the antidiuretic hormone. *Nature*. (1958) 182:1218–9. doi: 10.1038/1821218a0

18. Stridh S, Palm F, Hansell P. Inhibition of hyaluronan synthesis in rats reduces renal ability to excrete fluid and electrolytes during acute hydration. *Upsala J Med Sci*. (2013) 118:217–21. doi: 10.3109/03009734.2013.834013

19. Hansell P, Göransson V, Odlind C, Gerdin B, Hällgren R. Hyaluronan content in the kidney in different states of body hydration. *Kidney Int*. (2000) 58:2061–8. doi: 10.1111/j.1523-1755.2000.00378.x

20. Kobayashi T, Chanmee T, Itano N. Hyaluronan: metabolism and function. *Biomolecules*. (2020) 10:1525. doi: 10.3390/biom10111525

21. Fallacara A, Baldini E, Manfredini S, Vertuani S. Hyaluronic acid in the third millennium. *Polymers*. (2018) 10:701. doi: 10.3390/polym10070701

22. Rügheimer L, Johnsson C, Maric C, Hansell P. Hormonal regulation of renomedullary hyaluronan. *Acta Physiol (Oxf)*. (2008) 193:191–8. doi: 10.1111/j.1748-1716.2007.01795.x

23. Ivanova LN, Babina AV, Baturina GS, Katkova LE. Effect of vasopressin on the expression of genes for key enzymes of hyaluronan turnover in Wistar Albino Glaxo and Brattleboro rat kidneys. *Exp Physiol*. (2013) 98:1608–19. doi: 10.1113/expphysiol.2013.073163

24. Bolignano D, Cabassi A, Fiaccadori E, Ghigo E, Pasquali R, Peracino A, et al. Copeptin (CTproAVP), a new tool for understanding the role of vasopressin in pathophysiology. *Clin Chem Lab Med (CCLM)*. (2014) 52(10):1447–56. doi: 10.1515/cclm-2014-0379

25. Verzicco I, Tedeschi S, Graiani G, Bongrani A, Carnevali ML, Dancelli S, et al. Evidence for a prehypertensive water dysregulation affecting the development of hypertension: results of very early treatment of vasopressin V1 and V2 antagonism in spontaneously hypertensive rats. *Front Cardiovasc Med*. (2022) 9:897244. doi: 10.3389/fcvm.2022.897244

26. Sladek CD, Somponpun SJ. Estrogen receptors: Their roles in regulation of vasopressin release for maintenance of fluid and electrolyte homeostasis. *Front Neuroendocrinol*. (2008) 29:114–27. doi: 10.1016/j.yfrne.2007.08.005

27. Velasquez MT, Skelton MM, Cowley AW. Water loading and restriction in essential hypertension. *Hypertension*. (1987) 9:407–14. doi: 10.1161/01.HYP.9.4.407

28. Botzki A, Rigden DJ, Braun S, Nukui M, Salmen S, Hoechstetter J, et al. l-ascorbic acid 6-hexadecanoate, a potent hyaluronidase inhibitor. *J Biol Chem*. (2004) 279:45990–7. doi: 10.1074/jbc.M406146200

29. Jordan J, Shannon JR, Black BK, Ali Y, Farley M, Costa F, et al. The pressor response to water drinking in humans: A sympathetic reflex? *Circulation*. (2000) 101:504–9. doi: 10.1161/01.CIR.101.5.504

30. Shannon JR, Diedrich A, Biaggioni I, Tank J, Robertson RM, Robertson D, et al. Water drinking as a treatment for orthostatic syndromes. *Am J Med*. (2002) 112:355–60. doi: 10.1016/S0002-9343(02)01025-2

31. Geelen G, Greenleaf JE, Keil LC. Drinking-induced plasma vasopressin and norepinephrine changes in dehydrated humans. *J Clin Endocrinol Metab*. (1996) 81:2131–5. doi: 10.1210/jcem.81.6.8964840

32. Callegaro CC, Moraes RS, Negrão CE, Trombetta IC, Rondon MU, Teixeira MS, et al. Acute water ingestion increases arterial blood pressure in hypertensive and normotensive subjects. *J Hum Hypertens*. (2007) 21:564–70. doi: 10.1038/sj.jhh.1002188

33. Madhavulu B, Mohan PR, Sreebhushan. RD. Acute effect of excess water intake on blood pressure in healthy Individuals. *Asian Pac J Health Sci*. (2014) 1:496–9. doi: 10.21276/apjhs

34. Gibbons CH, Schmidt P, Biaggioni I, Frazier-Mills C, Freeman R, Isaacson S, et al. The recommendations of a consensus panel for the screening, diagnosis, and treatment of neurogenic orthostatic hypotension and associated supine hypertension. *J Neurol*. (2017) 264:1567–82. doi: 10.1007/s00415-016-8375-x

35. In Sinn D, Gibbons CH. Pathophysiology and treatment of orthostatic hypotension in parkinsonian disorders. *Curr Treat Options Neurol*. (2016) 18:28. doi: 10.1007/s11940-016-0410-9

36. Raj SR, Biaggioni I, Black BK, Rali A, Jordan J, Taneja I, et al. Sodium paradoxically reduces the gastropressor response in patients with orthostatic hypotension. *Hypertension*. (2006) 48:329–34. doi: 10.1161/01.HYP.0000229906.27330.4f

37. Rügheimer L, Olerud J, Johnsson C, Takahashi T, Shimizu K, Hansell P. Hyaluronan synthases and hyaluronidases in the kidney during changes in hydration status. *Matrix Biol*. (2009) 28:390–5. doi: 10.1016/j.matbio.2009.07.002

38. Göransson V. Renomedullary interstitial cells in culture; the osmolality and oxygen tension influence the extracellular amounts of hyaluronan and cellular expression of CD44. *Matrix Biol*. (2001) 20:129–36. doi: 10.1016/S0945-053X(01)00129-9

39. Ivanova LN, Melidi NN. Effects of vasopressin on hyaluronate hydrolase activities and water permeability in the frog urinary bladder. *Pflugers Arch*. (2001) 443:72–7. doi: 10.1007/s004240100575

40. Göransson V, Johnsson C, Nylander O, Hansell P. Renomedullary and intestinal hyaluronan content during body water excess: a study in rats and gerbils. *J Physiol*. (2002) 542:315–22. doi: 10.1113/jphysiol.2001.014894

41. Stridh S, Kerjaschki D, Chen Y, Rügheimer L, Åstrand ABM, Johnsson C, et al. Angiotensin converting enzyme inhibition blocks interstitial hyaluronan dissipation in the neonatal rat kidney via hyaluronan synthase 2 and hyaluronidase 1. *Matrix Biol*. (2011) 30:62–9. doi: 10.1016/j.matbio.2010.09.006

42. Fraser JR, Laurent TC, Laurent UB. Hyaluronan: its nature, distribution, functions and turnover. *J Intern Med*. (1997) 242:27–33. doi: 10.1046/j.1365-2796.1997.00170.x

43. Comper WD, Laurent TC. Physiological function of connective tissue polysaccharides. *Physiol Rev*. (1978) 58:255–315. doi: 10.1152/physrev.1978.58.1.255

44. Hughes AK, Kohan DE. Mechanism of vasopressin-induced contraction of renal medullary interstitial cells. *Nephron Physiol*. (2006) 103:119–24. doi: 10.1159/000092245

45. Dzgoev SG. Selective V2-agonist of vasopressin desmopressin stimulates activity of serum hyaluronidase. *Bull Exp Biol Med*. (2015) 159:424–6. doi: 10.1007/s10517-015-2981-y

46. Grassi D, Marraudino M, Garcia-Segura LM, Panzica GC. The hypothalamic paraventricular nucleus as a central hub for the estrogenic modulation of neuroendocrine function and behavior. *Front Neuroendocrinol*. (2022) 65:100974. doi: 10.1016/j.yfrne.2021.100974

47. Jin X, Kim WB, Kim MN, Jung WW, Kang HK, Hong EH, et al. Oestrogen inhibits salt-dependent hypertension by suppressing GABAergic excitation in magnocellular AVP neurons. *Cardiovasc Res*. (2021) 117:2263–74. doi: 10.1093/cvr/cvaa271

frontiers | Frontiers in Endocrinology

TYPE Original Research
PUBLISHED 30 September 2024
DOI 10.3389/fendo.2024.1348854

OPEN ACCESS

EDITED BY
Zongli Diao,
Capital Medical University, China

REVIEWED BY
Aimee Hanson,
University of Cambridge, United Kingdom
Shivani Sharma,
Mercer University, United States

*CORRESPONDENCE
Guangyan Cai
caiguangyan@sina.com

†These authors have contributed equally to this work

RECEIVED 03 December 2023
ACCEPTED 03 September 2024
PUBLISHED 30 September 2024

CITATION
Liang Y, Liang S, Xie D, Guo X, Yang C, Xiao T, Zhuang K, Xu Y, Wang Y, Wang B, Zhang Z, Chen X, Chen Y and Cai G (2024) Causal effects of serum calcium, phosphate, and 25-hydroxyvitamin D on kidney function: a genetic correlation, pleiotropic analysis, and Mendelian randomization study. *Front. Endocrinol.* 15:1348854. doi: 10.3389/fendo.2024.1348854

Causal effects of serum calcium, phosphate, and 25-hydroxyvitamin D on kidney function: a genetic correlation, pleiotropic analysis, and Mendelian randomization study

Yanjun Liang[1,2,3†], Shuang Liang[2†], Dayang Xie[1,2], Xinru Guo[4], Chen Yang[4], Tuo Xiao[1], Kaiting Zhuang[1], Yongxing Xu[1], Yong Wang[2], Bin Wang[2,5,6], Zhou Zhang[1,2], Xiangmei Chen[2], Yizhi Chen[2,5,6] and Guangyan Cai[2*]

[1]Medical School of Chinese People's Liberation Army (PLA), Beijing, China, [2]Department of Nephrology, First Medical Center of Chinese People's Liberation Army (PLA) General Hospital, Nephrology Institute of the Chinese People's Liberation Army, State Key Laboratory of Kidney Diseases, National Clinical Research Center for Kidney Diseases, Beijing Key Laboratory of Kidney Disease Research, Beijing, China, [3]Department of Nephrology, Characteristic Medical Center of Chinese People's Armed Police Force, Tianjin, China, [4]School of Medicine, Nankai University, Tianjin, China, [5]Department of Nephrology, Hainan Hospital of Chinese Chinese People's Liberation Army (PLA) General Hospital, Academician Chen Xiangmei of Hainan Province Kidney Diseases Research Team Innovation Center, Sanya, China, [6]The Second School of Clinical Medicine, Southern Medical University, Guangzhou, China

Background: Existing studies investigating the impact of serum calcium (Ca), phosphate (P), 25 hydroxyvitamin D (25[OH]D), and parathyroid hormone (PTH) levels on kidney function have produced inconsistent results. Further research is needed to establish the direct causal relationship between these factors and kidney function.

Methods: The study used genome-wide association study datasets for exposure and outcome, mainly derived from the UK Biobank and CKDGen Consortium, with sample sizes ranging from 3,310 to 480,699 individuals of European ancestry. Heritability and genetic correlations among these phenotypes were assessed using linkage disequilibrium score regression (LDSC) and phenotypes with a heritability z-score <4 were excluded from further analyses. Pleiotropic analyses were performed to identify potential horizontal pleiotropic variants at gene and LD-independent locus levels. Mendelian randomization (MR) analysis, using instrumental variables (IVs) based on two distinct selection criteria, was conducted to investigate the potential causal relationships between serum Ca, P, 25(OH)D, PTH, and kidney function.

Results: PTH was excluded from further analysis due to a heritability z-score < 4. Genetic correlations were observed between serum Ca and urine albumin-to-creatinine ratio (UACR) (rg = 0.202, P-value = 5.0E−04), between serum 25(OH)D and estimated glomerular filtration rate using serum creatinine (eGFRcrea) (rg = -0.094; P-value = 1.4E−05), and between serum 25(OH)D and blood urea nitrogen (BUN) (rg = 0.127; P-value = 1.7E−06). In univariable MR analysis using IVs based on

two different selection criteria, it consistently demonstrated that genetically predicted serum Ca consistently showed an increase in UACR (beta 0.11, *P*-value 2.0E−03; beta 0.13, *P*-value 2.0E−04). Similarly, serum P was associated with a decrease in eGFRcrea (beta −0.01, *P*-value 2.0E−04; beta −0.005, *P*-value 2.0E−03) and an increase in BUN (beta 0.02, *P*-value 3.0E−03; beta 0.02, *P*-value 7.5E−07). The influence of serum P on kidney function was further supported in multivariable MR analysis. However, genetically predicted 25(OH)D did not have a significant impact on kidney function.

Conclusions: Elevated serum Ca or P levels could both impair kidney function, whereas 25(OH)D has no impact on renal function.

KEYWORDS

calcium, phosphate, 25-hydroxyvitamin D, parathyroid hormone, kidney function, Mendelian randomization, genetic correlation, pleiotropic analysis

Introduction

Chronic kidney disease (CKD) is a significant contributor to the global burden of non-communicable diseases. Its common complications, including calcium (Ca) and phosphate (P) metabolic disorders, 25-hydroxyvitamin D (25[OH]D) deficiency, and hyperparathyroidism, worsen with the decline of renal function. Several clinical studies have focused on the potential impact of these complications on kidney function. However, the results were inconsistent, which may mainly be due to the interference of confounders or mediators and the uncertainty regarding the occurrence of the exposure factors, i.e., whether these occurred before the outcome.

For instance, a retrospective cohort study provided evidence that higher serum Ca levels were associated with a reduced risk of kidney failure (1). Conversely, another study indicated that increased Ca intake led to elevated serum Ca and creatinine levels, irrespective of random vitamin D intake (2). Moreover, in individuals with hypoparathyroidism, it was observed that prolonged hypercalcemia resulting from vitamin D and Ca supplementation was linked to a decline in renal function (3). Similar inconsistencies have been observed in studies investigating the impact of serum P levels on kidney function (1, 4–6).

In terms of parathyroid hormone (PTH) and its role in kidney function, a retrospective cohort analysis found that PTH levels>50 pg/mL in patients with CKD 3–4 were associated with an escalating combined risk of death or renal replacement therapy (7). Furthermore, a Phase 3 PaTHway Trial examined the efficacy and safety of TransCon PTH replacement therapy in individuals with hypoparathyroidism. The study findings revealed that participants receiving TransCon PTH experienced an increase in mean estimated glomerular filtration rate using serum creatinine (eGFRcrea) from 67.5 to 75.6 mL min^{-1} per 1.73 m^2, whereas no significant change in eGFRcrea was observed in the placebo group. However, it was important to note that other factors influenced by medication administration complicated the assessment of the protective effect of PTH on renal function, which fell beyond the scope of this trial (8).

Randomized controlled trial (RCT), which was widely regarded as the gold standard for establishing causation, could still yield false positive or false negative results due to limitations in sample size, duration of follow-up, and potential interference from unknown confounders. For instance, an RCT involving 61 CKD stage 3–4 patients found that oral vitamin D analogs administered over 6 months reduced urinary protein levels, irrespective of renin–angiotensin system inhibitor use (9). However, another RCT with 43 CKD stage 3–4 patients, using similar treatments and follow-up duration, failed to support these findings (10). Additionally, a meta-analysis suggested that the administration of vitamin D receptor agonists decreased the eGFRcrea (11).

To address the limitations of clinical studies, a combination of genetic analyses can be employed. Linkage disequilibrium score (LDSC) regression allows for the assessment of single-nucleotide variant (SNV)-based phenotype heritability and co-heritability between two traits, playing a pivotal role in providing valuable etiological insights and aiding in the prioritization of potential causal relationships (12). Pleiotropy refers to the phenomenon of one mutation affecting multiple traits. This includes vertical pleiotropy, where one variant influences both traits in succession, reflecting the causal relationship between the two traits, and horizontal pleiotropy, independently influencing the two traits, merely reflecting the correlation between the two traits. Pleiotropy analyses quantify horizontal pleiotropic relationships at gene and LD-independent locus levels, aiding in the detection of potential horizontal pleiotropic variants to prevent false positives in subsequent Mendelian randomization (MR) analyses. MR analysis refers to an analytic approach for assessing the causality of an observed association between a modifiable exposure and a

clinically relevant outcome, focusing on the vertical pleiotropy relationship. Because MR exploits the fact that genotypes are not generally susceptible to reverse causation and confounding due to their fixed nature and Mendel's first and second laws of inheritance (13). Univariable MR estimates the total causal effect of the exposure on the outcome. On the other hand, multivariable MR extends the analysis to consider a set of potentially correlated candidate exposure factors (>1). It evaluates the direct causal effect of each exposure factor on the outcome while accounting for the other exposure factors (14).

To our knowledge, there have been univariable MR studies that have found no effect of 25(OH)D on kidney function (15). However, there is a noticeable research gap in the literature when it comes to MR studies investigating the impact of Ca, P, and PTH on kidney function, as well as the use of multivariable MR to estimate the causal effects of Ca, P, PTH, and 25(OH)D on kidney function. Our research aims to address this gap and provide evidence for clinical decision-making and future research directions.

Materials and methods

Genome-wide association study datasets

We searched for published genome-wide association studies (GWASs) evaluating individuals of European ancestry on the GWAS Catalog and PubMed (the last search was performed in September 2023). Summary statistics of Ca and P were obtained from the Neale Laboratory with a sample size of 315,153 UK Biobank participants (16). The median, decile 1, and decile 9 values for Ca were 2.376 mmol/L, 2.268 mmol/L, and 2.497 mmol/L, respectively, whereas for P, the corresponding values were 1.165 mmol/L, 0.954 mmol/L, and 1.363 mmol/L. Summary statistics of 25(OH)D traits with a sample size of 417,580, were obtained from the UK Biobank, and the median, mean, and interquartile range of 47.9 mmol/L, 49.6 mmol/L, and 33.5–63.2 nmol/L, respectively (17). Summary statistics of PTH from the INTERVAL study with a sample size of less than 5,000 were used, and the range of PTH was not publicly available (18).

Summary statistics for kidney function traits, including CKD, CKD_Rapid3, CKDi25, eGFRcrea, eGFRcys (estimated glomerular filtration rate using serum cystatin C), BUN (blood urea nitrogen), UACR (urinary albumin–creatinine ratio), and microalbuminuria (MA), were obtained from several published GWAS meta-analyses (19–22). CKD was defined as eGFRcrea of<60 mL min^{-1} per 1.73 m^2. CKD_Rapid3 was characterized by an annual eGFRcrea decline of 3 mL min^{-1} per 1.73 m^2 or more and CKDi25 represented a decline of 25% or more in eGFRcrea with a final eGFRcrea below 60 mL min^{-1} per 1.73 m^2, among individuals with an initial eGFRcrea exceeding 60 mL min^{-1} per 1.73 m^2. MA was defined as UACR > 25 mg/g in women and > 17 mg/g in men. The majority of individual studies included in these meta-analyses were population-based, with less than 10% originating from diabetic populations, representing less than 5% of the total population in each meta-analysis. The GWASs for CKD, CKD_Rapid3, CKDi25, eGFRcrea, eGFRcys, BUN, UACR, and MA, included a subset of participants, representing 0.16%, 5.8%, 7.7%, 0.16%, 0.16%, 0.16%, 0%, and 0% respectively, from the UK Biobank. These subsets of participants overlapped with those included in GWAS analyses for other exposure factors. Detailed information regarding these studies can be found in Supplementary Table S1 or by referring to the original studies.

As all these GWASs were approved by their respective local research ethics committees and institutional review boards, no additional ethical approval was necessary for this study.

LDSC regression analysis

LDSC regression regressed SNV GWAS $\chi 2$ statistics for one phenotype to infer SNV-based heritability (h2) or $\chi 2$ statistics cross products for a pair of phenotypes to infer SNV-based coheritability on LDSC scores (23). To ensure sufficient statistical power, only phenotypes with a heritability z-score > 4, indicating a substantial proportion of phenotype variance explained by heredity, were included in subsequent analyses. The presence of an intercept close to 1, indicating polygenicity rather than population stratification or cryptic relatedness among samples, accounted for the majority of the observed increase in mean $\chi 2$ statistics. The LDSC v1.0.1 software (https://github.com/bulik/ldsc) was employed for this purpose.

Pleiotropic analyses

Pleiotropy at the gene level

Firstly, we assigned SNPs from GWAS summary statistics to genes via an annotation window of ±500 kb flanking the gene boundaries derived from the matched Ensembl build GRCh37 and 1000 G data (24) and then calculated *P*-values for each gene using the multimarker analysis of genomic annotation (MAGMA) v1.09 software (https://ctg.cncr.nl/software/magma) (25). A gene was considered related to a trait if the *P*-value was less than 0.05/the number of all annotated genes or five/the number of all annotated genes (if the number of significant genes was less than five). The next step was to calculate the proportion of genes that were simultaneously associated with both exposure factors and outcomes compared with the total number of genes associated with exposure factors. Additionally, we identified that the SNPs within these genes exhibited horizontal pleiotropy.

Pleiotropy at the level of LD-independent loci

The analysis employed the GWAS-PW v2.0.1 software (https://github.com/joepickrell/gwas-pw) (26), and posterior probabilities (PPA) were calculated for 1,703 predefined LD-independent loci (27) to support four scenarios for each locus: [i] the association only to exposure factor (PPA1), [ii] the association only to outcome (PPA2), [iii] shared association to both exposure and outcome via the same SNP (PPA3), and [iv] shared association to exposure and outcome but via two distinct SNPs (PPA4). A PPA3 ≥ 0.9 was used to define a pleiotropic-associated locus. The proportion of the independent loci that influenced the exposure factor also

influenced the outcome (ppa3/[ppa1+ppa3+ppa4]) was calculated to determine the possibility of pleiotropy between each exposure and outcome. SNPs meeting the threshold of the third scenario were considered potential horizontal pleiotropic SNPs.

Two-sample Mendelian randomization analyses

Assumptions

The MR analysis (Figure 1) was based on the following assumptions: the genetic variants used as instrumental variables (IVs) were associated with the exposure factor; the genetic variants were not associated with any confounders; and the genetic variants were associated with kidney traits through the exposure factor only, namely, non-horizontal pleiotropic variants. Although a direct test for the latter two assumptions was impossible, the analysis methods introduced below could relax these assumptions, serving as a sensitivity analysis.

Univariable Mendelian randomization analysis

The first step in univariable MR analysis was to construct effective IVs. As some exposure factors had a limited number of candidate IVs (*P*-value < 5E−08) or more than 65% of those (*P*-value < 5E−08) were not available in the GWAS results of the specific outcome, a relatively relaxed significance threshold was set at 5E−06 to improve statistical power. Hence, the first assumption of MR was satisfied. Subsequently, these IVs were grouped based on the 1000 Genomes Project LD structure and independent SNPs (R2 < 0.001 with any other SNP within 10,000 kb) with the most significant *P*-value. Moreover, to satisfy the latter two assumptions as much as possible, IVs associated with known confounders, such as hypertension, diabetes mellitus, lipid traits, body mass index, and gout, available at http://www.phenoscanner.medschl.cam.ac.uk/, were excluded. Following the removal of palindromic SNVs with intermediate allele frequencies, the IVs related to kidney traits (*P*-value [kidney traits] < *P*-value [exposure factors]), and weak IVs with an F value (beta2/se2) of <10, the initially selected IVs were constructed.

The next step was to perform an MR analysis with the initially selected IVs. In the absence of heterogeneity and pleiotropy, the IVW (inverse variance weighted) method combined information on all uncorrelated IVs into a single causal estimate with larger weights given to more precise IVs based on their inverse variances. In particular, the IVW radial as the main approach improved the performance of the IVW estimate and Cochran's Q statistics by using modified second-order weights (28). Heterogeneity was checked with the Cochran Q test and pleiotropy was tested with MR-Egger. The median-based and median-based approaches were conducted as a supplement given significant heterogeneity, whereas the Robust Adjusted Profile Score (RAPS) (29), which addressed idiosyncratic pleiotropy by robustifying the adjusted profile score, and MR-Egger were conducted as a supplement given significant

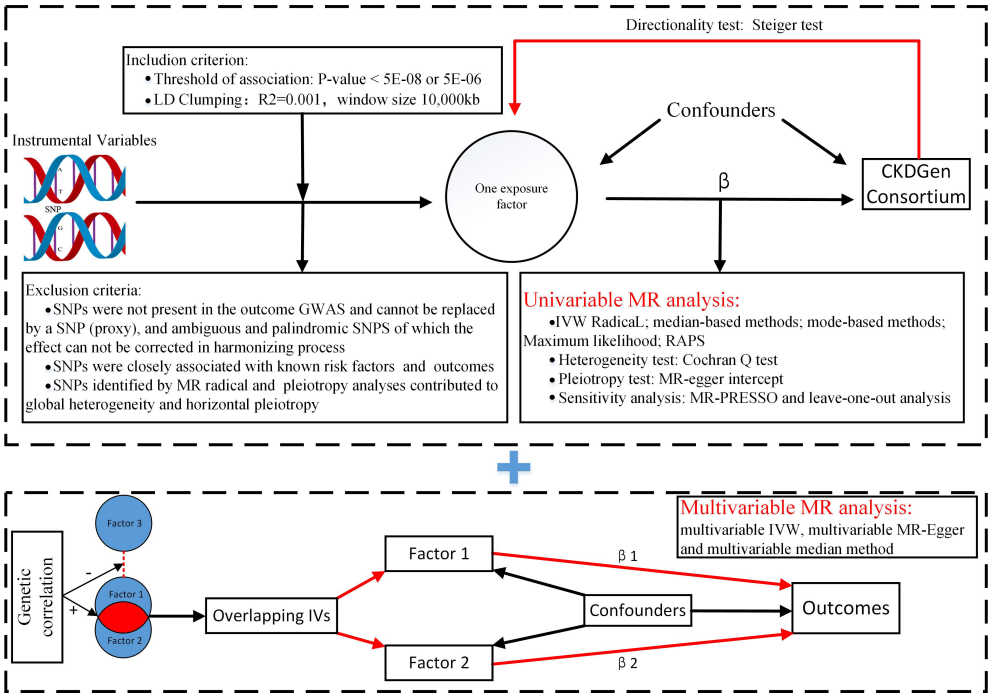

FIGURE 1
Flowchart of Mendelian randomization analysis. MR, Mendelian randomization; IVW, inverse variance weighted; RAPS, Robust Adjusted Profile Score; MR-PRESSO, Mendelian randomization pleiotropy residual sum and outlier; Lasso regression, least absolute shrinkage and selection operator regression.

pleiotropy. Causal directionality was evaluated with the Steiger test (30). The symmetrical funnel plot was generated to identify bias. Additionally, sensitivity analyses were conducted, such as the leave-one-out analysis with the IVW method to check whether the overall estimate was driven by a single SNP. In instances of substantial heterogeneity, the Mendelian Randomization Pleiotropy Residual Sum and Outlier (MR-PRESSO) method was employed for sensitivity analysis. This approach assessed heterogeneity by iteratively excluding each variant to identify horizontal pleiotropic outliers using the Residual Sum of Squares (RSS) (global test). Moreover, the method addressed horizontal pleiotropy by eliminating outliers and examined for significant differences in causal estimates before and after outlier removal (distortion test). When the global test results were significant, the corrected results of MR-PRESSO were considered more reliable than the raw results of that (31).

To further mitigate the risk of false positives, global heterogeneity, and reverse causality, pleiotropic SNPs identified from the pleiotropic analyses, outliers detected by IVW radial (28), and IVs potentially associated with kidney traits (with a *P*-value [kidney traits] < 0.05 if the IV threshold was 5E−08) were excluded to establish the final set of IVs. Subsequently, a new MR analysis was conducted using these final IVs, and the results were compared with those obtained using the initially selected IVs.

Multivariable Mendelian randomization analysis

The multivariable MR analysis included sets of exposure factors that exhibited genetic correlations among them. IVs were constructed by using multiple sets of overlapping SNPs from the GWASs for relevant exposure factors, which met the univariable MR inclusion criteria described previously. In the absence of heterogeneity and pleiotropy, the multivariable IVW method was the primary choice. If pleiotropy was detected, the multivariable Egger method was used, whereas the multivariable median method was recommended for addressing heterogeneity. Similar to univariable MR, we conducted multivariable MR analyses before and after removing pleiotropic SNPs.

The MR analyses mentioned were conducted using R software v4.1.0 and the following R packages: "TwoSampleMR" v0.5.5, "RadialMR" v2.2.1, and "MendelianRandomization" v0.4.4. The significance threshold for MR analyses mentioned was set at *P*-value = 0.05/12 = 4.2E−03 with Bonferroni correction applied due to the multiple testing (3 exposures × 4 outcomes = 12 tests).

Results

LDSC regression

Phenotypes with z-scores < 4, including PTH, CKD_Rapid3, CKDi25, eGFRcys, and MA, were excluded from subsequent analyses (Table 1). Genetic correlations were observed between serum 25(OH)D and eGFRcrea (rg −0.094; *P*-value 1.4E−05), as well as BUN (rg 0.127; *P*-value 1.7E−06). Serum Ca showed a significant genetic correlation with UACR (rg 0.202, *P*-value 5.0E−04). However, there was no statistically significant genetic correlation between serum P and CKD (*P*-value 0.03). Among the exposure factors, only serum 25(OH)D was correlated with serum P (rg 0.076; *P*-value 0.002) (Table 2).

Pleiotropic analyses

The characteristics of the annotated genes and related LD-independent loci are described in Supplementary Tables S2 and S3.

TABLE 1 LDSC regression estimates of all exposure factors and kidney traits.

Phenotype	Study design	Sample size	h^2 estimate (SE)	Z-score
Calcium	Population-based	315,153	0.115 (0.010)	11.5
Phosphate	Population-based	315,153	0.108 (0.01)	10.8
25-hydroxyvitamin D	Population-based	417,580	0.096 (0.014)	6.9
Parathyroid hormone	Population-based	3,310	0.137 (0.122)	1.1*
CKD	Meta-analysis	480,698	0.010 (0.001)	10.0
CKD_Rapid3	Meta-analysis	141,964	0.009 (0.003)	3.0*
CKDi25	Meta-analysis	195,145	0.010 (0.0022)	4.5*
eGFRcrea	Meta-analysis	567,460	0.071 (0.004)	17.8
eGFRcys	Meta-analysis	24,061	0.134 (0.055)	2.4*
BUN	Meta-analysis	243,029	0.064 (0.005)	12.8
UACR	Meta-analysis	54,450	0.046 (0.008)	5.8
MA	Meta-analysis	54,116	0.014 (0.007)	2.0*

LDSC, linkage disequilibrium score; h^2, heritability; CKD, chronic kidney disease; eGFRcrea, estimated glomerular filtration rate using serum creatinine; eGFRcys, estimated glomerular filtration rate using serum cystatin C; BUN, blood urea nitrogen; UACR, urinary albumin-to-creatinine ratio; MA, microalbuminuria.
aλGC refers to the genomic inflation factor. *Z-score < 4.

Figure 2 illustrates the proportion of horizontally pleiotropic genes for each exposure among all the genes associated with that particular exposure, as well as the percentage of horizontally pleiotropic LD-independent loci for each exposure among all the loci associated with that exposure. The potential pleiotropic SNPs located within the pleiotropic genes or loci are presented in Supplementary Table S4.

Two-sample Mendelian randomization analysis

Due to the unavailability of more than 65% of candidate IVs with a *P*-value less than 5E−08 in the GWAS results of UACR, a relatively relaxed significance threshold of 5E−06 was adopted when investigating UACR as the outcome.

TABLE 2 Genetic correlation estimates from LDSC regression.

Exposure	Outcome	rg (se)	rg intercept (se)	*P*-value
Calcium	Phosphate	−0.080 (0.049)	0.186 (0.013)	0.10
	25(OH)D	0.032 (0.024)	0.058 (0.010)	0.18
	CKD	0.010 (0.052)	0.016 (0.007)	0.85
	eGFRcrea	0.002 (0.029)	−0.013 (0.009)	0.95
	BUN	−0.034 (0.036)	0.023 (0.008)	0.34
	UACR	0.202 (0.058)	−0.002 (0.006)	5.0E−04*
25(OH)D	Calcium	0.032 (0.024)	0.058 (0.010)	0.18
	Phosphate	0.076 (0.025)	0.039 (0.008)	0.002*
	CKD	0.071 (0.042)	0.009 (0.007)	0.10
	eGFRcrea	−0.094 (0.022)	−0.019 (0.009)	1.4E−05*
	BUN	0.127 (0.027)	0.009 (0.007)	1.7E−06*
	UACR	0.006 (0.052)	−0.004 (0.007)	0.91
Phosphate	Calcium	−0.080 (0.049)	0.186 (0.013)	0.10
	25(OH)D	0.076 (0.025)	0.039 (0.008)	0.002
	CKD	−0.118 (0.055)	0.009 (0.007)	0.03
	eGFRcrea	0.057 (0.035)	−0.006 (0.009)	0.10
	BUN	0.041 (0.037)	0.003 (0.008)	0.27
	UACR	−0.037 (0.060)	0.002 (0.006)	0.54

LDSC, linkage disequilibrium score; 25-hydroxyvitamin D, 25(OH)D; CKD, chronic kidney disease; eGFRcrea, estimated glomerular filtration rate using serum creatinine; BUN, blood urea nitrogen; UACR, urinary albumin-to-creatinine ratio; rg, reflects the strength of the genetic relationship between the traits.
*P-value < 4.2E−03.

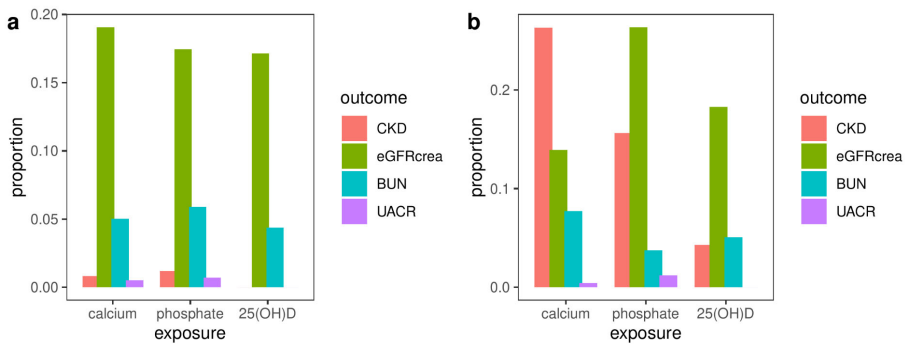

FIGURE 2
The proportion of horizontally pleiotropic genes **(A)** or loci **(B)** for each exposure among all the genes or loci associated with that particular exposure. CKD, chronic kidney disease; eGFRcrea, estimated glomerular filtration rate using serum creatinine; BUN, blood urea nitrogen; UACR, urinary albumin-to-creatinine ratio.

Univariable Mendelian randomization analysis

The characteristics of the initially selected effective IVs after removing confounding IVs (Supplementary Table S4), and the final set of effective IVs chosen after additional elimination of pleiotropic IVs (Supplementary Table S5), outliers (Supplementary Table S6), and IVs associated with the outcome, were detailed in Supplementary Tables S5–S30. Over 85% of the variants overlapped between outliers and IVs associated with the outcome.

There was no evidence of a violation of the causal directionality assumption in any of the univariable MR analyses (Supplementary Tables S31, S32). Initially selected IVs exhibited widespread heterogeneity but no evidence of horizontal pleiotropy. Upon using the finally selected IVs, the heterogeneity disappeared. However, horizontal pleiotropy was only evident for the relationship between 25(OH)D and BUN (*P*-value 0.04) (Supplementary Tables S33–S36). Although the global test of MR-PRESSO identified horizontal pleiotropic outliers only with initially selected IVs, except for the relationships involving Ca or 25(OH)D and UACR, the distortion test did not reveal significant differences in causal estimates before and after the removal of outliers (Supplementary Tables S37, S38). All symmetrical funnel plots indicated no disproportionate effects from selected IVs (Supplementary Figures S1–S4).

None of the MR analysis methods found any exposure factors associated with higher odds of CKD after the Bonferroni correction (*P*-value>4.2E-03) (Supplementary Tables S39, 40 and Supplementary Figures S5, S6).

In the analysis conducted with the initially selected IVs (Supplementary Table S41), the primary method, weighted median, supported both the associations between P and eGFRcrea (beta −0.01; *P*-value 2.0E−04), as well as between Ca and eGFRcrea (beta 0.009; *P*-value 8.0E−04). This finding was further confirmed by the main sensitivity analysis, MR-PRESSO (Figure 3) (Supplementary Table S37), rather than the leave-one-out analysis

a

Exposure&Outcome	Method	nSNPs	Beta(95%CI)	P−value
Calcium				
UACR	IVW radial	328−316−109	0.11(0.032,0.188)	2.0E−03
	MR−PRESSO(raw)	328−316−109	0.11(0.032,0.188)	2.0E−03
Phosphate				
eGFRcrea	Weighted median	160−152−128	−0.01(−0.016,−0.004)	2.0E−04
	Weighted mode	160−152−128	−0.009(−0.013,−0.005)	5.1E−05
	MR−PRESSO(corrected)	160−152−128	−0.01(−0.014,−0.006)	1.5E−06
BUN	Weighted median	160−152−126	0.02(0.008,0.032)	3.0E−03
	Weighted mode	160−152−126	0.02(0.01,0.03)	9.5E−05
	MR−PRESSO(corrected)	160−152−126	0.02(0.012,0.028)	1.0E−04
25(OH)D				
eGFRcrea	Weighted median	115−95−91	−0.003(−0.007,0.001)	0.09
	Weighted mode	115−95−91	−0.004(−0.006,−0.002)	0.01
	MR−PRESSO(corrected)	115−95−91	−0.005(−0.009,−0.001)	4.0E−03
BUN	Weighted median	115−95−92	0.006(−0.002,0.014)	0.13
	Weighted mode	115−95−92	0.006(0,0.012)	0.08
	MR−PRESSO(corrected)	115−95−92	0.009(0.001,0.017)	0.05

P−value < 4.2E−3 was considered statistically significant

b

Exposure&Outcome	Method	nSNPs	Beta(95%CI)	P−value
Calcium				
UACR	IVW radial	328−316−109−105	0.13(0.071,0.189)	2.0E−04
	MR−PRESSO(raw)	328−316−109−105	0.13(0.071,0.189)	3.0E−04
Phosphate				
eGFRcrea	IVW radial	160−152−128−78	−0.005(−0.01,0)	2.0E−03
	MR−PRESSO(raw)	160−152−128−78	−0.005(−0.009,−0.001)	2.0E−03
BUN	IVW radial	160−152−126−94	0.02(0.01,0.03)	7.5E−07
	MR−PRESSO(raw)	160−152−126−94	0.02(0.012,0.028)	3.3E−06
25(OH)D				
eGFRcrea	IVW radial	115−95−91−57	−0.003(−0.01,0)	0.11
	MR−PRESSO(raw)	115−95−91−57	−0.003(−0.007,0.001)	0.11
BUN	MR Egger	115−95−92−65	0.003(0,0.01)	0.45
	RAPS	115−95−92−65	0.008(0,0.01)	0.01
	MR−PRESSO(raw)	115−95−92−65	0.008(0.002,0.014)	4.0E−03

P−value < 4.2E−3 was considered statistically significant

FIGURE 3
The results of univariable Mendelian randomization analysis of calcium, phosphate, or 25(OH)D−eGFRcrea, BUN, or UACR. **(A)** Using the initially selected IVs; **(B)** using the finally selected IVs. 25(OH)D, 25-hydroxyvitamin D; eGFRcrea, estimated glomerular filtration rate using serum creatinine; BUN, blood urea nitrogen; UACR, urinary albumin-to-creatinine ratio; IVW, inverse variance weighted; RAPS, Robust Adjusted Profile Score; MR-PRESSO, Mendelian randomization pleiotropy residual sum and outlier. The four numbers in the nSNP column represent the remaining IVs after each IV selection step: step 1—threshold of association and LD clumping, step 2—harmony and excluding palindromic SNPs, step 3—deleting IVs with outcome correlation *P*-value less than exposure correlation *P*-value, step 4—removing pleiotropic SNPs, outliers detected by IVW radical, and IVs potentially associated with kidney traits (with a *P*-value [kidney traits] < 0.05 if the IV threshold was 5E−08).

(Supplementary Figure S7). In the analysis utilizing the finally selected IVs (Supplementary Table S42), the IVW radial method consistently affirmed the association between P and eGFRcrea (beta −0.005; *P*-value 2.0E−03), supported by sensitivity analyses with MR-PRESSO (Figure 3) and leave-one-out analysis (Supplementary Figure S8).

Causal estimates for BUN (Supplementary Tables S43, 44) indicated that with the initially selected IVs, only higher serum P was linked to a higher BUN, as evidenced by the weighted median (beta 0.02; *P*-value 3.0E−03), as well as sensitivity analyses using the MR-PRESSO (Figure 3) and the leave-one-out analysis (Supplementary Figure S9). Furthermore, in the analysis with the final IV selection, the primary analysis method, IVW radial approach, also validated the causal relationship between P and BUN (beta 0.02; *P*-value 7.5E−07), supported by sensitivity analyses using MR-PRESSO (Figure 3) and leave-one-out analysis (Supplementary Figure S10).

Regarding UACR (Supplementary Tables S45, S46), in the analysis using either the initially selected or the finally selected IVs, it was found that only genetically predicted higher Ca was related to the increase in UACR, as confirmed by the IVW radial method (beta 0.11, *P*-value 2.0E−03; beta 0.13, *P*-value 2.0E−04) and sensitivity analyses using the MR-PRESSO (Figure 3) and the leave-one-out analysis (Supplementary Figures S11, S12).

Multivariable Mendelian randomization analysis

The concurrent utilization of serum P and 25(OH)D as exposure variables in a multivariable MR analysis was driven by the identified genetic correlation between the two. The characteristics of the selected SNPs after excluding confounding IVs (Supplementary Table S47) and those finally selected after further removing pleiotropic IVs (Supplementary Table S48) are detailed in Supplementary Tables S49–S54. Both the initial and final IV sets showed extensive heterogeneity but no evidence of horizontal pleiotropy (Supplementary Tables S55, S56). The multivariable median method considered as the main method only showed that the associations between serum P and eGFRcrea or BUN were still significant (*P*-value < 4.2E-03) (Figure 4), regardless of the exclusion of pleiotropic IVs, consistent with the results in univariable MR analysis.

Discussion

Controversy exists regarding whether serum Ca, P, 25(OH)D, and PTH contribute to the deterioration of renal function, and clarifying these associations is essential for both nephrologists and the general population.

a

Exposure&Outcome	Method	nSNPs	Beta(95%CI)	P−value
Phosphate				
eGFRcrea	Multivariable IVW	187−181−169	−0.006(−0.01,−0.0008)	0.02
	Multivariable MR Egger	187−181−169	−0.006(−0.01,−0.0007)	0.02
	Multivariable median	187−181−169	−0.009(−0.01,−0.004)	2.0E−04
BUN	Multivariable IVW	187−185−178	0.02(0.010,0.03)	6.6E−05
	Multivariable MR Egger	187−185−178	0.02(0.010,0.03)	6.6E−05
	Multivariable median	187−185−178	0.02(0.008,0.03)	6.0E−04
25(OH)D				
eGFRcrea	Multivariable IVW	187−181−169	−0.005(−0.010,−0.0002)	0.04
	Multivariable MR Egger	187−181−169	−0.005(−0.01,0.0005)	0.04
	Multivariable median	187−181−169	−0.003(−0.007,0.0010)	0.14
BUN	Multivariable IVW	187−185−178	0.009(0.0007,0.02)	0.03
	Multivariable MR Egger	187−185−178	0.009(−0.0007,0.02)	0.03
	Multivariable median	187−185−178	0.008(−0.0003,0.02)	0.06

P−value < 4.2E−3 was considered statistically significant

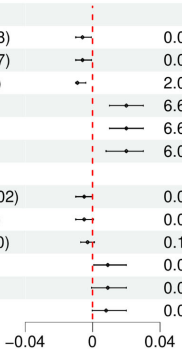

b

Exposure&Outcome	Method	nSNPs	Beta(95%CI)	P−value
Phosphate				
eGFRcrea	Multivariable IVW	187−181−169−168	−0.006(−0.011,−0.001)	0.02
	Multivariable MR Egger	187−181−169−168	−0.006(−0.011,−0.001)	0.03
	Multivariable median	187−181−169−168	−0.009(−0.014,−0.004)	0
BUN	Multivariable IVW	187−185−178−177	0.019(0.01,0.029)	0
	Multivariable MR Egger	187−185−178−177	0.019(0.01,0.029)	0
	Multivariable median	187−185−178−177	0.018(0.008,0.029)	1.0E−03
25(OH)D				
eGFRcrea	Multivariable IVW	187−181−169−168	−0.005(−0.01,0)	0.04
	Multivariable MR Egger	187−181−169−168	−0.005(−0.01,0.001)	0.08
	Multivariable median	187−181−169−168	−0.003(−0.007,0.001)	0.14
BUN	Multivariable IVW	187−185−178−177	0.009(0.001,0.018)	0.03
	Multivariable MR Egger	187−185−178−177	0.009(−0.001,0.019)	0.07
	Multivariable median	187−185−178−177	0.008(0,0.016)	0.06

P−value < 4.2E−3 was considered statistically significant

FIGURE 4
The results of multivariable Mendelian randomization analysis of serum phosphate and 25(OH)D−eGFRcrea or BUN. **(A)** Using the initially selected IVs; **(B)** using the finally selected IVs. IVW, inverse variance weighted; 25(OH)D, 25-hydroxyvitamin D; eGFRcrea, estimated glomerular filtration rate using serum creatinine; BUN, blood urea nitrogen. The four numbers in the nSNP column represent the remaining IVs after each IV selection step: step 1—threshold of association and LD clumping, step 2—harmony and excluding palindromic SNPs, step 3—deleting IVs with outcome correlation *P*-value less than exposure correlation *P*-value, step 4—removing pleiotropic SNPs.

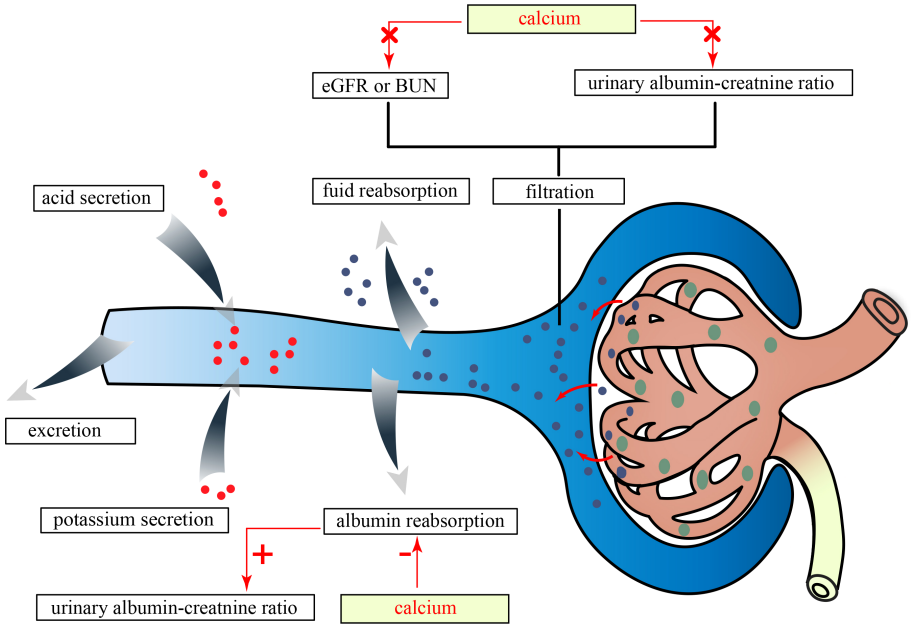

FIGURE 5
The effects of serum Ca on kidney traits in this study. eGFRcrea, estimated glomerular filtration rate using serum creatinine; BUN, blood urea nitrogen; Ca, calcium; P, phosphate.

Although genetic correlations between 25(OH)D and eGFRcrea or BUN were significant, both univariable and multivariable MR analyses in our study indicated that these correlations did not represent causal relationships. This finding was consistent with a previous MR study (15) that only conducted univariable MR analysis. The reason behind this lack of causality can be attributed to the fact that the serum 25(OH)D levels were associated with various health conditions beyond serum Ca and P levels, including diseases closely related to renal function such as glucose metabolism disorders, weight gain, infectious diseases, immune function, and cancer (32). The extensive phenotypic effects of genetic variants in the GWAS data for 25(OH)D that did not meet the threshold for MR resulted in the genetic correlation between 25(OH)D and kidney function. Similarly, clinical studies influenced or mediated by these conditions may not yield reliable results.

Interestingly, our findings revealed a causal and detrimental relationship between serum Ca and UACR, but no such relationship was observed with BUN. Despite the absence of genetic correlations between serum Ca and eGFRcrea, the use of initially selected IVs in MR analysis, rather than finally selected IVs, supported this causal effect. Notably, a high proportion (92.5%) of outliers identified by the IVW radical among the initially selected IVs were potentially associated with the outcome (P-value < 0.05), suggesting potential bias if these IVs were included in the MR analysis. Moreover, excluding these outcome-related IVs led to non-significant results (nSNPs 112, beta 0.002, P-value 0.20) aligning with the analysis with finally selected IVs. Consequently, the causal effect of Ca on eGFRcrea cannot be conclusively established.

Considering the evidence that the normal kidney filtered nephrotic levels of albumin retrieved by proximal tubule cells (33), our findings suggested that serum Ca might only damage the albumin reabsorption function of PTEC instead of the surface area of the glomerular capillary wall, and its permeability to small solutes and water mainly determined eGFRcrea and BUN (Figure 5). *In vitro* studies have shown that elevated extracellular Ca for 18 h–20 h could induce damage in human PTEC (34). Another study demonstrated that high Ca levels for 24 h, through the activation of reactive oxygen species derived from nicotinamide adenine dinucleotide phosphate oxidase subunit 4 via protein kinase C, caused oxidative stress damage and apoptosis in PTECs (35). However, short-term activation of PTEC-specific CaSR (calcium-sensing receptor) by perfusion with varying Ca concentrations for 2 to 8 min only enhances fluid reabsorption without causing damage (36). These findings suggested that the duration of high Ca exposure had different effects on PTECs. *In vivo*, a study suggested that long-term inactivation of CaSR may protect renal function. Specifically, treatment with the CaSR antagonist ronacaleret for 3 months can help maintain the expression of klotho and nephrin, preserve renal function, and reduce serum P and proteinuria in rats with 5/6 nephrectomy without affecting blood pressure, PTH, 1,25(OH)D, or serum Ca levels (37). However, another study supporting the renal protective effects of CaSR activation showed that cinacalcet reduced toxin-induced proteinuria and glomerular damage in mice on the 10th and 12th days after a 2-day administration (38). We speculated that this protective effect might be due to decreased renin activity induced by acute CaSR activation with 2-day treatment, which was independent of PTH and could not be induced by chronic CaSR activation over 7 days in juxtaglomerular cells (39). Based on the results of our MR analyses and in consideration of prior research,

we speculated that long-term elevation of serum Ca may impair kidney function through the activation of CaSR.

Research conducted on animal models of CKD has provided substantial evidence for a significant association between the intake of dietary P and the progression of CKD (40, 41). Previous studies have found that the mediation of serum P signaling by type III sodium-dependent phosphate transporters occurred independently of their P transport function, possibly involving downstream modulation of ERK signaling, thereby contributing to glomerular damage (42). Our study employing univariable MR analysis and multivariable MR analysis in conjunction with 25(OH)D has consistently supported the causal effect of serum P on eGFRcrea or BUN. Nevertheless, the effect size (beta −0.005) was relatively small, indicating that larger sample sizes and longer follow-up durations may be required to achieve sufficient statistical power in RCT. This could explain why the effects of serum P on kidney function have not been observed in an RCT with 31 participants and a 3-week follow-up period (43).

There were some limitations in the present study: (1) Our findings may not be generalizable to other ancestries due to the GWAS dataset being sourced solely from European populations; (2) due to low heritability, several related traits could not be included in the MR analysis using existing GWAS studies; (3) despite efforts to mitigate population specificity, population stratification, and potential sample overlap, it was not possible to completely eliminate these factors; (4) our findings have not been verified through experimental studies, as this was beyond the scope of our study. Therefore, further research should be designed to address these limitations.

Conclusions

Based on the genetic analyses conducted in our study, it was crucial to closely monitor serum Ca levels to prevent potential kidney toxicity resulting from elevated serum Ca during the administration of Ca supplements or vitamin D therapy. Additionally, it was important to acknowledge the progressive decline in residual renal function that can occur due to high serum phosphate levels. Finally, there is no evidence to suggest that vitamin D analogs directly improve renal function.

Data availability statement

The original contributions presented in the study are included in the article/Supplementary Material. Further inquiries can be directed to the corresponding author.

Author contributions

YL: Conceptualization, Formal Analysis, Methodology, Writing – original draft. SL: Methodology, Writing – original draft, Writing – review & editing. DX: Methodology, Software, Writing – review & editing. XG: Software, Writing – review & editing. CY: Writing – review & editing. TX: Writing – review & editing. KZ: Writing – review & editing. YX: Writing – review & editing. YW: Writing – review & editing. BW: Writing – review & editing. ZZ: Writing – review & editing. XC: Writing – review & editing. YC: Writing – review & editing. GC: Writing – review & editing.

Funding

The author(s) declare that financial support was received for the research, authorship, and/or publication of this article. This work was supported by the Natural Science Foundation of China (NSFC) (82170686 and 82000675), the National Key Research and Development Program of China (2022YFC3602900), the Grant for GYC (22KJLJ001), the National Key Technology R&D Program (2018YFA0108800), the Science and Technology Project of Beijing (D181100000118004), and the National Key Technology R&D Program (2015BAI12B06).

Conflict of interest

The authors declare that the research was conducted in the absence of any commercial or financial relationships that could be construed as a potential conflict of interest.

Publisher's note

Supplementary material

The Supplementary Material for this article can be found online at: https://www.frontiersin.org/articles/10.3389/fendo.2024.1348854/full#supplementary-material

References

1. Tangri N, Inker LA, Hiebert B, Wong J, Naimark D, Kent D, et al. A dynamic predictive model for progression of ckd. *Am J Kidney Dis*. (2017) 69:514–20. doi: 10.1053/j.ajkd.2016.07.030

2. Barry EL, Mott LA, Melamed ML, Rees JR, Ivanova A, Sandler RS, et al. Calcium supplementation increases blood creatinine concentration in a randomized controlled trial. *PloS One*. (2014) 9:e108094. doi: 10.1371/journal.pone.0108094

3. Mitchell DM, Regan S, Cooley MR, Lauter KB, Vrla MC, Becker CB, et al. Long-term follow-up of patients with hypoparathyroidism. *J Clin Endocrinol Metab*. (2012) 97:4507–14. doi: 10.1210/jc.2012-1808

4. Da J, Xie X, Wolf M, Disthabanchong S, Wang J, Zha Y, et al. Serum phosphorus and progression of CKD and mortality: A meta-analysis of cohort studies. *Am J Kidney Dis*. (2015) 66:258–65. doi: 10.1053/j.ajkd.2015.01.009

5. Wang M, Zhang J, Kalantar-Zadeh K, Chen J. Focusing on phosphorus loads: from healthy people to chronic kidney disease. *Nutrients*. (2023) 15:1236. doi: 10.3390/nu15051236

6. Chang AR, Anderson C. Dietary phosphorus intake and the kidney. *Annu Rev Nutr*. (2017) 37:321–46. doi: 10.1146/annurev-nutr-071816-064607

7. Asche CV, Marx SE, Kim J, Unni SK, Andress D. Impact of elevated intact parathyroid hormone on mortality and renal disease progression in patients with chronic kidney disease stages 3 and 4. *Curr Med Res Opin*. (2012) 28:1527–36. doi: 10.1185/03007995.2012.716029

8. Khan AA, Rubin MR, Schwarz P, Vokes T, Shoback DM, Gagnon C, et al. Efficacy and safety of parathyroid hormone replacement with transcon pth in hypoparathyroidism: 26-week results from the phase 3 pathway trial. *J Bone Miner Res*. (2023) 38:14–25. doi: 10.1002/jbmr.4726

9. Fishbane S, Chittineni H, Packman M, Dutka P, Ali N, Durie N. Oral paricalcitol in the treatment of patients with ckd and proteinuria: a randomized trial. *Am J Kidney Dis*. (2009) 54:647–52. doi: 10.1053/j.ajkd.2009.04.036

10. Hadjiyannakos D, Filiopoulos V, Trompouki S, Sonikian M, Karatzas I, Panagiotopoulos K, et al. Treatment with oral paricalcitol in daily clinical practice for patients with chronic kidney disease stage 3-4: a preliminary study. *Clin Kidney J*. (2013) 6:164–68. doi: 10.1093/ckj/sfs188

11. Zhang Q, Li M, Zhang T, Chen J. Effect of vitamin d receptor activators on glomerular filtration rate: a meta-analysis and systematic review. *PloS One*. (2016) 11: e147347. doi: 10.1371/journal.pone.0147347

12. Bulik-Sullivan B, Finucane HK, Anttila V, Gusev A, Day FR, Loh PR, et al. An atlas of genetic correlations across human diseases and traits. *Nat Genet*. (2015) 47:1236–41. doi: 10.1038/ng.3406

13. Sekula P, Del Greco MF, Pattaro C, Köttgen A. Mendelian randomization as an approach to assess causality using observational data. *J Am Soc Nephrol*. (2016) 27:3253–65. doi: 10.1681/ASN.2016010098

14. Burgess S, Thompson SG. Multivariable Mendelian randomization: the use of pleiotropic genetic variants to estimate causal effects. *Am J Epidemiol*. (2015) 181:251–60. doi: 10.1093/aje/kwu283

15. Adi M, Ghanbari F, Downie ML, Hung A, Robinson-Cohen C, Manousaki D. Effects of 25-hydroxyvitamin d levels on renal function: a bidirectional mendelian randomization study. *J Clin Endocrinol Metab*. (2023) 108:1442–51. doi: 10.1210/clinem/dgac724

16. Neale lab: UK-Biobank GWAS results round2 . Available online at: http://www.nealelab.is/uk-biobank (Accessed 1st August 2018).

17. Revez JA, Lin T, Qiao Z, Xue A, Holtz Y, Zhu Z, et al. Genome-wide association study identifies 143 loci associated with 25 hydroxyvitamin D concentration. *Nat Commun*. (2020) 11:1647. doi: 10.1038/s41467-020-15421-7

18. Sun BB, Maranville JC, Peters JE, Stacey D, Staley JR, Blackshaw J, et al. Genomic atlas of the human plasma proteome. *Nature*. (2018) 558:73–9. doi: 10.1038/s41586-018-0175-2

19. Wuttke M, Li Y, Li M, Sieber KB, Feitosa MF, Gorski M, et al. A catalog of genetic loci associated with kidney function from analyses of a million individuals. *Nat Genet*. (2019) 51:957–72. doi: 10.1038/s41588-019-0407-x

20. Gorski M, van der Most PJ, Teumer A, Chu AY, Li M, Mijatovic V, et al. 1000 Genomes-based meta-analysis identifies 10 novel loci for kidney function. *Sci Rep*. (2017) 7:45040. doi: 10.1038/srep45040

21. Teumer A, Tin A, Sorice R, Gorski M, Yeo NC, Chu AY, et al. Genome-wide association studies identify genetic loci associated with albuminuria in diabetes. *Diabetes*. (2016) 65:803–17. doi: 10.2337/db15-1313

22. Gorski M, Jung B, Li Y, Matias-Garcia PR, Wuttke M, Coassin S, et al. Meta-analysis uncovers genome-wide significant variants for rapid kidney function decline. *Kidney Int*. (2021) 99:926–39. doi: 10.1016/j.kint.2020.09.030

23. Bulik-Sullivan BK, Loh PR, Finucane HK, Ripke S, Yang J, Schizophrenia Working Group of the Psychiatric Genomics Consortium, et al. LD Score regression distinguishes confounding from polygenicity in genome-wide association studies. *Nat Genet*. (2015) 47:291–5. doi: 10.1038/ng.3211

24. 1000 Genomes Project Consortium, Auton A, Brooks LD, Durbin RM, Garrison EP, Kang HM, et al. A global reference for human genetic variation. *Nature*. (2015) 526:68–74. doi: 10.1038/nature15393

25. de Leeuw CA, Mooij JM, Heskes T, Posthuma D. MAGMA: generalized gene-set analysis of GWAS data. *PloS Comput Biol*. (2015) 11:e1004219. doi: 10.1371/journal.pcbi.1004219

26. Pickrell JK, Berisa T, Liu JZ, Ségurel L, Tung JY, Hinds DA. Detection and interpretation of shared genetic influences on 42 human traits. *Nat Genet*. (2016) 48:1296. doi: 10.1038/ng.3570

27. Berisa T, Pickrell JK. Approximately independent linkage disequilibrium blocks in human populations. *Bioinformatics*. (2016) 32:283–5. doi: 10.1093/bioinformatics/btv546

28. Bowden J, Spiller W, Del Greco MF, Sheehan N, Thompson J, Minelli C, et al. Improving the visualization, interpretation and analysis of two-sample summary data Mendelian randomization via the Radial plot and Radial regression. *Int J Epidemiol*. (2018) 47:1264–78. doi: 10.1093/ije/dyy101

29. Zhao Q, Chen Y, Wang J, Small DS. Powerful three-sample genome-wide design and robust statistical inference in summary-data Mendelian randomization. *Int J Epidemiol*. (2019) 48:1478–92. doi: 10.1093/ije/dyz142

30. Hemani G, Tilling K, Davey Smith G. Orienting the causal relationship between imprecisely measured traits using GWAS summary data. *PloS Genet*. (2017) 13: e1007081. doi: 10.1371/journal.pgen.1007081

31. Verbanck M, Chen CY, Neale B, Do R. Detection of widespread horizontal pleiotropy in causal relationships inferred from Mendelian randomization between complex traits and diseases. *Nat Genet*. (2018) 50:693–8. doi: 10.1038/s41588-018-0099-7

32. Holick MF. High prevalence of vitamin D inadequacy and implications for health. *Mayo Clin Proc*. (2006) 81:353–73. doi: 10.4065/81.3.353

33. Russo LM, Sandoval RM, McKee M, Osicka TM, Collins AB, Brown D, et al. The normal kidney filters nephrotic levels of albumin retrieved by proximal tubule cells: retrieval is disrupted in nephrotic states. *Kidney Int*. (2007) 71:504–13. doi: 10.1038/sj.ki.5002041

34. Hodeify R, Ghani A, Matar R, Vazhappilly CG, Merheb M, Zouabi HA, et al. Adenosine triphosphate protects from elevated extracellular calcium-induced damage in human proximal kidney cells: using deep learning to predict cytotoxicity. *Cell Physiol Biochem*. (2022) 56:484–99. doi: 10.33594/000000571

35. Xun Y, Zhou P, Yang Y, Li C, Zhang J, Hu H, et al. Role of nox4 in high calcium-induced renal oxidative stress damage and crystal deposition. *Antioxid Redox Signal*. (2022) 36:15–38. doi: 10.1089/ars.2020.8159

36. Capasso G, Geibel PJ, Damiano S, Jaeger P, Richards WG, Geibel JP. The calcium sensing receptor modulates fluid reabsorption and acid secretion in the proximal tubule. *Kidney Int*. (2013) 84:277–84. doi: 10.1038/ki.2013.137

37. Takenaka T, Inoue T, Miyazaki T, Nishiyama A, Ishii N, Hayashi M, et al. Antialbuminuric actions of calcilytics in the remnant kidney. *Am J Physiol Renal Physiol*. (2015) 309:F216–26. doi: 10.1152/ajprenal.00003.2015

38. Muhlig AK, Steingrover J, Heidelbach HS, Wingerath M, Sachs W, Hermans-Borgmeyer I, et al. The calcium-sensing receptor stabilizes podocyte function in proteinuric humans and mice. *Kidney Int*. (2022) 101:1186–99. doi: 10.1016/j.kint.2022.01.036

39. Atchison DK, Ortiz-Capisano MC, Beierwaltes WH. Acute activation of the calcium-sensing receptor inhibits plasma renin activity in vivo. *Am J Physiol Regul Integr Comp Physiol*. (2010) 299:R1020–6. doi: 10.1152/ajpregu.00238.2010

40. Lumlertgul D, Burke TJ, Gillum DM, Alfrey AC, Harris DC, Hammond WS, et al. Phosphate depletion arrests progression of chronic renal failure independent of protein intake. *Kidney Int*. (1986) 29:658–66. doi: 10.1038/ki.1986.49

41. Haut LL, Alfrey AC, Guggenheim S, Buddington B, Schrier N. Renal toxicity of phosphate in rats. *Kidney Int*. (1980) 17:722–31. doi: 10.1038/ki.1980.85

42. Kulesza T, Piwkowska A. The impact of type III sodium-dependent phosphate transporters (Pit 1 and pit 2) on podocyte and kidney function. *J Cell Physiol*. (2021) 236:7176–85. doi: 10.1002/jcp.30368

43. Chang AR, Miller ER, Anderson CA, Juraschek SP, Moser M, White K. Phosphorus additives and albuminuria in early stages of ckd: a randomized controlled trial. *Am J Kidney Dis*. (2017) 69:200–09. doi: 10.1053/j.ajkd.2016.08.029

Glossary

MR	Mendelian randomization
LDSC	linkage disequilibrium score
MAGMA	multimarker analysis of genomic annotation
GWAS	genome-wide association studies
SNV	single-nucleotide variant
SNP	single-nucleotide polymorphism
h2	heritability
IVs	instrumental variables
IVW	inverse variance weighted
MR-PRESSO	Mendelian randomization pleiotropy residual sum and outlier
RAPS	Robust Adjusted Profile Score
Ca	calcium
P	phosphate
ALP	alkaline phosphatase
25(OH)D	25-hydroxyvitamin D
Mg	magnesium
PTH	parathyroid hormone
FGF23	fibroblast growth factor 23
EPO	erythropoietin
CKD	chronic kidney disease
eGFRcrea	estimated glomerular filtration rate using serum creatinine
eGFRcys	estimated glomerular filtration rate using serum cystatin C
BUN	blood urea nitrogen
UACR	urinary albumin–creatinine ratio
MA	microalbuminuria
CaSR	calcium-sensing receptor.

frontiers | Frontiers in Endocrinology

TYPE Original Research
PUBLISHED 25 October 2024
DOI 10.3389/fendo.2024.1358124

OPEN ACCESS

EDITED BY
Lin Chen,
Northwest University, China

REVIEWED BY
Akira Sugawara,
Tohoku University, Japan
Saravanan Subramaniam,
Massachusetts College of Pharmacy and Health Sciences, United States

*CORRESPONDENCE
Qing He
qing.he@whu.edu.cn

†These authors have contributed equally to this work

RECEIVED 19 December 2023
ACCEPTED 10 July 2024
PUBLISHED 25 October 2024

CITATION
Zuo Y, Zha D, Zhang Y, Yang W, Jiang J, Wang K, Zhang R, Chen Z and He Q (2024) Dysregulation of the 3β-hydroxysteroid dehydrogenase type 2 enzyme and steroid hormone biosynthesis in chronic kidney disease.
Front. Endocrinol. 15:1358124.
doi: 10.3389/fendo.2024.1358124

Dysregulation of the 3β-hydroxysteroid dehydrogenase type 2 enzyme and steroid hormone biosynthesis in chronic kidney disease

Yiyi Zuo[1†], Dongqing Zha[2†], Yue Zhang[1], Wan Yang[1], Jie Jiang[1], Kangning Wang[1], Runze Zhang[1], Ziyi Chen[1] and Qing He[1*]

[1]State Key Laboratory of Oral & Maxillofacial Reconstruction and Regeneration, Key Laboratory of Oral Biomedicine Ministry of Education, Hubei Key Laboratory of Stomatology, School & Hospital of Stomatology, Wuhan University, Wuhan, China, [2]Division of Nephrology, Zhongnan Hospital of Wuhan University, Wuhan, China

Introduction: Chronic kidney disease (CKD) presents a critical global health challenge, marked by the progressive decline of renal function. This study explores the role of the 3β-hydroxysteroid dehydrogenase type 2 enzyme (HSD3B2) and the steroid hormone biosynthesis pathway in CKD pathogenesis and progression.

Methods: Using an adenine-induced CKD mouse model, we conducted an untargeted metabolomic analysis of plasma samples to identify key metabolite alterations associated with CKD. Immunohistochemistry, Western blotting, and qPCR analyses were performed to confirm HSD3B2 expression in both human and mouse tissues. Additionally, Nephroseq and Human Protein Atlas data were utilized to assess the correlation between HSD3B2 and kidney function. Functional studies were conducted on HK2 cells with HSD3B2 knockdown to evaluate the impact on cell proliferation and apoptosis.

Results: Metabolic characteristics revealed significant shifts in CKD, with 61 metabolites increased and 65 metabolites decreased, highlighting the disruption in steroid hormone biosynthesis pathways influenced by HSD3B2. A detailed examination of seven key metabolites underscored the enzyme's central role. HSD3B2 exhibited a strong correlation with kidney function, supported by data from Nephroseq and the Human Protein Atlas. Immunohistochemistry, Western blotting, and qPCR analyses confirmed a drastic reduction in HSD3B2 expression in CKD-affected kidneys. Suppressed proliferation and increased apoptosis rates in HSD3B2 knocked down HK2 cells further demonstrated the enzyme's significance in regulating renal pathophysiology.

Discussion: These findings underscore the potential of HSD3B2 as a clinical diagnostic and therapeutic target in CKD. While further studies are warranted to fully elucidate the mechanisms, our results provide valuable insights into the intricate interplay between steroid hormone biosynthesis and CKD. This offers a promising avenue for precision medicine approaches and personalized treatment strategies.

KEYWORDS

chronic kidney disease, metabolomics, HSD3B2, steroid hormone biosynthesis, therapeutic target

1 Introduction

Chronic kidney disease (CKD) stands as a significant global health concern, affecting over 10% of the worldwide population and resulting from a diverse range of diseases that progressively alter renal structure and function (1). With its debilitating consequences and rising prevalence, CKD has become a focal point in healthcare. The International Society of Nephrology (ISN) reported an alarming 41.5% increase in global absolute CKD prevalence from 1990 to 2017, projecting an impending rise in CKD-related deaths to 2.2 to 4.0 million by 2040 (1–3). The overlap between CKD and cardiovascular disease (CVD) further accentuates the complexity of managing this condition and underscores the need for holistic healthcare approaches (4, 5).

CKD is categorized into stages based on estimated glomerular filtration rate (eGFR) and the presence of kidney damage, with severity increasing as eGFR decreases. The terminal stage, CKD stage 5, also known as end-stage renal disease (ESRD), necessitates artificial filtration or kidney transplantation for survival, severely compromising quality of life (6). Notably, IgA nephropathy and diabetic nephropathy stand out as the two leading causes of end-stage renal failure. Presently, there are no available treatments that have shown the capability to impede the advancement of diabetic and IgA nephropathy to end-stage renal failure (7, 8). Consequently, there is an urgent requirement for innovative therapeutic strategies to proficiently manage diabetic nephropathy. The current therapeutic strategy for CKD mainly centers on mitigating kidney damage progression, achieved primarily through risk factor management and symptom alleviation (9–11). Although these approaches are integral, the identification of novel therapeutic targets for CKD and its associated comorbidities remains a pressing need.

To comprehend the intricate mechanisms underlying CKD, animal models have been instrumental. Among these, the adenine-induced CKD mouse model offers an avenue to study the disease's pathogenesis without the requirement for surgery or genetic manipulation (12). This model involves administering an adenine-enriched diet, mimicking CKD-like structural and functional changes, such as proteinuria, renal atrophy, fibrosis, and oxidative stress (13–15). It represents a relevant platform for investigating CKD progression.

Metabolomics has emerged as a powerful tool to investigate the underlying molecular intricacies of diseases (16–18). In CKD, it has proven invaluable in identifying biomarkers and shedding light on pathological mechanisms (19). This technology facilitates the profiling of low-molecular-weight metabolites, providing insights into cellular functions, pathways, and metabolic dysregulation associated with CKD (20). Advanced analytical techniques have enabled comprehensive assessments of metabolomic changes, such as alterations in amino acids, lipids, and organic acids, associated with oxidative stress, inflammation, and impaired renal function (18, 21, 22). Metabolomics has the potential to unravel novel diagnostic and prognostic markers and advance personalized medicine in CKD.

This study employs the adenine-induced CKD mouse model and metabolomics analysis to investigate the role of the 3β-hydroxysteroid dehydrogenase type 2 enzyme (HSD3B2) and the steroid hormone biosynthesis pathway in CKD. We explore the potential implications of HSD3B2 and steroid hormone metabolism in CKD pathogenesis, progression, and possible therapeutic interventions. This research not only broadens our understanding of CKD mechanisms but also presents novel avenues for precision medicine approaches tailored to individual CKD patients.

2 Materials and methods

2.1 Experimental animals and induction of chronic kidney disease

Eight-week-old female C57BL/6 mice were obtained from the Hubei Provincial Center for Disease Control and Prevention (Hubei CDC) and were raised in a specific pathogen-free facility. After 3 days of adaption, animals were divided into two groups: the control group (normal diet, n=8) and the CKD group (0.2% adenine diet, n=6). Chronic kidney disease was induced in mice using the well-established adenine diet model (13), which mimics end-stage renal failure. Mice in the control group received a normal adenine-free diet, while those in the CKD group received a customed diet containing 0.2% adenine (Jiangsu Xietong Bioengineering Co., Ltd) for six weeks. At the end of the study, all mice were anesthetized using a combination of Sutex (75 mg/kg) and xylazine hydrochloride (10 mg/kg), administered via intraperitoneal injection. Following anesthesia, the mice were euthanized by decapitation to obtain blood samples. This method ensured that the animals were fully anesthetized before euthanasia, minimizing any potential suffering.

All animal experiments and procedures performed in this study followed ethical guidelines for animal studies and were approved by the Animal Welfare and Ethics Committee of the School and Hospital of Stomatology at Wuhan University (S07922040A).

2.2 Clinical samples

Human kidney biopsy samples were obtained from 6 female patients, including 3 individuals with eGFR higher than 90 mL/min/1.73 m^2 (Control group) and 3 with eGFR under 30 mL/min/1.73 m^2 (CKD group), at Zhongnan Hospital of Wuhan University. The staging criteria for CKD were determined by multiple pathologists based on clinical presentation and histological assessment. The experimental protocol was approved by the Medical Ethics Committee of Zhongnan Hospital of Wuhan University (protocol number: 2021074), and all participants provided written informed consent. This study was conducted in accordance with the Declaration of Helsinki.

2.3 Biochemical assessment for kidney injury

To evaluate kidney function, blood samples were collected before and at 1, 3, 4, and 6 weeks into the adenine diet.

Overnight fasting preceded blood collection. At 0, 1, 3, and 4 weeks, blood samples were obtained by tail nicking into heparin tubes. During euthanasia, whole blood was collected by decapitation. Plasma was separated from blood cells by centrifugation (1,000~2,000 rcf, 10 minutes, 4°C). The supernatant was stored at -80°C until analysis. Serum creatinine (700460, Cayman Chemical, MI, USA), blood urea nitrogen (BUN; 0580-250, Stanbio Laboratory, Boerne, TX, USA), and phosphate concentrations (ab65622, ABclonal, Wuhan, China) were measured using commercial kits respectively, following the manufacturer's instructions. Levels of adrenocorticotropic hormone (ACTH), interleukin 6 (IL6), and tumor necrosis factor alpha (TNFα) in plasma were measured using enzyme-linked immunosorbent assay (ELISA) kits according to the manufacturer's protocol (ACTH, E-EL-M0079, Elabscience; IL6, Proteintech, KE10007; TNFα, Proteintech, KE10002). OD values were measured using a microplate reader (Biotech, USA). OD values from at least three independent experiments were analyzed with GraphPad Prism.

2.4 Kidney histology

Kidneys were rapidly harvested and fixed in 4% paraformaldehyde (PFA) at 4°C for 24 hours. After dehydration and paraffin embedding, 5 μm sections were cut for histological analysis. Hematoxylin and eosin (H&E) staining was performed to visualize cell morphology, interstitium, glomeruli, and tubules.

2.5 Immunohistochemistry

Kidney and adrenal gland sections underwent deparaffinization and hydration through dimethyl benzene and ethanol. Antigen retrieval was achieved by boiling in 10 mM sodium citrate buffer (pH 6.0) for 10 min in a microwave. An HRP polymer anti-rabbit IHC kit (Maixin, Fuzhou, China) was used according to the manufacturer's instructions. The primary antibody of HSD3B2 (A1823, ABclonal, Wuhan, China) for mouse samples was applied at a 1:10 concentration. The primary antibody of HSD3B2 (122513, Zen Bio, Chengdu, China) for human samples was applied at a 1:50 concentration. Subsequent staining involved using a diaminobenzidine (DAB) reagent kit (Maixin, Fuzhou, China) after incubation with HRP secondary antibody. Slides were sealed and left to air dry overnight at room temperature. As a negative control, the primary antibody was replaced with PBS alone.

2.6 Cell culture

Human renal proximal tubule (HK2) cells were purchased from ATCC and cultured in DMEM/F12 medium (C11330500BT, Gibco, China). The medium included 10% fetal bovine serum (FBS; 10270-106, Gibco, Brazil) and 1% penicillin-streptomycin (SV30010, Cytiva, USA). Cells were maintained in a humidified atmosphere of 5% CO2 and 95% air at 37°C. Fresh growth medium was added every 2~3 days until confluent.

2.7 Small Hairpin RNA Plasmid Construction and Lentivirus Infection

The shRNA plasmids targeting human HSD3B2 gene (ENSG00000203859) were constructed according to the protocol of the Broad Institute. We inserted the target sequences of human HSD3B2 (ENST00000369416; 201-exon4) into PLKO.1 vector. The circular PLKO.1 plasmid was digested by AgeI (R3552L, NEB, Ipswich, MA, USA) and EcoRI (R3101L, NEB, Ipswich, MA, USA), and the prepared open vector was then ligated with the annealed oligo pair. The ligated plasmid was amplified by transferring it into DH5α (KTSM101L, AlpalifeBio, Shenzhen, China) for clone selection. Finally, the recombinant plasmids were identified by DNA sequencing.

To perform cell transfection, Lipofectamine™ 2000 (Thermo Fisher Scientific, Waltham, MA, USA) was used according to the following protocol. A 2.4 μg plasmid (containing 1.2 μg target plasmid packaged with the 0.9 μg pSPAX2 and 0.3 μg pMD2.G) was mixed with 150 μL serum-free Opti-MEM medium, and then mixed with an additional 150 μL serum-free Opti-MEM medium containing 6 μL Lipofectamine™ 2000. The mixture was incubated at room temperature for 20 minutes and then added to HEK293T cells in 6-well plates. Cells were incubated with the mixture of transfection reagent and plasmid at 37°C for 10 hours before replacement. 48 hours after replacement, recombinant lentivirus was collected and stored at -80°C.

To generate a stable HSD3B2 knockdown cell line, HK2 cells were infected with the recombinant lentivirus for 8 hours and then cultured for 48 hours before stable selection by incubating in a complete medium (as described above) containing 4 μg/mL puromycin dihydrochloride (ST551, Beyotime Biotechnology, Shanghai, China). The medium was changed every 2 days to maintain selection pressure. The primers for shRNA sequences are listed in Table 1 and were synthesized by Wuhan AuGCT DNA-SYN Biotechnology Co., Ltd (Wuhan, China).

2.8 Cell viability assay

To assess cell viability, HK2 cells were seeded at 5,000 cells/well in 96-well plates and cultured at 37°C for 24 hours. Subsequently, cells were cultured for varying time points (0, 12, 24, 48, and 72 hours), and viability was determined using the Cell Counting Kit-8 assay (CCK-8; CK04, Dojindo, Kumamoto, Japan) following the manufacturer's instructions. Briefly, 10 μL of CCK-8 solution was added to each well and incubated for 4 hours at 37°C. Absorbance at 450 nm was measured using a microplate reader (Biotech, USA). OD values from at least six independent experiments were analyzed with GraphPad Prism.

2.9 Apoptosis assay

Cells at 90% confluency in complete medium were dissociated using 0.25% trypsin solution (SH40003.01, Cytiva, USA). A cell

10.3389/fendo.2024.1358124

TABLE 1 Primers used for quantitative real-time PCR and shRNA.

Name of genes or shRNAs	Organism	Forward primer	Reverse primer	Product size (bp)
β-actin	Mouse	GATCTGGCACCACACCTTCT	GGGGTGTTGAAGGTCTCAAA	138
HSD3B2	Mouse	GAGATCAGGGTCCTGGACAA	CAATGATGGCAGCAGTATGG	169
β-actin	Human	TGACGTGGACATCCGCAAAG	CTGGAAGGTGGACAGCGAGG	205
HSD3B2	Human	ACAAGGCCTTCAGACCAGAA	ACACAGGCCTCCAACAGTAG	232
HSD3B2-sh1	Human	CCGGATTCCTTTCTGCCAGTA TAAACTCGAGTTTATACTGGC AGAAAGGAATTTTTTG	AATTCAAAAAATTCCTTTCTG CCAGTATAAACTCGAGTTTAT ACTGGCAGAAAGGAAT	
HSD3B2-sh2	Human	CCGGCTTCCTACTCAGCCCAA TTTACTCGAGTAAATTGGGCT GAGTAGGAAGTTTTTG	AATTCAAAAACTTCCTACTCA GCCCAATTTACTCGAGTAAAT TGGGCTGAGTAGGAAG	

suspension of 195μl containing 50,000~100,000 cells was prepared with PBS and moved to a centrifuge tube. Staining with Annexin V-fluorescein isothiocyanate (Annexin V-FITC) and propidium iodide-phycoerythrin (PI) was done using an apoptosis detection kit (C1067M, Beyotime Biotechnology, Shanghai, China). After 20 minutes' incubation in the dark, a flow cytometer (Beckman Coulter, Inc., Brea, CA, USA) was used for the apoptosis assay. Removal of dead cells and debris relied on forward scatter area (FSC-A) vs. side scatter area (SSC-A) analysis, with doublet exclusion using FSC-A vs. forward scatter height (FSC-H). Healthy cells showed negative Annexin V and PI staining, while early apoptotic cells displayed positive Annexin V and negative PI staining. Results indicating the percentage of early apoptotic cells were analyzed using CytExpert version 2.0 software (Beckman Coulter, Inc., Brea, CA, USA). Apoptosis rates from at least three independent experiments were analyzed with GraphPad Prism.

2.10 Quantitative real-time PCR analysis

Total RNA was isolated from whole kidneys and HK2 cells using Trizol Reagent (15596026, Ambion, USA) and the HP Total RNA Kit (R6812-02, Omega bio-tek, Norcross, GA, USA), respectively. cDNA synthesis utilized HiScript III qRT Supermix for qPCR (R323, Vazyme, Nanjing, China). Real-time PCR reaction mix contained 2 μL cDNA, 10 μL qPCR SYBR Green Master Mix (11201ES08, Yeasen, Shanghai, China), 0.5μL forward primers (10 μmol/L), and 0.5 μL reverse primers (10 μmol/L), adjusted to 20 μL with ddH2O. RT-PCR was conducted in a two-step procedure: cDNA synthesis (RT, 37°C for 15 min, 85°C for 5 sec), followed by cDNA amplification (95°C for 5 s, 60°C for 30 s) in 39 cycles using a CFX Connect Real-Time PCR Detection System (Bio-Rad, Hercules, CA, USA). Relative gene expression used β-actin as an internal control gene, calculated via the 2-ΔΔCt method. qPT-PCR results are representative of three independent experiments. PCR primer details for each gene are provided in Table 1.

2.11 Western blot

Kidney tissues were lysed using NP40 lysis buffer (P0013F, Beyotime Biotechnology, Shanghai, China), and protein concentrations were measured using a BCA protein assay kit (23225, Thermo Fisher Scientific, Waltham, MA, USA). For electrophoresis, 30 μg of protein from each sample was separated by 10% sodium dodecyl sulfate–polyacrylamide gel electrophoresis and transferred onto NC membrane (HATF00010, Merck KGaA, Darmstadt, Germany). After blocking for 1 hour at room temperature with 5% nonfat milk in TBST (Tris-buffered saline with 0.05% Tween 20), membranes were incubated overnight at 4°C with primary antibodies: rabbit anti-HSD3B2 (1:500, A1823, ABclonal, Wuhan, China), rabbit anti-vimentin (1:000, PAB30692, Bioswamp, Wuhan, China), rabbit anti-α-SMA (1:1000, PAB30319, Bioswamp, Wuhan, China), and mouse anti-β-actin(1:10000, 66009-1, Proteintech, Chicago, IL, USA). Membranes were washed three times in TBST before incubation

with appropriate HRP-conjugated secondary antibodies (goat anti-rabbit, ANT020; goat anti-mouse, ANT020; both from AntGene, Wuhan, China) at a dilution of 1:4000 for 1 hour at room temperature. After three 5-minute washes in TBST, protein bands were visualized with WesternBrightTM ECL solution (Advansta, San Jose, CA, USA) and detected by an Odyssey CLx Imaging System (LI-COR, NE, USA). Protein levels were quantified using ImageJ software (National Institutes of Health, Bethesda, MD). β-actin was used as a loading control. Western blot results are representative of at least three independent experiments.

2.12 Untargeted metabolomic profiling

2.12.1 Chemicals and reagents

Analytical grade formic acid (FA) was supplied by Sinopharm Chemical Reagent Co., Ltd. (Shanghai, China). HPLC-grade methanol (MeOH) and acetonitrile (ACN) were supplied by Merck (Darmstadt, Germany). Ultra-pure water used was prepared by a Milli-Q apparatus (Millipore, Bedford, MA).

2.12.2 Sample preparations

Blood samples were collected from the control group (n=8) and the CKD group (n=6) at the end of the 6-week study period. Plasma was separated from blood cells by centrifugation (1,000~2,000 rcf, 10 minutes, 4°C), followed by storage at -80°C until analysis. Plasma samples were thawed at 4°C before use. For each sample, 100 µL plasma was deproteinized by addition of 400 µL MeOH. The mixture was vortexed for 60 s and stored at -20°C for 20 min, and then centrifuged at 13000 rpm for 10 min at 4°C. The supernatant was collected and dried under nitrogen, and then redissolved in 100 µL methanol/water (1/1, v/v) before LC-MS analysis. The quality control (QC) sample was prepared through mixing an equal aliquot (10 µL) from all plasma samples. The same procedure was used for each QC aliquot and individual sample. Throughout the experiment, plasma samples were analyzed randomly, with the QC sample analyzed every 5 samples for the purposes of data filtering, analytical variability evaluation and normalization.

2.12.3 LC-MS analysis

The UHPLC-LTQ-Orbitrap MS system was used for plasma samples analysis, consisting of a Dionex Ultimate 3000 UHPLC system (Thermo Scientific, Sunnyvale, CA, USA) and an LTQ-Orbitrap Elite mass spectrometer (Thermo Scientific, Waltham, MA, USA) with an electrospray ionization source (ESI). LC separation was achieved on a ZORBAX Eclipse Plus C18 Column (50 × 2.1 mm, 1.8 µm, Agilent Technologies) with a flow rate of 0.35 mL/min at 40°C. FA in water (0.1%, v/v, solvent A) and FA in ACN (0.1%, v/v, solvent B) were used as mobile phases. A gradient of 0–1 min at 2% B, 1–9 min from 2% to 98% B, 9–12 min at 98% B, 12–12.1 min from 98% to 2% B, and 12.1–15 min at 2% B was applied. The injection volume was 10 µL.

The MS analysis was performed under both the positive ion mode and negative ion mode with full scan detection of m/z 70-1000 at the resolution of 60000. The ESI parameters were set as follows: heater temperature, 300°C; sheath gas, 35 arb; aux gas, 7 arb or 10 arb for positive or negative mode, respectively; spray voltage, 3500 V; capillary temperature, 350°C. Data-dependent acquisition mode (DDA) was used to acquire the MS2 spectra according to the top 6 intensities with the resolution of 15000. And the MS2 fragment ions were acquired under higher energy dissociation (HCD) with 40% normalized collision energy, 2.0 m/z isolation width, 0.1 ms activation time and 10 s dynamic exclusion duration.

2.12.4 Data Processing and Analysis

Raw data were acquired by Thermo Xcalibur Software (version 2.1, MA, USA). Compound discoverer software (version 3.0) was used for features extraction, retention time correction, peak alignment, and blank subtraction to generate peak table, and QC-based LOESS normalization to generate a comprehensive feature list (23, 24). QC samples were injected in every batch at a regular interval of 5 samples, were used for data filtering. For metabolites detected by two or more platforms, only the values with the lowest relative standard deviation (RSD) in QC samples were retained, and metabolites with RSDs less than 30% in QC samples were selected for further analysis. Before conducting statistical analysis, the data underwent log-transformation to achieve an approximate normal distribution. The detected metabolites were annotated by matching their MS2 spectra against the mzCloud database through Compound discoverer.

For fold change analysis, volcano plot visualization, two-dimensional principal component analysis (PCA), and the identification of CKD-influenced metabolic pathways (Mus musculus), these analyses were conducted using the web-based tool MetaboAnalyst 5.0 (https://www.metaboanalyst.ca/, accessed on 26 January 2023).

2.13 Statistical analysis

All data were presented as mean ± standard deviation (SD) from at least three independent experiments. GraphPad Prism software (v. 8.3.1) was used for statistical analyses. Student's t-test was used for experiments with two groups, while one-way analysis of variance (ANOVA) followed by the Bonferroni *post hoc* test was used for experiments with more than two groups. A P value <0.05 was considered significant.

3 Results

3.1 Adenine-enriched diet induces chronic renal failure

In this study, we employed 8-week-old female mice subjected to either a normal or adenine-enriched diet for 6 weeks. Blood samples were collected at intervals of 0, 1, 3, and 4 weeks, with final whole-blood

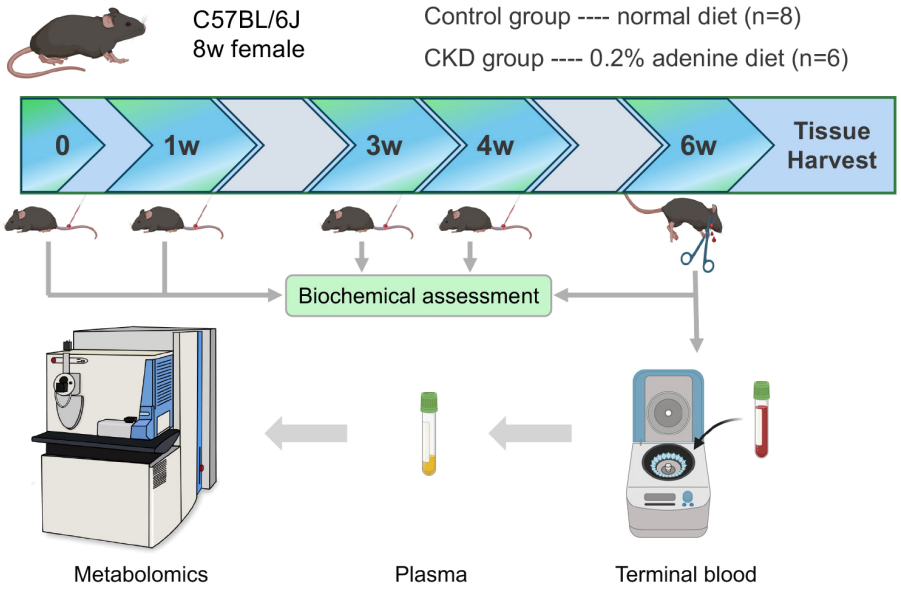

FIGURE 1
Schematic of the overall experimental workflow performed in this study that involves normal and adenine diet groups of adult female C57BL/6 mice, time points and methods of plasma extraction, and metabolomics analysis.

sampling at the 6-week mark (Figure 1). At the end of the dietary regimen, mice in the adenine-induced CKD group displayed significant weight loss (Figure 2A). Additionally, we assessed renal function markers including blood urea nitrogen (BUN), serum creatinine, and serum phosphate levels. Notably, all markers exhibited marked elevation in the CKD group compared to controls, confirming renal impairment and reduced function in CKD-afflicted mice. BUN levels increased by 1.9-fold ($P < 0.01$) at the 3rd week, 2.2-fold ($P < 0.01$) at the 4th week, and 2.6-fold ($P < 0.0001$) at the 6th week in the CKD group compared to controls (Figure 2B). Serum creatinine, a well-established risk factor for morbidity and mortality in CKD patients, significantly rose following the 6-week adenine diet, indicating substantial kidney damage (Figure 2C). Moreover, CKD-related renal failure was accompanied by elevated serum phosphate (7.1 ± 0.05 mg/dl in control group vs. 9.8 ± 0.8 mg/dl in AD group, $P < 0.05$) at the 3rd week after adenine-enriched diet initiation (Figure 2D). Hematoxylin-eosin (HE) staining of kidney histological sections showcased distinct features of extensive nephropathy in both renal tubules and glomeruli, confirming CKD-associated histopathological changes (Figure 2E). Western blot analysis detected heightened expression of the mesenchymal marker vimentin and α-SMA, indicative of activated fibroblasts, in the kidneys of CKD group mice compared to controls (Figure 2F). Statistical evaluation underscored a 4 to 7-fold increase in vimentin and α-SMA in the AD group kidneys ($P < 0.001$) (Figures 2G, H). Together, these findings validate the establishment of the CKD mouse model. Additionally, it has been suggested that perturbations occur in the hypothalamic-pituitary-adrenal (HPA) axis in CKD (25). In line with this, we investigated plasma levels of adrenocorticotropic hormone (ACTH), which were significantly elevated in CKD compared to the controls ($p < 0.01$), as depicted in Figure 2I. We also discovered that plasma cytokine levels, including IL-6 and TNF-α, were significantly increased in CKD mice (Figures 2J, K), indicating a heightened inflammatory state.

3.2 Plasma metabolome changes in adenine-induced CKD

Untargeted liquid chromatography–mass spectrometry (LC–MS) analysis of plasma samples from 8 control group mice and 6 adenine-induced CKD group mice after 6 weeks of diet revealed 675 identified metabolites. Comparison of relative changes in metabolites unveiled 226 significantly altered compounds. Among these, 94 metabolites were downregulated (log2 FC(Adenine/Control) < -1), while 132 metabolites were upregulated (log2 FC (Adenine/Control) > 1) (Supplementary Figure 1A). Notably, the plasma metabolome profiles underwent profound transformations in CKD. A volcano plot confirmed differential clustering, with 126 significantly altered components, comprising 65 downregulated and 61 upregulated metabolites (Figure 3A, Supplementary Table 1). Two-dimensional principal component analysis (PCA) underscored distinct segregation between control and CKD group samples, reflecting the intricate changes induced by the adenine diet (Figure 3B).

3.3 Pathway analysis revealed the key pathway and enzyme altered in CKD

Pathway analysis of significantly changed metabolites ($p < 0.05$) in Metaboanalyst 5.0 illuminated altered functional patterns associated with CKD progression (Figure 3C). Notably, steroid hormone

10.3389/fendo.2024.1358124

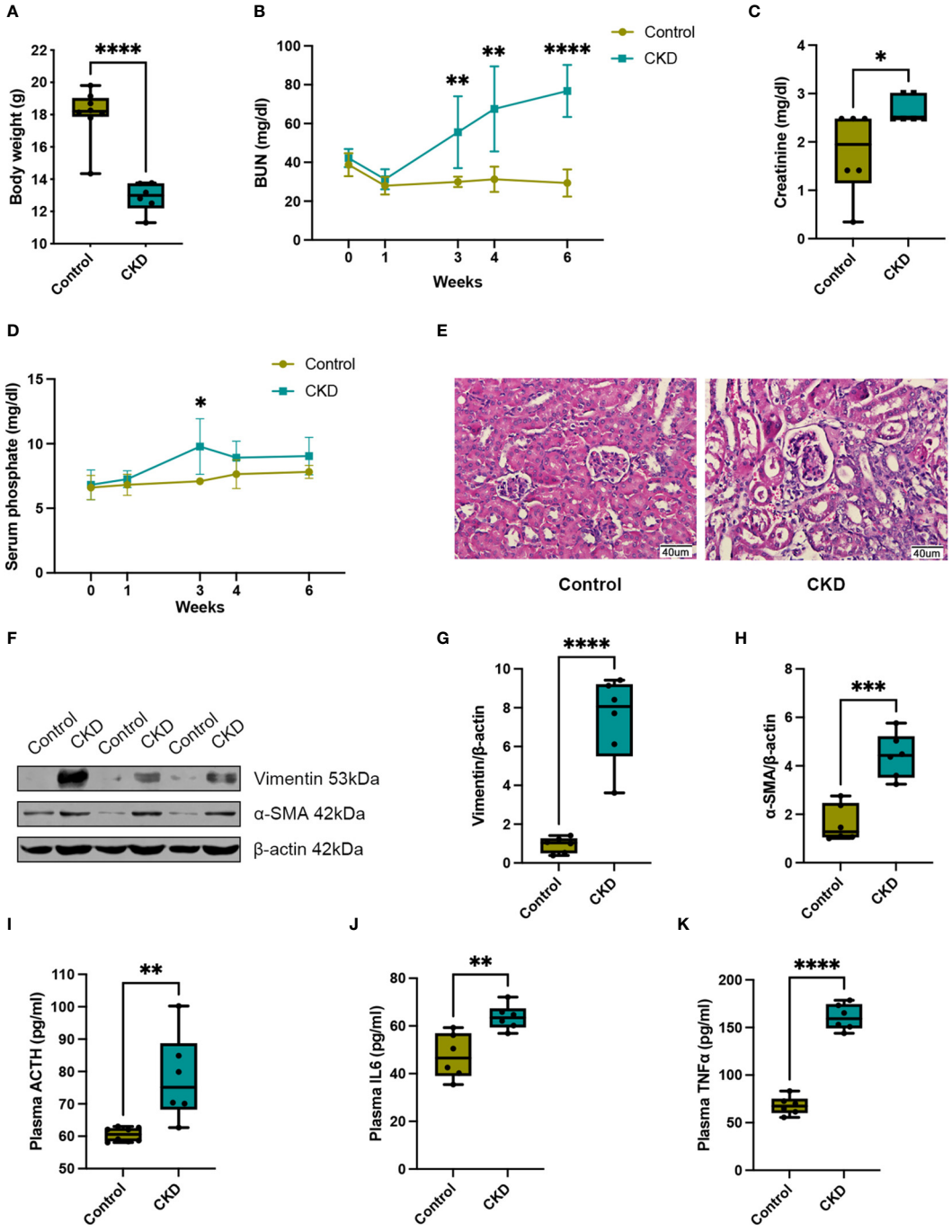

FIGURE 2
Adenine-enriched diet induced chronic renal failure. **(A)** Box and whisker plots comparing body weight between control and adenine-induced CKD mice at the end of the 6-week feeding period. Control group (n=8), CKD group (n=6). **(B)** Changes of renal function parameters represent by blood urea nitrogen (BUN) concentrations between control and adenine-induced CKD mice. Control group (n=6), CKD group (n=6). **(C)** Box and whisker plots comparing serum creatinine concentrations between control and adenine-induced CKD mice at the end of the 6-week feeding period. Control group (n=6), CKD group (n=6). **(D)** Changes of renal function parameters represent by serum phosphate concentrations between control and adenine-induced CKD mice. Control group (n=5), CKD group (n=5). **(E)** Representative HE staining of kidneys from control or adenine-induced CKD group mice. Scale bar = 40 μm. **(F)** Western blot of vimentin and α-SMA in the kidneys of control or adenine-induced CKD mice. β-actin was used as a loading control. Western blot results are representative of at least three independent experiments. **(G)** Box and whisker plots comparing vimentin and **(H)** α-SMA expression in the kidneys of control and adenine-induced CKD mice. Control (n=6), CKD (n=6). **(I)** Box and whisker plots comparing adrenocorticotropic hormone (ACTH) levels in plasma between control and adenine-induced CKD mice at the end of the 6-week feeding period. Control group (n=8), CKD group (n=6). **(J)** Box and whisker plots comparing interleukin 6 (IL6) levels in plasma between control and adenine-induced CKD mice at the end of the 6-week feeding period. Control group (n=6), CKD group (n=6). **(K)** Box and whisker plots comparing tumor necrosis factor alpha (TNFα) levels in plasma between control and adenine-induced CKD mice at the end of the 6-week feeding period. Control group (n=6), CKD group (n=6). For box and whisker plots, the median expression level is indicated by the central line within each box, while the box represents the interquartile range (IQR). Whiskers extend to the minimum and maximum values within a 1.5 * IQR range. All data are presented as the means ± SEM. Unpaired Student's t-test was performed to determine the statistical significance, with * $p < 0.05$, ** $p < 0.01$, *** $p < 0.001$, and **** $p < 0.0001$ versus control group.

10.3389/fendo.2024.1358124

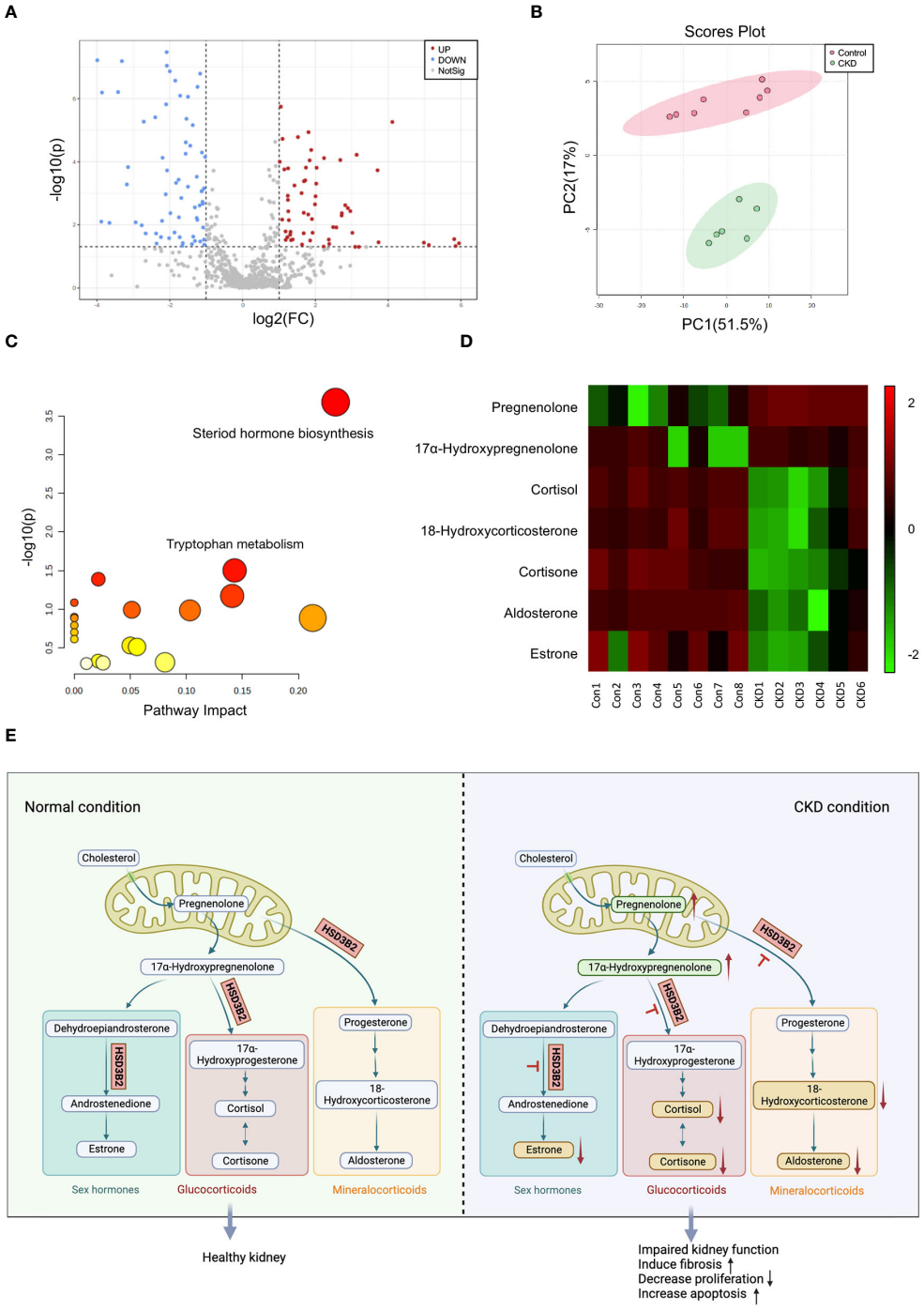

FIGURE 3
Metabolic analysis of plasma metabolites between control and adenine-induced CKD groups. **(A)** Volcano plots of metabolites that differ between control and adenine-induced CKD groups plasma. Grey dots represent metabolites that were not significantly different between the two groups, while the red and blue dots represent those that are significantly upregulated and downregulated ($p < 0.05$). **(B)** The 2D PCA analysis comparing the altered metabolites of the plasma samples from control and adenine-induced CKD groups shows two apparent clusters. Red circle and dots represent the control group, while green circle and dots represent the CKD group. **(C)** Analysis of the disordered pathways based on metabolite alterations between control and adenine-induced CKD groups, visualized by a bubble plot. Steroid hormone biosynthesis pathway is mainly identified. The size of the bubble is relative to the impact of each pathway, and the color of the bubble indicates significance, from highest in red to lowest in white; a small p-value and a large pathway impact factor indicate that the pathway is highly influenced. **(D)** Heatmap of the differential metabolites in the steroid hormone biosynthesis pathway measured in the control and adenine-induced CKD groups. Each small square on the X axis depicts individual sample of two groups, while Y axis depicts individual metabolites. The degrees of red or green color indicate higher and lower relative contents of the metabolites. Vertical colored bar is on the right of the heatmap. **(E)** Pathway map illustrating steroid hormone biosynthesis under normal and CKD conditions. Upward arrows indicate upregulated compounds, while downward arrows indicate downregulated compounds.

biosynthesis emerged as a pivotal pathway of interest, boasting a lower p-value and greater pathway impact factor, enriched with the most differential metabolites. Within this pathway, 7 distinct metabolites underwent significant alterations (Supplementary Figure 1B). A heatmap comparing the quantifiable metabolites within this pathway demonstrated marked regulation (Figure 3D). Schematic representation of the classic steroid hormone biosynthesis pathway unveiled the elevation of precursors like pregnenolone and 17α-hydroxypregnenolone in CKD plasma (Figure 3E). Subsequent metabolic steps yield glucocorticoids, mineralocorticoids, and sex hormones, reliant on hydroxysteroid dehydrogenase (HSD) and cytochrome P450 (CYP) family enzymes. Intriguingly, we observed a reduction in end products such as 18-hydroxycorticosterone, aldosterone, cortisone, cortisol, and estrone. Collectively, elevated precursors and reduced end products suggest an impact on the enzyme HSD3B2, which is pivotal across all branches of this pathway.

3.4 HSD3B2 expression was decreased in renal tubular cells of both human and mouse CKD models

Association analysis in the Nephroseq clinical biomarker module revealed correlations between HSD3B2 expression and kidney function indicators, with notable clinical relevance. HSD3B2 mRNA level was closely correlated with GFR in different databases of human samples (Figure 4A, Supplementary Figures 2A, B). Proteinuria and serum creatinine levels, indicators for renal function, also displayed strong correlation with HSD3B2 mRNA expression (Supplementary Figures 2C, D). Expression profiling of western blotting and immunohistochemistry staining collectively demonstrated substantial HSD3B2 presence in renal proximal tubules, a finding validated by single-cell RNA-seq data from the Human Protein Atlas database (Figures 4B, C). Immunohistochemistry using human and mouse kidney samples further confirmed this expression pattern (Figure 4D). Additionally, a drastic reduction in HSD3B2 expression in CKD-affected kidneys was observed, particularly in atrophied tubules, in both human and mouse tissues (Figures 4D, E). Western blot and real-time PCR analyses corroborated these findings, revealing significantly diminished HSD3B2 levels in the adenine-induced CKD group at the 6-week endpoint (Figures 4F–H). Collectively, these data underscore the substantial reduction of HSD3B2 in CKD kidneys and imply the critical role of HSD3B2 in maintaining kidney function.

3.5 Knockdown of HSD3B2 affects proliferation and apoptosis of HK2 cells

To unravel HSD3B2's role in CKD renal tubular cells, we employed shRNA targeting HSD3B2 (Human-201-exon4) to knock down HSD3B2 in HK2 cells, a proximal tubular cell line derived from normal kidney. The HSD3B2 targeting shRNAs transduced HK2 cells showed significant knockdown efficiency, exceeding 50% reduction ($P < 0.05$) by both sh1 and sh2 (Figure 5A). Using the CCK-8 assay kit, we assessed HK2 cell viability and observed suppressed cell proliferation upon HSD3B2 knockdown (Figure 5B). Apoptosis, a hallmark of CKD-related renal tubular cell pathology, was investigated through Annexin V/PI staining following flow cytometry analysis. The results showed a significant increase in apoptotic cells following HSD3B2 knockdown, compared to the control (Figures 5C, D). Collectively, these results highlight HSD3B2's role in regulating renal tubular cell proliferation and apoptosis within the context of CKD, which contribute to CKD progression.

4 Discussion

This study delves into the intricate relationship between the 3β-hydroxysteroid dehydrogenase type 2 enzyme (HSD3B2), the steroid hormone biosynthesis pathway, and chronic kidney disease (CKD). The findings illuminate novel perspectives on CKD pathogenesis and offer potential therapeutic avenues, while acknowledging certain limitations and avenues for future research.

Discovering HSD3B2's central role in steroid hormone biosynthesis enriches our comprehension of CKD, shifting the focus beyond the traditionally studied hormones like aldosterone and cortisol to a wider spectrum of steroidogenesis impacts on CKD's advancement (26–29). In some relevant studies on human renal diseases, plasma metabolites were assessed in controls and diabetic subjects with impaired kidney function, revealing a negative correlation between Pregnenolone sulfate and eGFR. Pregnenolone sulfate is one of key precursors in steroid synthesis pathways (30). Our findings of elevated pregnenolone levels in CKD models echo these observations, suggesting a disrupted steroid biosynthesis pathway. Interestingly, early diabetic conditions in rats have been shown to suppress renal steroidogenic activity, pointing to a broader disruption of steroidogenesis in renal diseases (31). However, the specific role of HSD3B2 in CKD progression remained unexplored until now. Our study's revelation of a marked decrease in HSD3B2 expression in CKD-affected kidneys underscores its potential significance in renal pathology, possibly contributing to key processes like inflammation, fibrosis, and oxidative stress. This opens up new therapeutic possibilities, where modulating HSD3B2 to adjust steroid hormone levels could offer a novel approach to restoring renal balance and slowing CKD progression.

Our investigation into HSD3B2 expression levels revealed that HSD3B2 is also substantially expressed in the kidneys compared to the adrenal glands in wild-type mice (Supplementary Figures 3A–C). This finding supports previous reports indicating the kidney's potential as an extra-glandular steroidogenic organ, with significant transcript levels of HSD3B1 and HSD3B2 detected in kidneys and an observed increase in steroidogenic capacity during development (32–34). Therefore, our results indicate that the decrease in HSD3B2 expression in CKD kidneys may play a significant role in disrupting systemic steroid biosynthesis. Interestingly, our immunohistochemistry staining data indicate that this reduction in kidney HSD3B2 expression

10.3389/fendo.2024.1358124

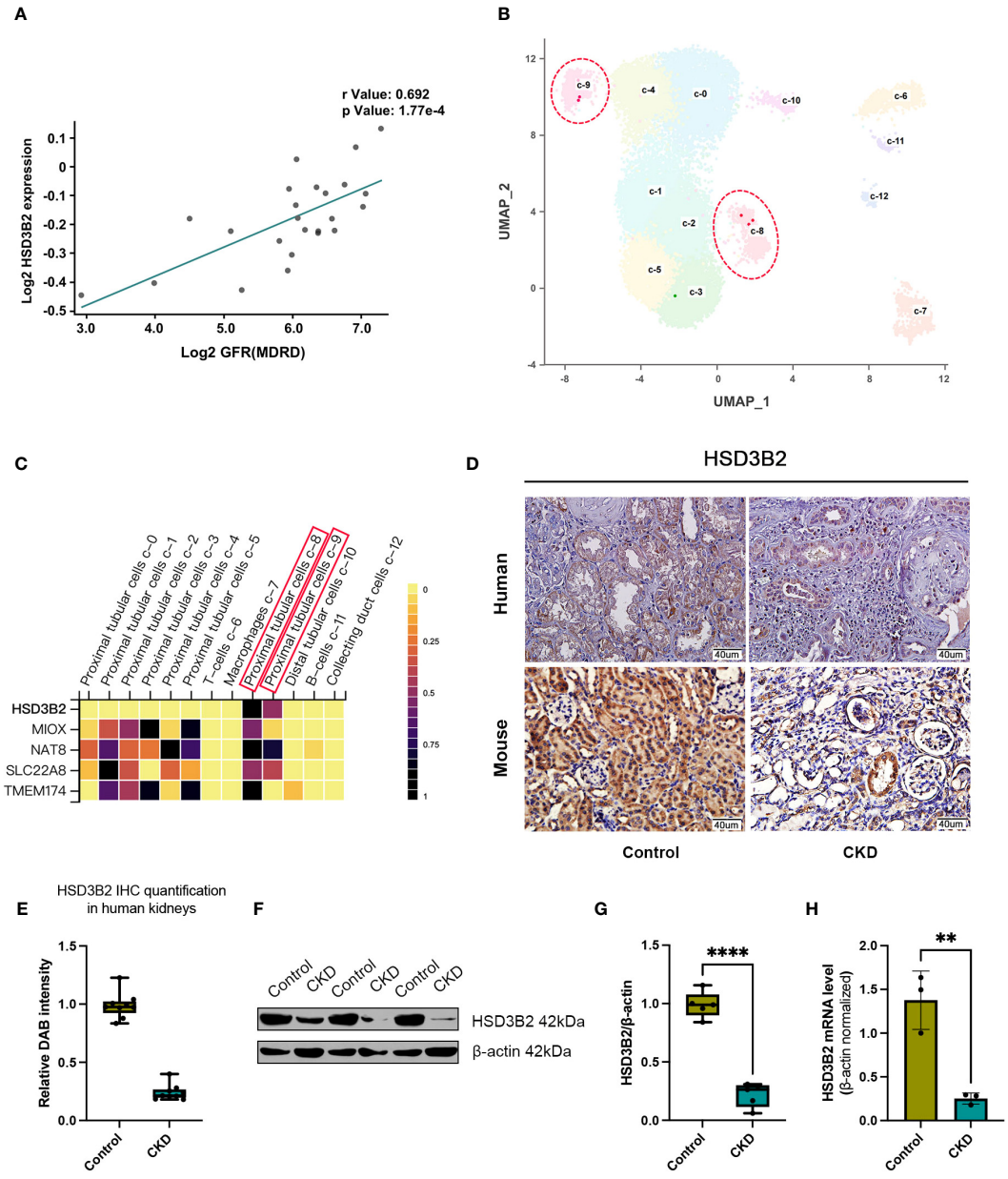

FIGURE 4
HSD3B2 expression was decreased in renal tubular cells of both human and mouse CKD models. **(A)** Correlation between GFR and renal HSD3B2 expression levels in the Reich IgAN TubInt dataset. HSD3B2 expression level exhibited a positive correlation with GFR in IgA nephropathy samples from CKD patients. **(B)** UMAP clustering of single cell data from the Human Protein Atlas dataset. Cells are clustered and annotated with cluster labels in two dimensions using the dimensionality reduction technique. The cell cluster label in the UMAP correspond to the cell types in the heatmap. **(C)** Heatmap of gene expression levels in different cell clusters of human kidney samples from the Human Protein Atlas dataset. Each small square on the X axis depicts individual cell clusters of the kidney, while Y axis depicts individual genes. Vertical colored bar is on the right of the heatmap. **(D)** Immunohistochemical detection of HSD3B2 in the kidneys of control or CKD group human and mice. Scale bar = 40 μm. **(E)** Box and whisker plots comparing relative DAB intensity of HSD3B2 immunohistochemical staining in control and CKD human kidneys. Control group (n=3), CKD group (n=3). **(F)** Western blot of HSD3B2 in the kidneys of control or adenine-induced CKD group mice. β-actin was used as a loading control. Western blot results are representative of at least three independent experiments. **(G)** Box and whisker plots comparing HSD3B2 expression in the kidneys of control and adenine-induced CKD mice. Control (n=5), CKD (n=5). **(H)** Quantitative real-time PCR analysis of HSD3B2 in the kidneys of control or adenine-induced CKD group mice. Control (n=3), CKD (n=3). β-actin was used as a house keeping gene. qPT-PCR results are representative of three independent experiments. For box and whisker plots, the median expression level is indicated by the central line within each box, while the box represents the interquartile range (IQR). Whiskers extend to the minimum and maximum values within a 1.5 * IQR range. All data are presented as the means ± SEM. Unpaired Student's t-test was performed to determine the statistical significance, with * $p < 0.05$, ** $p < 0.01$, *** $p < 0.001$, and **** $p < 0.0001$ versus control group.

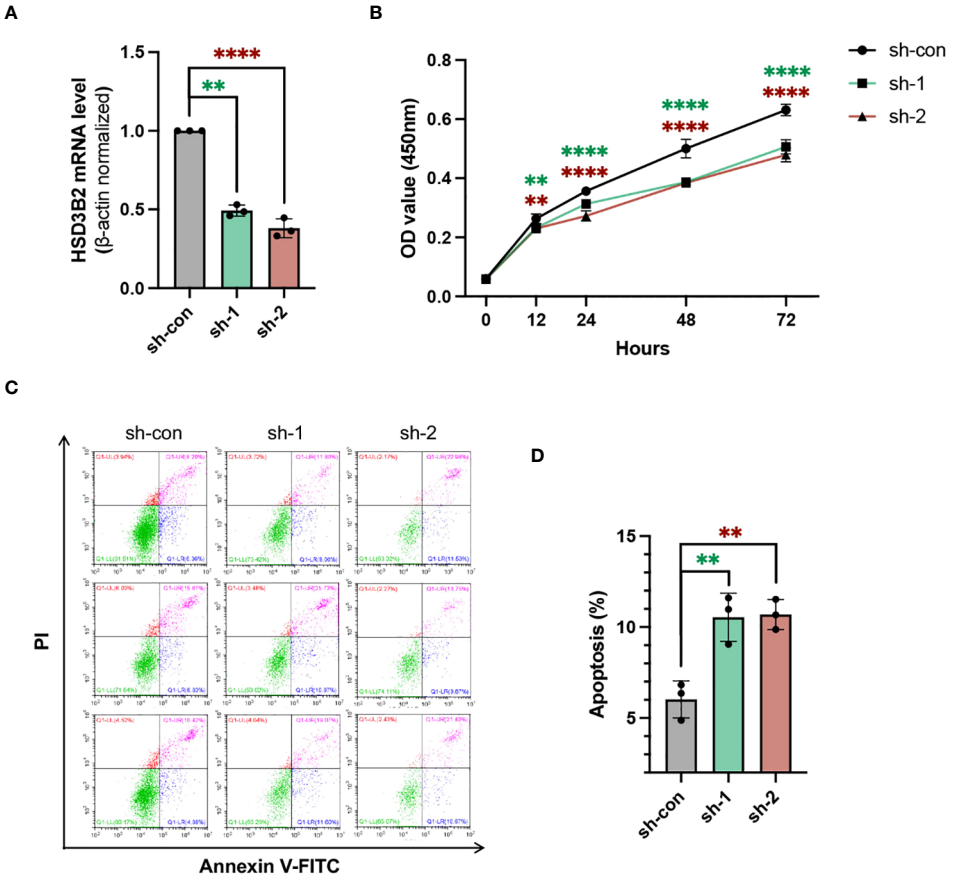

FIGURE 5
Knockdown of HSD3B2 affects proliferation and apoptosis of HK2 cells. **(A)** Evaluation of the knockdown efficiency of HSD3B2 in HK2 cells following shRNA infection using quantitative real-time PCR analysis (n=3 per group). β-actin was used as a house keeping gene. qPT-PCR results are representative of three independent experiments. **(B)** Cell viability of control and HSD3B2 knockdown groups of HK2 cells was detected by CCK-8 assay (n=6 per group). **(C)** Cell apoptosis of control and HSD3B2 knockdown groups of HK2 cells was detected by flow cytometry analysis of Annexin V and PI staining (n=3 per group). Results of flow cytometry analysis are representative of three independent experiments. **(D)** Quantification of flow cytometry analysis. All data are presented as the means ± SEM. Unpaired Student's t-test was performed to determine the statistical significance, with * $p < 0.05$, ** $p < 0.01$, *** $p < 0.001$, and **** $p < 0.0001$ versus control group.

does not extend to the adrenal glands (Supplementary Figure 3D). This result aligns with previous studies suggesting that late-stage CKD patients may not manifest adrenocortical function failure (35, 36). Thus, the specific decline of HSD3B2 in renal tissue highlights a unique aspect of CKD pathology, suggesting a localized disruption in steroid synthesis that does not affect adrenal gland function.

Understanding the precise mechanisms by which HSD3B2 influences CKD, and the steroid hormone biosynthesis pathway is imperative before translating these findings into therapeutic interventions. Investigating the downstream effects of HSD3B2 dysregulation and its potential interaction with established pathways, such as the renin-angiotensin-aldosterone system (RAAS), will be crucial to assessing its therapeutic potential. Moreover, it's important to consider the dysregulation of the hypothalamic-pituitary-adrenal (HPA) axis in CKD, which may lead to increased levels of adrenocorticotropic hormone (ACTH). Previous research has highlighted the variability in the function of the HPA axis in CKD patients, particularly regarding ACTH levels (25, 37, 38). While some studies have reported elevated ACTH levels in CKD compared to control groups, others have found no significant differences (39, 40). Interestingly, a discernible trend emerges, suggesting that ACTH elevations are more commonly observed in advanced CKD cohorts, while they may be less evident in the early stages of the disease (29). These findings underscore the complexity of HPA axis dysregulation in CKD and emphasize the need for further investigation into its role in disease progression and management.

In this study, we noted that adenine-induced CKD mice exhibited increased blood viscosity and a shorter coagulation time compared to control mice. This observation is in line with clinical case reports in the literature, which have documented changes in coagulation function and a hypercoagulable state in CKD patients (41). Clinical studies have consistently reported that patients with CKD exhibit altered hemostatic profiles, characterized by an increased tendency for blood clotting (42). These changes include elevated levels of procoagulant factors such as fibrinogen, factor VII (FVII), and factor VIII (FVIII), as well as higher von Willebrand factor (vWF) antigen

and activity. These abnormalities contribute to a hypercoagulable state, predisposing CKD patients to thromboembolic events (43). Our findings of increased blood viscosity and faster coagulation in CKD mice induced by an adenine diet mirror these clinical observations, suggesting that this mouse model accurately reflects the hemostatic alterations seen in human CKD.

The identification of HSD3B2's association with CKD opens new avenues for biomarker discovery. These biomarkers could be pivotal for early disease detection, risk stratification, and predicting treatment responses. Integration of HSD3B2-related biomarkers with other clinical and molecular markers could facilitate precision medicine approaches, tailoring interventions to individual patient needs. Furthermore, deeper insights into HSD3B2's role in CKD could enable the identification of patient subgroups that may particularly benefit from targeted interventions, enabling personalized treatment plans. For future studies, we propose exploring alternative approaches to modulate HSD3B2 activity in renal tissues. A promising direction could be deploying AAV9 vectors aimed at the kidneys, to boost HSD3B2 expression in renal cells, aiming to restore renal function both *in vivo* and *in vitro*. This novel therapeutic strategy may offer potential benefits with minimal impact on overall steroid metabolism.

Several limitations warrant consideration. The present study only utilized plasma samples for metabolomics analysis. Combining both kidney tissue and plasma samples in the metabolomics analysis could provide a more comprehensive assessment of metabolic pathway changes in CKD, capturing both systemic and renal-specific alterations. Untargeted metabolomic studies involve the simultaneous measurement of metabolites from each sample, aiming to achieve a global and unbiased perspective. However, the vast physiochemical diversity of the metabolome imposes limitations on the number of compounds that can be effectively measured in a single experiment. Factors such as solvent selection, separation strategies, and instrumentation platforms strongly influence which metabolites can be detected (44). Additionally, untargeted metabolomic analysis often relies on comparing experimental spectra with spectral databases for metabolite identification. Nevertheless, these databases may not encompass the entire metabolome, posing challenges in accurately identifying all detected metabolites (45).

All controls and CKD mice utilized in this study were female. The decision to use female mice was based on existing evidence indicating that female mice are more tolerant to adenine supplementation compared to males, which is reflected in decreased mortality rates and delayed occurrence of kidney damage following adenine supplementation (46). Male mice exposed to long-term adenine-enriched diet often exhibit significant reductions in body weight and signs of poor health, making further characterization challenging. It appears that sex hormones may be the cause of greater susceptibility of male kidneys to progressive renal injury in mice (47). Therefore, to ensure the feasibility and reliability of our experimental model, female mice were chosen for this study. While female mice were selected to ensure the study's viability and consistency, it's important to note that CKD prevalence globally is higher in women than in men (48, 49). Future studies might benefit from including both male and female subjects to explore gender-related differences in CKD progression and response to interventions.

In conclusion, this study sheds light on the pivotal role of HSD3B2 and the steroid hormone biosynthesis pathway in CKD. The findings expand our understanding of CKD pathogenesis, offering new insights into steroid hormone dysregulation's potential impact on renal function and pathology. The identification of HSD3B2 as a potential therapeutic target opens exciting possibilities for developing interventions aimed at modulating steroid hormone levels and ameliorating kidney dysfunction. While further research is necessary to elucidate the precise mechanisms and therapeutic potential, these findings provide a foundation for advancing CKD diagnostics and treatment strategies through personalized medicine approaches.

Data availability statement

The metabolomics data presented in the study are deposited in the MetaboLights repository, accession number MTBLS10715 https://www.ebi.ac.uk/metabolights/editor/MTBLS10715/descriptors.

Ethics statement

The studies involving humans were approved by the Medical Ethics Committee of Zhongnan Hospital of Wuhan University (protocol number: 2021074). The studies were conducted in accordance with the local legislation and institutional requirements. The participants provided their written informed consent to participate in this study. The animal study was approved by Animal Ethics Committee in Wuhan University (protocol number. WP20210561). The study was conducted in accordance with the local legislation and institutional requirements.

Author contributions

YZu: Conceptualization, Investigation, Methodology, Validation, Writing – original draft, Writing – review & editing. DZ: Data curation, Formal analysis, Investigation, Resources, Writing – review & editing. YZh: Investigation, Methodology, Project administration, Validation, Visualization, Writing – review & editing. WY: Methodology, Writing – review & editing, Formal analysis, Software, Visualization. JJ: Investigation, Methodology, Writing – review & editing, Validation. KW: Visualization, Writing – review & editing, Investigation. RZ: Investigation, Visualization, Writing – review & editing. ZC: Investigation, Visualization, Writing – review & editing. QH: Investigation, Visualization, Writing – review & editing, Conceptualization, Funding acquisition, Methodology, Supervision, Writing – original draft.

Funding

The author(s) declare financial support was received for the research, authorship, and/or publication of this article. This work was supported by National Natural Science Foundation of China 82072483, the Key Research and Development Program of Hubei Province (2022BCA052), and National Planning Project of Innovation and Entrepreneurship Training of Undergraduate of Wuhan University.

Acknowledgments

We would like to express our sincere appreciation to all the people involved in this research for their cooperation. Especially to Professor Yuqi Feng and Dr Anna for their invaluable help in performing the LC-MS analysis for this experiment at the Department of Chemistry, Wuhan University, Wuhan 430072, China. Similarly, we are grateful to Dr. DZ from the Department of Nephrology, Zhongnan Hospital of Wuhan University, Wuhan, China, for providing paraffin specimen sections of kidney biopsy samples from 6 patients.

Conflict of interest

The authors declare that the research was conducted in the absence of any commercial or financial relationships that could be construed as a potential conflict of interest.

Publisher's note

Supplementary material

The Supplementary Material for this article can be found online at: https://www.frontiersin.org/articles/10.3389/fendo.2024.1358124/full#supplementary-material

References

1. Kovesdy CP. Epidemiology of chronic kidney disease: an update 2022. *Kidney Int Suppl.* (2022) 12:7–11. doi: 10.1016/j.kisu.2021.11.003

2. Foreman KJ, Marquez N, Dolgert A, Fukutaki K, Fullman N, McGaughey M, et al. Forecasting life expectancy, years of life lost, and all-cause and cause-specific mortality for 250 causes of death: reference and alternative scenarios for 2016-40 for 195 countries and territories. *Lancet.* (2018) 392:2052–90. doi: 10.1016/S0140-6736(18)31694-5

3. Bikbov B, Purcell C, Levey AS, Smith M, Abdoli A, Abebe M, et al. Global, regional, and national burden of chronic kidney disease, 1990-2017: A systematic analysis for the global burden of disease study 2017. *Lancet.* (2020) 395:709–33. doi: 10.1016/S0140-6736(20)30045-3

4. Buckley LF, Schmidt IM, Verma A, Palsson R, Adam D, Shah AM, et al. Associations between kidney histopathologic lesions and incident cardiovascular disease in adults with chronic kidney disease. *JAMA Cardiol.* (2023) 8:357–65. doi: 10.1001/jamacardio.2023.0056

5. Jankowski J, Floege J, Fliser D, Bohm M, Marx N. Cardiovascular disease in chronic kidney disease pathophysiological insights and therapeutic options. *Circulation.* (2021) 143:1157–72. doi: 10.1161/CIRCULATIONAHA.120.050686

6. Augustine J. Kidney transplant: new opportunities and challenges. *Clev Clin J Med.* (2018) 85:138–44. doi: 10.3949/ccjm.85gr.18001

7. Rodrigues JC, Haas M, Reich HN. Iga nephropathy. *Clin J Am Soc Nephrol.* (2017) 12:677–86. doi: 10.2215/CJN.07420716

8. Samsu N. Diabetic nephropathy: challenges in pathogenesis, diagnosis, and treatment. *BioMed Res Int.* (2021) 2021:1497449. doi: 10.1155/2021/1497449

9. Breyer MD, Susztak K. Developing treatments for chronic kidney disease in the 21st century. *Semin Nephrol.* (2016) 36:436–47. doi: 10.1016/j.semnephrol.2016.08.001

10. Kalantar-Zadeh K, Li PKT. Strategies to prevent kidney disease and its progression. *Nat Rev Nephrol.* (2020) 16:129–30. doi: 10.1038/s41581-020-0253-1

11. Shabaka A, Cases-Corona C, Fernandez-Juarez G. Therapeutic insights in chronic kidney disease progression. *Front Med-Lausanne.* (2021) 8:645187. doi: 10.3389/fmed.2021.645187

12. Zaloszyc A, Bernardor J, Bacchetta J, Laverny G, Schmitt CP. Mouse models of mineral bone disorders associated with chronic kidney disease. *Int J Mol Sci.* (2023) 24:5325. doi: 10.3390/ijms24065325

13. Yokozawa T, Zheng PD, Oura H, Koizumi F. Animal-model of adenine-induced chronic-renal-failure in rats. *Nephron.* (1986) 44:230–4. doi: 10.1159/000183992

14. Yokozawa T, Oura H, Okada T. Metabolic effects of dietary purine in rats. *J Nutr Sci Vitaminol.* (1982) 28:519–26. doi: 10.3177/jnsv.28.519

15. de Frutos S, Luengo A, Garcia-Jerez A, Hatem-Vaquero M, Griera M, O'Valle F, et al. Chronic kidney disease induced by an adenine rich diet upregulates integrin linked kinase (Ilk) and its depletion prevents the disease progression. *Bba-Mol Basis Dis.* (2019) 1865:1284–97. doi: 10.1016/j.bbadis.2019.01.024

16. Hocher B, Adamski J. Metabolomics for clinical use and research in chronic kidney disease. *Nat Rev Nephrol.* (2017) 13:269–84. doi: 10.1038/nrneph.2017.30

17. Johnson CH, Ivanisevic J, Siuzdak G. Metabolomics: beyond biomarkers and towards mechanisms. *Nat Rev Mol Cell Bio.* (2016) 17:451–9. doi: 10.1038/nrm.2016.25

18. Zhang AH, Sun H, Wang P, Han Y, Wang XJ. Recent and potential developments of biofluid analyses in metabolomics. *J Proteomics.* (2012) 75:1079–88. doi: 10.1016/j.jprot.2011.10.027

19. Liu XH, Zhang B, Huang SY, Wang FC, Zheng L, Lu JD, et al. Metabolomics analysis reveals the protection mechanism of Huangqi-Danshen decoction on adenine-induced chronic kidney disease in rats. *Front Pharmacol.* (2019) 10:992. doi: 10.3389/fphar.2019.00992

20. Darmayanti S, Lesmana R, Meiliana A, Abdulah R. Genomics, proteomics and metabolomics approaches for predicting diabetic nephropathy in type 2 diabetes mellitus patients. *Curr Diabetes Rev.* (2021) 17. doi: 10.2174/1573399817666210101105253

21. Gagnebin Y, Boccard J, Ponte B, Rudaz S. Metabolomics in chronic kidney disease: strategies for extended metabolome coverage. *J Pharmaceut BioMed.* (2018) 161:313–25. doi: 10.1016/j.jpba.2018.08.046

22. Ryan D, Robards K, Prenzler PD, Kendall M. Recent and potential developments in the analysis of urine: A review. *Anal Chim Acta.* (2011) 684:17–29. doi: 10.1016/j.aca.2010.10.035

23. Gagnebin Y, Pezzatti J, Lescuyer P, Boccard J, Ponte B, Rudaz S. Toward a better understanding of chronic kidney disease with complementary chromatographic methods hyphenated with mass spectrometry for improved polar metabolome coverage. *J Chromatogr B Analyt Technol BioMed Life Sci.* (2019) 1116:9–18. doi: 10.1016/j.jchromb.2019.03.031

24. An N, Zhang M, Zhu Q-F, Chen Y-Y, Deng Y-L, Liu X-Y, et al. Metabolomic analysis reveals association between decreased ovarian reserve and in vitro fertilization outcomes. *Metabolites.* (2024) 14:143. doi: 10.3390/metabo14030143

25. Oguz Y, Oktenli C, Ozata M, Ozgurtas T, Sanisoglu Y, Yenicesu M, et al. The midnight-to-morning urinary cortisol increment method is not reliable for the assessment of hypothalamic-pituitary-adrenal insufficiency in patients with end-stage kidney disease. *J Endocrinol Invest.* (2003) 26:609–15. doi: 10.1007/BF03347016

26. Ames MK, Atkins CE, Pitt B. The renin-angiotensin-aldosterone system and its suppression. *J Vet Intern Med.* (2019) 33:363–82. doi: 10.1111/jvim.15454

27. Epstein M, Kovesdy CP, Clase CM, Sood MM, Pecoits R. Aldosterone, mineralocorticoid receptor activation, and ckd: a review of evolving treatment paradigms. *Am J Kidney Dis*. (2022) 80:658–66. doi: 10.1053/j.ajkd.2022.04.016

28. Frimodt-Moller M, Persson F, Rossing P. Mitigating risk of aldosterone in diabetic kidney disease. *Curr Opin Nephrol Hy*. (2020) 29:145–51. doi: 10.1097/MNH.0000000000000557

29. Sagmeister MS, Harper L, Hardy RS. Cortisol excess in chronic kidney disease - a review of changes and impact on mortality. *Front Endocrinol*. (2023) 13:1075809. doi: 10.3389/fendo.2022.1075809

30. Nilavan E, Sundar S, Shenbagamoorthy M, Narayanan H, Nandagopal B, Srinivasan R. Identification of biomarkers for early diagnosis of diabetic nephropathy disease using direct flow through mass spectrometry. *Diabetes Metab Synd*. (2020) 14:2073–8. doi: 10.1016/j.dsx.2020.10.017

31. Pagotto MA, Roldán ML, Molinas SM, Raices T, Pisani GB, Pignataro OP, et al. Impairment of renal steroidogenesis at the onset of diabetes. *Mol Cell Endocrinol*. (2021) 524:111170. doi: 10.1016/j.mce.2021.111170

32. Savchuk I, Morvan ML, Antignac JP, Kurek M, Le Bizec B, Söder O, et al. Steroidogenic potential of human fetal kidney at early gestational age. *Steroids*. (2019) 149:108417. doi: 10.1016/j.steroids.2019.05.009

33. Zhao HF, Labrie C, Simard J, Delaunoit Y, Trudel C, Martel C, et al. Characterization of rat 3-beta-hydroxysteroid dehydrogenase delta-5-delta-4 isomerase cdnas and differential tissue-specific expression of the corresponding messenger-rnas in steroidogenic and peripheral-tissues. *J Biol Chem*. (1991) 266:583–93. doi: 10.1016/S0021-9258(18)52475-3

34. Dalla Valle L, Toffolo V, Vianello S, Belvedere P, Colombo L. Expression of cytochrome P450c17 and other steroid-converting enzymes in the rat kidney throughout the life-span. *J Steroid Biochem*. (2004) 91:49–58. doi: 10.1016/j.jsbmb.2004.01.008

35. Rodriguez-Gutierrez R, Gonzalez-Gonzalez JG, Martinez-Rodriguez A, Burciaga-Jimenez E, Cesar Solis R, Gonzalez-Colmenero AD, et al. Adrenal functional reserve in the full spectrum of chronic kidney disease. *Gac Med Mex*. (2021) 157:502–7. doi: 10.24875/GMM.M21000605

36. Clodi M, Riedl M, Schmaldienst S, Vychytil A, Kotzmann H, Kaider A, et al. Adrenal function in patients with chronic renal failure. *Am J Kidney Dis*. (1998) 32:52–5. doi: 10.1053/ajkd.1998.v32.pm9669424

37. Huang WY, Molitch ME. Prolactin and other pituitary disorders in kidney disease. *Semin Nephrol*. (2021) 41:156–67. doi: 10.1016/j.semnephrol.2021.03.010

38. Meuwese CL, Carrero JJ. Chronic kidney disease and hypothalamic-pituitary axis dysfunction: the chicken or the egg? *Arch Med Res*. (2013) 44:591–600. doi: 10.1016/j.arcmed.2013.10.009

39. Raff H, Trivedi H. Circadian rhythm of salivary cortisol, plasma cortisol, and plasma acth in end-stage renal disease. *Endocr Connect*. (2013) 2:24–32. doi: 10.1530/EC-12-0058

40. Asao T, Oki K, Yoneda M, Tanaka J, Kohno N. Hypothalamic-pituitary-adrenal axis activity is associated with the prevalence of chronic kidney disease in diabetic patients. *Endocr J*. (2016) 63:119–26. doi: 10.1507/endocrj.EJ15-0360

41. Pavlou EG, Georgatzakou HT, Fortis SP, Tsante KA, Tsantes AG, Nomikou EG, et al. Coagulation abnormalities in renal pathology of chronic kidney disease: the interplay between blood cells and soluble factors. *Biomolecules*. (2021) 11:1309. doi: 10.3390/biom11091309

42. Baaten C, Sternkopf M, Henning T, Marx N, Jankowski J, Noels H. Platelet function in ckd: A systematic review and meta-analysis. *J Am Soc Nephrol*. (2021) 32:1583–98. doi: 10.1681/ASN.2020101440

43. Huang MJ, Wei RB, Wang Y, Su TY, Di P, Li QP, et al. Blood coagulation system in patients with chronic kidney disease: A prospective observational study. *BMJ Open*. (2017) 7:e014294. doi: 10.1136/bmjopen-2016-014294

44. Patti GJ. Separation strategies for untargeted metabolomics. *J Sep Sci*. (2011) 34:3460–9. doi: 10.1002/jssc.201100532

45. Gauglitz JM, West KA, Bittremieux W, Williams CL, Weldon KC, Panitchpakdi M, et al. Enhancing untargeted metabolomics using metadata-based source annotation. *Nat Biotechnol*. (2022) 40:1774–U20. doi: 10.1038/s41587-022-01368-1

46. Si H, Banga RS, Kapitsinou P, Ramaiah M, Lawrence J, Kambhampati G, et al. Human and murine kidneys show gender- and species-specific gene expression differences in response to injury. *PloS One*. (2009) 4:e4802. doi: 10.1371/journal.pone.0004802

47. Elliot SJ, Berho M, Korach K, Doublier S, Lupia E, Striker GE, et al. Gender-specific effects of endogenous testosterone:: female A- estrogen receptor-deficient C57bl/6j mice develop glomerulosclerosis. *Kidney Int*. (2007) 72:464–72. doi: 10.1038/sj.ki.5002328

48. Tong A, Evangelidis N, Kurnikowski A, Lewandowski M, Bretschneider P, Oberbauer R, et al. Nephrologists' Perspectives on gender disparities in ckd and dialysis. *Kidney Int Rep*. (2022) 7:424–35. doi: 10.1016/j.ekir.2021.10.022

49. Lewandowski MJ, Krenn S, Kurnikowski A, Bretschneider P, Sattler M, Schwaiger E, et al. Chronic Kidney Disease Is More Prevalent among Women but More Men Than Women Are under Nephrological Care Analysis from Six Outpatient Clinics in Austria. *Wien Klin Wochenschr*. (2023) 135:89–96. doi: 10.1007/s00508-022-02074-3

Frontiers in Endocrinology

Explores the endocrine system to find new therapies for key health issues

The second most-cited endocrinology and metabolism journal, which advances our understanding of the endocrine system. It uncovers new therapies for prevalent health issues such as obesity, diabetes, reproduction, and aging.

Discover the latest Research Topics

See more →

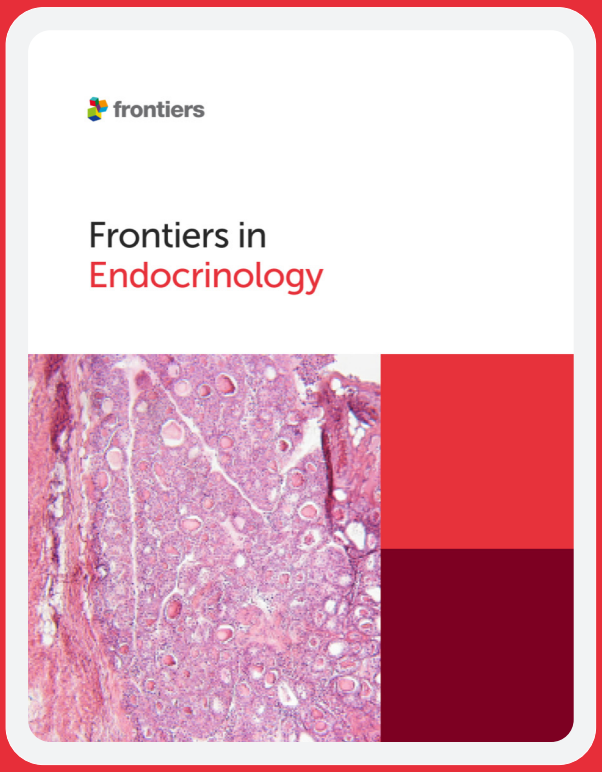

Frontiers

Avenue du Tribunal-Fédéral 34
1005 Lausanne, Switzerland
frontiersin.org

Contact us

+41 (0)21 510 17 00
frontiersin.org/about/contact